UNCLASSIFIED

AD NUMBER
ADC025102
CLASSIFICATION CHANGES
TO: unclassified
FROM: confidential
LIMITATION CHANGES
TO: Approved for public release, distribution unlimited
FROM: Controlling DoD Organization: Naval Ocean Research and Development Activity, Stennis Space Center, MS 39529.
AUTHORITY
ONR ltr, 31 Jan 2006; ONR ltr, 31 Jan 2006

THIS PAGE IS UNCLASSIFIED

CONFIDENTIAL

Copy No. 93

CHURCH STROKE II - CRUISE 5 PAR/ACODAC ENVIRONMENTAL ACOUSTIC MEASUREMENTS AND ANALYSIS (U)

Karl C. Focke

Jack A. Shooter

Nancy R. Bedford

Stephen K. Mitchell

APPLIED RESEARCH LABORATORIES
THE UNIVERSITY OF TEXAS AT AUSTIN
POST OFFICE BOX 8029, AUSTIN, TEXAS 78712

AD C025102

29 October 1979

Technical Report

Prepared for:

NAVAL OCEAN RESEARCH AND DEVELOPMENT ACTIVITY
NSTL STATION, MS 39529

"NATIONAL SECURITY INFORMATION"
"Unauthorized Disclosure Subject to Criminal Sanctions"

DTIC ELECTE JUN 4 1981 A

DTIC FILE COPY

DD 254, 26 March 1980,
Contract N00014-78-C-0329,
CLASSIFIED BY: OPNAVINST S5513.5, ID 05-42.2, 30 May 1980

REVIEW FOR DECLASSIFICATION ON: 29 October 1999

"Original contains color plates: All DTIC reproductions will be in black and white"

CONFIDENTIAL

81 6 04 502

CONFIDENTIAL

SECURITY CLASSIFICATION OF THIS PAGE (When Data Entered)

REPORT DOCUMENTATION PAGE

READ INSTRUCTIONS BEFORE COMPLETING FORM

1. REPORT NUMBER

2. GOVT ACCESSION NO. AD C025102

3. RECIPIENT'S CATALOG NUMBER

4. TITLE (and Subtitle)
CHURCH STROKE II - CRUISE 5 PAR/ACODAC ENVIRONMENTAL ACOUSTIC MEASUREMENTS AND ANALYSIS. (U)

5. TYPE OF REPORT & PERIOD COVERED
technical reports

6. PERFORMING ORG. REPORT NUMBER
ARL-TR-79-52

7. AUTHOR(s)
Karl C. Focke, Nancy R. Bedford, Jack A. Shooter, Stephen K. Mitchell

8. CONTRACT OR GRANT NUMBER(s)
N00014-78-C-0329

9. PERFORMING ORGANIZATION NAME AND ADDRESS
Applied Research Laboratories
The University of Texas at Austin
Austin, Texas 78712

10. PROGRAM ELEMENT, PROJECT, TASK AREA & WORK UNIT NUMBERS
12 247

11. CONTROLLING OFFICE NAME AND ADDRESS
Commanding Officer
Naval Ocean Research and Development Activity
NSTL Station, MS 39529

12. REPORT DATE
29 October 1979

13. NUMBER OF PAGES

14. MONITORING AGENCY NAME & ADDRESS (if different from Controlling Office)

15. SECURITY CLASS. (of this report)
CONFIDENTIAL

15a. DECLASSIFICATION DOWNGRADING SCHEDULE
See reverse side.

16. DISTRIBUTION STATEMENT (of this Report)

"NATIONAL SECURITY INFORMATION"
"Unauthorized Disclosure Subject to Criminal Sanctions"

17. DISTRIBUTION STATEMENT (of the abstract entered in Block 20, if different from Report)

"Original ... plates: All DTIC reproductions will be in black and white."

18. SUPPLEMENTARY NOTES

19. KEY WORDS (Continue on reverse side if necessary and identify by block number)

ambient noise, cw propagation loss, SUS propagation loss, ACODAC, PAR, bottom loss, geoacoustic parameters, Parece Vela Basin, Philippine Sea, bottom limited, depth excess, West Philippine Sea, storm noise

20. ABSTRACT (Continue on reverse side if necessary and identify by block number)

(C) Environmental acoustical analysis of cw, SUS, and ambient noise are reported for the Parece Vela Basin and the Western Philippine Sea Basin. These data were collected during the exercise CHURCH STROKE II Cruise 5, held in the Philippine Sea during the fall of 1977. Raw acoustic data were recorded on remote bottom moored ACODAC and PAR systems. During the recording periods ambient noise, ship signatures, and storm noise were recorded as well as cw and SUS data. Bottom loss and propagation loss are reported for the different basins. The

DD FORM 1473, 1 JAN 73 EDITION OF 1 NOV 65 IS OBSOLETE

404434

CONFIDENTIAL

SECURITY CLASSIFICATION OF THIS PAGE (When Data Entered)

15a.
DD 254, 25 Mar 80, Cont. N00014-78-C-0329
CLASSIFIED BY: OPNAVINST S5513.5, ID 05-42.2, 30 May 80
REVIEW FOR DECLASSIFICATION ON: 29 October 1999

20. (cont'd)

(C) Parece Vela Basin is characterized as bottom limited and high bottom loss for grazing angles greater than 40°. The Western Philippine Sea Basin is characterized as an area of depth excess and high bottom loss.

9

TABLE OF CONTENTS

(The reverse of this page is blank.)

LIST OF FIGURES

LIST OF FIGURES (Cont'd)

LIST OF FIGURES

LIST OF FIGURES

LIST OF FIGURES (Cont'd)

LIST OF FIGURES (Cont'd)

LIST OF FIGURES (Cont'd)

LIST OF FIGURES (Cont'd)

LIST OF FIGURES (Cont'd)

(The reverse of this page is blank.)

LIST OF TABLES

(The reverse of this page is blank.)

I. INTRODUCTION

(C) CHURCH STROKE II, Cruise 5, was conducted in November and December 1977, in the Philippine Sea. The planning for Cruise 5 of the exercise was presented in "Exercise Plan for CHURCH STROKE II Cruise 5" (U).[1] Acoustic measurement systems deployed included the LAMDBA (large aperture mobile data base array) systems, two PAR (programmable acoustic receiver) systems, and two ACODAC (acoustic data capsule) systems. Data recorded on the PAR and ACODAC systems have been processed at ARL:UT under this contract. The subjects of this report are bottom loss, propagation loss, and ambient noise measurements from both the ACODAC and PAR systems. Figure 1.1 presents the locations of sites from which data have been processed; these data were acquired on 15-20 November at Site B, 27-29 November at Site EN, and 17 November at Site C.

(U) The data objectives of the ACODAC were bottom loss versus angle and frequency; propagation loss and signal excess versus source range and depth, and receiver depth; ambient noise as a function of wind speed and receiver depth; and the effects of extended bottom limited propagation conditions in the Philippine Sea on ambient noise and propagation loss. The data objectives of the PAR were: sensor performances for omnidirectional, vertical line arrays (VLA), and DIFAR sensors based on ambient noise and cw projector tows. The recorded data have been processed at ARL:UT using computer programs operating upon digitized samples of the recorded data.

(U) The main purpose of this report is to present the processed data obtained from the ACODAC and PAR deployments during Cruise 5; observations and analyses are presented in Chapter 6 of this report. The complete set of measurements is stored on digital computer tapes, which are available to CHURCH STROKE II technical investigators.

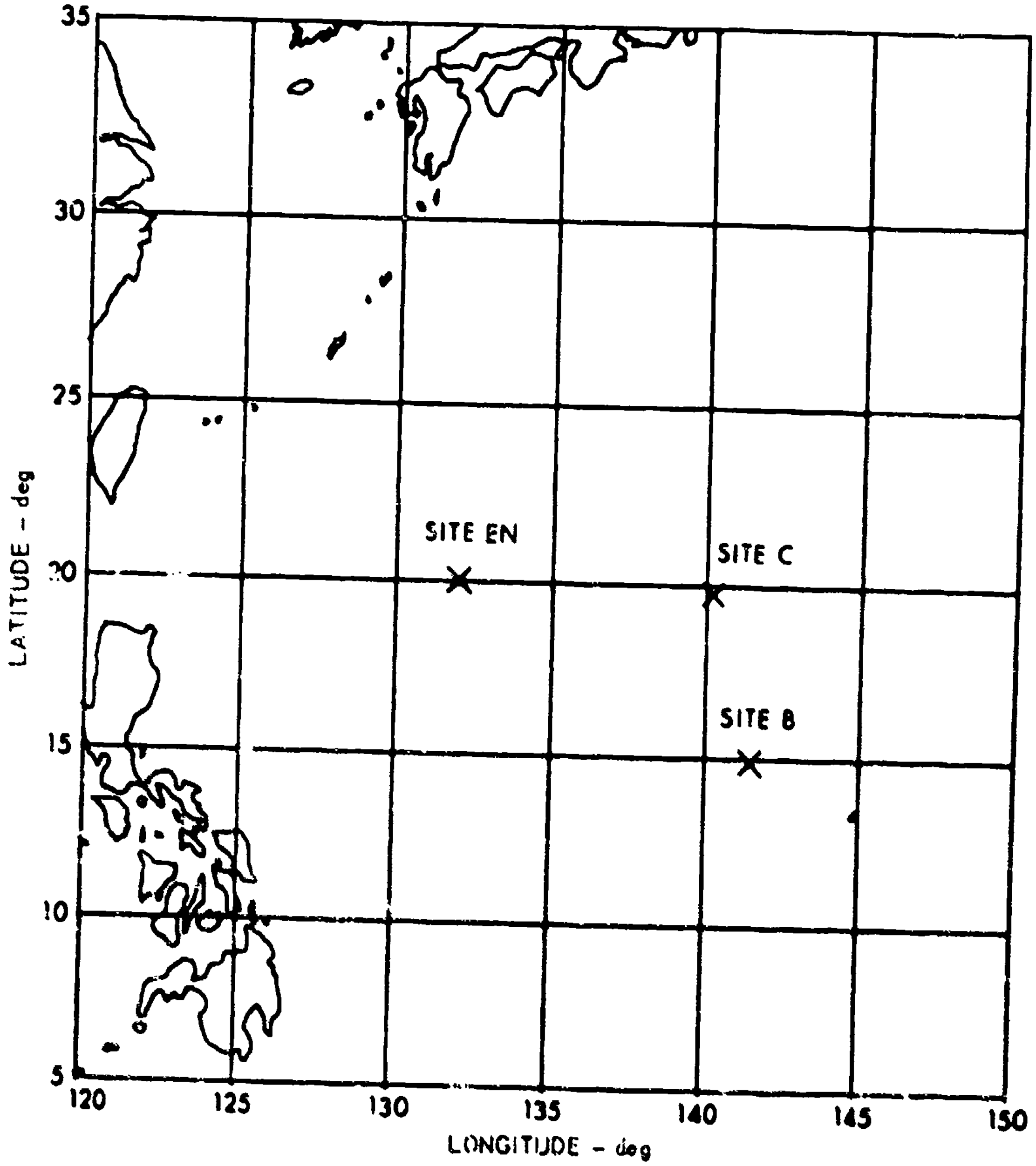

FIGURE 1.1
CHURCH STROKE II - EXERCISE AREA (U)

ARL:UT
AS-78-1838
KCF-GA
11-30-78

(U) ACODAC recording systems[2] were deployed at Sites B and EN to record ambient noise and cw and SUS propagation events. Each ACODAC was set up to record 12 data channels and 2 time code channels. At Site B the ACODAC recorded for 5 days and at Site EN, for 10 days.

(U) PAR recording systems[3] were deployed at Sites B, C, and EN to record ambient noise and cw propagation events. Each PAR was set up to record one time code channel, and 13 data channels: 11 omnidirectional channels and 2 horizontally directive channels. The PARs recorded for 6 days at Site B, 2 days at Site C, and over 10 days at Site EN.

(U) The same ACODAC hydrophone configuration was used at Sites B and EN. This configuration is shown in Fig. 1.2. Hydrophone 1 rested on the bottom and hydrophones 2 through 8 were distributed throughout the lower 1000 m of the water column. Hydrophones 9 and 10 were well up into the sound channel. The receiving sensitivities of hydrophones 8 and 10 were appropriate to measure SUS events, while the sensitivities of the remaining hydrophones were appropriate to measure the cw events and ambient noise. Problems with the ACODAC recordings,[4] however, limited the data processed to data from one uncalibrated SUS hydrophone (No. 8) at both sites and five cw/AN hydrophones (No.'s 2, 3, 4, 6, and 7) at Site EN only. As will be discussed in Chapters II and III, these recording problems meant that calibrated total propagation loss measurements from SUS sources could not be made (they have been estimated). However, bottom loss measurements could be made from the SUS sources recorded on the cw/AN hydrophones. Within the constraints of these problems, the available data which were processed should be good enough to achieve most of the ACODAC objectives.

(U) A single hydrophone array configuration was used for all PAR deployments. This configuration is shown in Fig. 1.3. Hydrophone 1 was 15.2 m off the bottom. The remaining omnidirectional hydrophones (2-4 and 7-13) were uniformly spaced 3.8 m (12.5 ft) from the adjacent hydrophones. The directional hydrophones 5 and 6 were located in close proximity to omnidirectional hydrophone 7. All of the PAR hydrophones were set up

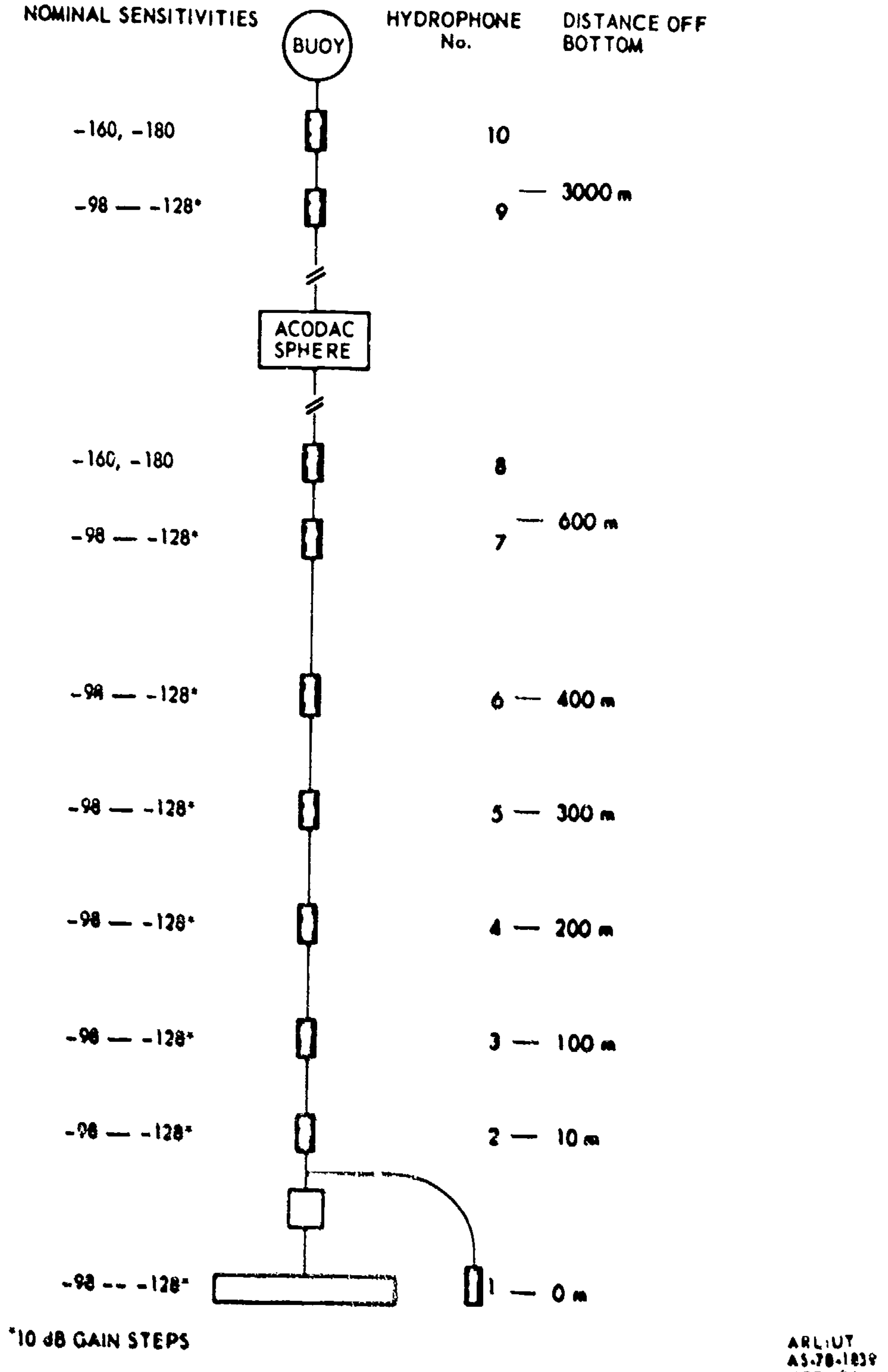

FIGURE 1.2
ACODAC ARRAY SPACING

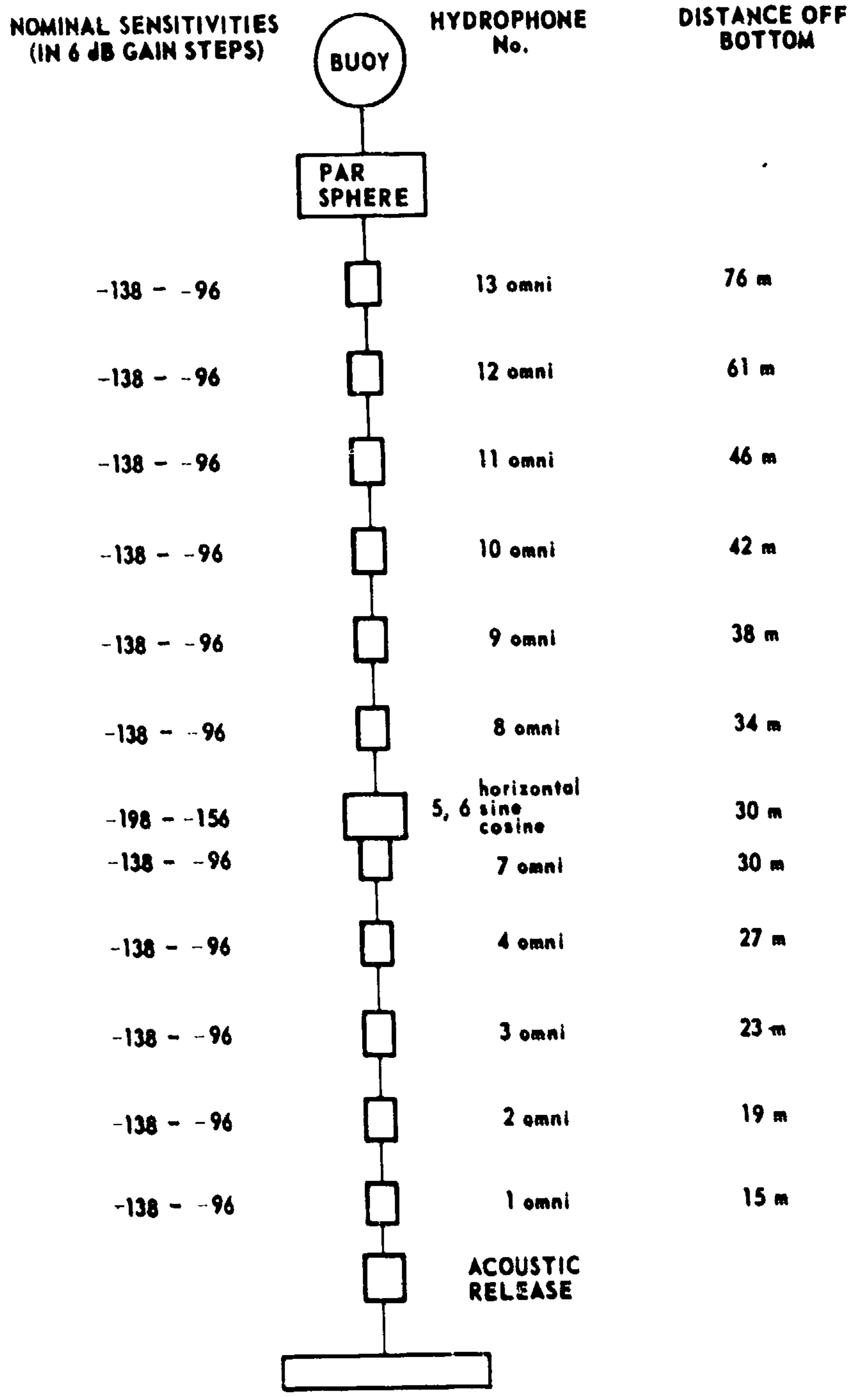

FIGURE 1.3
PAR ARRAY SPACING

ARL:UT
AS-79-990
KCF-GA
5-9-79

(U) with receiving sensitivities appropriate for measuring the cw and ambient noise events. Problems with the PAR recordings,[4] however, limited any processing to the omnidirectional data at selected time intervals. Although sensor performance comparisons were unattainable, the quality of the available data warranted processing of selected time intervals to supplement the ACODAC data set.

(U) The times of events during which the ACODACs were recording are presented in Figs. 1.4 and 1.5. The times when the PAR systems were recording are shown in Figs. 1.6 and 1.7. The shaded areas in these figures indicate the times and events which were processed and are reported here.

(C) Ambient noise and cw propagation data were processed for Sites B, C, and EN. At each of these sites data from only one PAR hydrophone was processed. At Site B, data from three ACODAC hydrophones were also processed for ambient noise. The ACODAC data from all five working cw/AN hydrophones at Site EN were processed. These data were analyzed in narrowband spectra with a frequency resolution of 0.147 Hz over the system bandwidth of 10 to 500 Hz. One power spectrum per minute was produced and stored on digital tape. Additional processing details are given in Appendix A.

(U) The SUS data at Site B and the aircraft SUS event at Site EN were processed for propagation loss and bottom loss. These shot data were analyzed in 1/3 octave bands between 12.5 Hz and 600 Hz using the techniques given in Appendices B and C. As mentioned above, problems with the ACODAC recording system prevented calibrated measurements of propagation loss from the SUS sources.

(C) Bottom loss and propagation loss computed from the SUS data were calculated using source levels published by Gaspin and Shuler.[5] The cw propagation loss calculations were based on the source levels presented in Table I-1 for the short ranges at Site B, and in Table I-2 for all other tows. Ancillary exercise data sources are listed in Refs. 6-11.

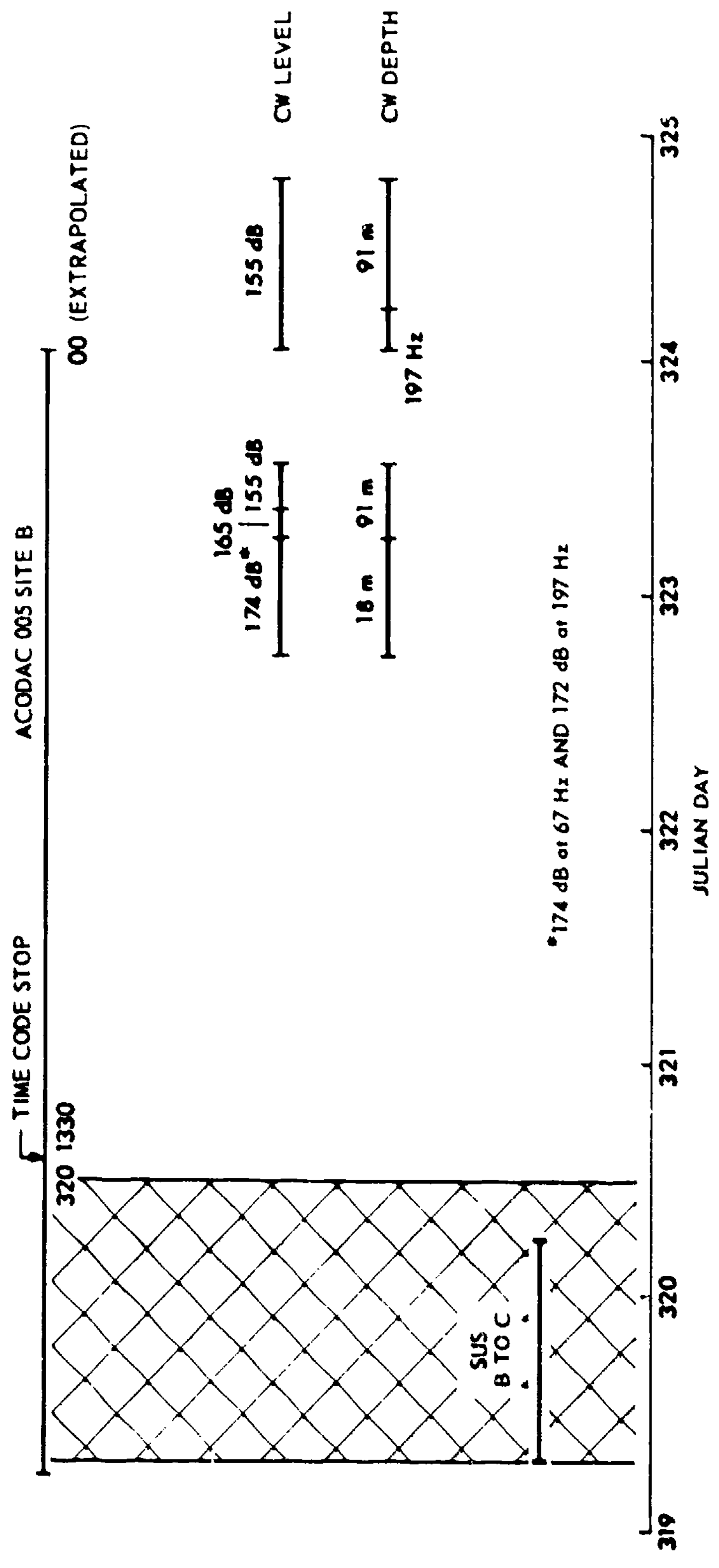

FIGURE 1.4
CHURCH STROKE II
PHASE 1
ACODAC RECORDING, CW,
AND SUS EVENT TIMES

ARL:UT
AS-78-1840
KCF-GA
11-30-78

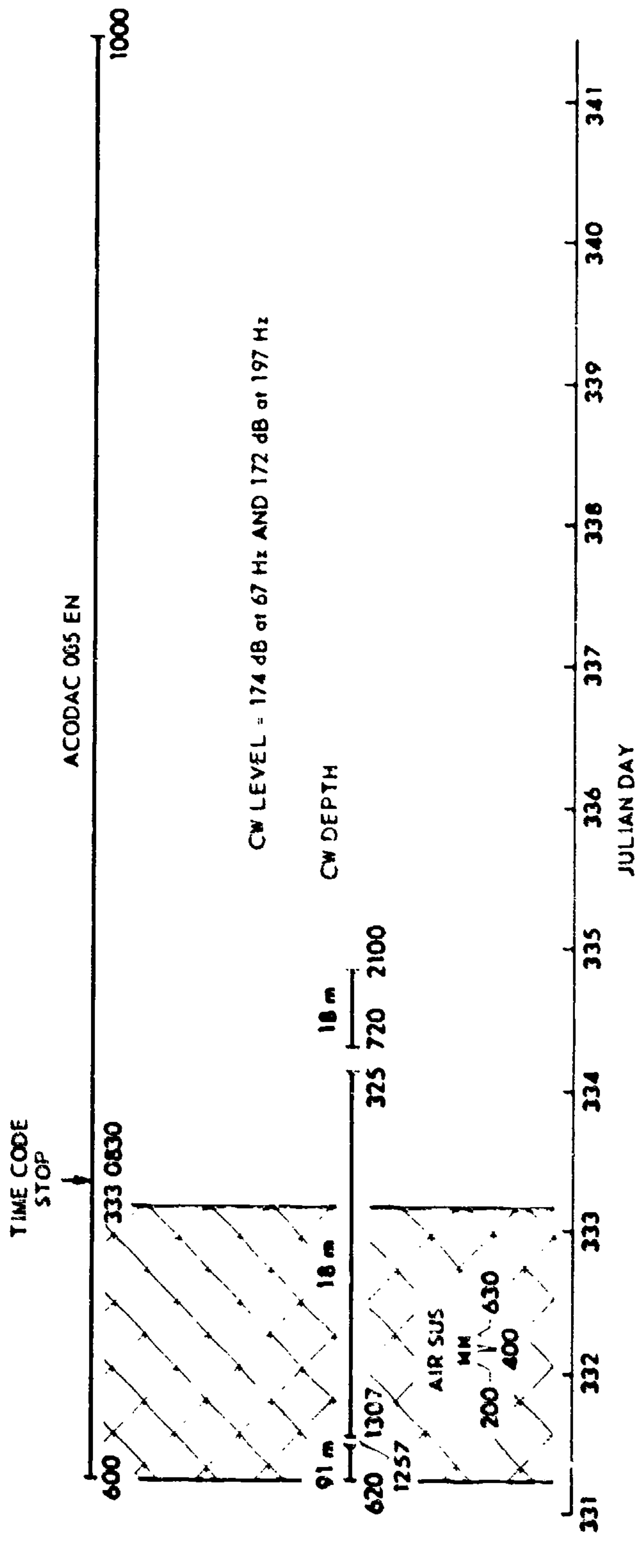

FIGURE 1.5
CHURCH STROKE II
PHASE 2
ACODAC RECORDING, CW, AND SUS EVENT TIMES

ARL:UT
AS-78-1841
KCF-GA
11-30-78

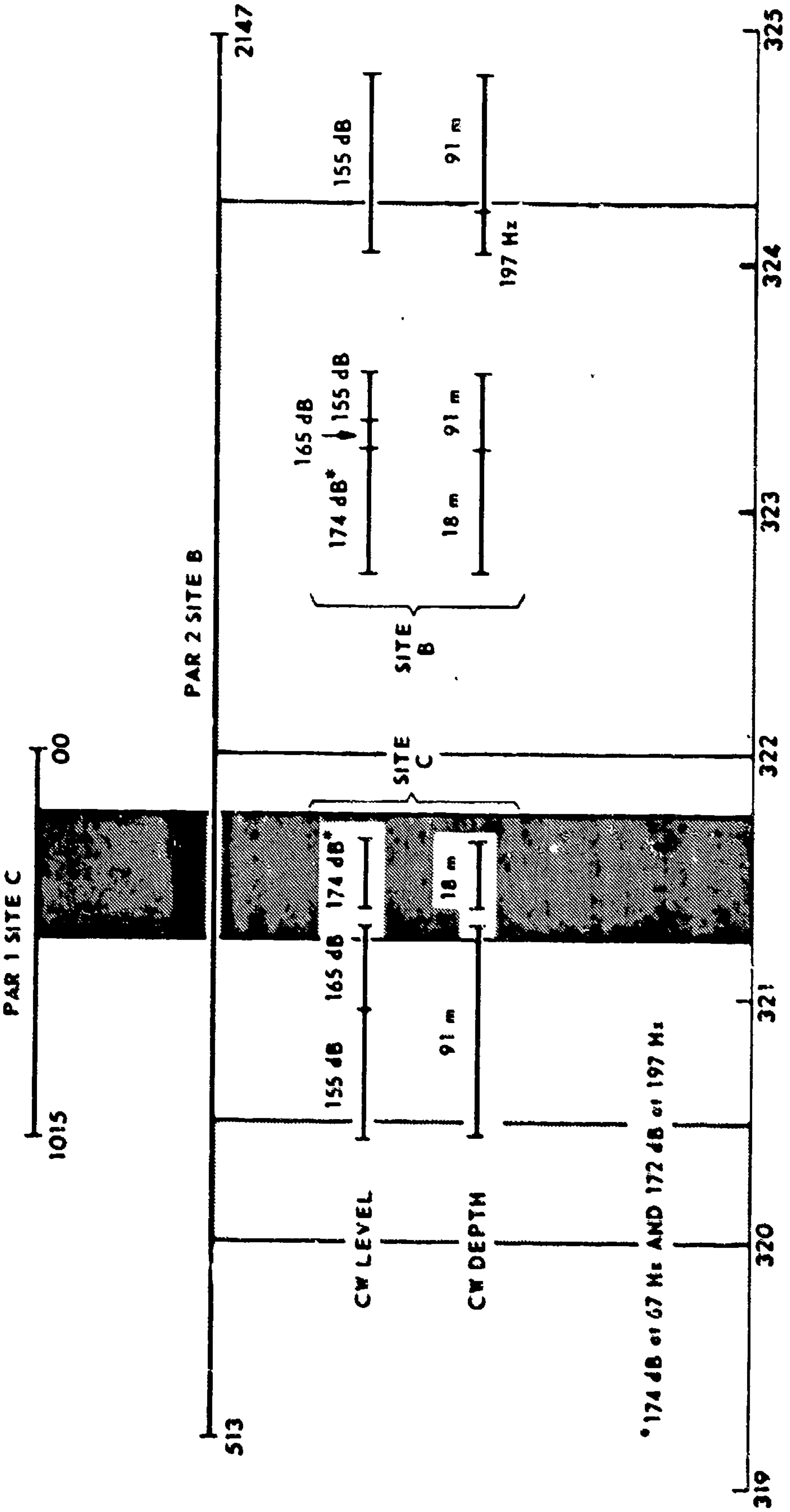

FIGURE 1.6
CHURCH STROKE II
PAR RECORDING AND CW EVENT TIMES
PHASE 1

ARL UT
AS-79-992
KCF - GA
5 - 9 - 79

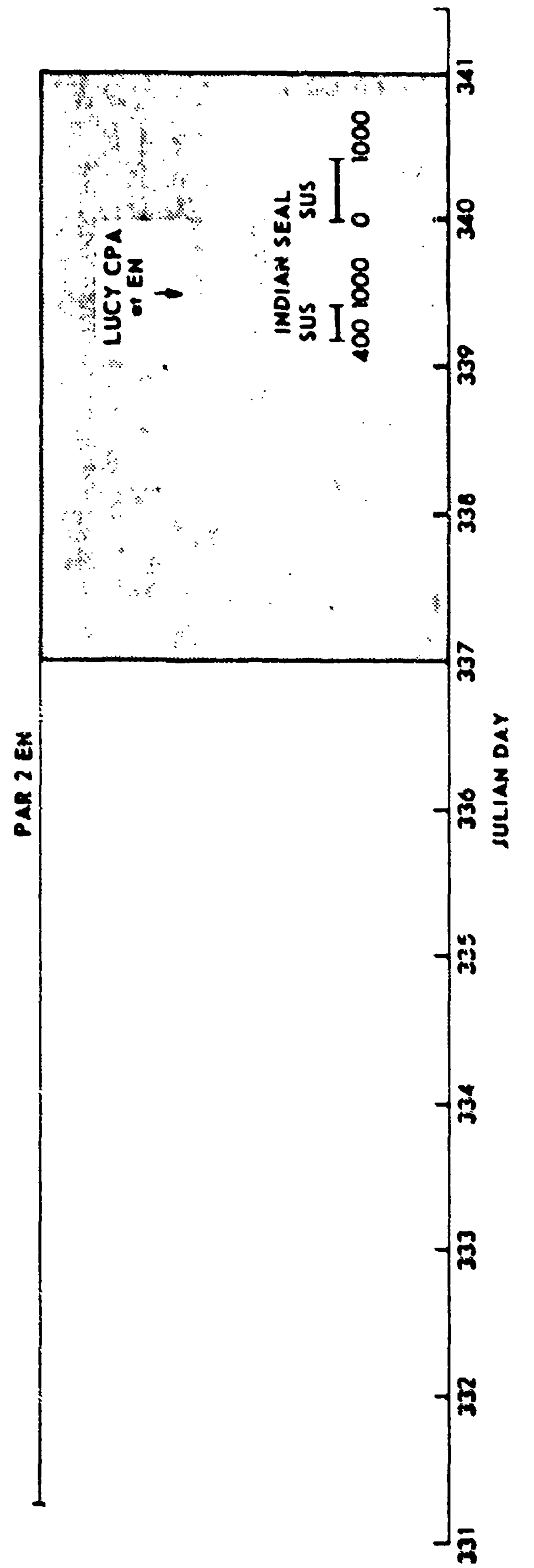

FIGURE 1.7
CHURCH STROKE II
PAR RECORDING AND SUS EVENT TIMES
PHASE 2

ARL UT
AS-79-991
KCF-GA
5-9-79

(U) TABLE I-1

SITE B - SHORT RANGE ACOUSTIC SOURCE LEVEL[6]

Range Interval (km)	Level (dB//μPa)
0 - 22	155
22 - 37	165

(U) TABLE I-2

ACOUSTIC PROJECTOR SOURCE LEVEL[6]

Frequency (Hz)	Level (dB//μPa)
67	174
197	172

II. SITE B ENVIRONMENTAL ACOUSTIC DATA

(C) Figure 2.1 presents the Site B location and the SUS shot run processed for this site. The site location was 14°54.5' N, 141°31.2' E;[11] the SUS source event commenced at 0740, 15 November 1977, and was concluded at 1716, 16 November 1977. This run was on an approximate bearing of 340° relative to the site. The data processed was for a range interval extending from 35 km to 500 km.[7,8] The entire event was conducted within the bottom limited basin shown in Fig. 2.1.

(U) Shots detonated at depths of 91 m and 244 m and received at a hydrophone depth of 3572 m (1000 m off the ocean floor) have been analyzed. There were two hydrophones deployed at this depth. One hydrophone with a nominal receiving sensitivity of -151 dB//V/µPa was designed to measure the shot data, and another hydrophone, with a nominal receiving sensitivity of -128 to -98 dB//V/µPa (varying gain) was designed to measure ambient noise and cw data.

(U) The predeployment calibration signals for the shot hydrophone exceeded the saturation level of the recording tape, and therefore the data received on this hydrophone was uncalibrated. Since the high sensitivity hydrophone was designed to measure ambient noise, the peak level of the first and second multipath arrivals of almost all of the shots saturated the tape recordings. Bottom loss measurements were made using the unsaturated higher order arrivals received on the ambient noise hydrophones. However, total propagation loss could not be accurately measured because of the above problems. To get an estimate of total propagation loss, data from both the shot hydrophone and the ambient noise hydrophone have been processed for propagation loss. The data from the shot hydrophone (uncalibrated though unsaturated) have been plotted as relative sound pressure level (SPL) to present the structure of the propagation loss as a function of range. The data from the ambient noise hydrophone

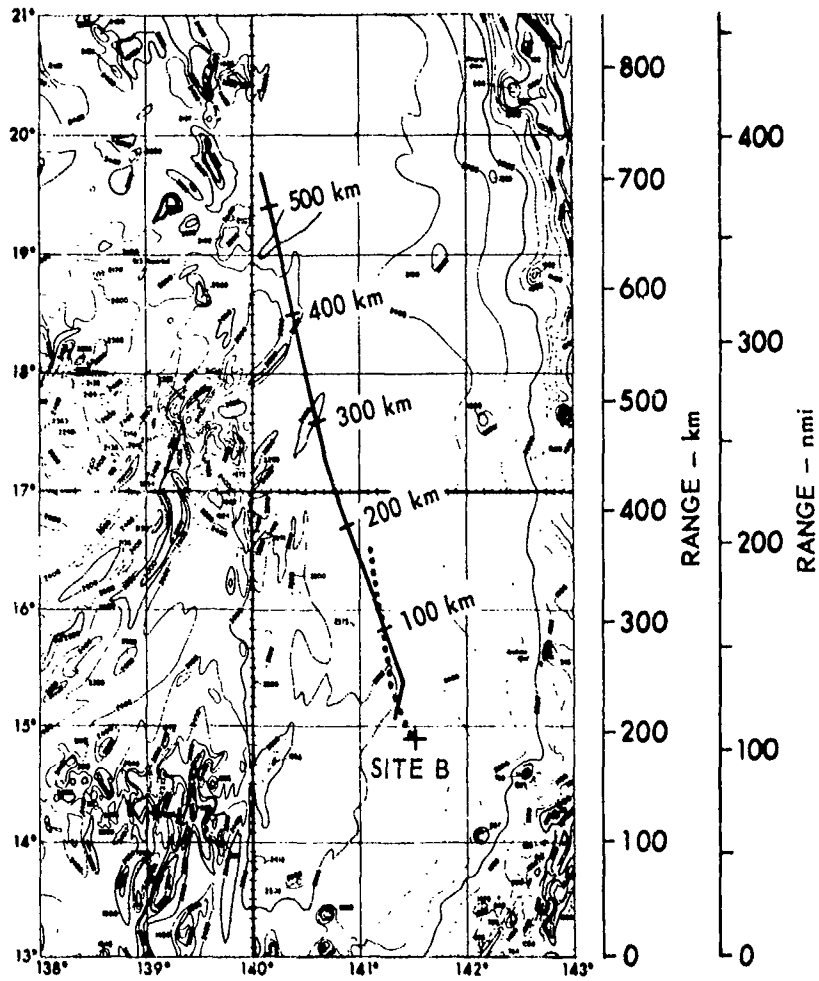

FIGURE 2.1
CHURCH STROKE II - SITE B (U)
—— SUS SOURCE TRACK - INDIAN SEAL
······ CW SOURCE TRACK - INDIAN SEAL

ARL:UT
AS-78-1842
KCF - GA
11-30-78

(U) (calibrated though saturated) have been plotted as propagation loss to provide an upper bound on the propagation loss. All of the propagation loss data have been plotted with symbols to indicate the signal-to-noise ratio (S/N) within the measurement band. The meaning of each symbol is given below.

X: S/N ≥ 3 dB,

+: 0 dB ≤ S/N < 3 dB,

S: Saturation on some peaks,

□: -3 dB ≤ S/N < 0 dB, and

Δ: S/N < -3 dB.

The term saturation refers to recorded shots which have a peak amplitude exceeding the maximum recording level.

(C) The INDIAN SEAL towed a cw projector approximately along the 345° radial of Site B from 1740 18 November to 1200 19 November 1977. The tow started at a range of 180 km and finished at the site. Data recorded on the PAK during this time interval have been processed for cw propagation loss and ambient noise. The hydrophone had a nominal receiving sensitivity of -138 to -96 dB//V/μPa and was at a depth of 4542 m (30 m above the bottom). At ranges greater than 36 km the source depth was 18 m, while at closer range the source was at 91 m.

2.1 Bottom Loss at Site B

(U) Bottom loss measurements are presented as the loss per bounce as a function of bottom grazing angle; the data processing is given in Appendix B. The bottom loss measurements for each multipath arrival are presented in Figs. 2.2 and 2.3. The symbol plotted for a given measurement indicates the total number of bottom bounces for that arrival.

(U) A scalloping effect can be seen in the 25 Hz and 50 Hz bottom loss measurements from the 91 m SUS (Fig. 2.2). It is felt that the bottom loss does not actually follow such a pattern. This type of behavior arises from small discrepancies between the values of parameters such as source range

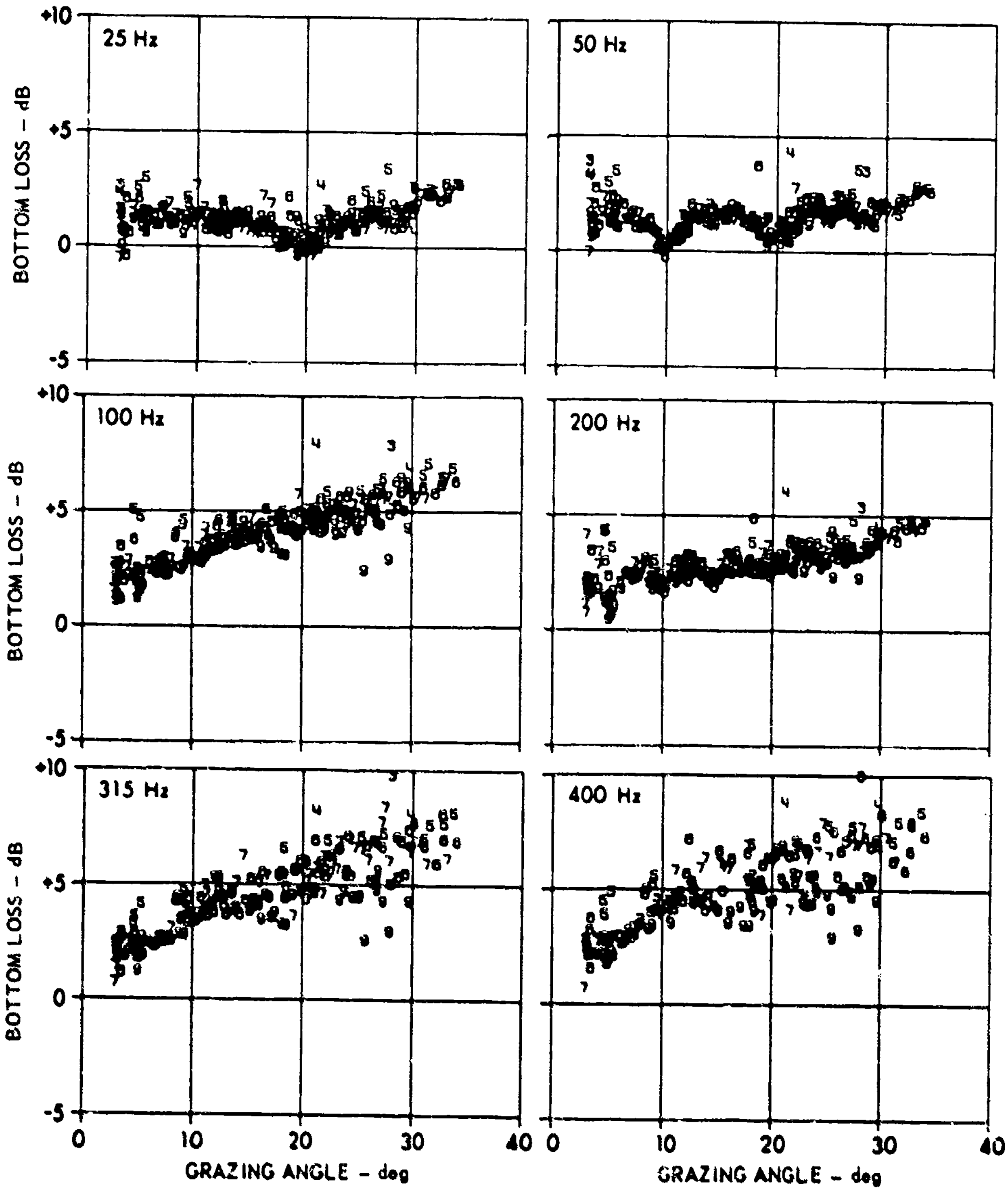

FIGURE 2.2
BOTTOM LOSS ESTIMATES versus GRAZING ANGLE (U)
CHURCH STROKE II - SITE B - 3572 m RECEIVER DEPTH
91 m SOURCE DEPTH

ARL:UT
AS-78-1833
KCF - GA
11-30-78

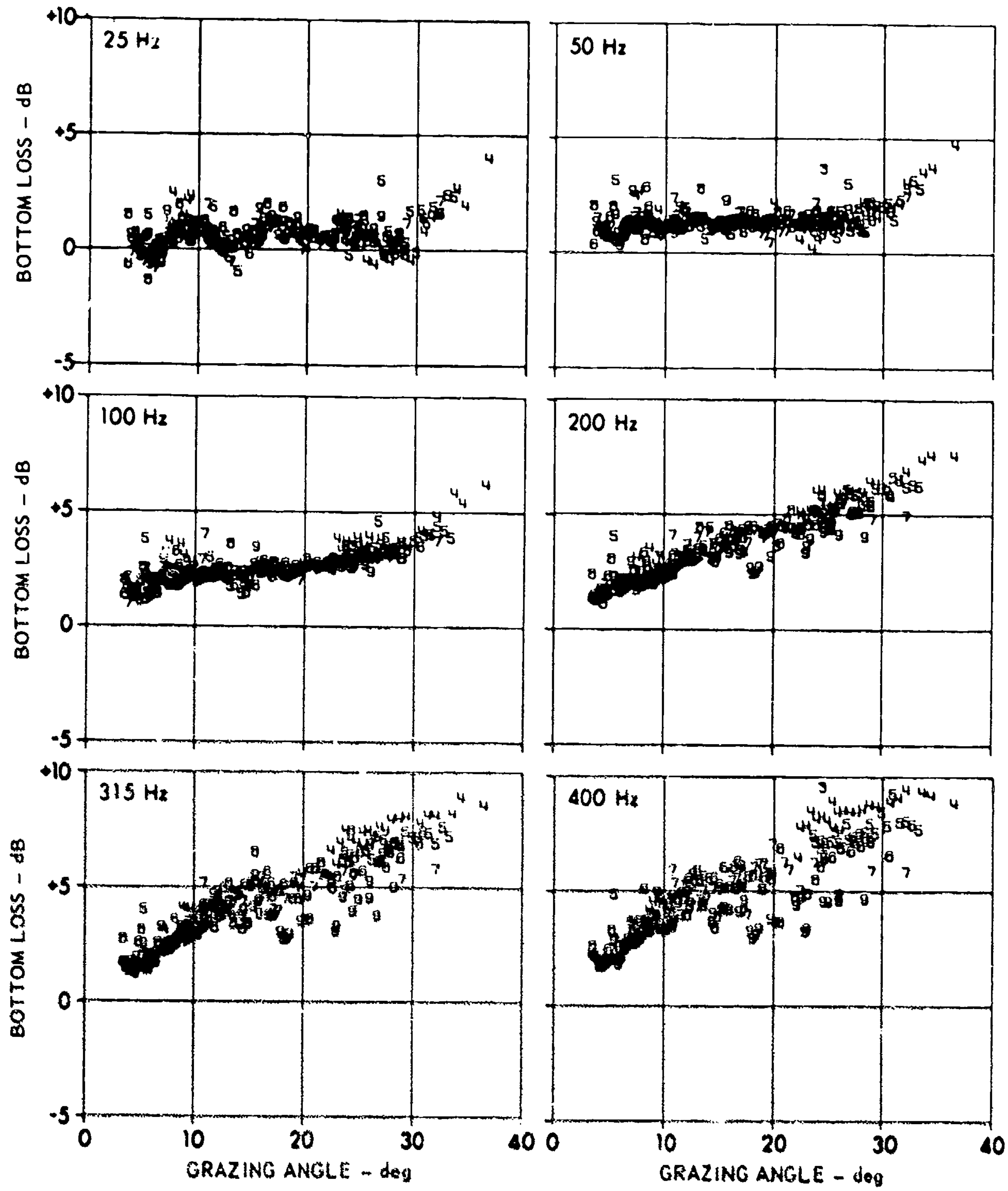

FIGURE 2.3

BOTTOM LOSS ESTIMATES versus GRAZING ANGLE (U)

CHURCH STROKE II - SITE B - 3572 m RECEIVER DEPTH

214 m SOURCE DEPTH

ARL:UT
AS-78-1832
KCF - GA
11-30-78

(U) or source depth which were used for data reduction and the actual value(s) during the experiment. One may understand this by considering the propagation loss measurements and reference calculations going into Figs. 2.2 and 2.3; the material of Appendix C and Ref. 12 are relevant to this consideration. Figure 2.4 presents the calculated reference propagation loss as a function of bottom grazing angle (see Appendix C). The scalloping in this figure is due to surface image interference (Lloyd's Mirror Effect). In Fig. 2.5 the individual measured arrivals are seen to be blurred, due, probably, to problems in the experiment. For example, variations in the source depth or the navigation data result in slight errors in predicting the bottom angle of a given arrival and blur the effects of the surface image. In turn, this results in a slight scalloping in the measured bottom loss curves, as in Fig. 2.2; the influence of this effect is diminished by averaging over grazing angle.

(U) Figure 2.6 presents the average bottom loss at Site B. Data from the two source depths were combined and then averaged in 5° bins. These averages have been plotted at the midpoint of the angular bin. Table II-1 presents these average values along with the standard deviation and the number of points used in each average.

(U) The bottom loss measurements were limited to bottom grazing angles less than 35°; the arrivals predicted at angles greater than 35° were not detectable in the shots processed. For example, Fig. 2.7 shows the envelope of one of the Site B SUS arrivals. Bottom reflection angles calculated for that shot are shown in the figure. As may be seen, the arrivals at angles above 35° become abruptly absent. This is consistent with known sediment thickness in the Site B basin which is approximately 350 m.[13] Assuming typical sound velocity gradients in the sediment, one may calculate that rays steeper than 35° at the bottom will fully penetrate the sediment and be scattered from the basalt basement. For that reason, at angles above 35° it is recommended that 10 to 15 dB of bottom loss be assumed, as indicated in Table II-1.

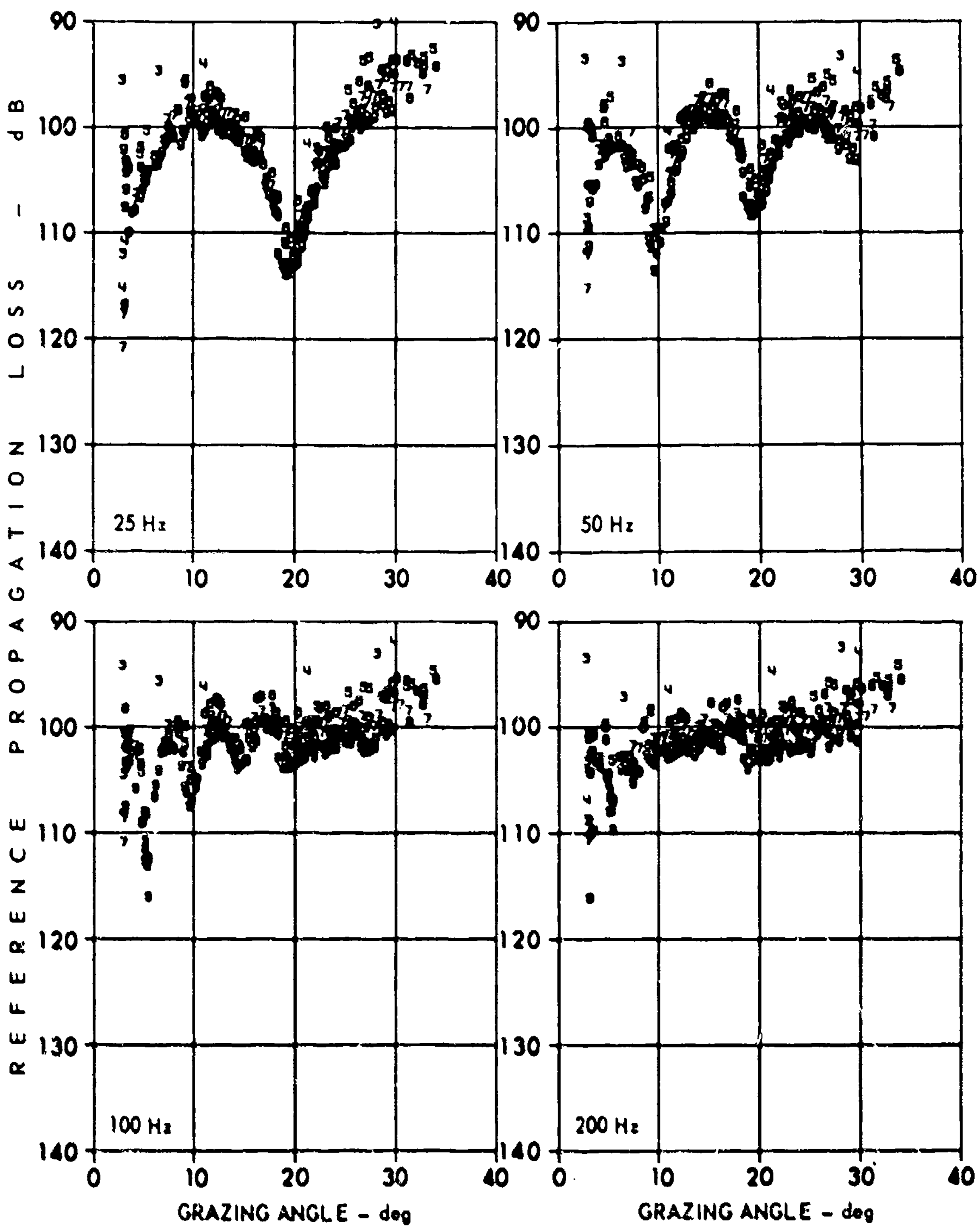

FIGURE 2.4
REFERENCE PROPAGATION LOSS FOR
EACH MULTIPATH ARRIVAL (U)
CHURCH STROKE II - SITE B - 3572 m RECEIVER DEPTH
91 m SOURCE DEPTH

ARL:UT
AS-78-1962
KCF - GA
12-13-78

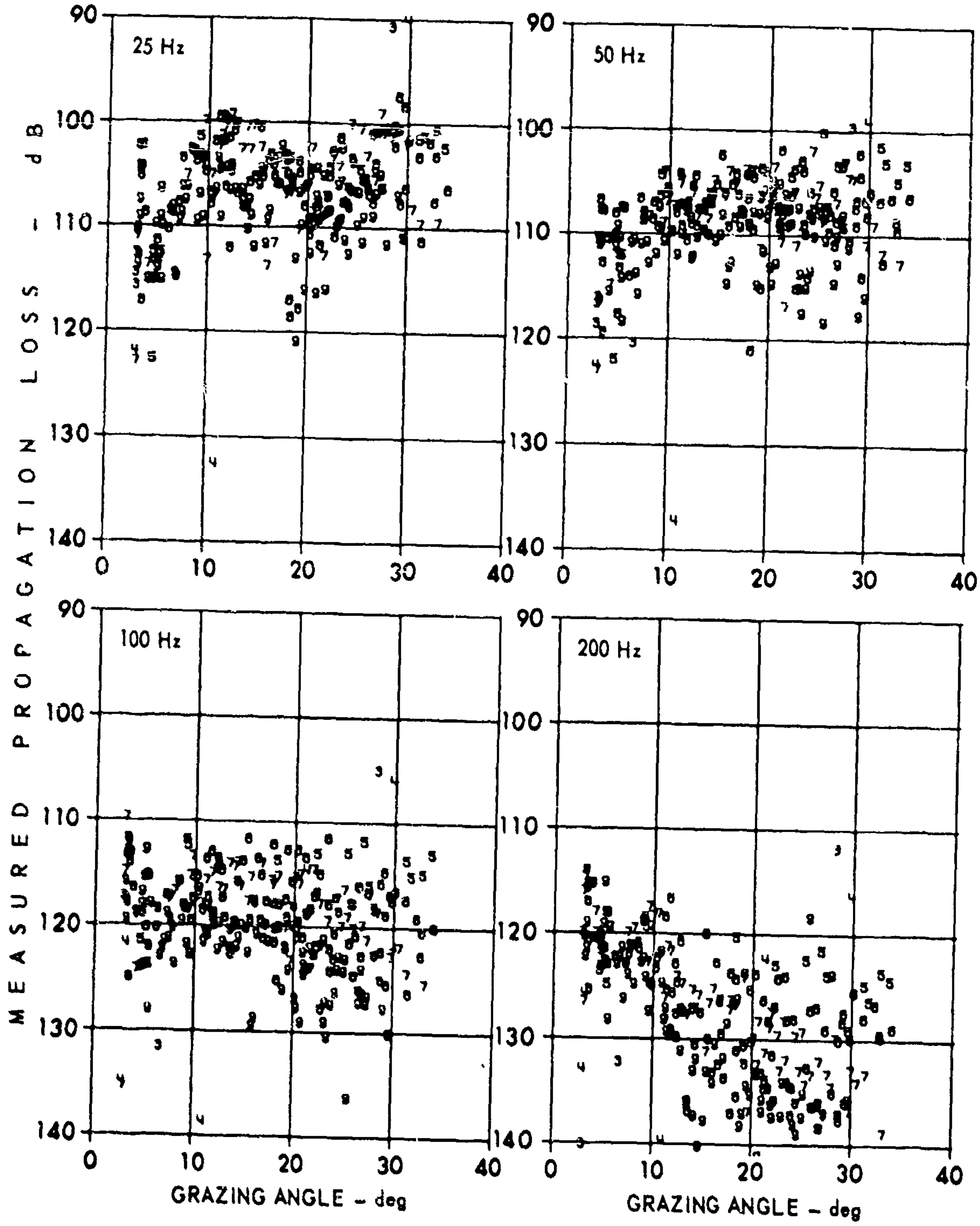

FIGURE 2.5
MEASURED PROPAGATION LOSS
FOR EACH MULTIPATH ARRIVAL (U)
SITE B - 3572 m RECEIVER
91 m SOURCE DEPTH

ARL:UT
AS-78-1963
KCF - GA
12-13-78

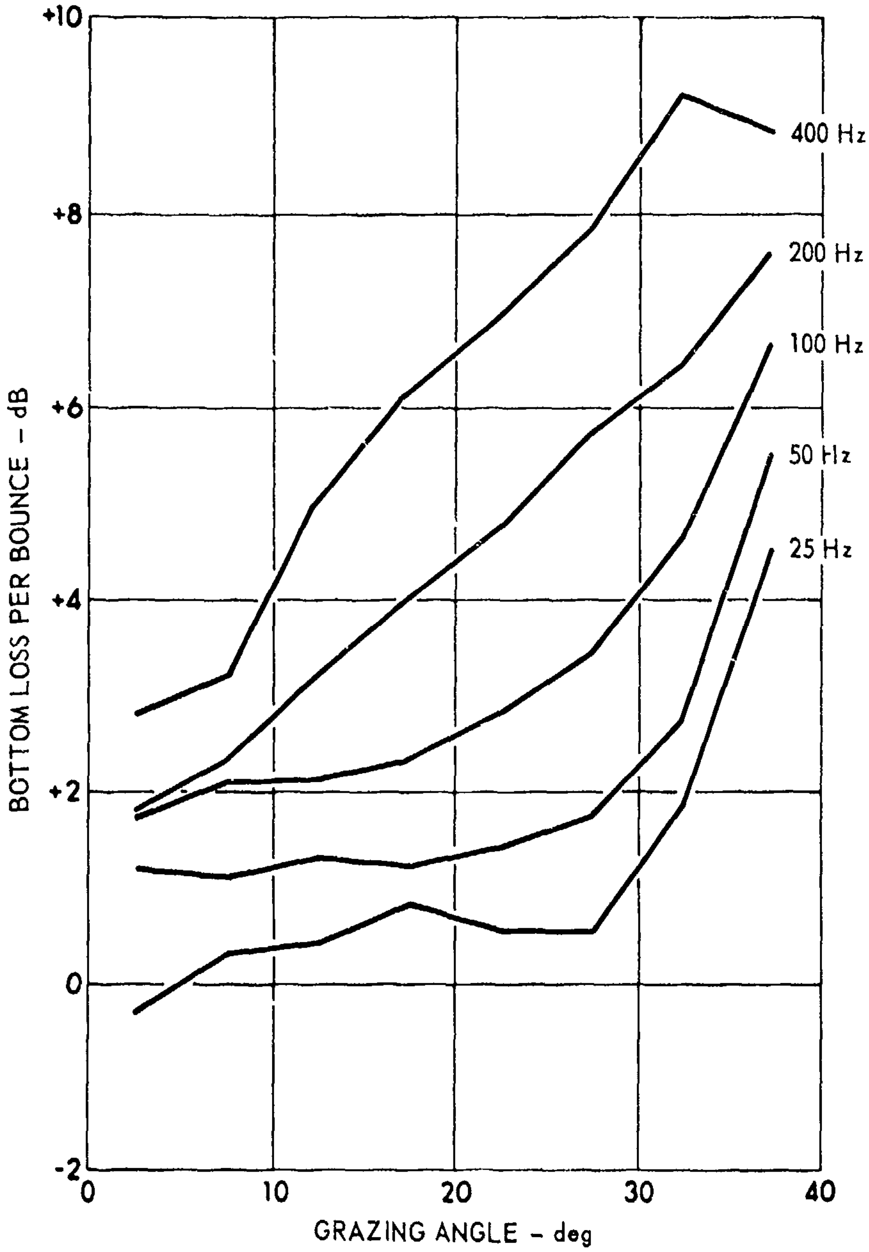

FIGURE 2.6
(U) AVERAGED BOTTOM LOSS (5° INTERVALS)
CHURCH STROKE II – SITE B
SEE TABLE 2.1

ARL:UT
AS-78-1878
KCF-GA
12-6-78

(C) TABLE II-1

AVERAGED BOTTOM LOSS DATA CHURCH STROKE II - SITE B (U)

91 m and 244 m SUS
Receiver Depth - 3572 m
Bounces 3-12

25 Hz

Grazing Angle Interval-Deg		Mean	Std Dev	Number Samples
0	5	-0.3	1.5	312
5	10	0.3	0.8	672
10	15	0.4	0.6	627
15	20	0.8	0.5	375
20	25	0.5	0.7	414
25	30	0.5	0.7	357
30	35	1.8	0.8	93
35	40	4.5	0.5	6

50 Hz

Grazing Angle Interval-Deg		Mean	Std Dev	Number Samples
0	5	1.2	1.7	357
5	10	1.1	0.6	831
10	15	1.3	0.4	681
15	20	1.2	0.4	390
20	25	1.4	0.5	447
25	30	1.7	0.5	369
30	35	2.7	1.0	99
35	40	5.5	1.0	9

100 Hz

Grazing Angle Interval-Deg		Mean	Std Dev	Number Samples
0	5	1.7	1.8	276
5	10	2.1	0.7	453
10	15	2.1	0.5	408
15	20	2.3	0.4	261
20	25	2.8	0.5	294
25	30	3.4	0.5	258
30	35	4.6	1.1	78
35	40	6.6	1.0	9

200 Hz

Grazing Angle Interval-Deg		Mean	Std Dev	Number Samples
0	5	1.8	1.6	243
5	10	2.3	0.8	435
10	15	3.2	0.8	213
15	20	4.0	0.7	135
20	25	4.7	1.0	156
25	30	5.7	1.0	153
30	35	6.4	0.7	39
35	40	7.6	0.0	3

400 Hz

Grazing Angle Interval-Deg		Mean	Std Dev	Number Samples
0	5	2.8	1.7	207
5	10	3.2	1.2	168
10	15	5.0	0.9	54
15	20	6.1	1.3	45
20	25	6.7	1.8	75
25	30	7.8	1.9	69
30	35	9.2	0.2	15
35	40	8.8	0.0	3

NOTE: Arrivals above 40° grazing angles not detected. Recommend using 12 dB loss above 40° at all frequencies.

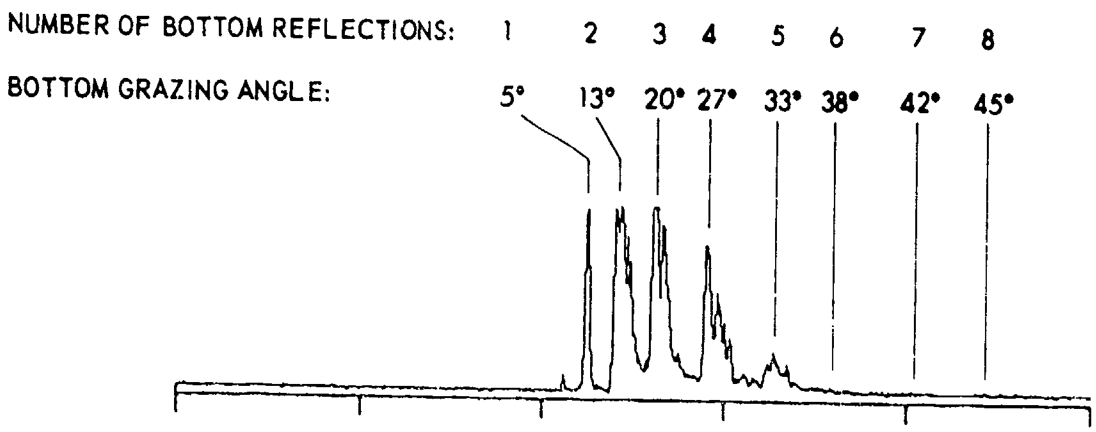

FIGURE 2.7
ENVELOPE OF 244 m SUS AT 40 nmi RANGE
FROM CHURCH STROKE II-SITE B

ARL - UT
AS-78-2006
KCF - GA
12-12-78

2.2 Propagation Loss at Site B

(U) Since there were no calibrated SUS propagation results because of equipment problems, we are presenting two types of results here to provide a picture of SUS propagation in the area.

(U) The SUS hydrophones were approximately calibrated by matching the levels received at the SUS hydrophone and the ambient noise hydrophone at the same depth. Only individual SUS multipath arrivals which were not saturated on the ambient noise hydrophone and which had a positive S/N on the shot hydrophone were used. Figures 2.8 through 2.13 show estimated propagation loss as measured from the uncalibrated shot hydrophone channel. On these figures, all results at a given frequency are comparable. For example, the differences between propagation losses from the 91 m and 244 m SUS at 25 Hz, seen in Fig. 2.8, are accurate. The source depth dependence of these results arises from the fact that the area is bottom limited. The 244 m SUS, but not the 91 m SUS, are below the conjugate depth of the sound velocity profile. From the 244 m SUS, bottom refracting (vice only bottom reflecting) propagation is possible; hence, the convergence zone structure in the 244 m source data.

(U) As an estimate of this lower bound of propagation loss, measurements from the saturated AN/cw hydrophone channel are given in Figs. 2.14 through 2.20. An "S" symbol means that some of the multipath arrivals from a shot saturated the recording, while other portions of the signal were properly recorded. Notice that, because of signal saturation, the convergence zone structure--the periodic high signal levels of the 244 m data--seen in Figs. 2.8 through 2.13 is absent in Figs. 2.14 through 2.20.

(U) Table II-2 summarizes the cw projector data from the PAR system at Site B; 67 Hz and 197 Hz tones were broadcast for the entire range of 180 km. At a range of 22 km the source level for both frequencies was increased by approximately 10 dB. At 37 km the source level was again increased by 10 dB and the source depth was decreased from 91 m to 18 m.

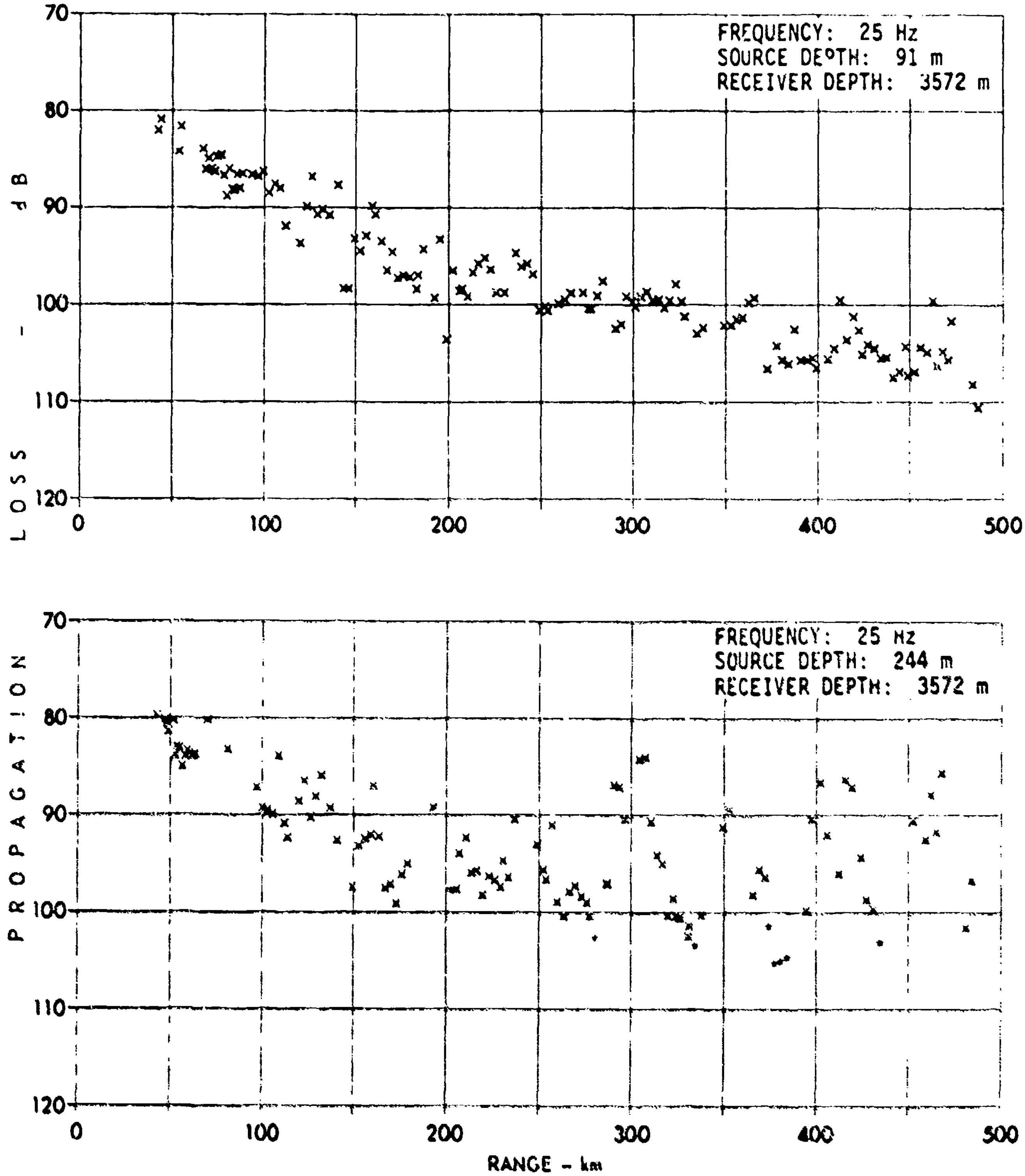

FIGURE 2.8
ESTIMATED PROPAGATION LOSS AT 25 Hz
CHURCH STROKE II-SITE B (U)
91 m AND 244 m SUS

ARL UT
AS-78-1955
KCF - GA
12-12-78

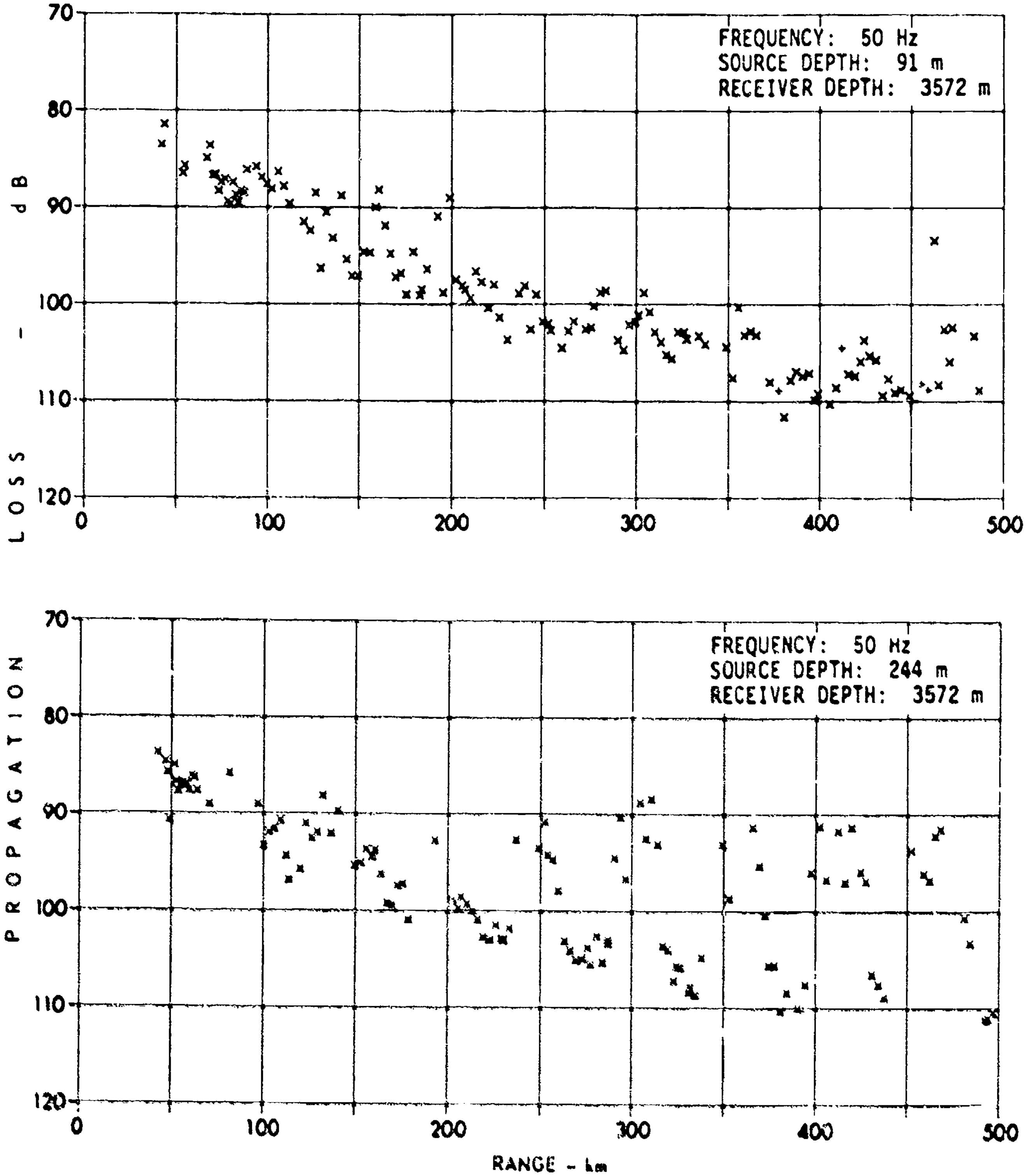

FIGURE 2.9
ESTIMATED PROPAGATION LOSS AT 50 Hz
CHURCH STROKE II-SITE B (U)
91 m AND 244 m SUS

ARL UT
AS-78-1956
KCF-GA
12-12-78

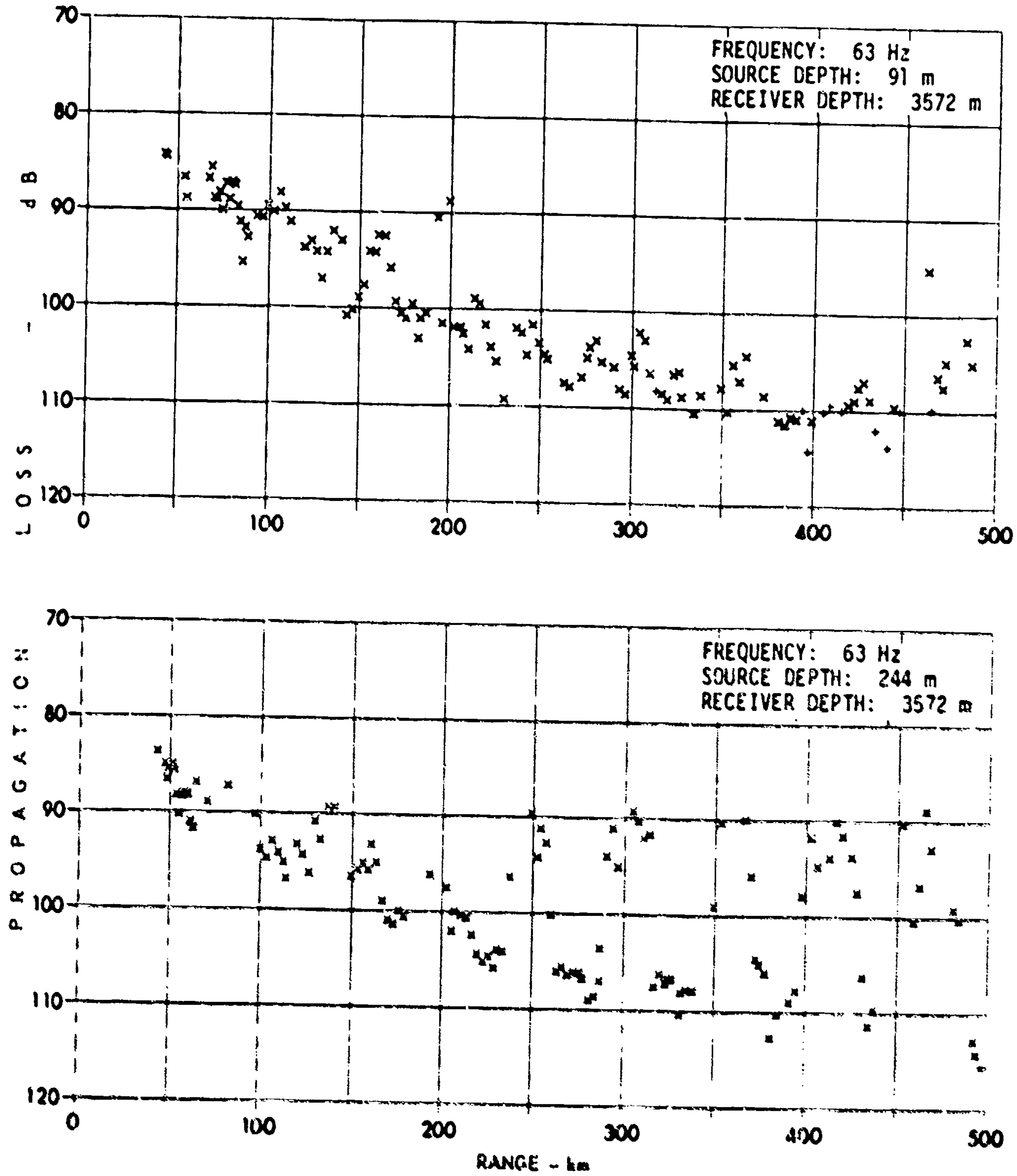

FIGURE 2.10
ESTIMATED PROPAGATION LOSS AT 63 Hz
CHURCH STROKE II-SITE B (U)
91 m AND 244 m SUS

ARL UT
AS-78-1957
KCF-GA
12-12-78

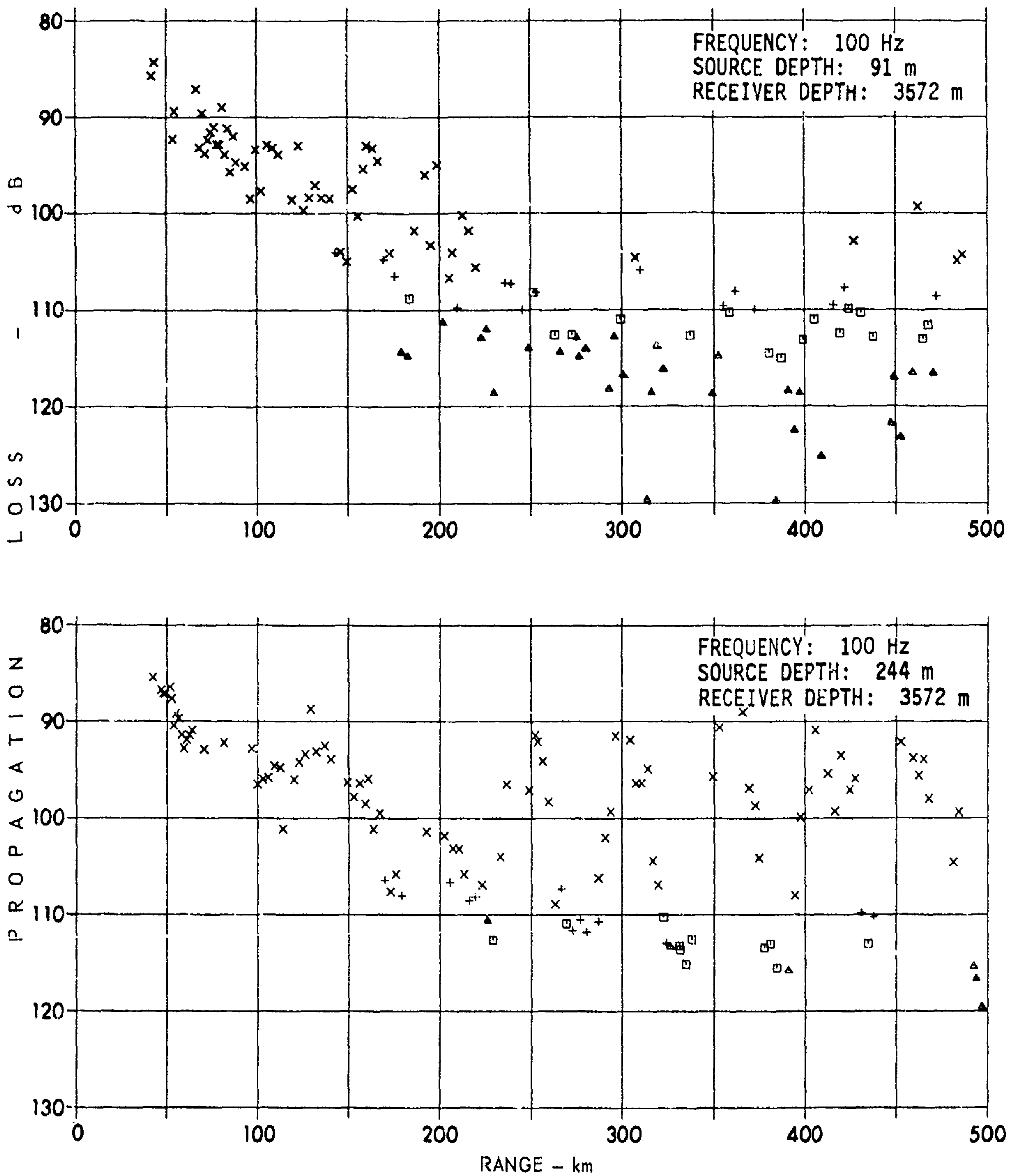

FIGURE 2.11
ESTIMATED PROPAGATION LOSS AT 100 Hz
CHURCH STROKE II-SITE B (U)
91 m AND 244 m SUS

ARL:UT
AS-78-1958
KCF-GA
12-12-78

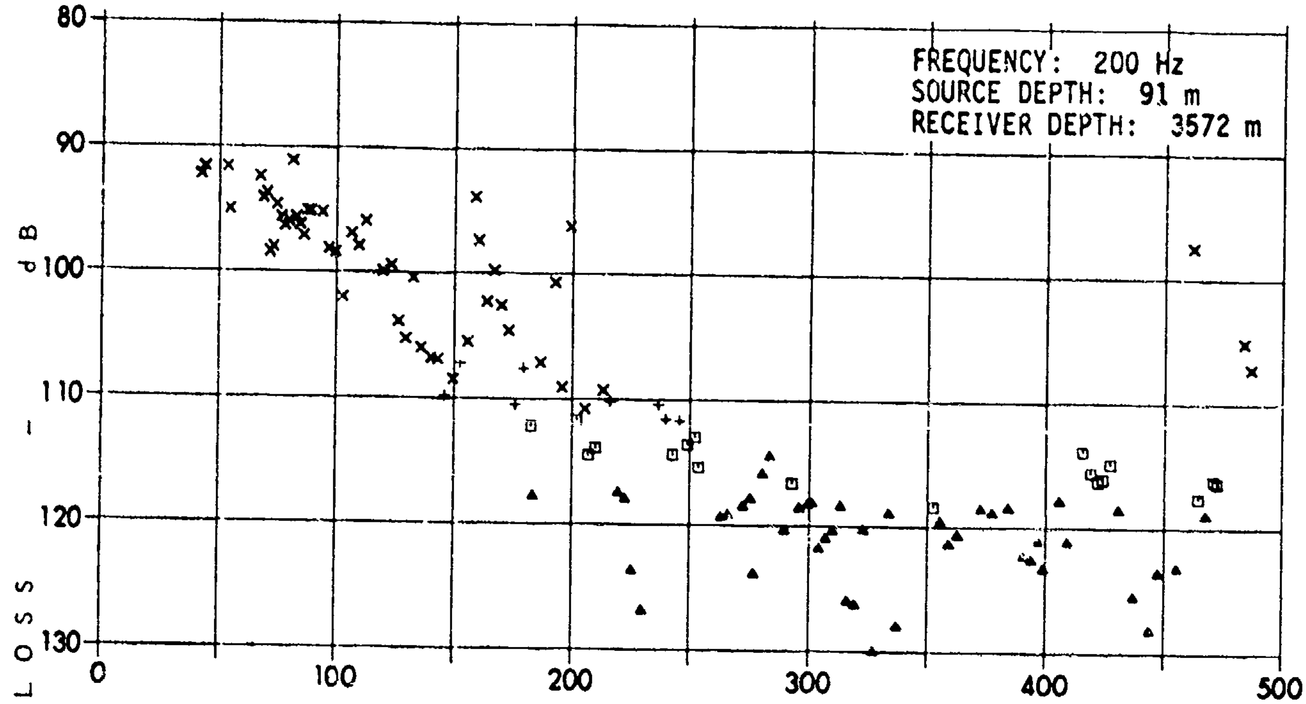

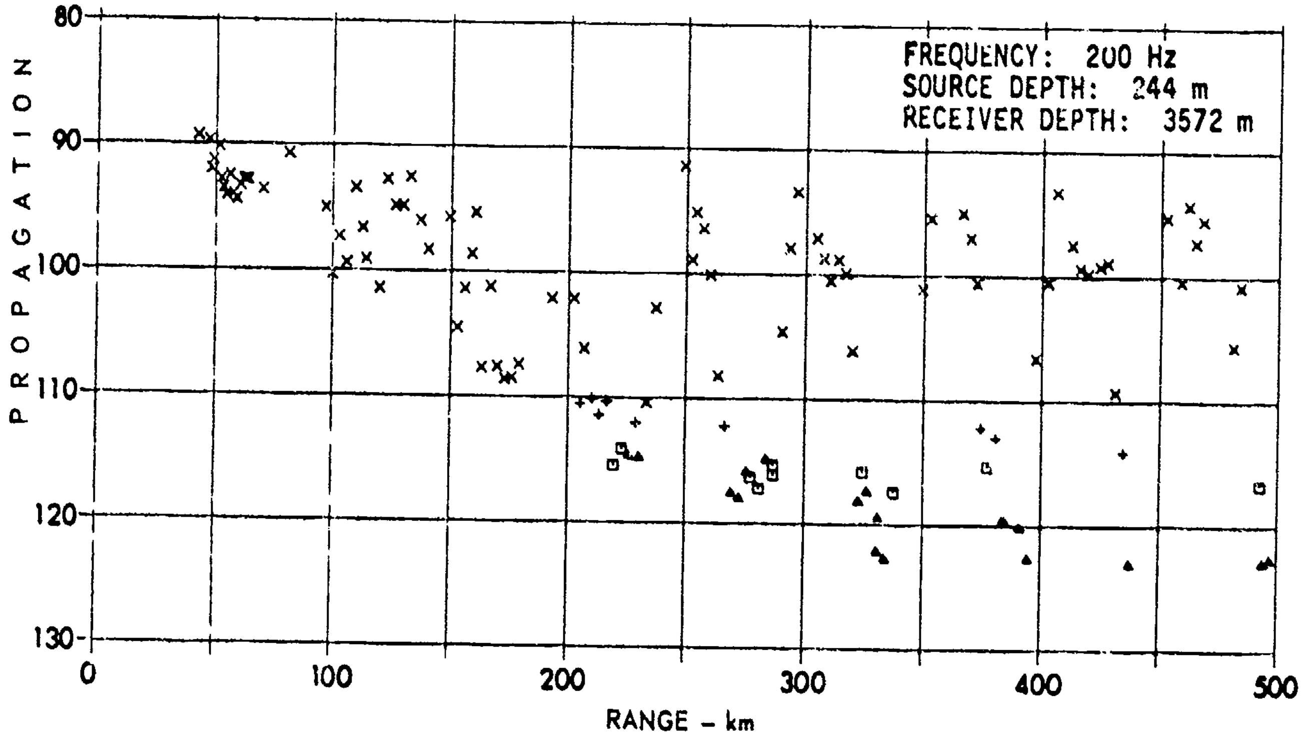

FIGURE 2.12
ESTIMATED PROPAGATION LOSS AT 200 Hz
CHURCH STROKE II-SITE B (U)
91 m AND 244 m SUS

ARL:UT
AS-78-1959
KCF - GA
12-12-78

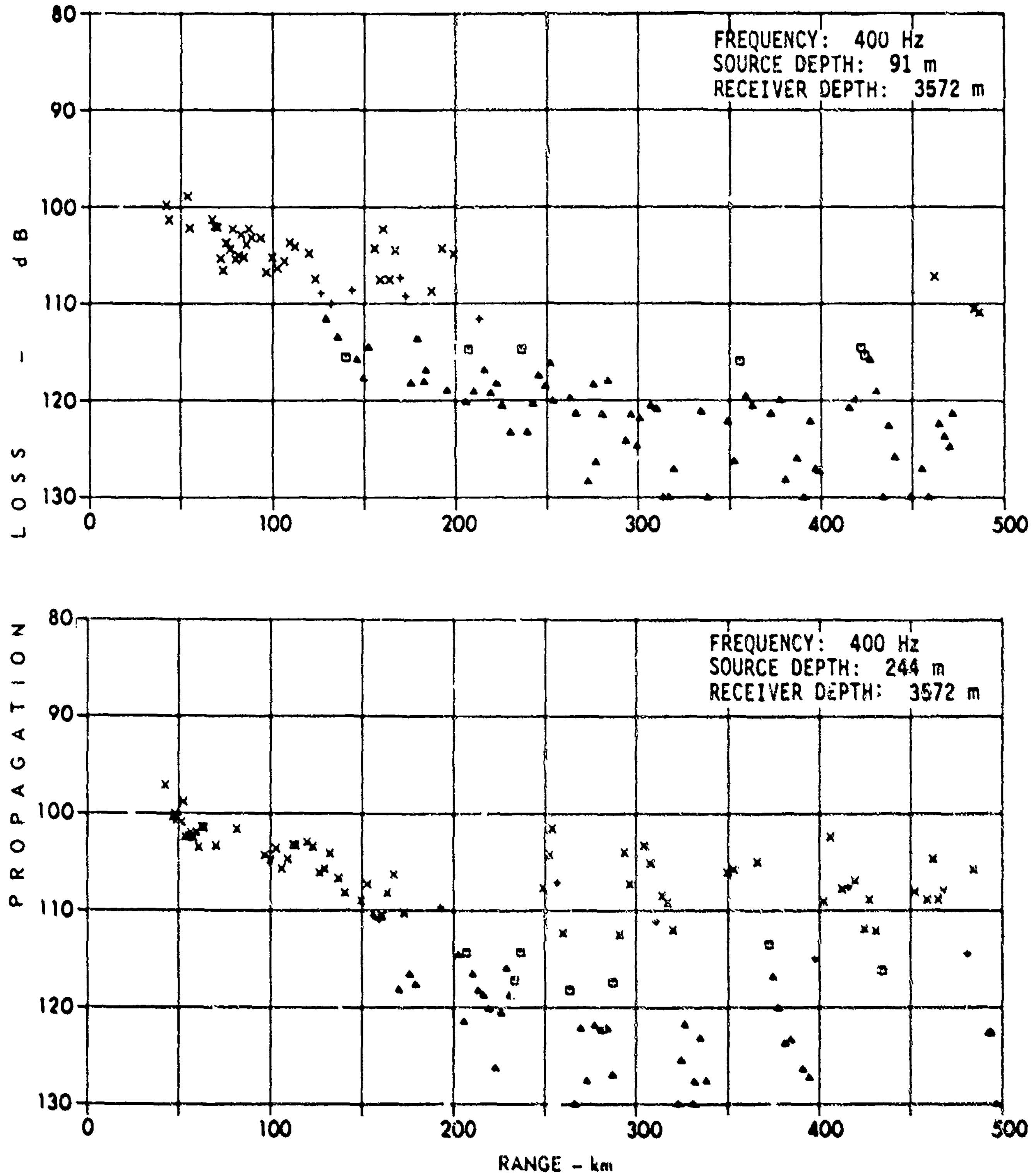

FIGURE 2.13
ESTIMATED PROPAGATION AT 400 Hz
CHURCH STROKE II-SITE B (U)
91 m AND 244 m SUS

ARL:UT
AS-78-1960
KCF - GA
12-12-78

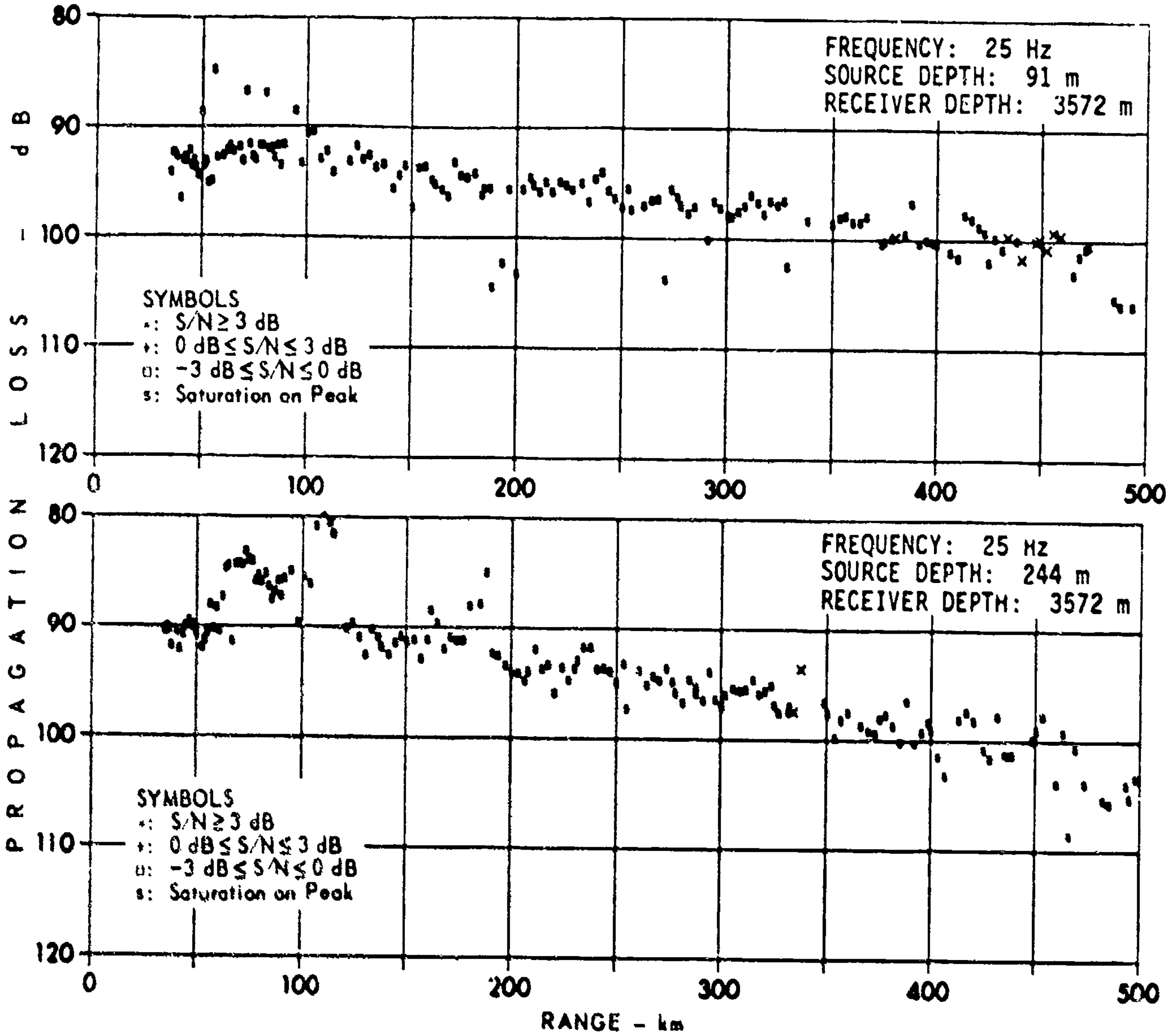

FIGURE 2.14
PROPAGATION LOSS AT 25 Hz* (U)
CHURCH STROKE SITE B
91 m AND 244 m SUS

*SATURATED - SEE TEXT

ARL UT
AS-78-1848
KCF - GA
12 - 4 - 78

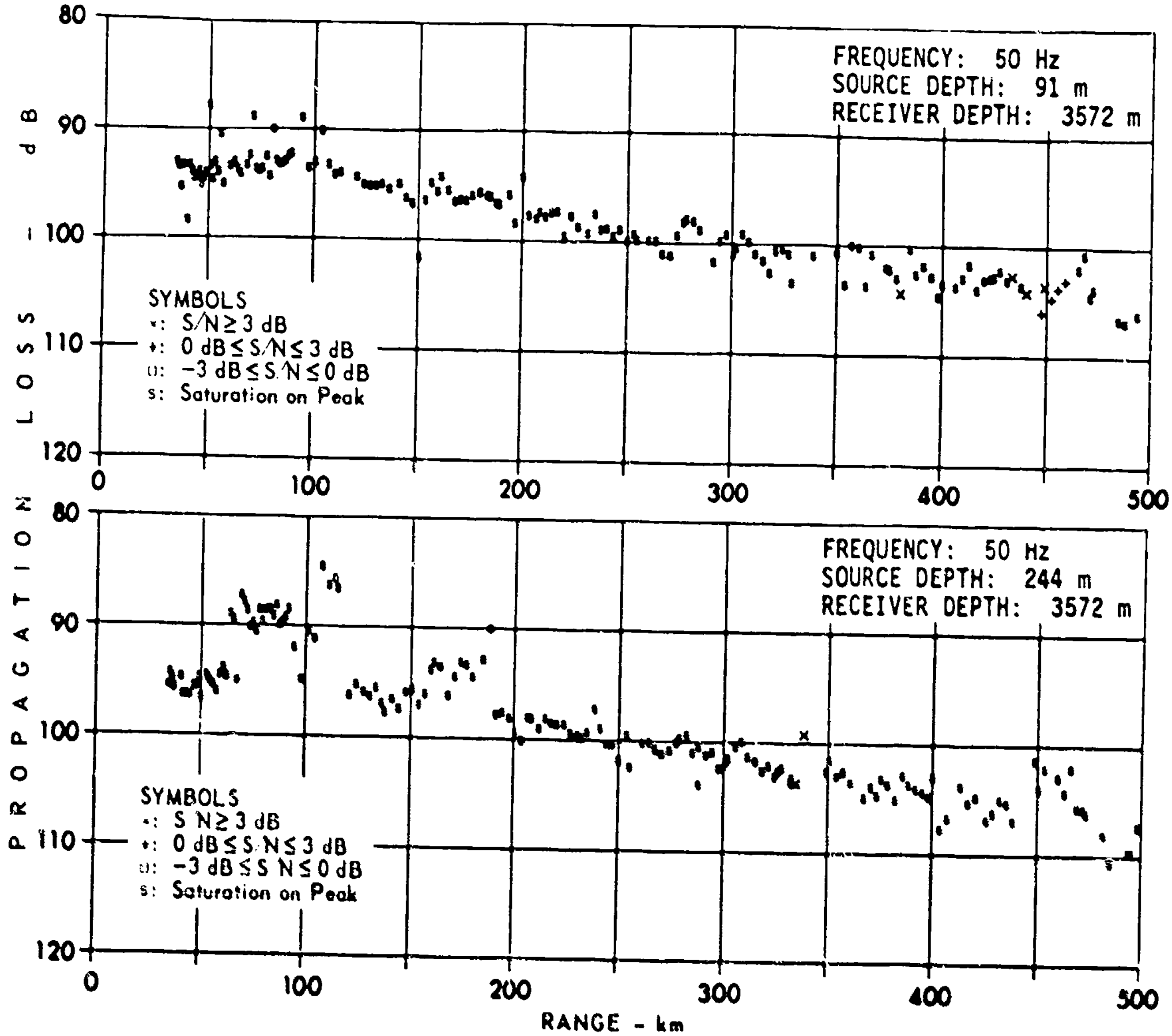

FIGURE 2.15
PROPAGATION LOSS AT 50 Hz* (U)
CHURCH STROKE SITE B
91 m AND 244 m SUS

*SATURATED - SEE TEXT

ARL UT
AS-78-1849
KCF - GA
12 - 4 - 78

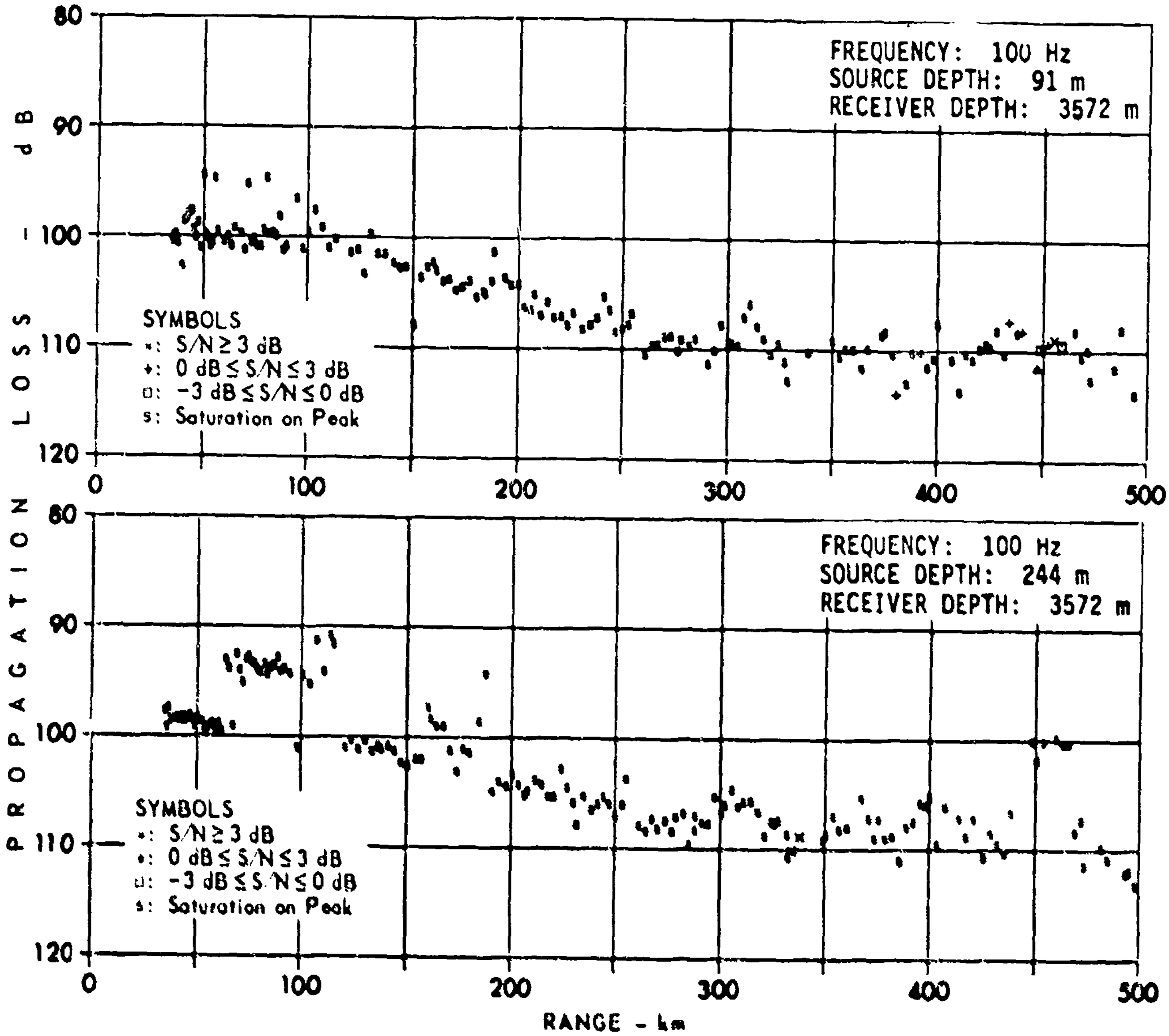

FIGURE 2.16
PROPAGATION LOSS AT 100 Hz* (U)
CHURCH STROKE SITE B
91 m AND 244 m SUS

*SATURATED - SEE TEXT

ARL UT
AS-78-1850
KCP - GA
12 - 4 - 78

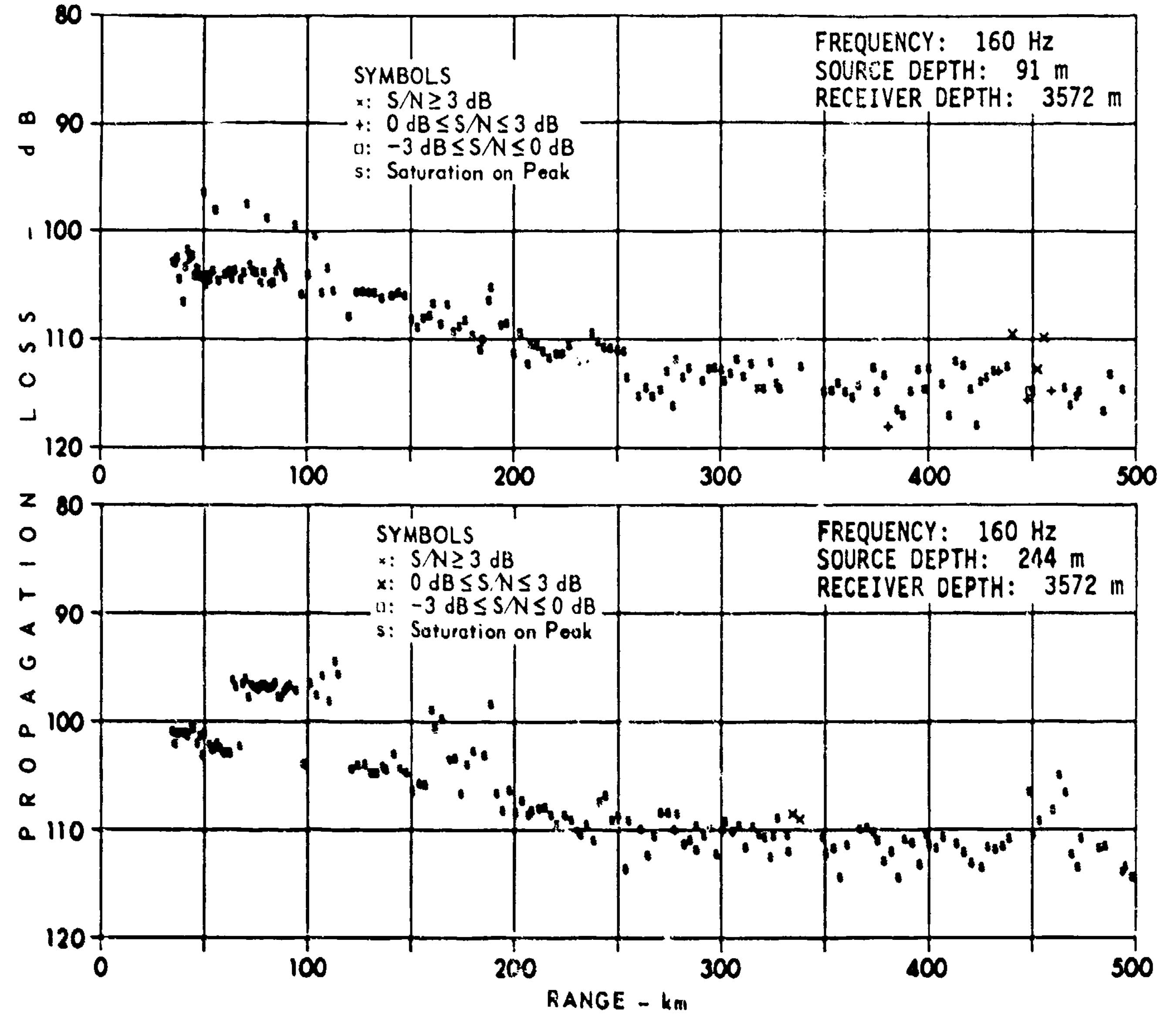

FIGURE 2.17
PROPAGATION LOSS AT 160 Hz* (U)
CHURCH STROKE SITE B
91 m AND 244 m SUS

*SATURATED – SEE TEXT

ARL:UT
AS-78-1851
KCF - GA
12-4-78

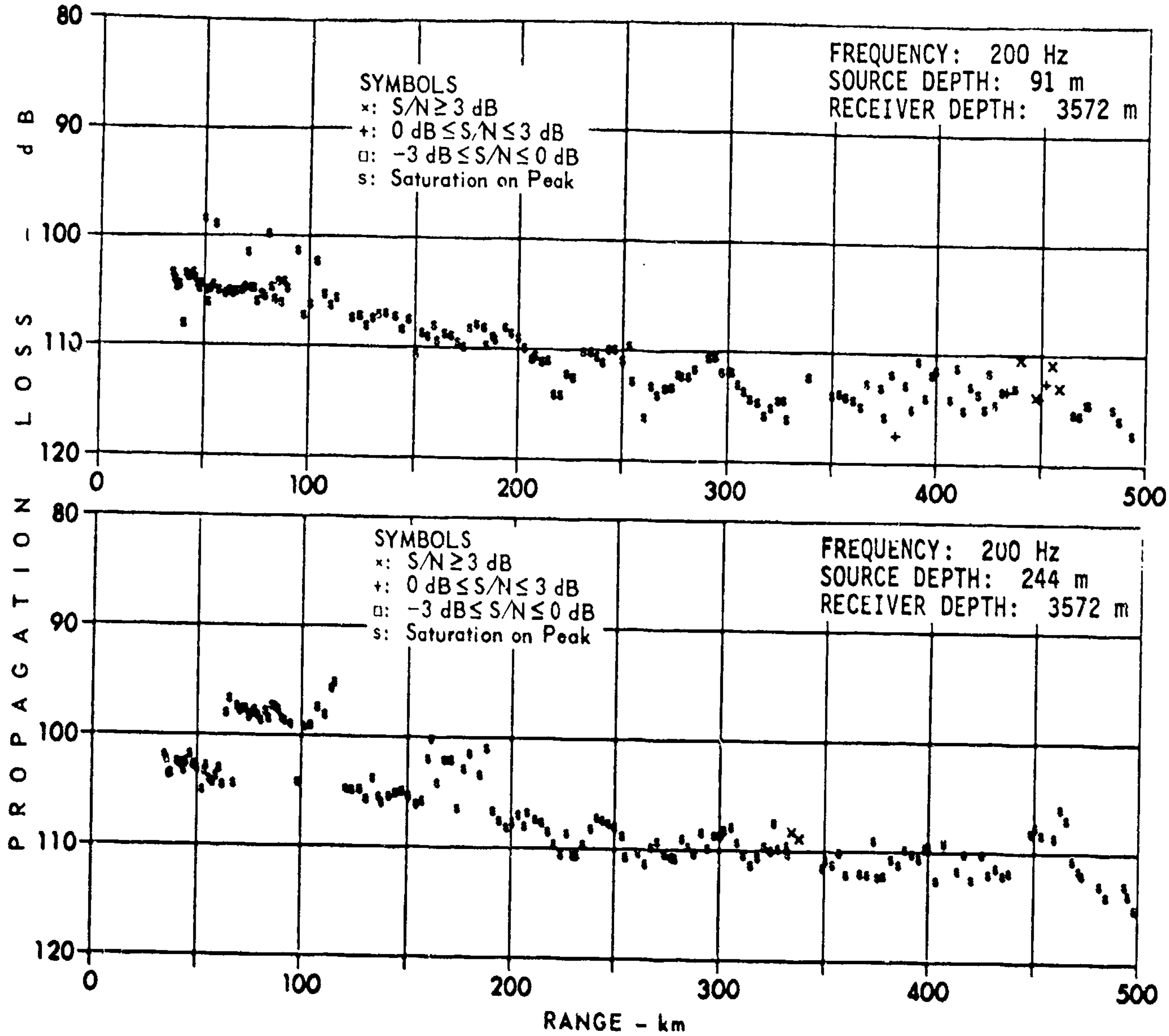

FIGURE 2.18
PROPAGATION LOSS AT 200 Hz* (U)
CHURCH STROKE SITE B
91 m AND 244 m SUS

*SATURATED – SEE TEXT

ARL:UT
AS-78-1852
KCF - GA
12 - 4 - 78

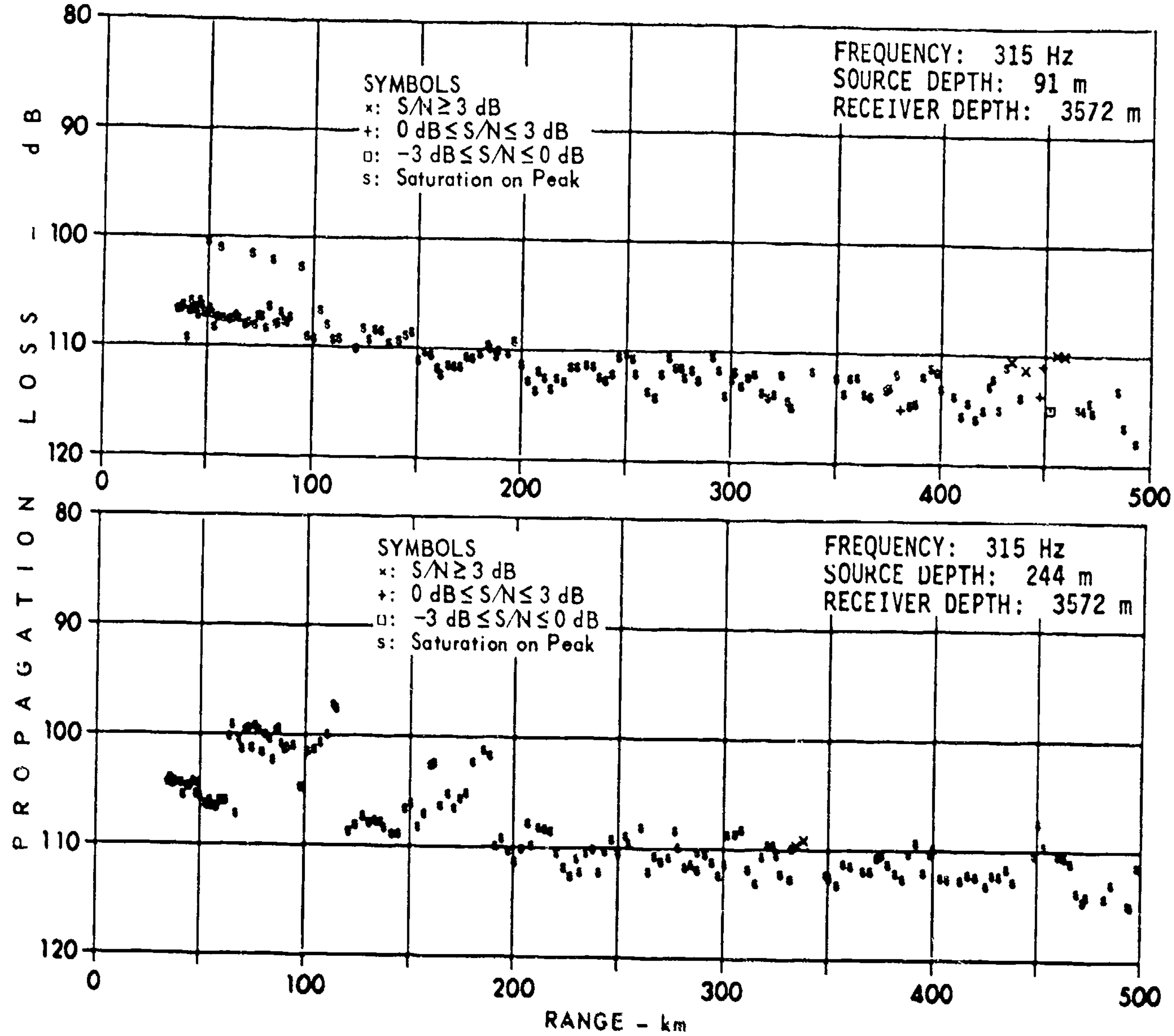

FIGURE 2.19
PROPAGATION LOSS AT 315 Hz* (U)
CHURCH STROKE SITE B
91 m AND 244 m SUS

*SATURATED - SEE TEXT

ARL:UT
AS-78-1853
KCF - GA
12 - 4 - 78

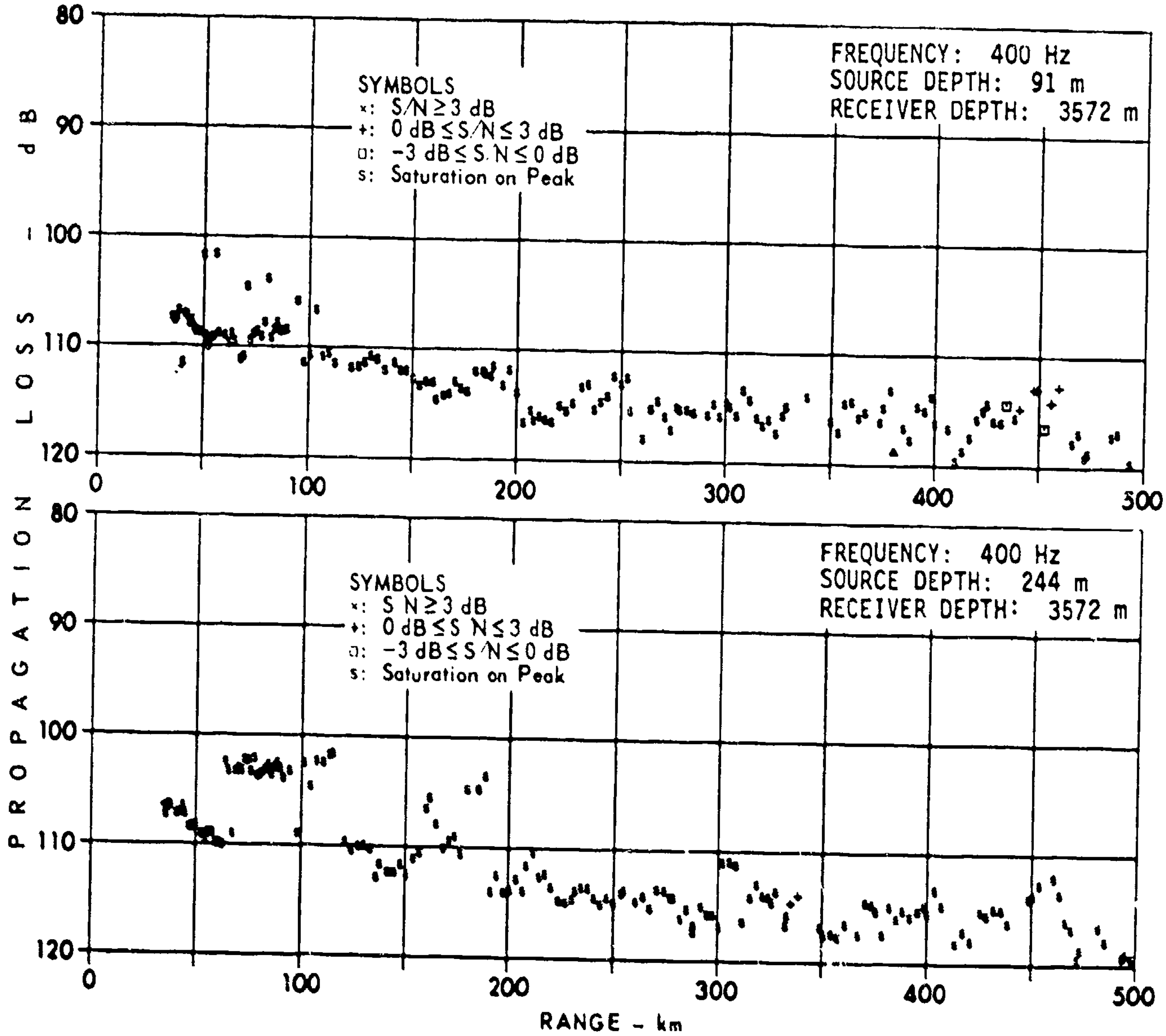

FIGURE 2.20
PROPAGATION LOSS AT 400 Hz* (U)
CHURCH STROKE SITE B
91 m AND 244 m SUS

*SATURATED – SEE TEXT

ARL UT
AS-78-1854
KCF - GA
12 - 4 - 78

(C)

TABLE II-2

CHURCH STROKE II - Site B

Projector Tow Summary (U)

Range Interval (km)	Source Depth (m)	Source Level (dB) 67 Hz	197 Hz	Propagation Loss Figure Number
0 - 22	91	155	155	2.21
22 - 36	91	165	165	2.21
37 - 180	18	174	172	2.22

(U) Propagation loss for the 91 m source is presented in Fig. 2.21; propagation loss for the 18 m source is presented in Fig. 2.22.

(U) Signal excess and ambient noise level (in an adjacent frequency band) during the projector tows at Site B are presented in Figs. 2.23 through 2.26. Both the 91 m and 18 m source depths are included in these figures.

2.3 Ambient Noise

(C) Data were selected from PAR channel 4, from a hydrophone 30 m above the bottom, for the time periods 322/0000 through 324/0600. Selected 1/10 octave band time series for that channel are shown in Fig. 2.27. The merchant ship JJCD was identified during this time and will be discussed in Chapter V on ship signatures. Percentile spectral levels for this period are shown in Fig. 2.28; at 50 Hz the median level is near 74 dB and the minimum level was found to be 63 dB. During this period the dynamic range in level covered 40 dB across most of the spectrum. Included in Fig. 2.28 is the system electronic noise spectrum, which can be used to assess where the data are corrupted by electronic noise.

(C) Data from the time period 330/0000 through 330/1200 was selected for three channels from the ACODAC to study depth dependence of the noise. PAR data during the same period were also processed to crosscheck calibration between the two systems. The 1/10 octave band time series followed by their respective percentile spectral plots are shown in Figs. 2.29 through 2.36. These data show a general decrease in level with time over the 12 h period for all frequencies. The decreasing level with time corresponds to a departing unknown ship and decreasing wind speed. The spectral levels range over 15 dB for the receiver 1000 m above the bottom (ACODAC channel 4) and 25 dB for the near-bottom receivers (PAR channel 4, 30 m above bottom, and ACODAC channel 14, on the bottom). The most significant observation is that the noise decreases in level with depth over the last 1000 m above the bottom, as shown in Figs. 2.37 and 2.38. The change in level is 7 or 8 dB, somewhat of a surprise because Site B is bottom limited. A second surprise is the spectral level

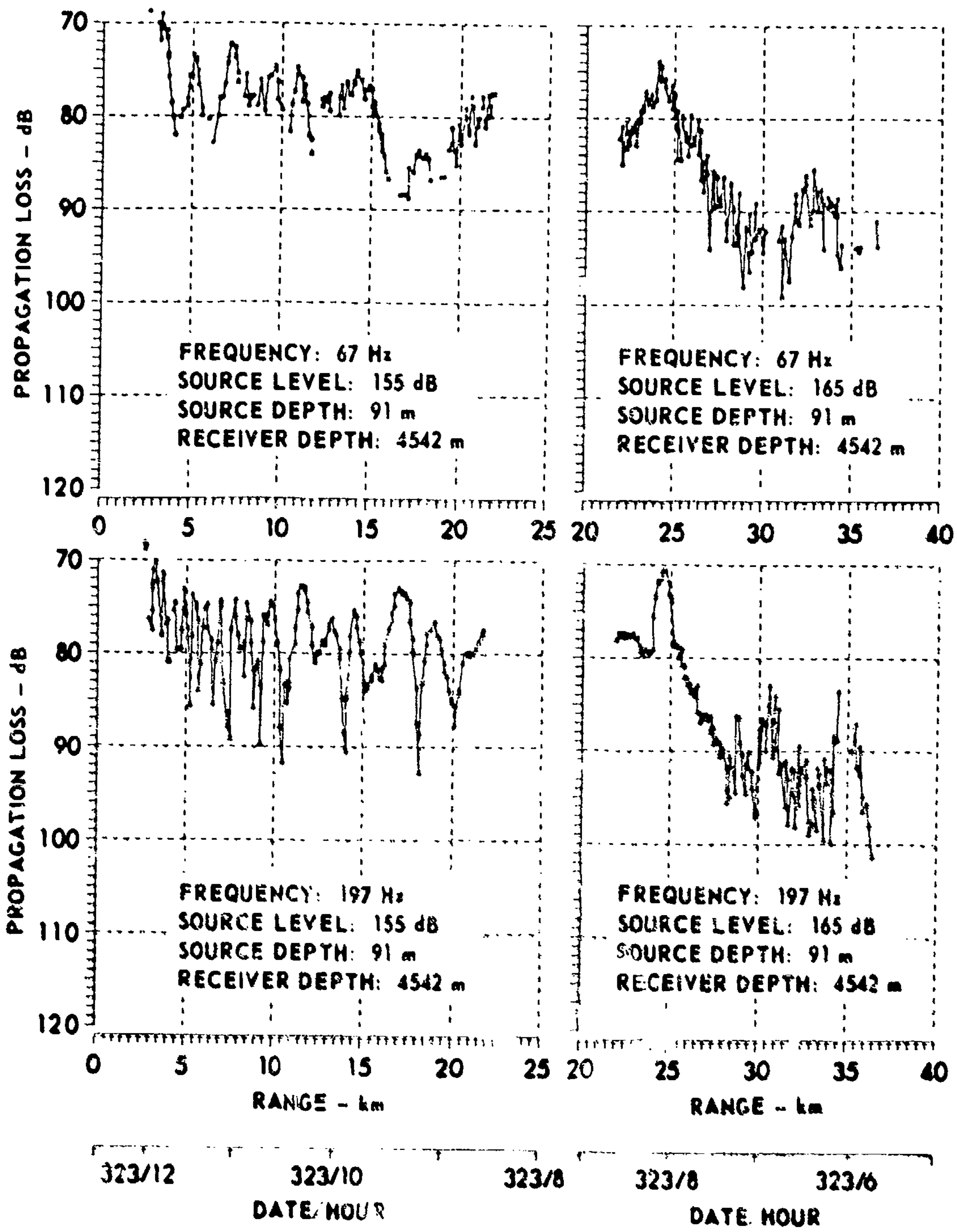

FIGURE 2.21
PROPAGATION LOSS TO 4542 m RECEIVER
CHURCH STROKE II SITE B PAR (U)

ARL UT
AS-79-836
KCF - GA
4 - 30 - 79

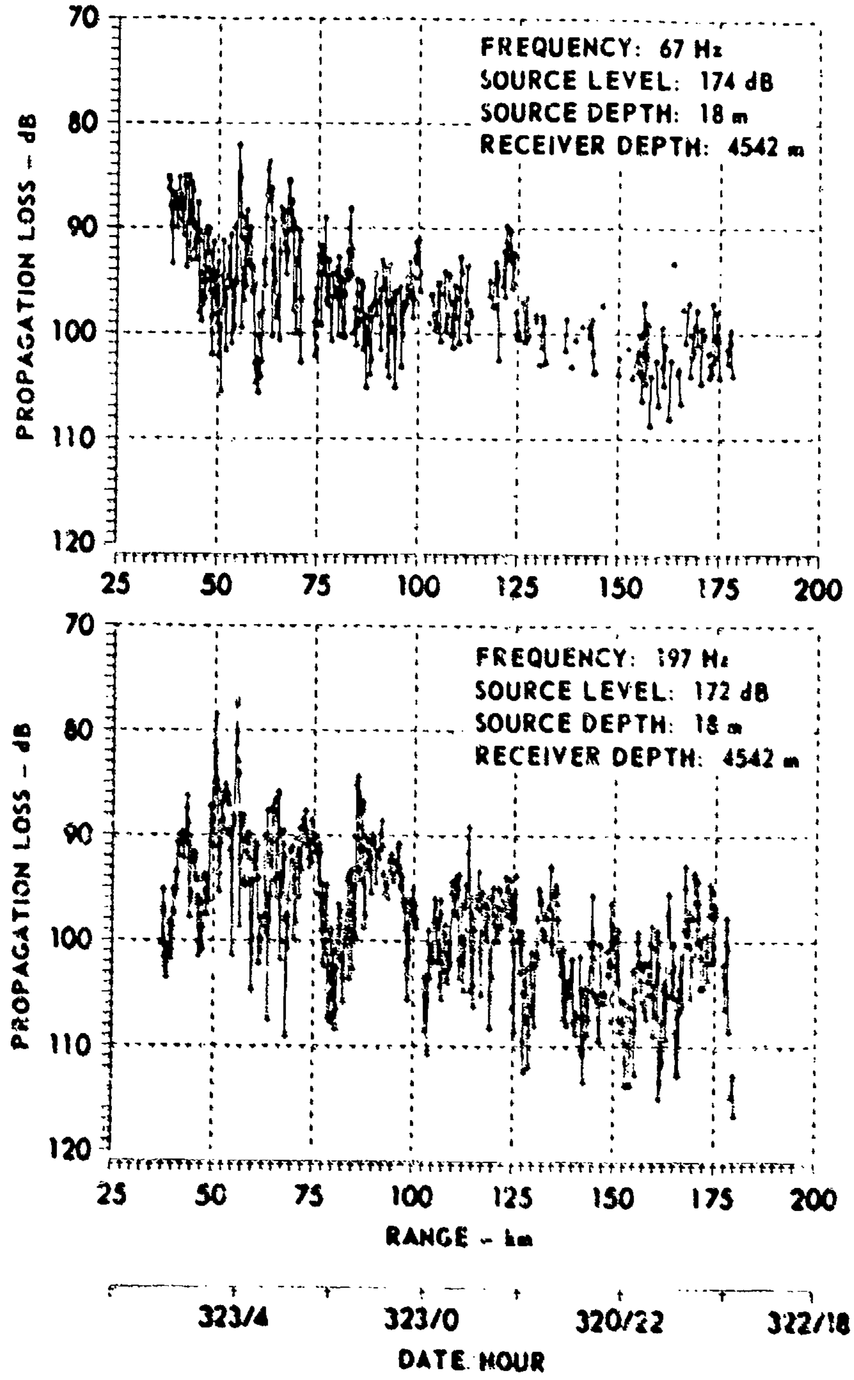

FIGURE 2.22
PROPAGATION LOSS TO 4542 m RECEIVER
CHURCH STROKE II SITE B PAR (U)

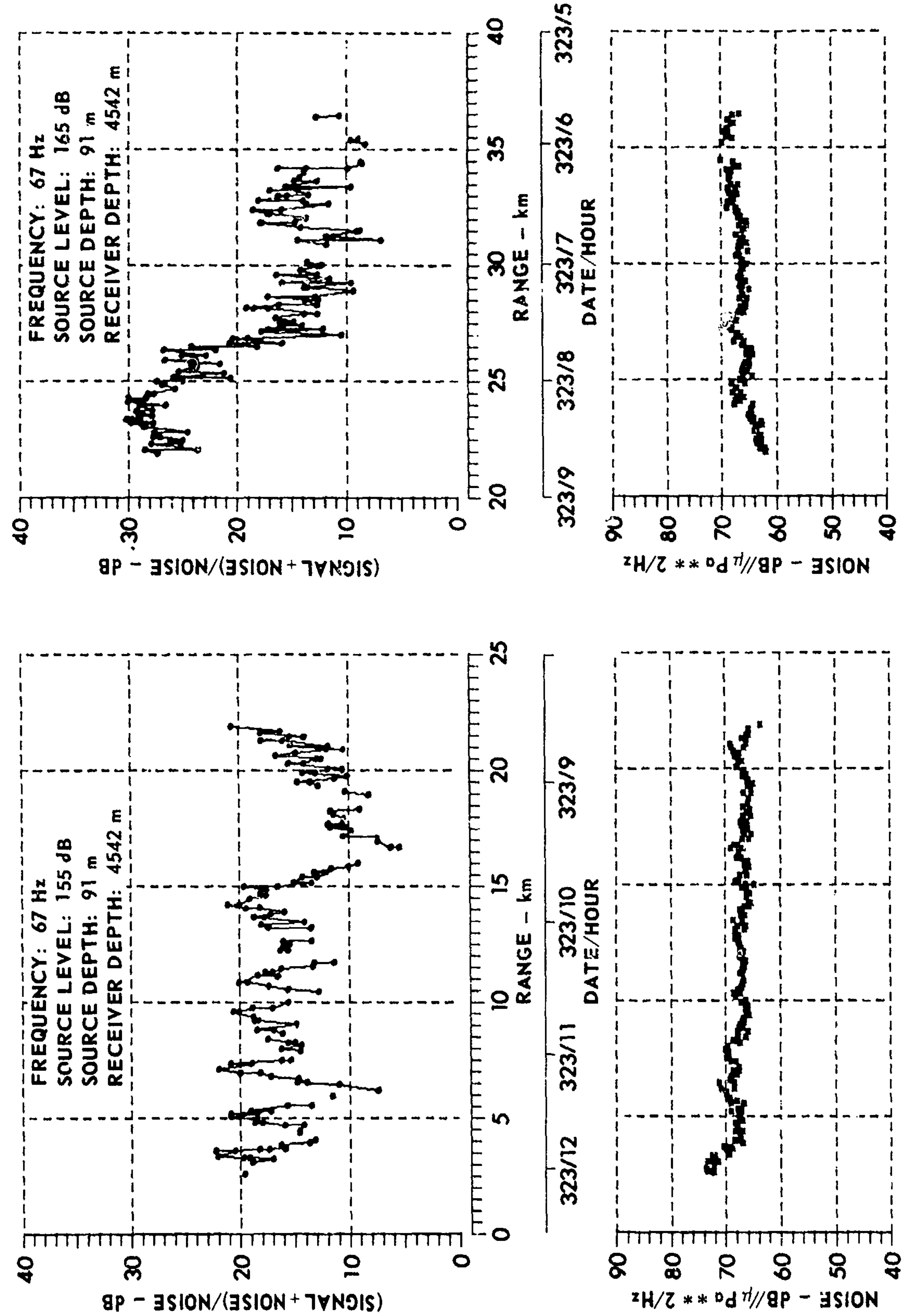

FIGURE 2.23
NOISE AND SIGNAL EXCESS FOR 4542 m RECEIVER
AT 67 Hz CHURCH STROKE II SITE B PAR (U)
SOURCE DEPTH: 91 m

ARL:UT
AS-79-861
KCF-GA
4-30-79

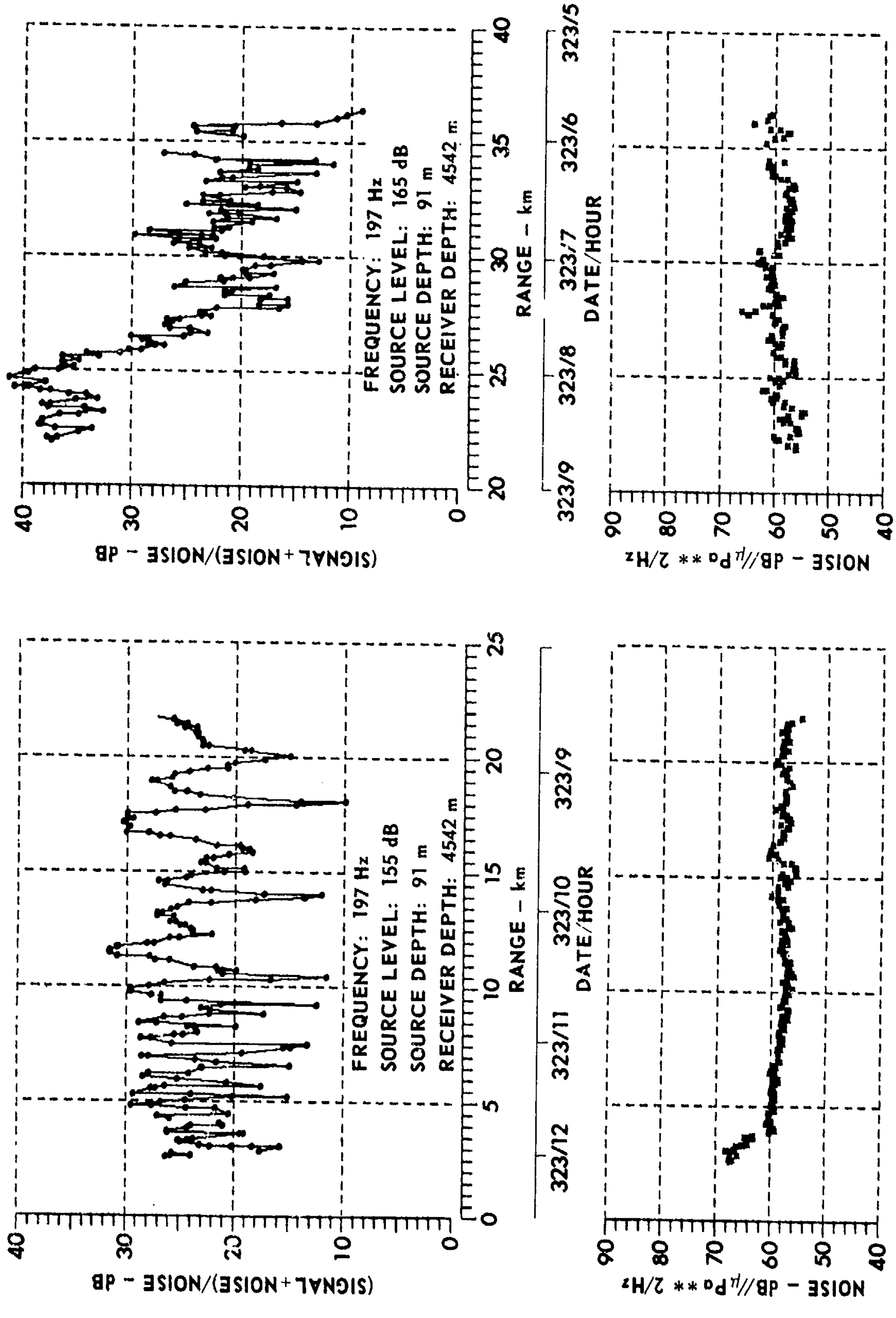

FIGURE 2.24
NOISE AND SIGNAL EXCESS FOR 4542 m RECEIVER
AT 197 Hz CHURCH STROKE II SITE B PAR (U)
SOURCE DEPTH: 91 m

ARL:UT
AS-79-862
KCF - GA
4 - 30 - 79

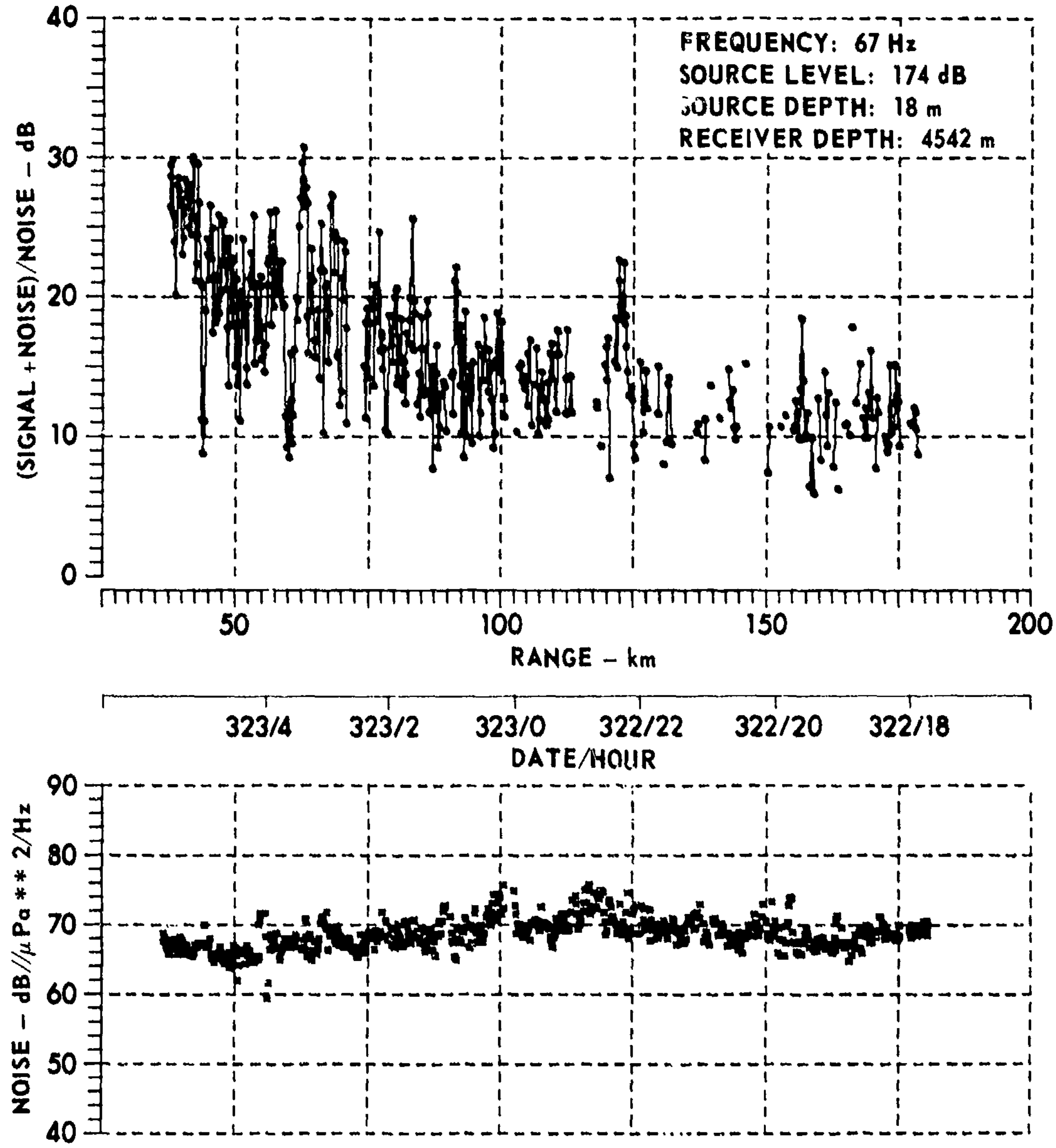

FIGURE 2.25
NOISE AND SIGNAL EXCESS FOR 4542 m RECEIVER
AT 67 Hz CHURCH STROKE II SITE B PAR (U)
SOURCE DEPTH: 18 m

ARL:UT
AS-79-857
KCF - GA
4 - 30 - 79

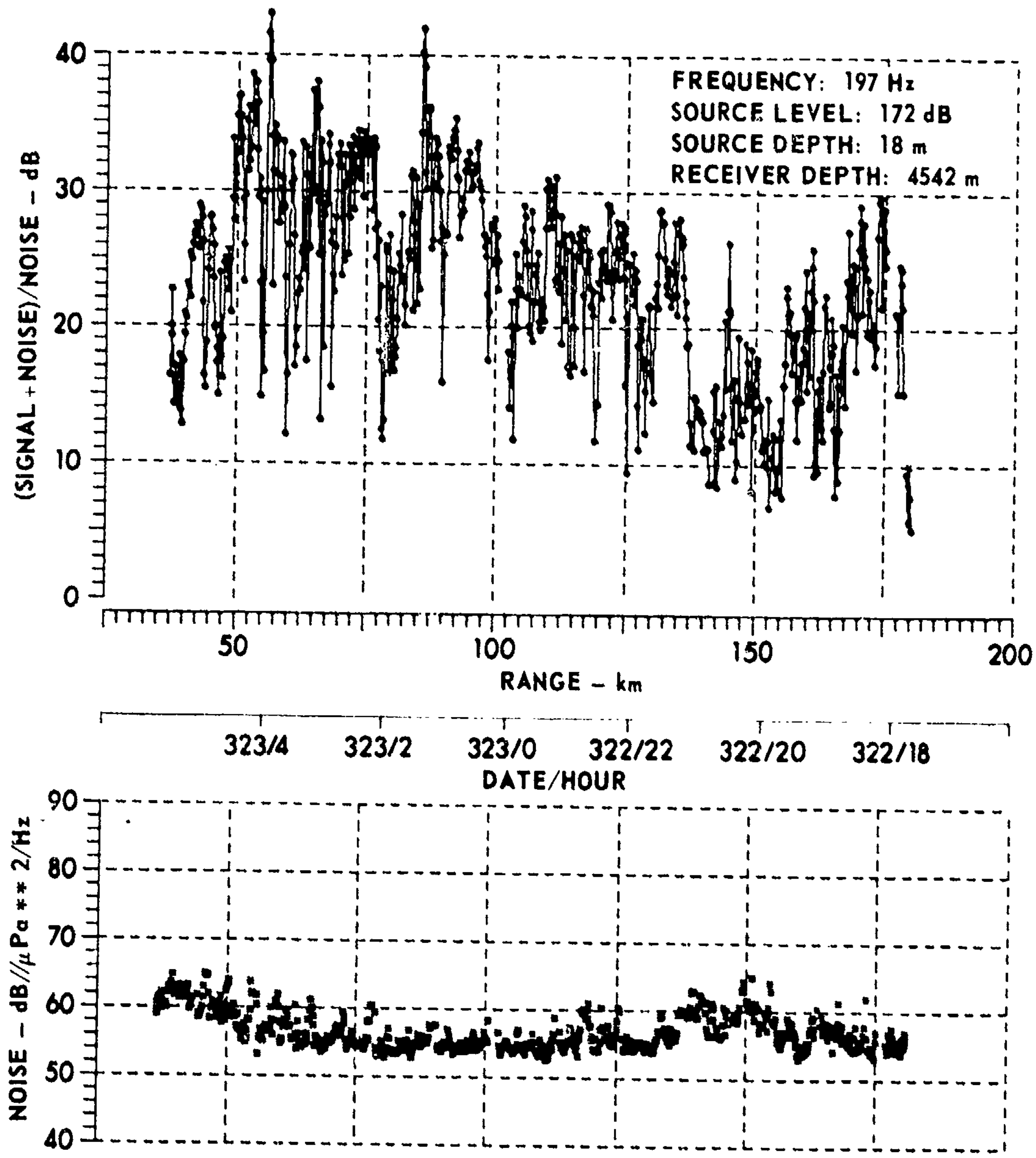

FIGURE 2.26
NOISE AND SIGNAL EXCESS FOR 4542 m RECEIVER
AT 197 Hz CHURCH STROKE II SITE B PAR (U)
SOURCE DEPTH: 18 m

ARL:UT
AS-79-858
KCF-GA
4-30-79

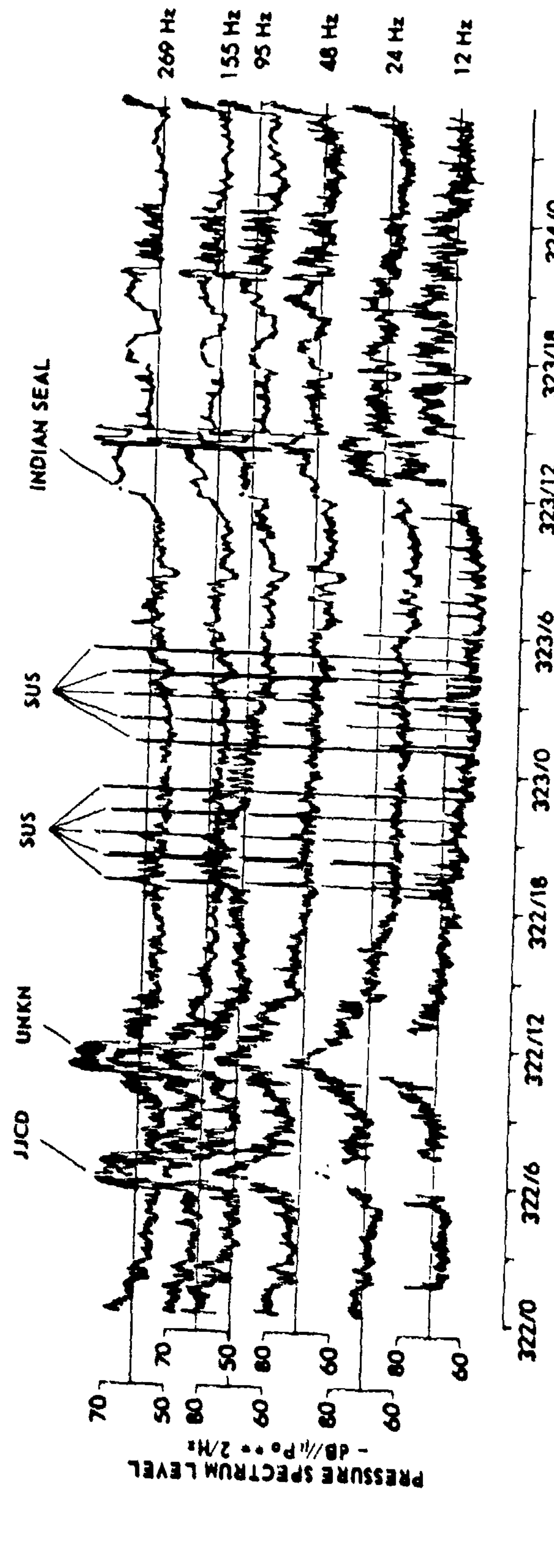

FIGURE 2.27
AMBIENT NOISE TIME SERIES – 4542 m RECEIVER
CHURCH STROKE II SITE B PAR (U)

ARL UT
AS-79-865
KCF - GA
5 - 1 - 79

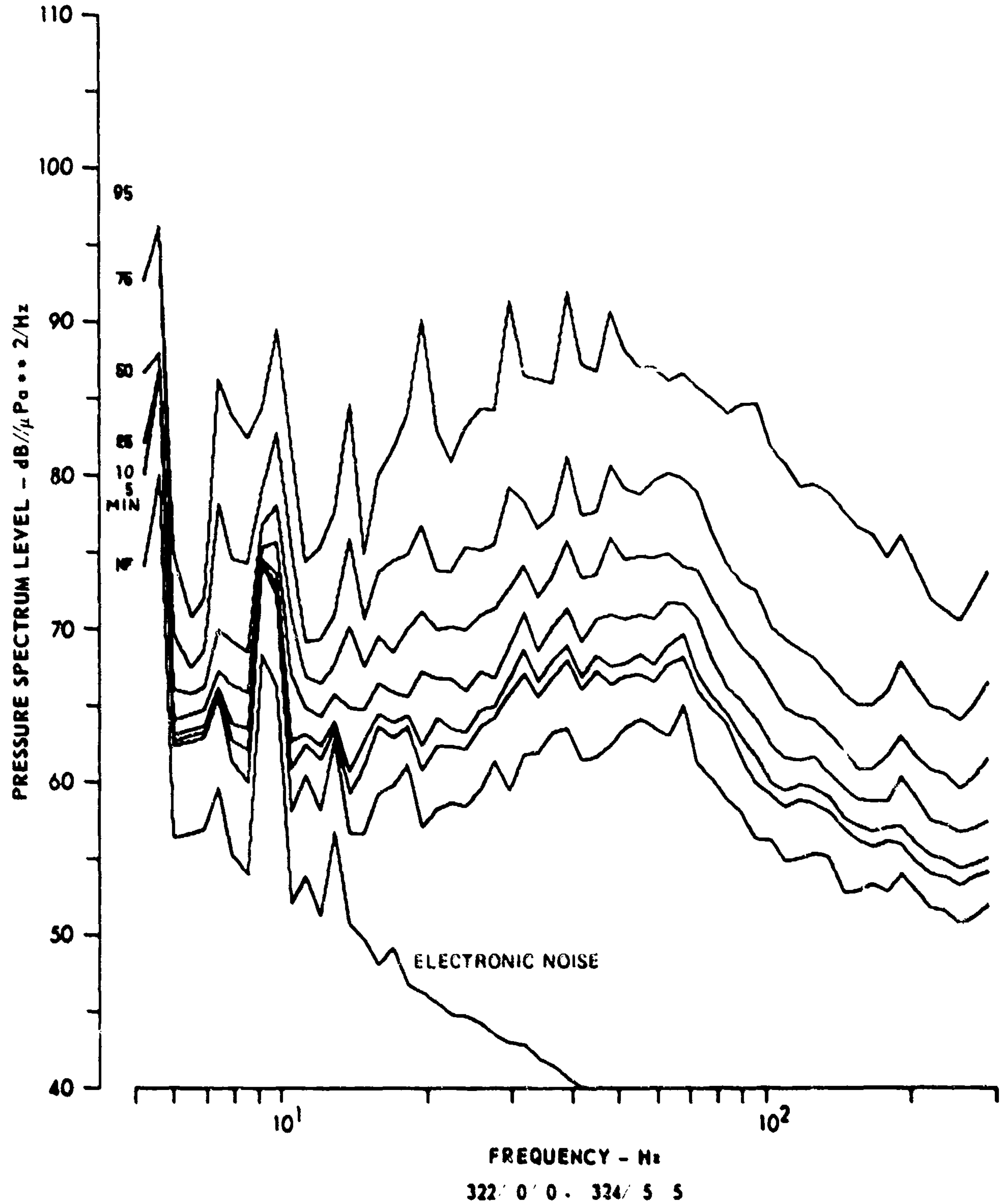

322/ 0/ 0 - 324/ 5 5

FIGURE 2.28
PERCENTILE SPECTRAL LEVELS FOR CHURCH STROKE II SITE B PAR (U)

CHANNEL 4 4542 m

ARL UT
AS-79-972
KCF - GA
5 - 8 - 79

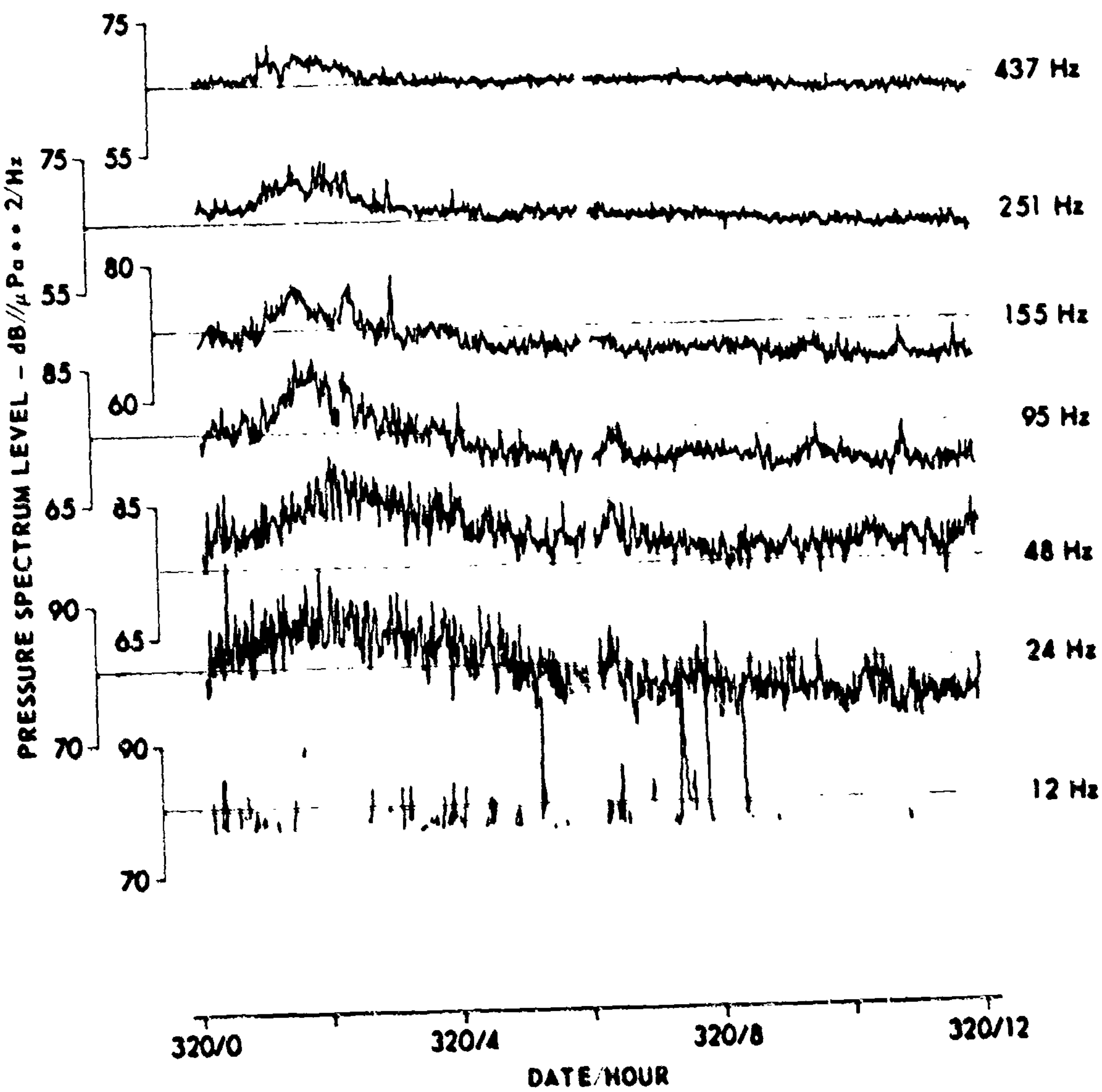

FIGURE 2.29
AMBIENT NOISE TIME SERIES CHURCH STROKE II SITE B-3572 m RECEIVER (U)

ARL UT
AS-79-984
KCF-GA
5-8-79

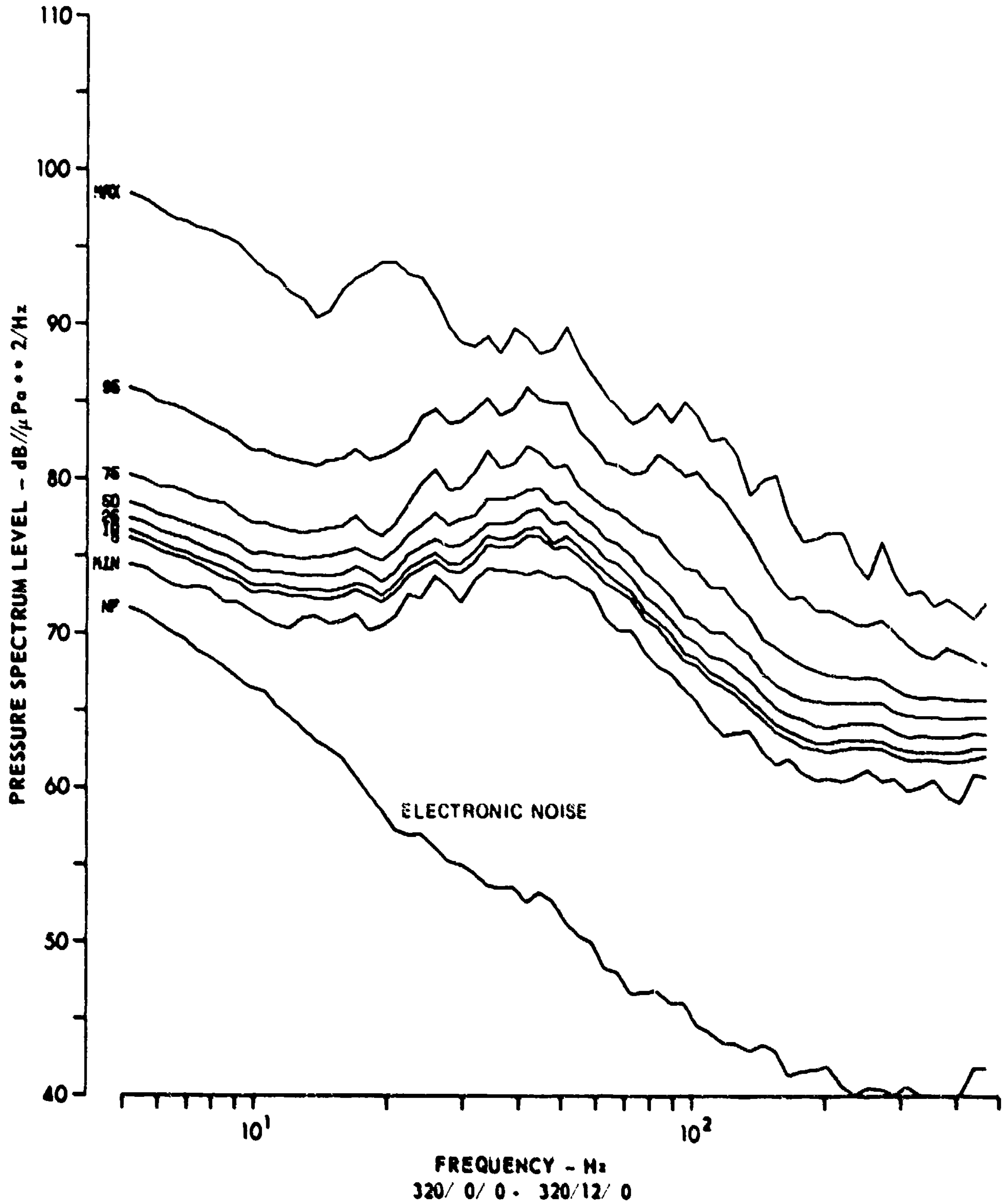

FIGURE 2.30
AMBIENT NOISE
PERCENTILE SPECTRUM LEVELS
CHURCH STROKE II SITE B-3572 m RECEIVER (U)

ARL UT
AS-79-1368
KCF - GA
7-16-79

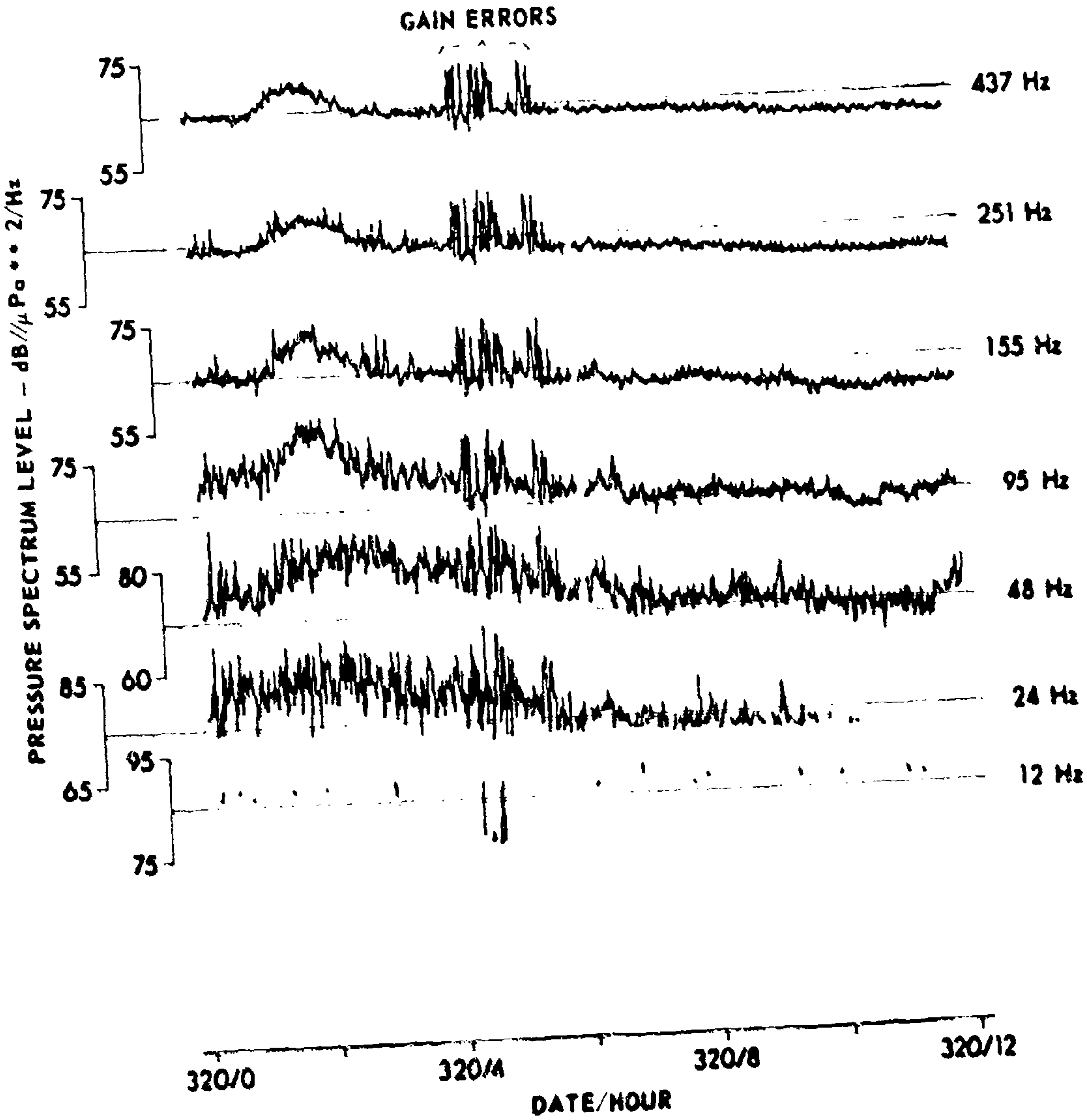

FIGURE 2.31
AMBIENT NOISE TIME SERIES CHURCH STROKE II SITE B - 4272 m RECEIVER (U)

ARL UT
AS-79-983
KCF - GA
5 - 8 - 79

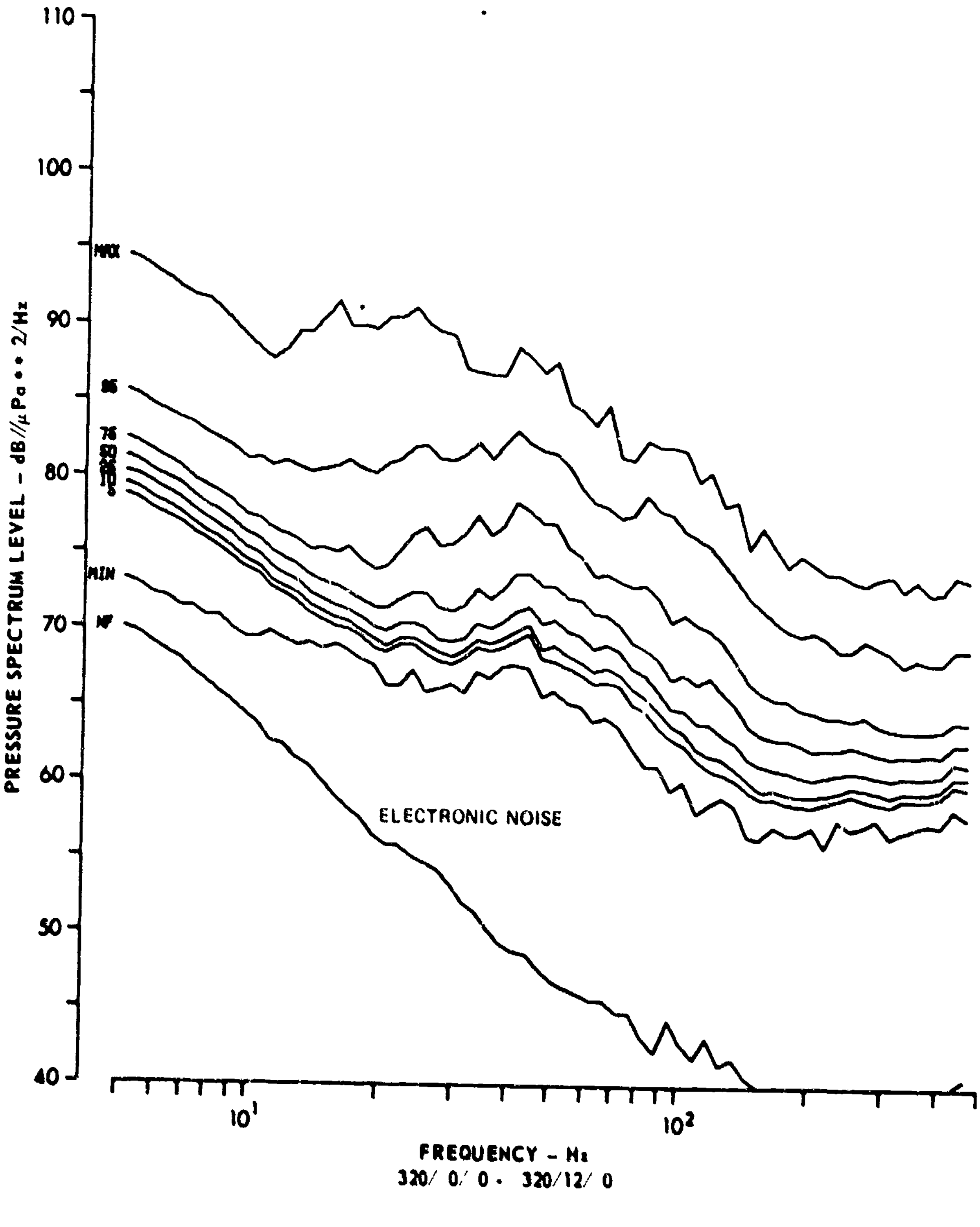

FIGURE 2.32
AMBIENT NOISE
PERCENTILE SPECTRUM LEVELS
CHURCH STROKE II SITE B-4272 m RECEIVER (U)

ARL UT
AS-79-1369
KCF - GA
7-16-79

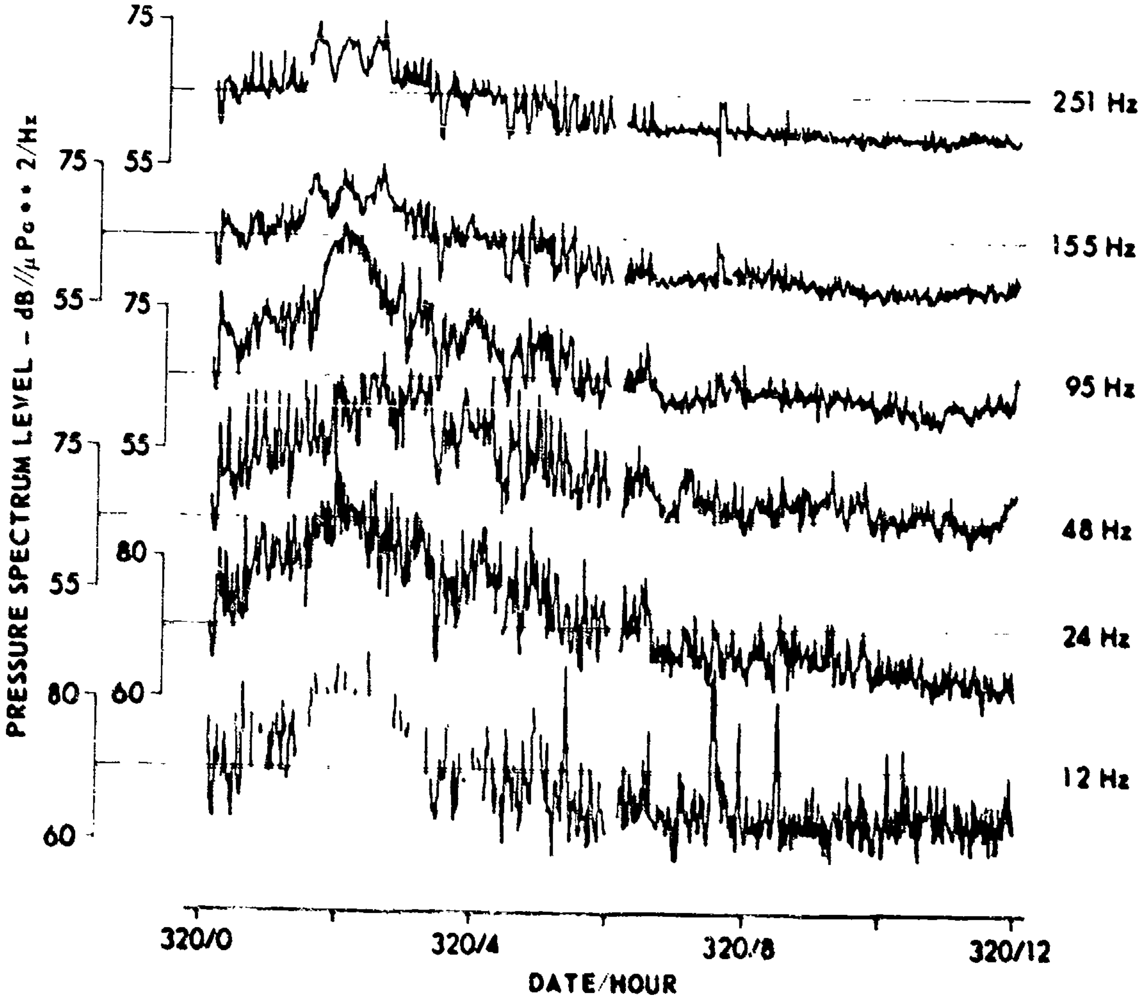

FIGURE 2.33
AMBIENT NOISE TIME SERIES CHURCH STROKE II
SITE B PAR-4542 m RECEIVER (U)

ARL UT
AS-79-986
KCF-GA
5-8-79

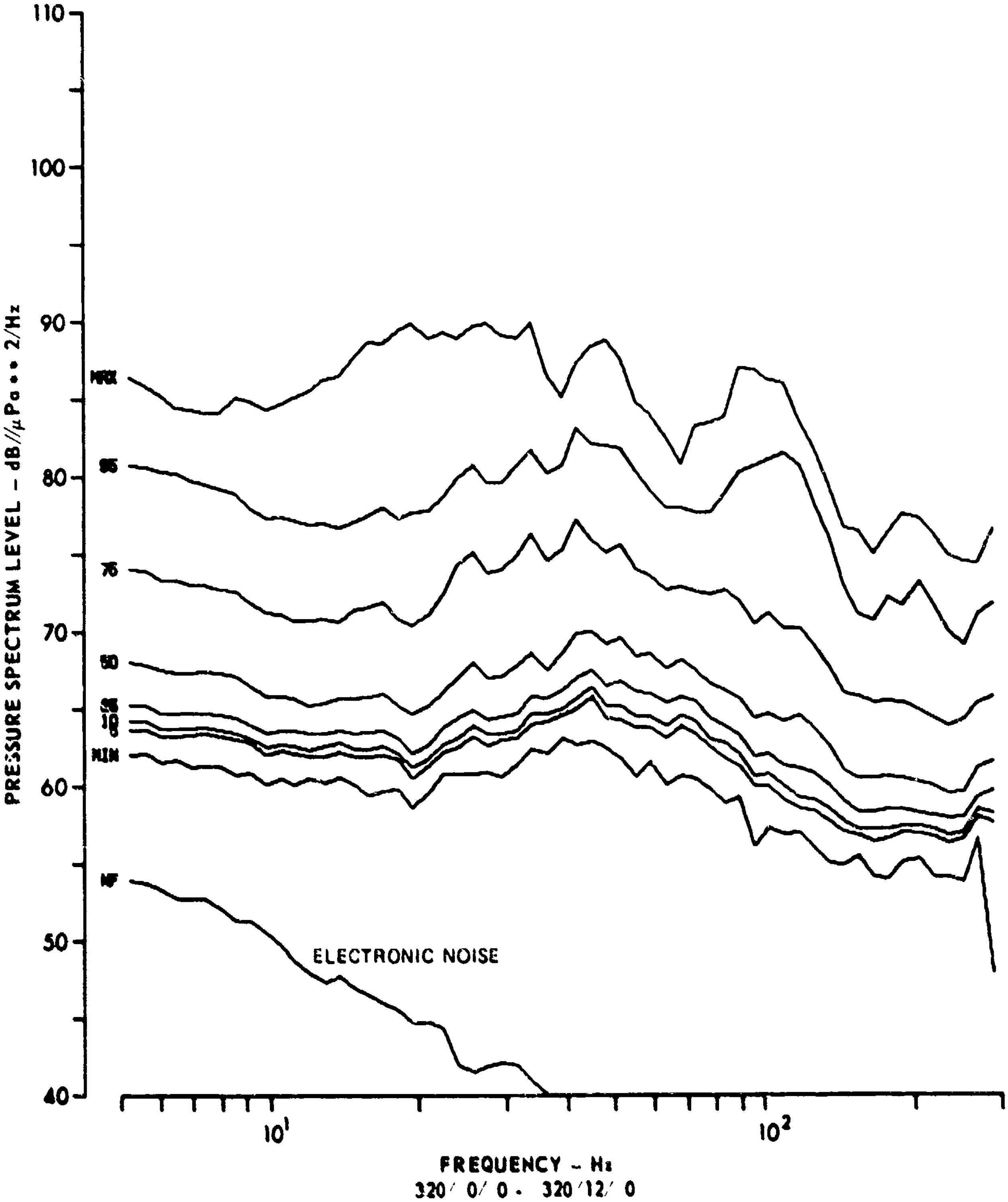

FIGURE 2.34
AMBIENT NOISE
PERCENTILE SPECTRUM LEVELS
CHURCH STROKE II SITE B PAR-4542 m RECEIVER (U)

ARL UT
AS-79-1370
KCF-GA
7-16-79

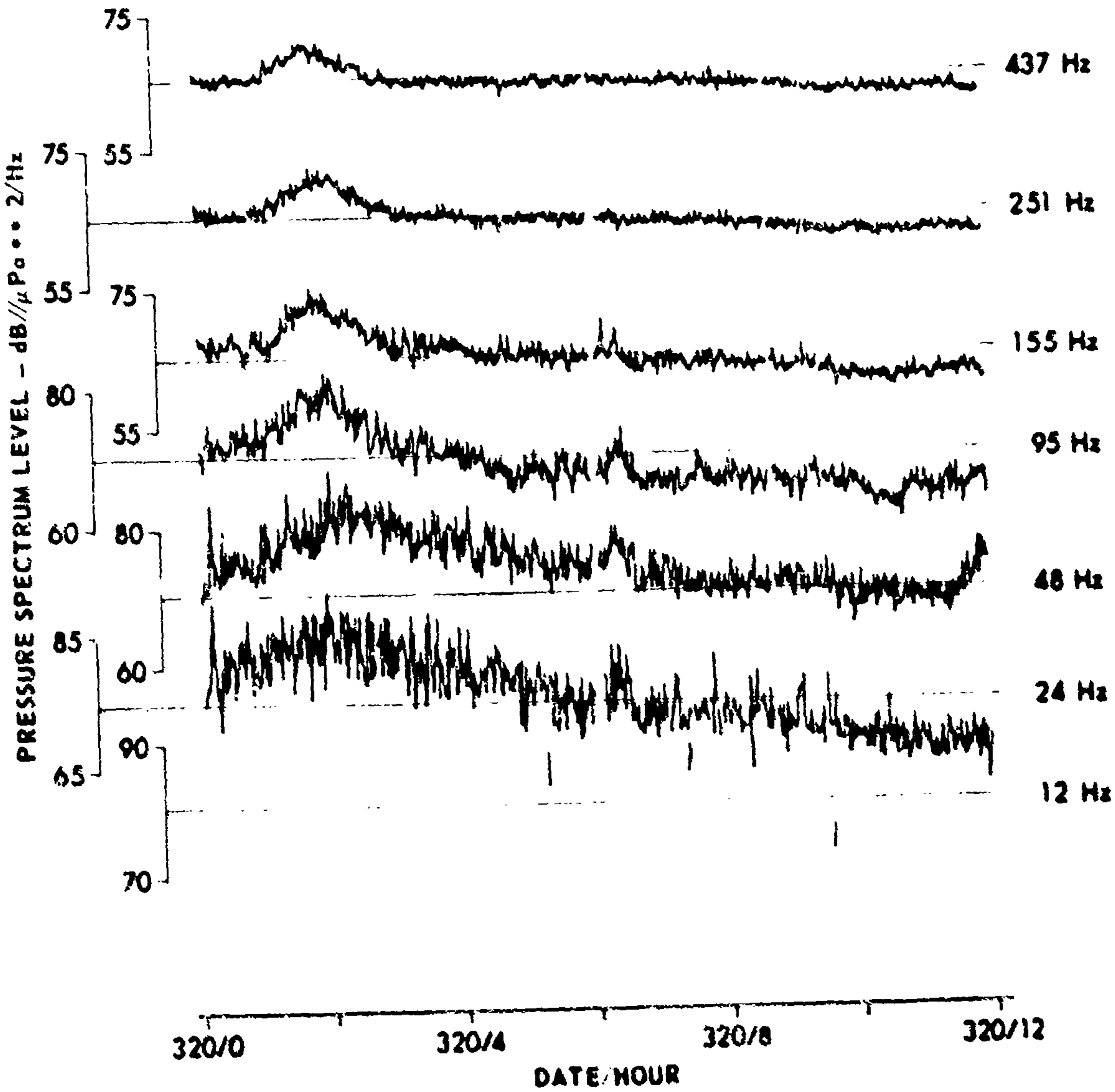

FIGURE 2.35
AMBIENT NOISE TIME SERIES CHURCH STROKE II SITE B-4542 m RECEIVER (U)

ARL UT
AS-79-985
KCF-GA
5-8-79

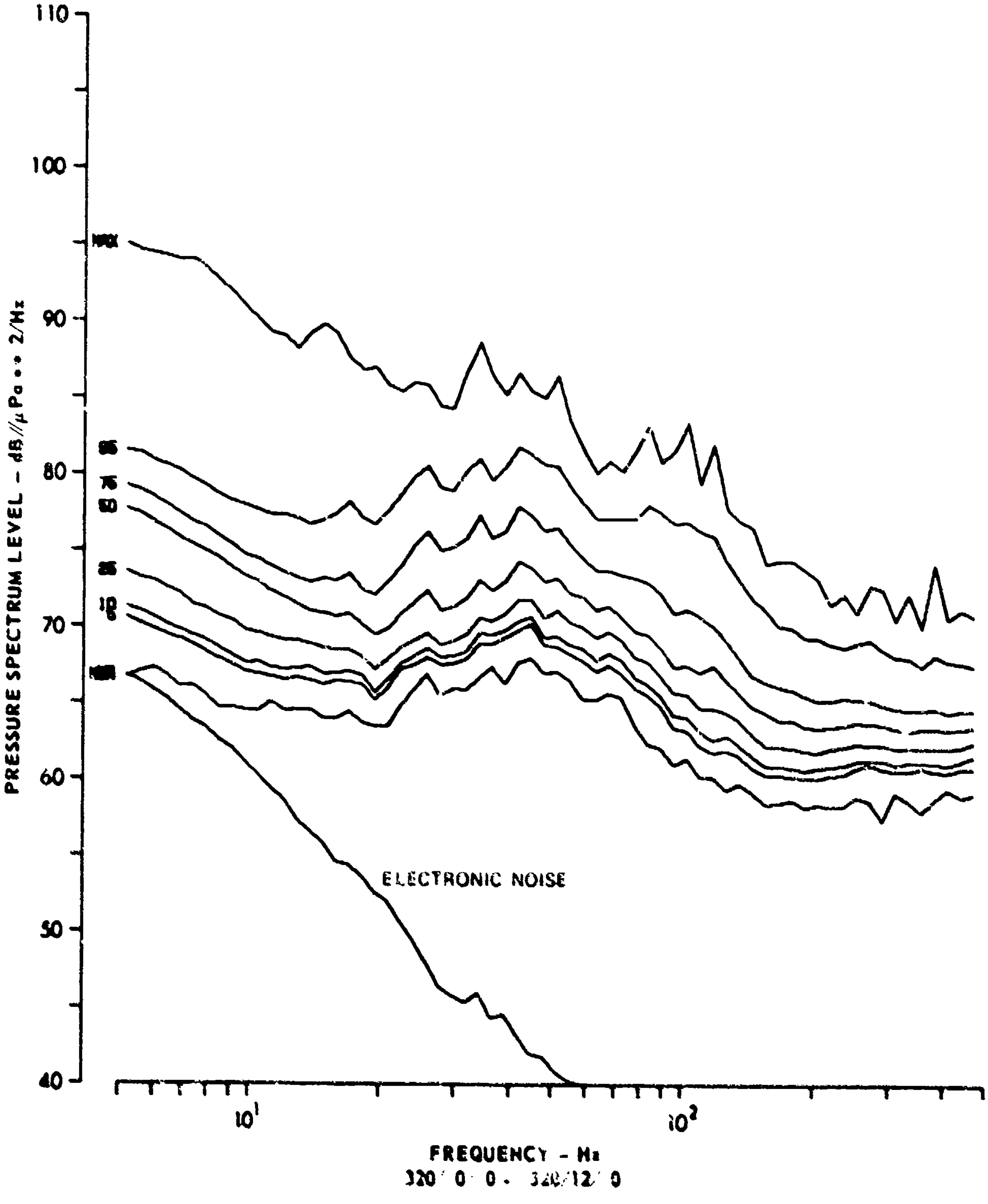

FIGURE 2.36
AMBIENT NOISE
PERCENTILE SPECTRUM LEVELS
CHURCH STROKE II SITE B-4572 m RECEIVER (U)

ARL UT
AS-79-1321
KCP - GA
7-16-79

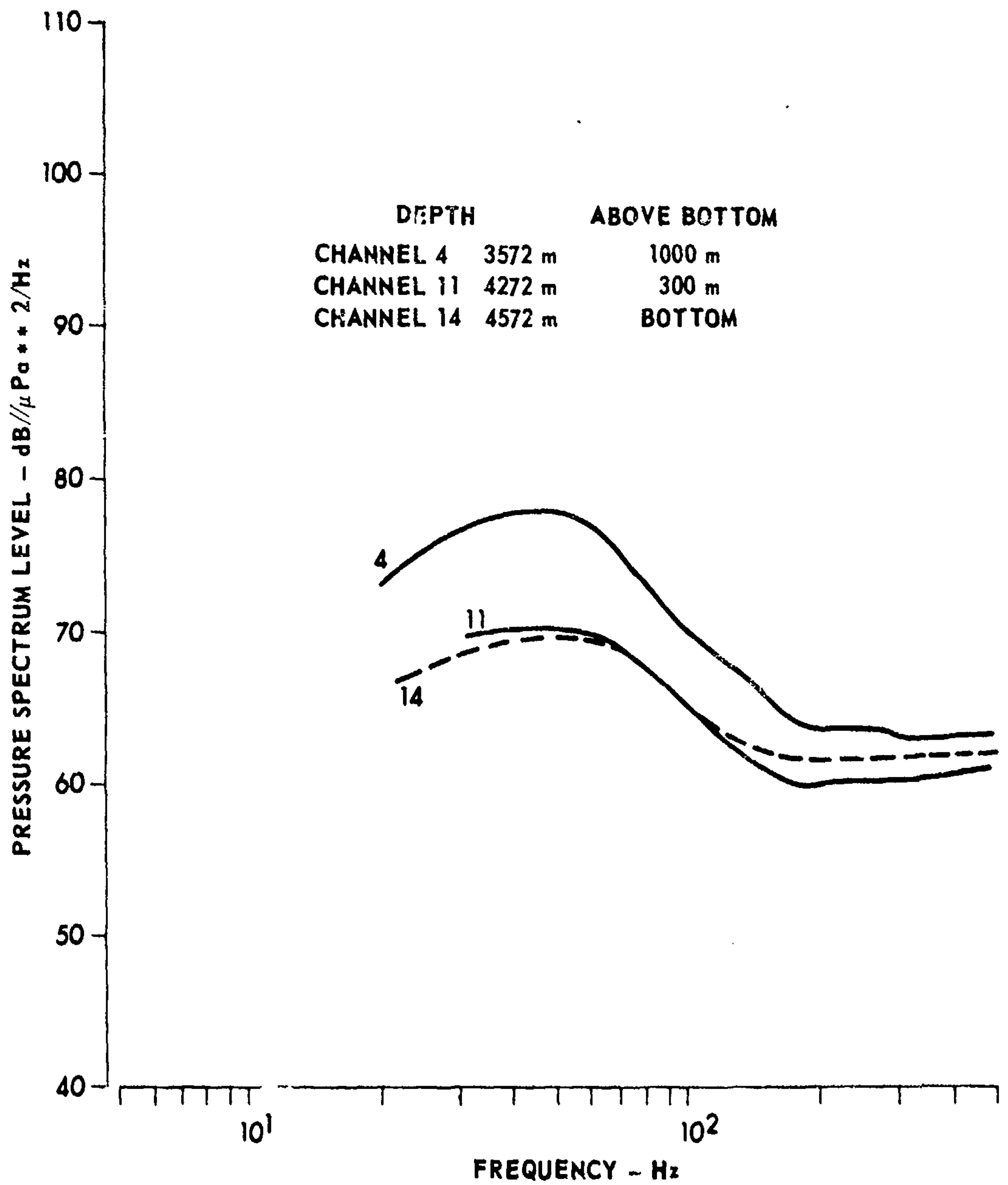

FIGURE 2.37
AMBIENT NOISE LEVELS FROM ACODAC AT SITE B (U)
WIND SPEED = 22 kt, LIGHT SHIPPING, 10 min AVERAGE
320/11/0

ARL:UT
AS-79-975
KCF - GA
5 - 8 - 79

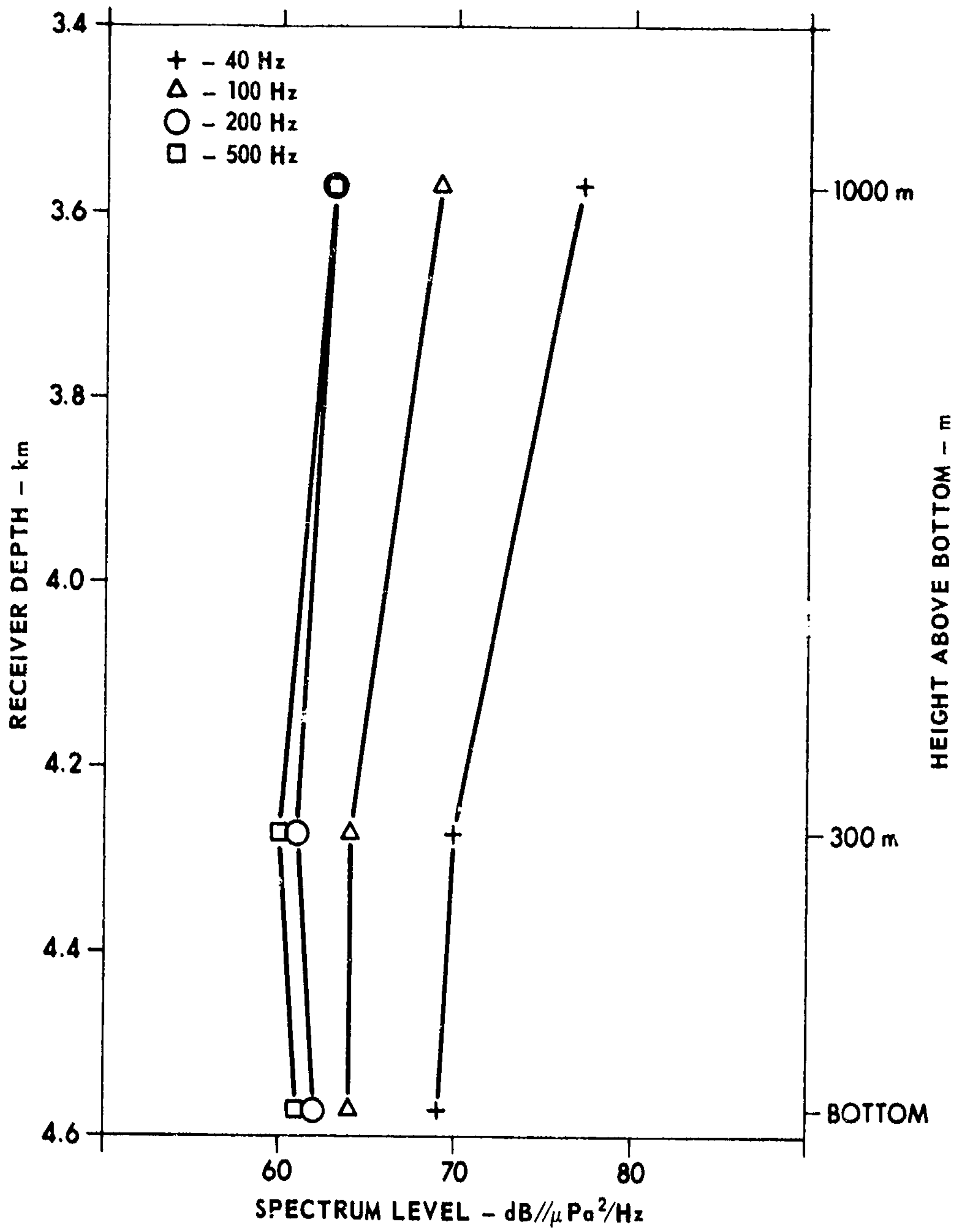

FIGURE 2.38
SPECTRUM LEVEL AT FOUR FREQUENCIES AS A FUNCTION OF RECEIVER DEPTH AT SITE B (U)

ARL:UT
AS-79-974
KCF-GA
5-8-79

(C) for frequencies between 200 and 500 Hz. During the 10 min interval for which the spectra, shown in Fig. 2.37, were computed, the wind speed given by the site anemometer, 10 m above the surface, was 22 kt. The spectral level according to, for example, Ref. 11a, would be 66 dB at 500 Hz instead of the 60 to 63 dB for the three receivers shown. The wind speed as reported by Fleet Numerical Weather Central (FNWC) and the data from the site anemometer are shown in Fig. 2.39. The spectral level output of the PAR is compared with that of the ACODAC in Fig. 2.40 (for the same time period as shown in Fig. 2.37). There are some differences which are possibly calibration errors due to missing hydrophone information. Some of the differences may be actual differences in level due to the fact that the PAR and ACODAC were separated by 0.79 nmi and a ship was in the background. Near the ship's CPA, shown in Fig. 2.32 (ACODAC) and Fig. 2.34 (PAR), a significant difference is seen which can easily be attributed to different source-receiver geometries.

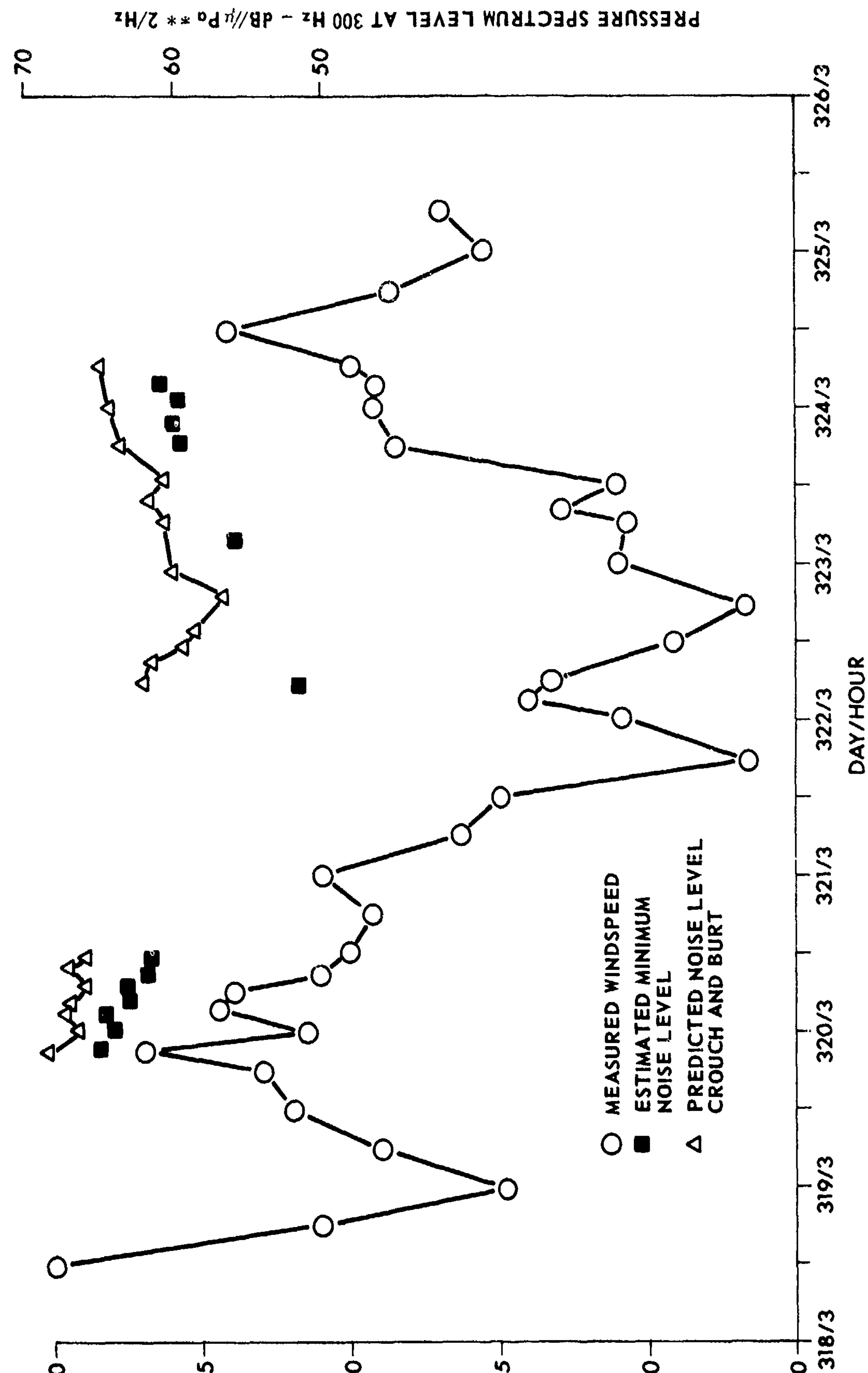

FIGURE 2.39
WINDSPEED/NOISE LEVEL COMPARISON GRAPH
SITE B

ARL:UT
AS-79-965
KCF - GA
5 - 8 - 79

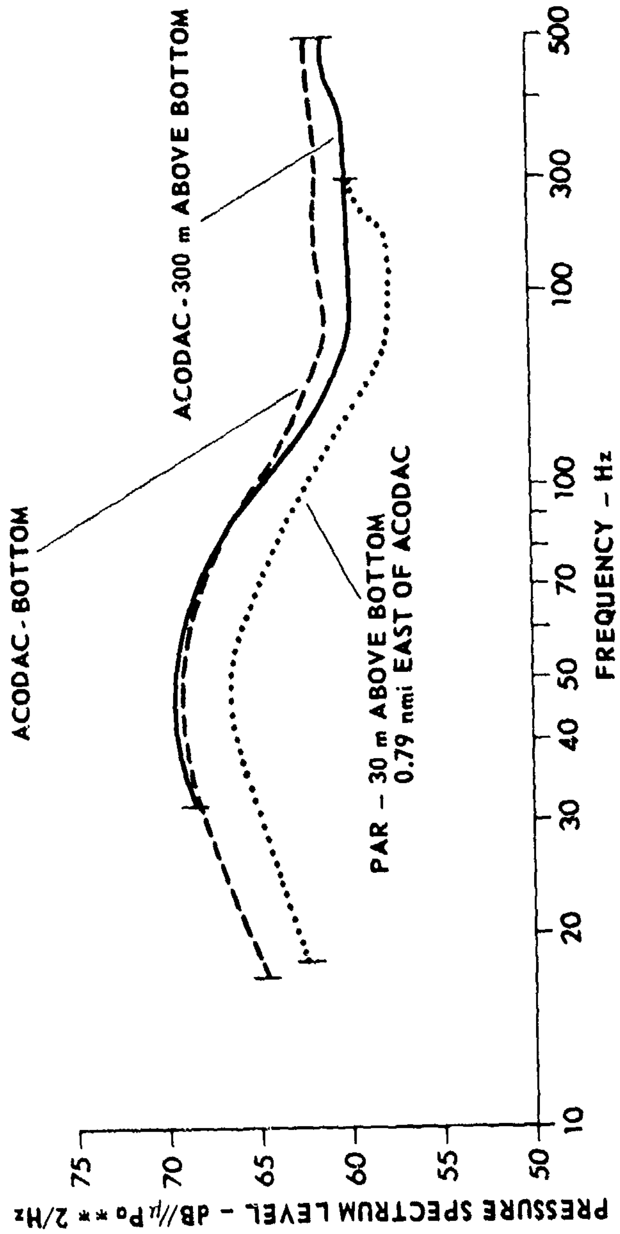

FIGURE 2.40
STYLIZED SPECTRAL LEVELS FOR THE PAR AND ACODAC RECORDING SYSTEMS AT SITE B
CHURCH STROKE II (U)

ARL:UT
AS-79-973
KCF-GA
5 - 8 - 79

III. SITE EN ENVIRONMENTAL ACOUSTIC DATA

(C) Figure 3.1 shows the Site EN location, 20°05.9' N, 132°05.0' E,[11] and the source events processed for this site.

(U) There was one cw projector tow by the INDIAN SEAL out to 450 km along the 180° radial to EN from 0629, 27 November, to 0345, 29 November 1977. These data have been processed for propagation loss and ambient noise. Receiver depths were 4982 m (1000 m off the bottom), 5582 m (400 m off the bottom), 5782 m (200 m off the bottom), 5882 m (100 m off the bottom), and 5972 m (10 m off the bottom).[6] These AN/cw channels had nominal receiver sensitivities of -128 to -98 dB//V/μPa. It should be noted that the cw projector depth was 91 m out to a range of approximately 53 km, and 18 m depth beyond that.

(U) VP aircraft dropped 18 m and 91 m depth SUS along the tracks shown in Fig. 3.1; they were received at a hydrophone depth of 4982 m (1000 m above the bottom). The SUS data recordings at Site EN were subject to the same problems that occurred at Site B, discussed in Chapter II. For Site EN, since calibrated propagation loss data were available from the cw source, only the SUS data from the AN/cw receiver were processed for bottom loss and propagation loss.

3.1 Bottom Loss at Site EN

(U) As mentioned, the SUS charges at Site EN were aircraft deployed. The primary practical effects of airdropping charges upon bottom loss measurements are that fewer samples are available and that navigation errors (and hence errors in bottom loss data reduction) are greater. However, adequate data were obtained to estimate bottom loss in the area; the results show that the bottom loss at Site EN is higher than at Site B.

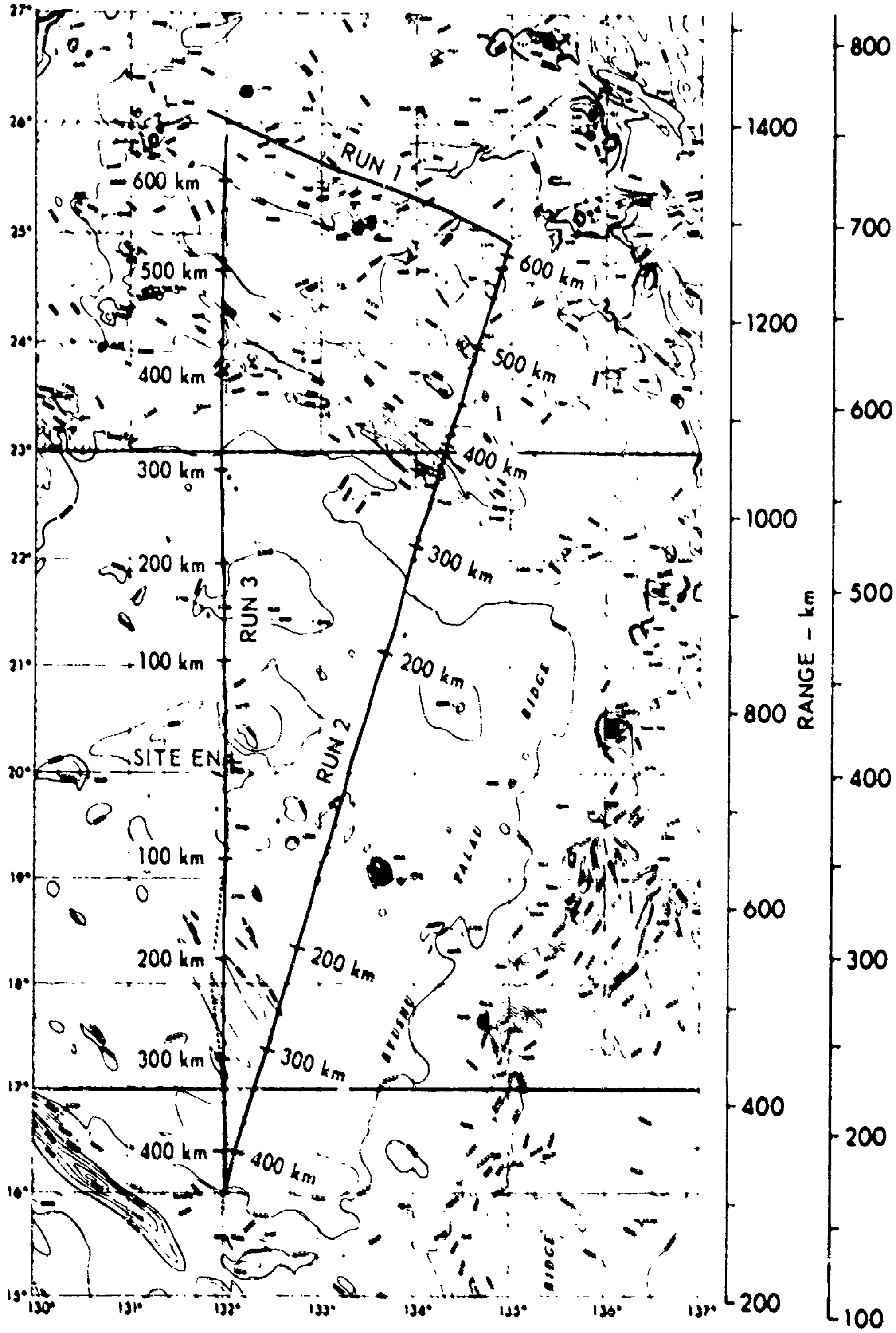

FIGURE 3.1
CHURCH STROKE II - SITE EN (U)
SOURCE TRACKS
——— AIRCRAFT SUS
.... INDIAN SEAL cw

ARL:UT
AS-78-1843
KCF - GA
11-30-78

(U) Individual arrival estimates of bottom loss from 18 m and 91 m depth SUS are shown in Figs. 3.2 and 3.3, respectively. There is larger scatter in these samples than was seen in the data at Site B (Figs. 2.2 and 2.3) from the ship dropped SUS. In addition, the anomalous oscillations in the 25 Hz and 50 Hz results of Fig. 3.3 reflect the navigation uncertainties of the aircraft dropped SUS.

(U) Averaged values of bottom loss at Site EN are shown in Fig. 3.4. These are averages at 5° increments of 18 m source data at 25 and 50 Hz, and of 18 m and 91 m source data at the higher frequencies.

(U) The averaged values are also given in Table III-1. The values for angles above 20° are estimates, based on the fact that no signal arrivals could be detected at angles above those plotted, as was the case for high angle values at Site B.

3.2 Propagation Loss at Site EN

(U) For the first 53 km of the cw projector tow, the source was at 91 m depth. Propagation loss from the 67 Hz and 197 Hz tones to the different receiver depths are shown in Figs. 3.5 through 3.9. Beyond 53 km, the same frequencies were projected for 18 m source depth, and the propagation loss is shown in Figs. 3.10 through 3.14. It should be noted that data on the 5882 m and the 5972 m depth receivers were contaminated by ACODAC recording system problems. These are shown on Figs. 3.13 and 3.14.

(U) Signal excess and the ambient noise level (in an adjacent frequency band) during the projector tow at Site EN are given in Figs. 3.15 through 3.24 for the 91 m source at short range, and Figs. 3.25 through 3.34, for the 18 m source at longer ranges.

(U) Because of recording system problems, only a few of the SUS propagation loss results are included here. These results suffice to show the acoustic blockage by the shoaling approximately 400 km north of Site EN.

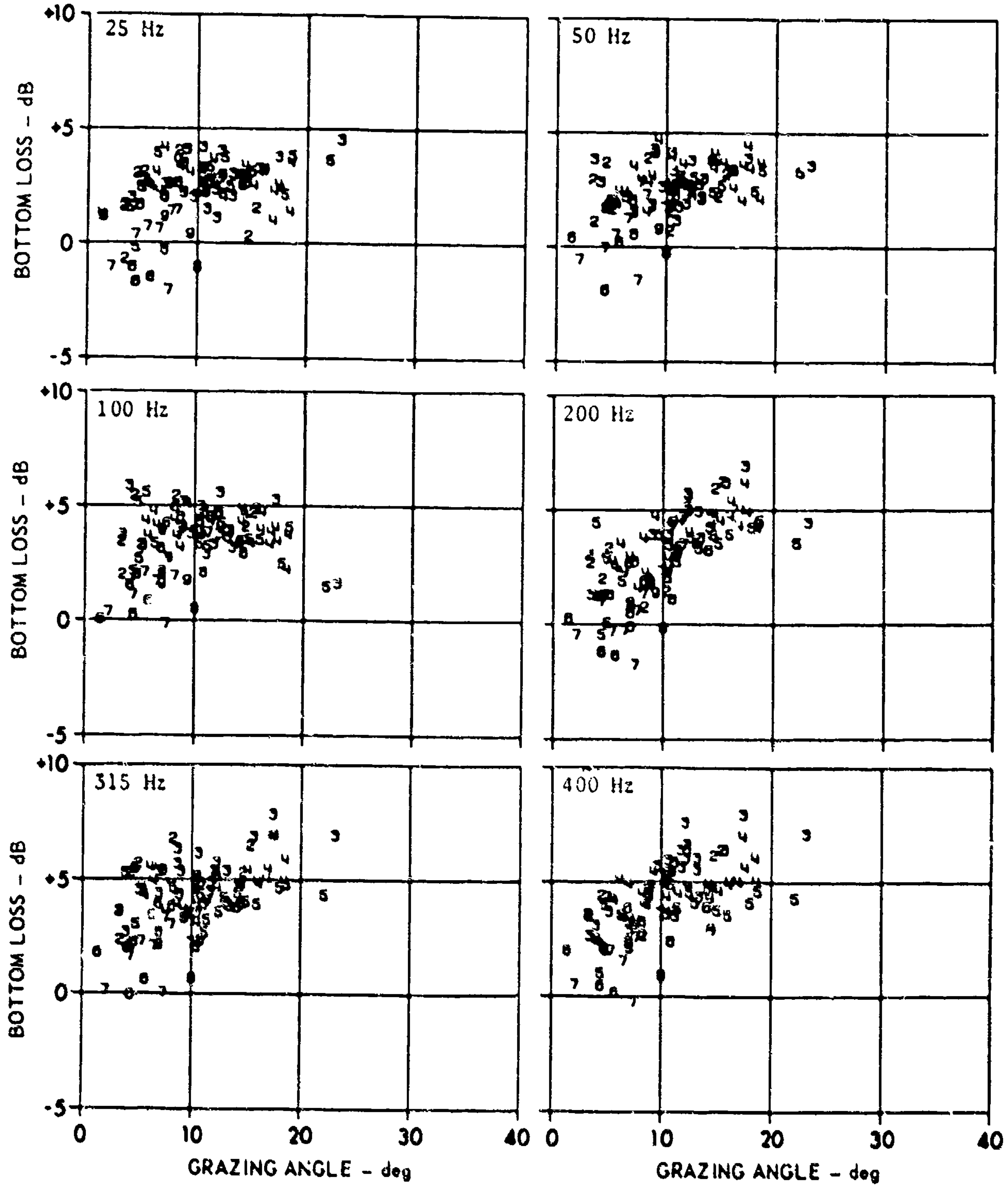

FIGURE 3.2
BOTTOM LOSS ESTIMATES versus GRAZING ANGLE (U)
SITE EN - 4982 m RECEIVER
18 m SOURCE

ARL:UT
AS-78-1834
KCF-GA
11-30-78

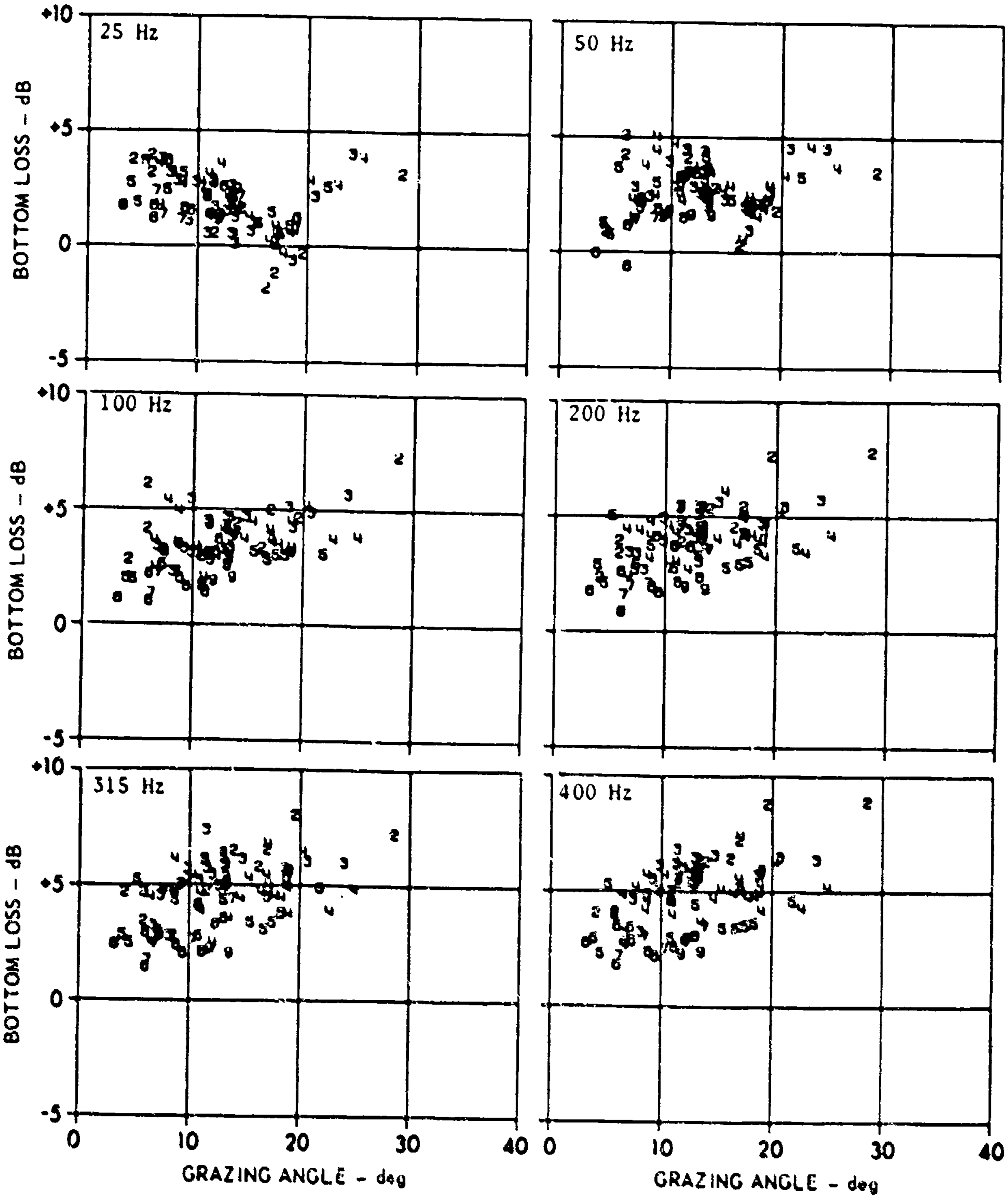

FIGURE 3.3
BOTTOM LOSS ESTIMATES versus GRAZING ANGLE (U)
SITE EN - 4982 m RECEIVER
91 m SOURCE

ARL:UT
AS-78-1835
KCF-GA
11-30-78

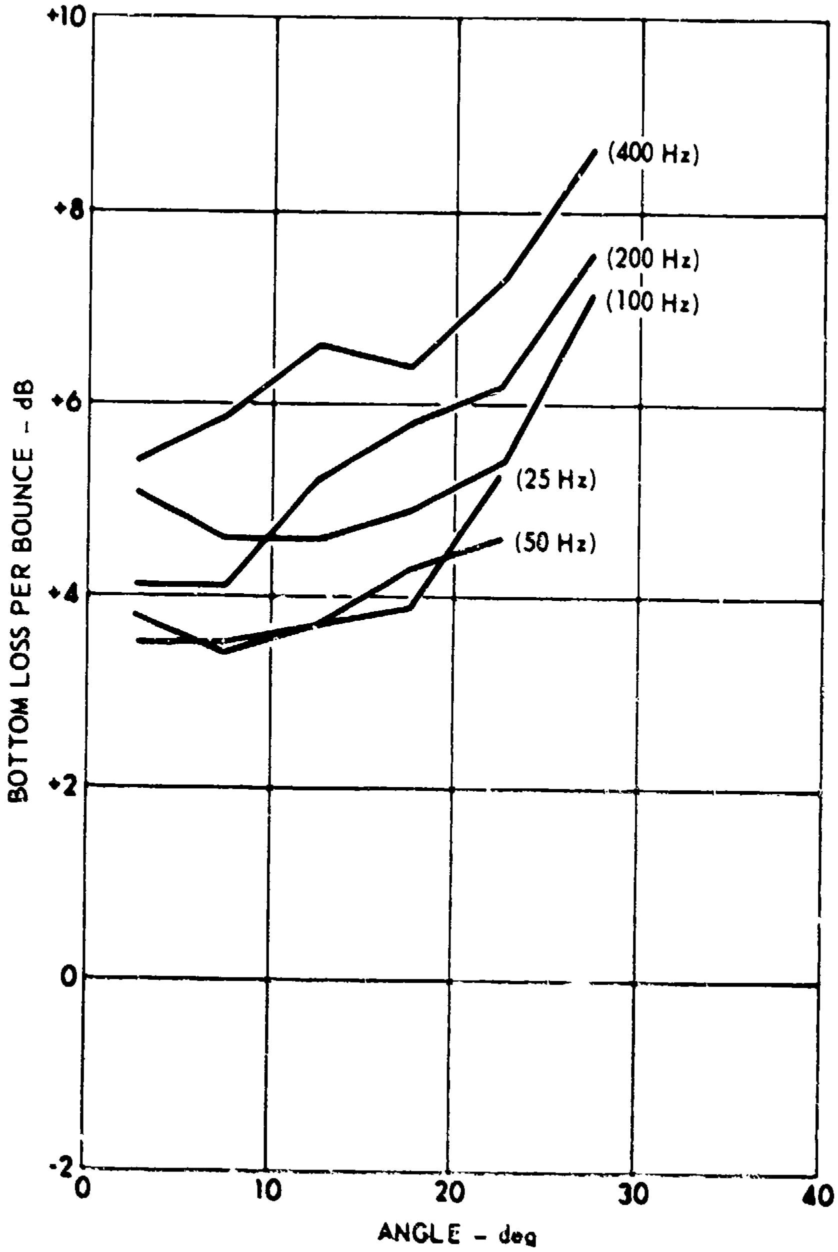

FIGURE 3.4

(U) AVERAGED BOTTOM LOSS
CHURCH STROKE II - SITE EN

SEE TABLE 21

ARL UT
AS-78-1954
KCF - GA
12-12-78

(C) TABLE III-1

AVERAGED BOTTOM LOSS DATA
CHURCH STROKE II - SITE EN (U)

18 m and 91 m SUS
Receiver Depth 4982 m
Bounces 2-9

25 Hz

Grazing Angle Interval-deg		Mean	Std Dev	Number Samples
0	5	3.5	2.4	50
5	10	3.5	1.5	55
10	15	3.7	1.0	38
15	20	3.9	1.0	17
20	25	5.3	0.7	2
25	30	0.0	0.0	0
30	35	0.0	0.0	0
35	40	0.0	0.0	0
40	45	0.0	0.0	0
45	50	0.0	0.0	0

50 Hz

Grazing Angle Interval-deg		Mean	Std Dev	Number Samples
0	5	3.8	2.8	46
5	10	3.4	1.4	52
10	15	3.7	1.0	37
15	20	4.3	0.7	17
20	25	4.6	0.5	2
25	30	0.0	0.0	0
30	35	0.0	0.0	0
35	40	0.0	0.0	0
40	45	0.0	0.0	0
45	50	0.0	0.0	0

100 Hz

Grazing Angle Interval-deg		Mean	Std Dev	Number Samples
0	5	5.1	2.7	69
5	10	4.6	1.4	97
10	15	4.6	1.2	76
15	20	4.9	1.1	38
20	25	5.4	2.2	8
25	30	7.2	2.3	2
30	35	0.0	0.0	0
35	40	0.0	0.0	0

200 Hz

Grazing Angle Interval-deg		Mean	Std Dev	Number Samples
0	5	4.1	3.0	69
5	10	4.1	1.9	98
10	15	5.2	1.6	75
15	20	5.8	1.3	39
20	25	6.2	1.8	8
25	30	7.6	2.3	2
30	35	0.0	0.0	0
35	40	0.0	0.0	0

400 Hz

Grazing Angel Interval-deg		Mean	Std Dev	Number Samples
0	5	5.4	2.4	67
5	10	5.9	1.6	77
10	15	6.6	1.3	55
15	20	6.4	1.7	26
20	25	7.3	2.0	7
25	30	8.7	2.4	2
30	35	0.0	0.0	0
35	40	0.0	0.0	0

NOTE: Arrivals above 30° grazing angle not detected. Recommend using 12 dB loss above 30° at all frequencies, 25 and 50 Hz - 18 m SUS only.

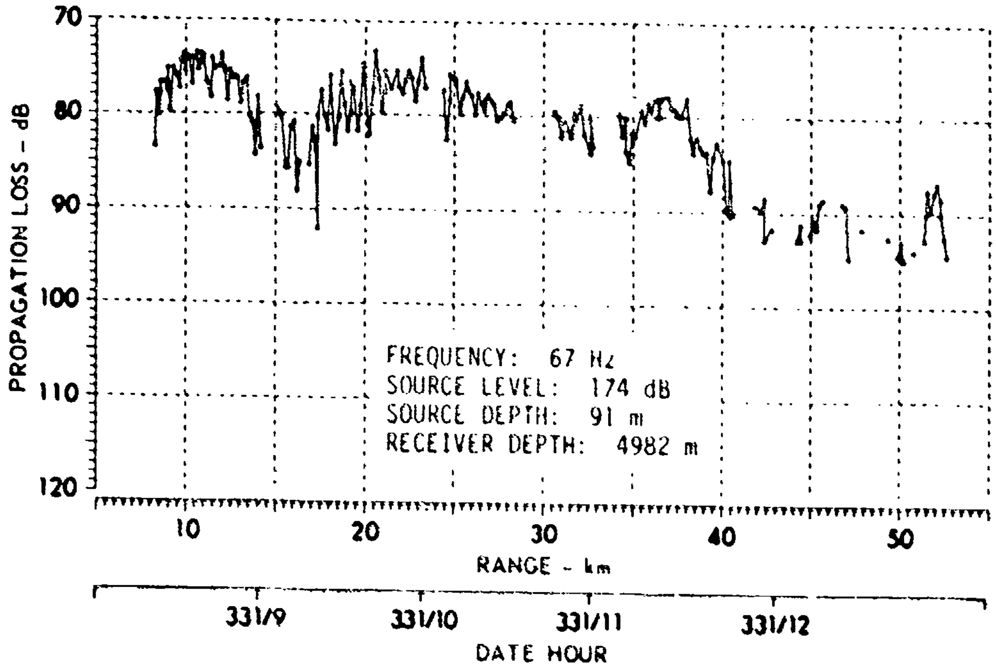

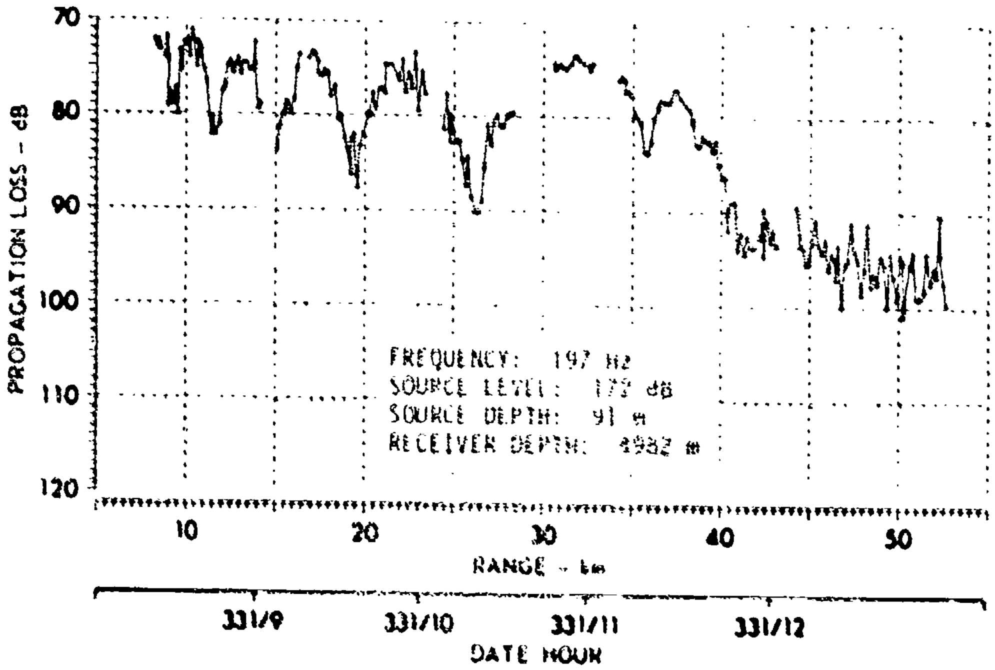

FIGURE 3 5
PROPAGATION LOSS TO 4982 m RECEIVER
CHURCH STROKE II - PHASE 2 SITE EN (U)
SOURCE DEPTH 91 m

ARL UT
AS-78-1785
KCF-GA
11-30-78

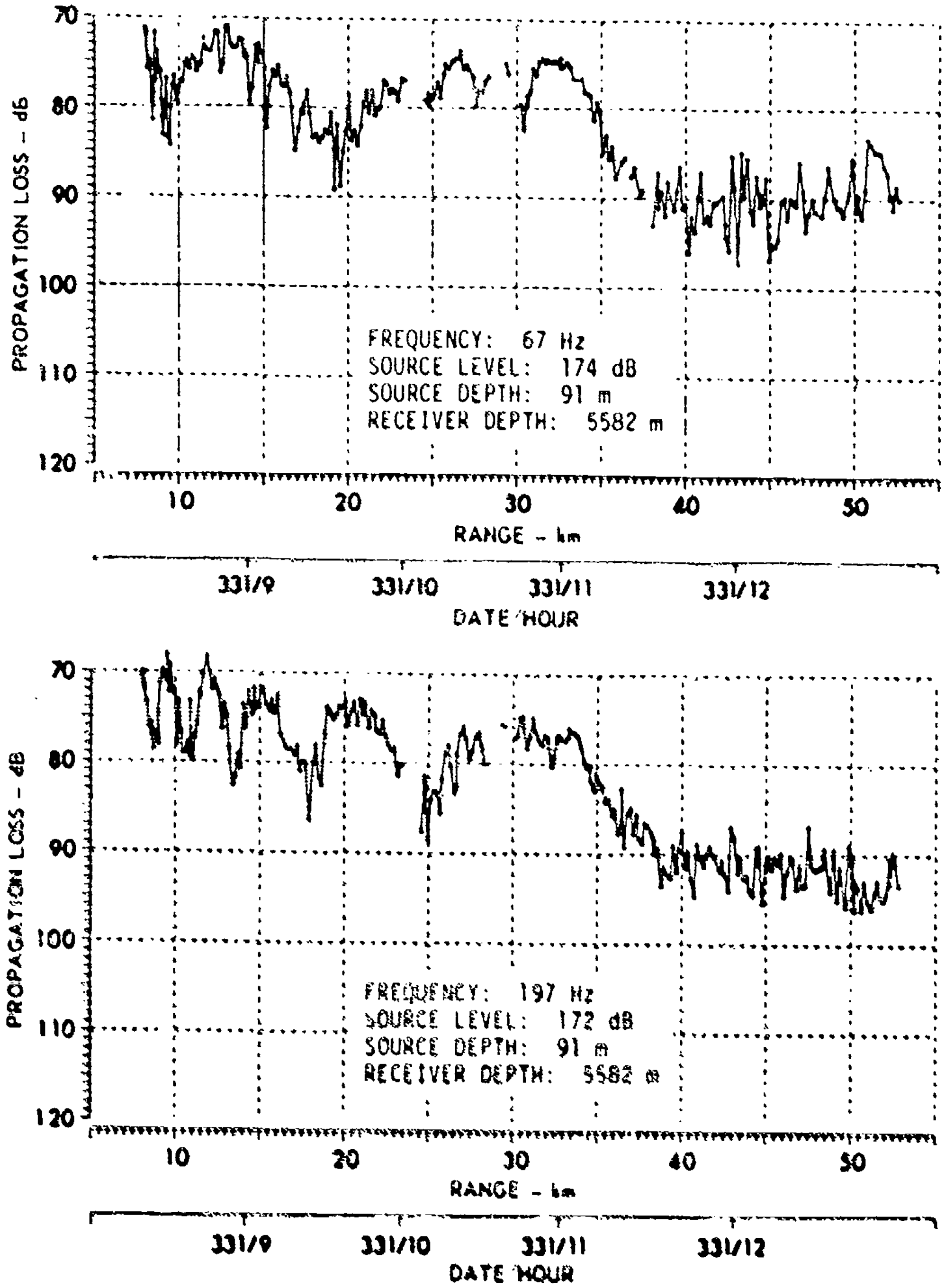

FIGURE 3.6
PROPAGATION LOSS TO 5582 m RECEIVER
CHURCH STROKE II - PHASE 2 SITE EN (U)
SOURCE DEPTH 91 m

ARL UT
AS-78-1787
KCF-GA
11-30-78

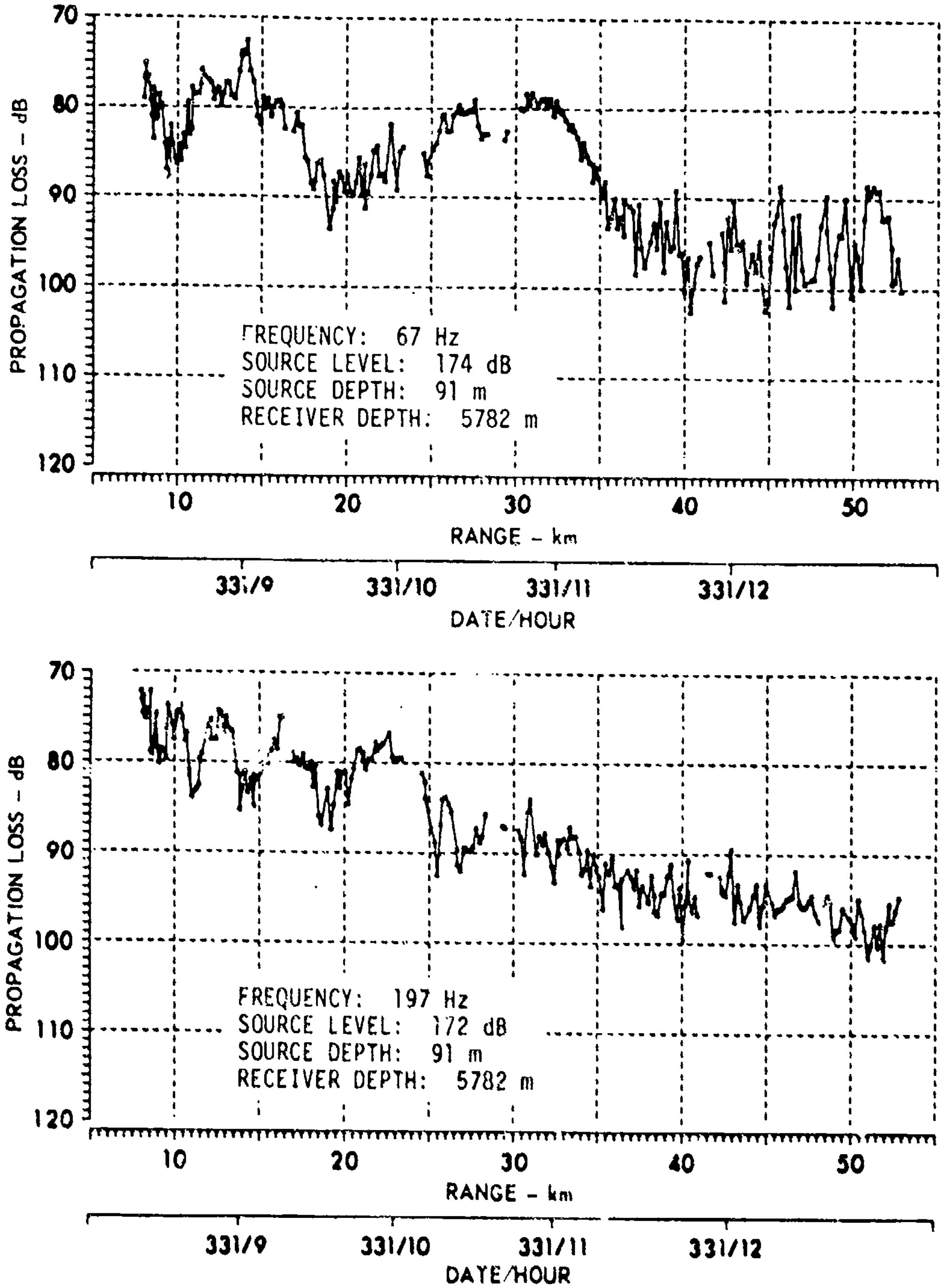

FIGURE 3.7
PROPAGATION LOSS TO 5782 m RECEIVER
CHURCH STROKE II - PHASE 2 SITE EN (U)
SOURCE DEPTH: 91 m

ARL:UT
AS-78-1789
KCF - GA
11-30-78

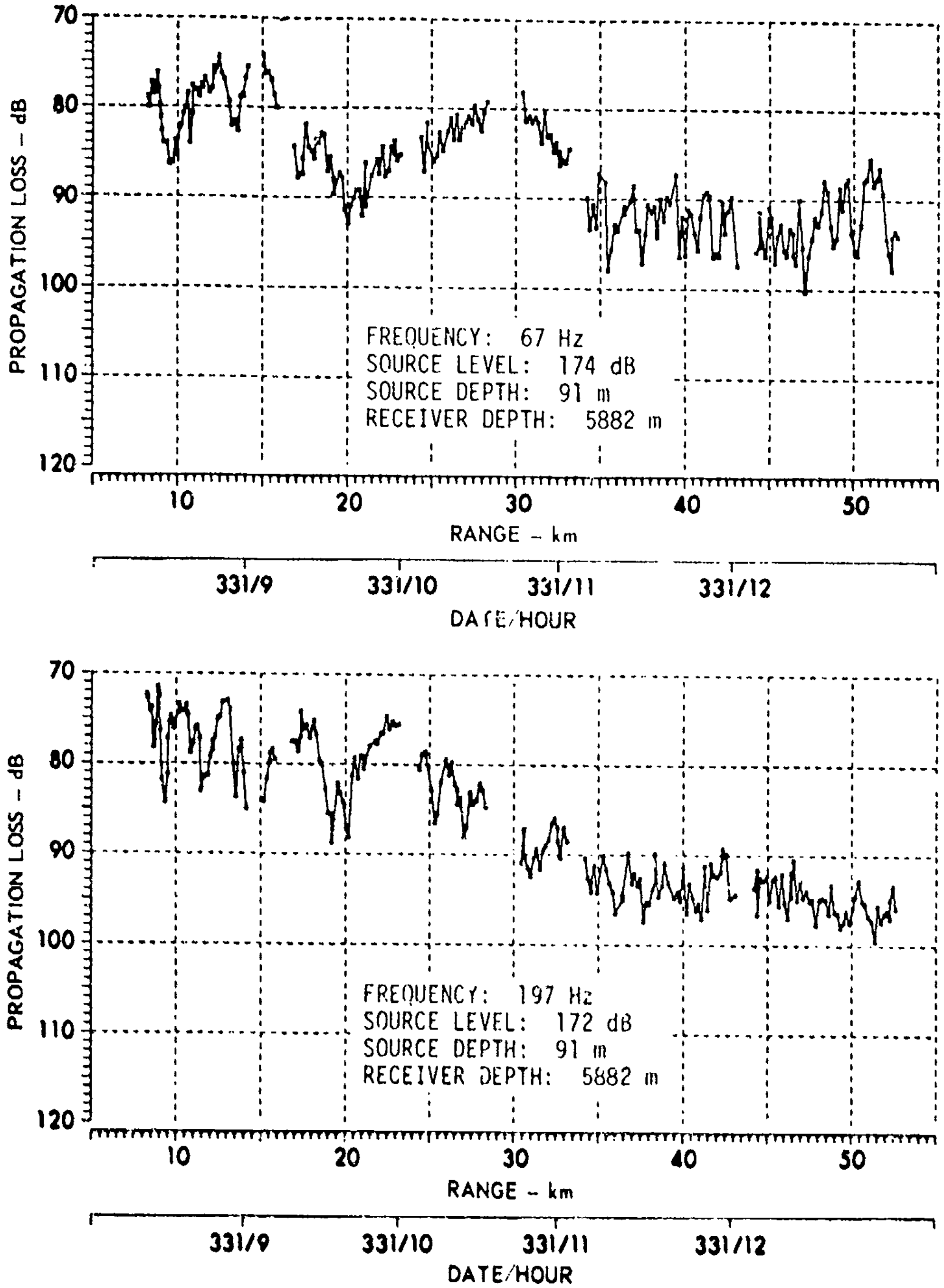

FIGURE 3.8
PROPAGATION LOSS TO 5882 m RECEIVER
CHURCH STROKE II - PHASE 2 SITE EN (U)
SOURCE DEPTH: 91 m

ARL:UT
AS-78-1793
KCF-GA
11-30-78

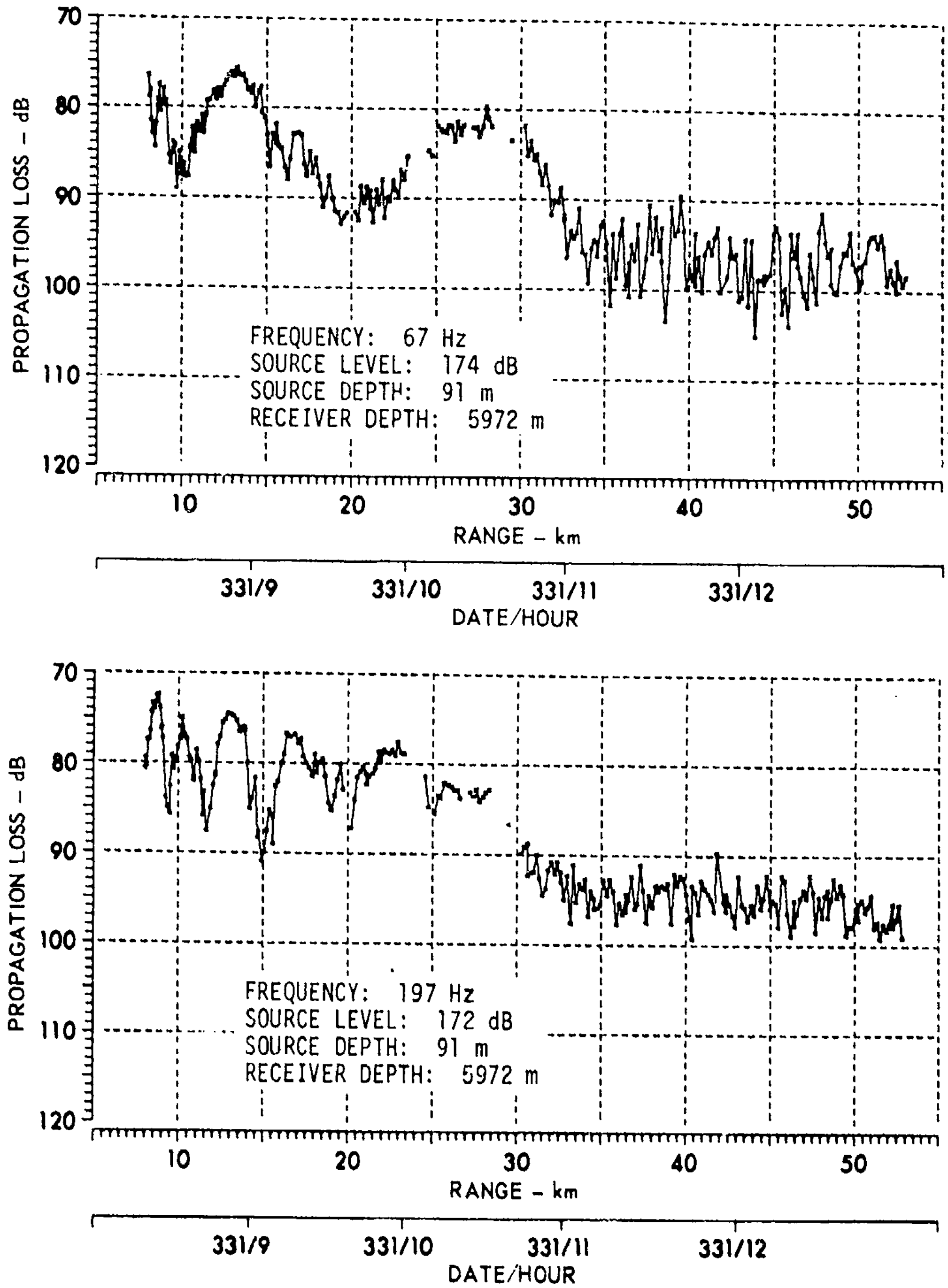

FIGURE 3.9
PROPAGATION LOSS TO 5972 m RECEIVER
CHURCH STROKE II - PHASE 2 SITE EN (U)
SOURCE DEPTH: 91 m

ARL:UT
AS-78-1791
KCF-GA
11-30-78

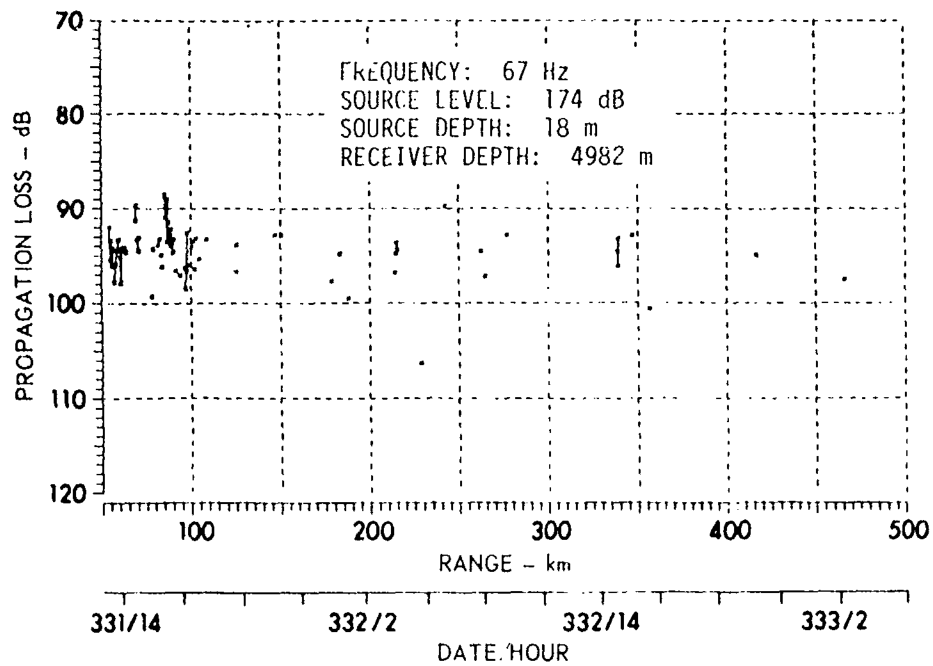

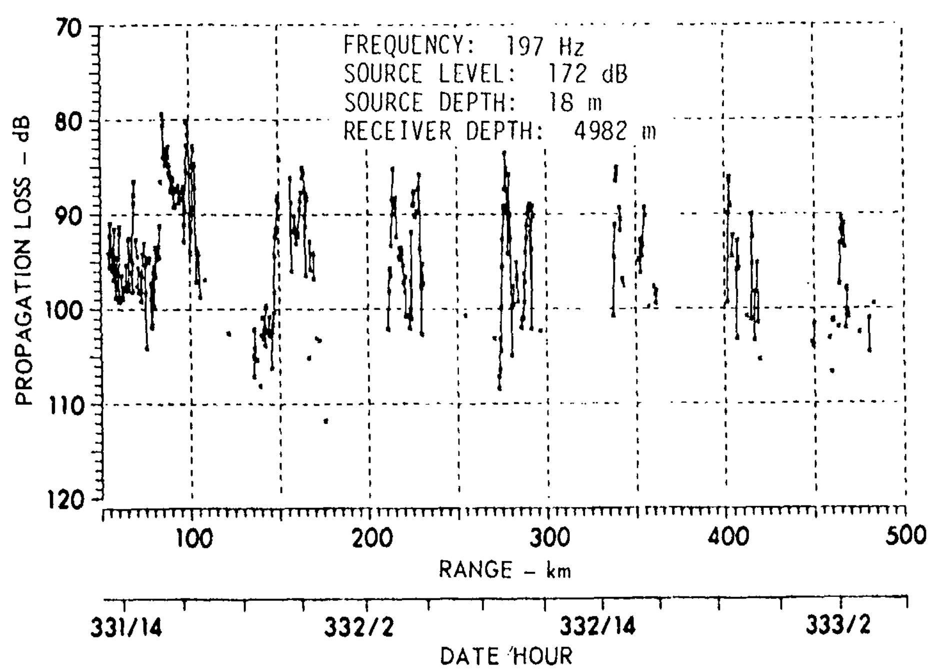

FIGURE 3.10
PROPAGATION LOSS TO 4982 m RECEIVER
CHURCH STROKE II - PHASE 2 SITE EN (U)
SOURCE DEPTH: 18 m

ARL:UT
AS-78-1786
KCF-GA
11-30-78

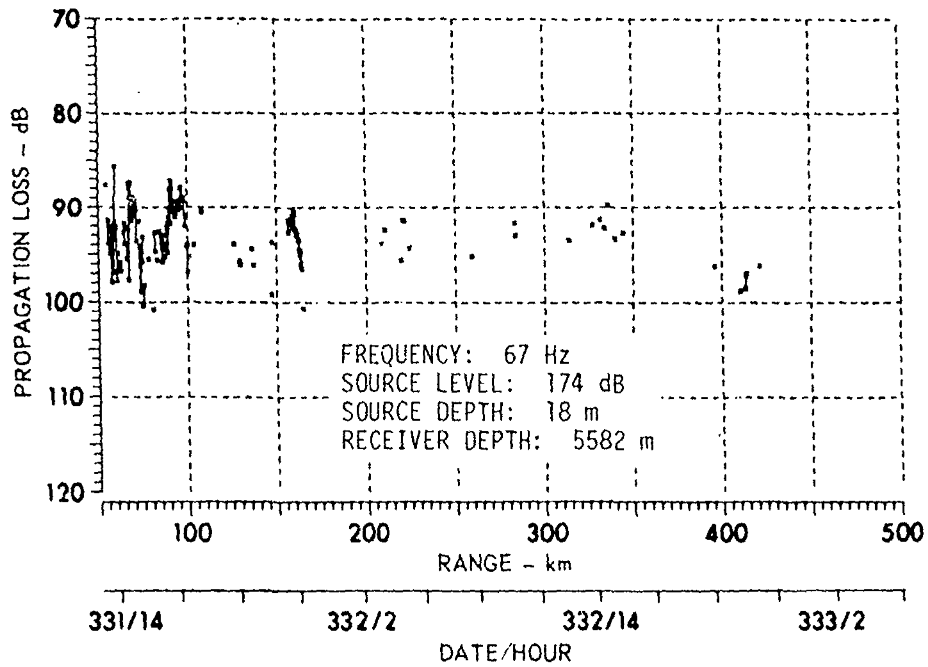

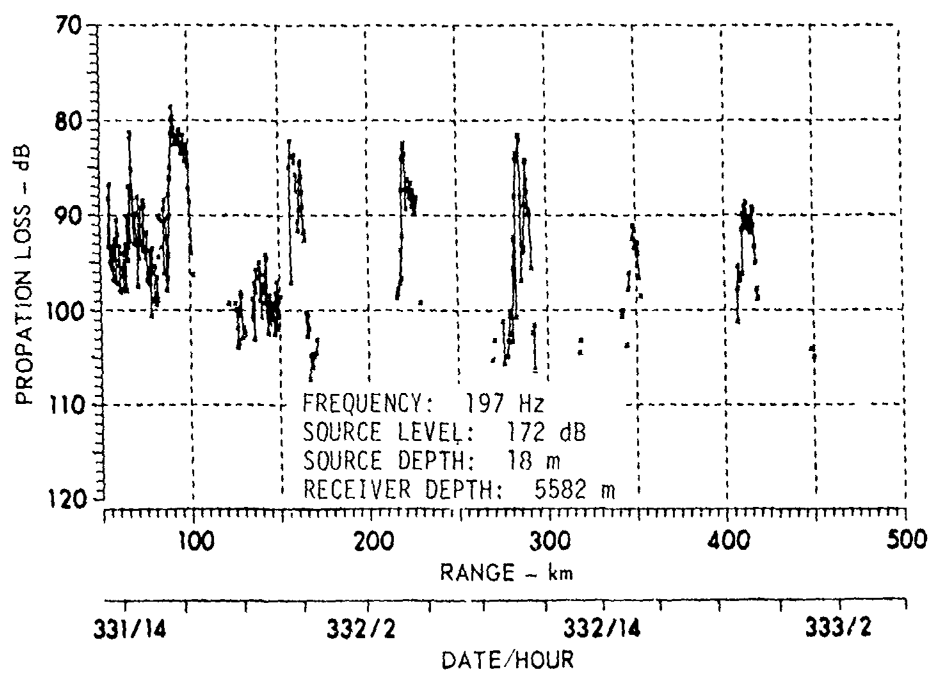

FIGURE 3.11
PROPAGATION LOSS TO 5582 m RECEIVER
CHURCH STROKE II - PHASE 2 SITE EN (U)
SOURCE DEPTH: 18 m

ARL:UT
AS-78-1788
KCF-GA
11-30-78

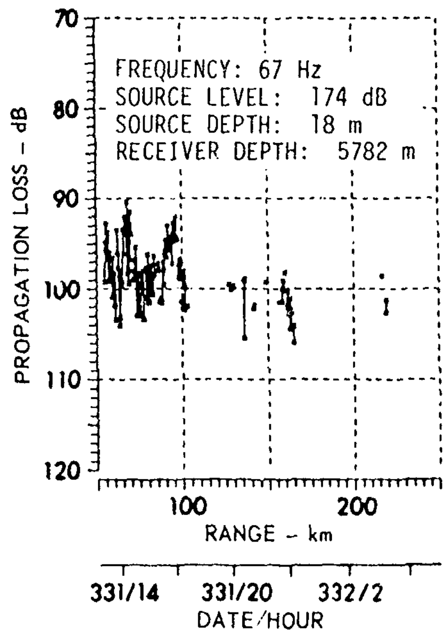

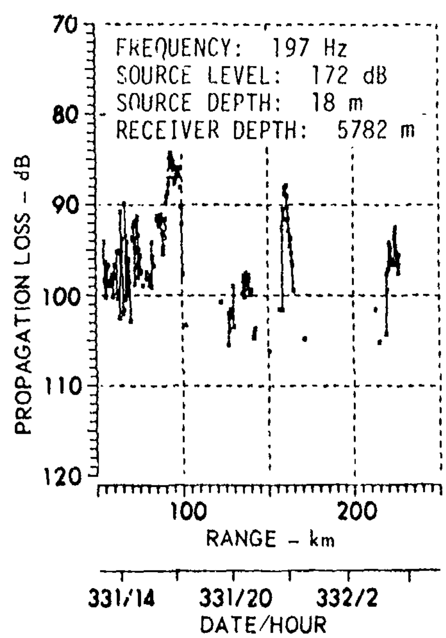

FIGURE 3.12
PROPAGATION LOSS TO 5782 m RECEIVER
CHURCH STROKE II - PHASE 2 SITE EN (U)
SOURCE DEPTH: 18 m

ARL:UT
AS-78-1790
KCF-GA
11-30-78

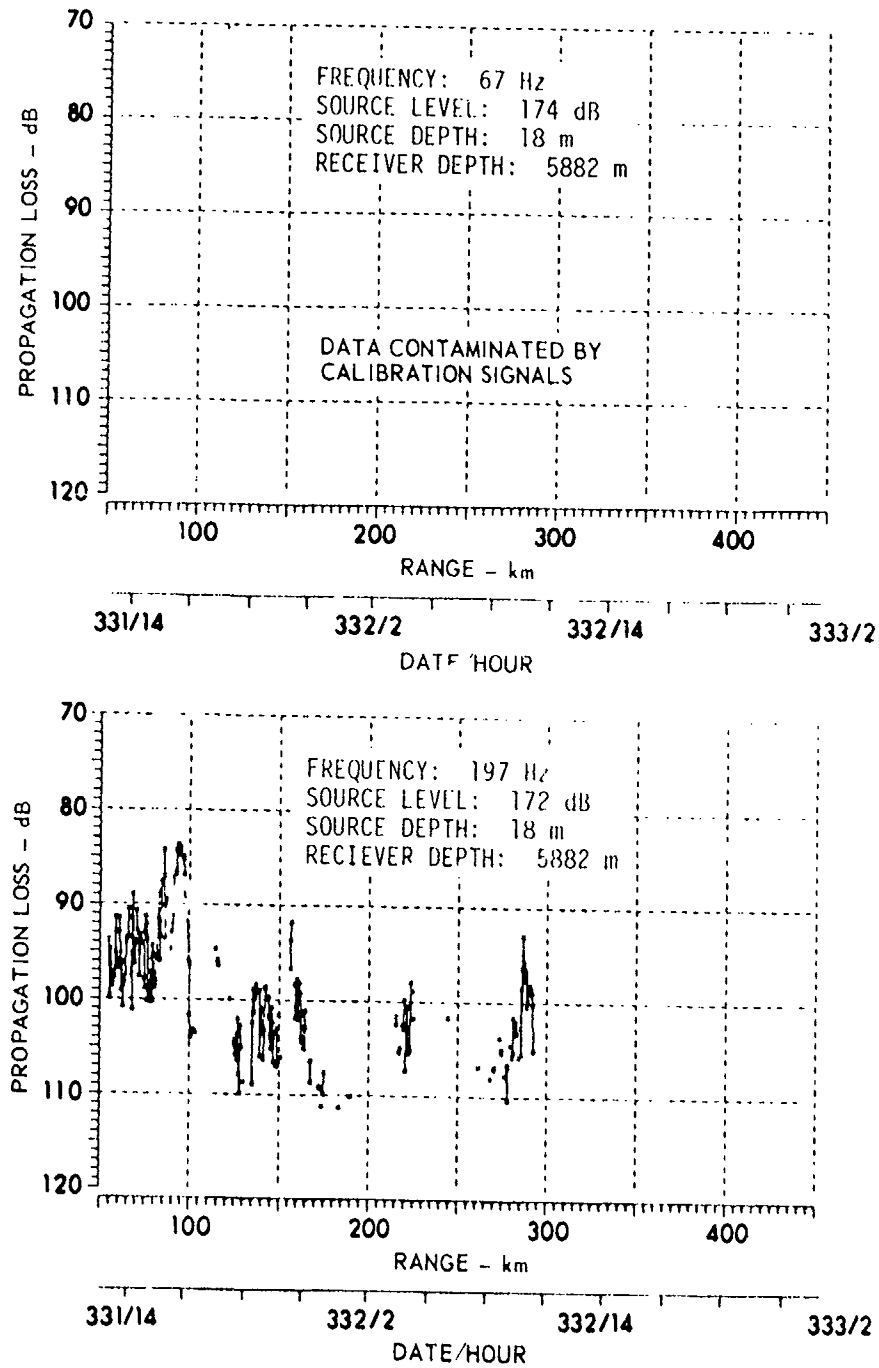

FIGURE 3.13
PROPAGATION LOSS TO 5882 m RECEIVER
CHURCH STROKE II - PHASE 2 SITE EN (U)
SOURCE DEPTH: 18 m

ARL UT
AS-78-1794
FCF-GA
11-30-78

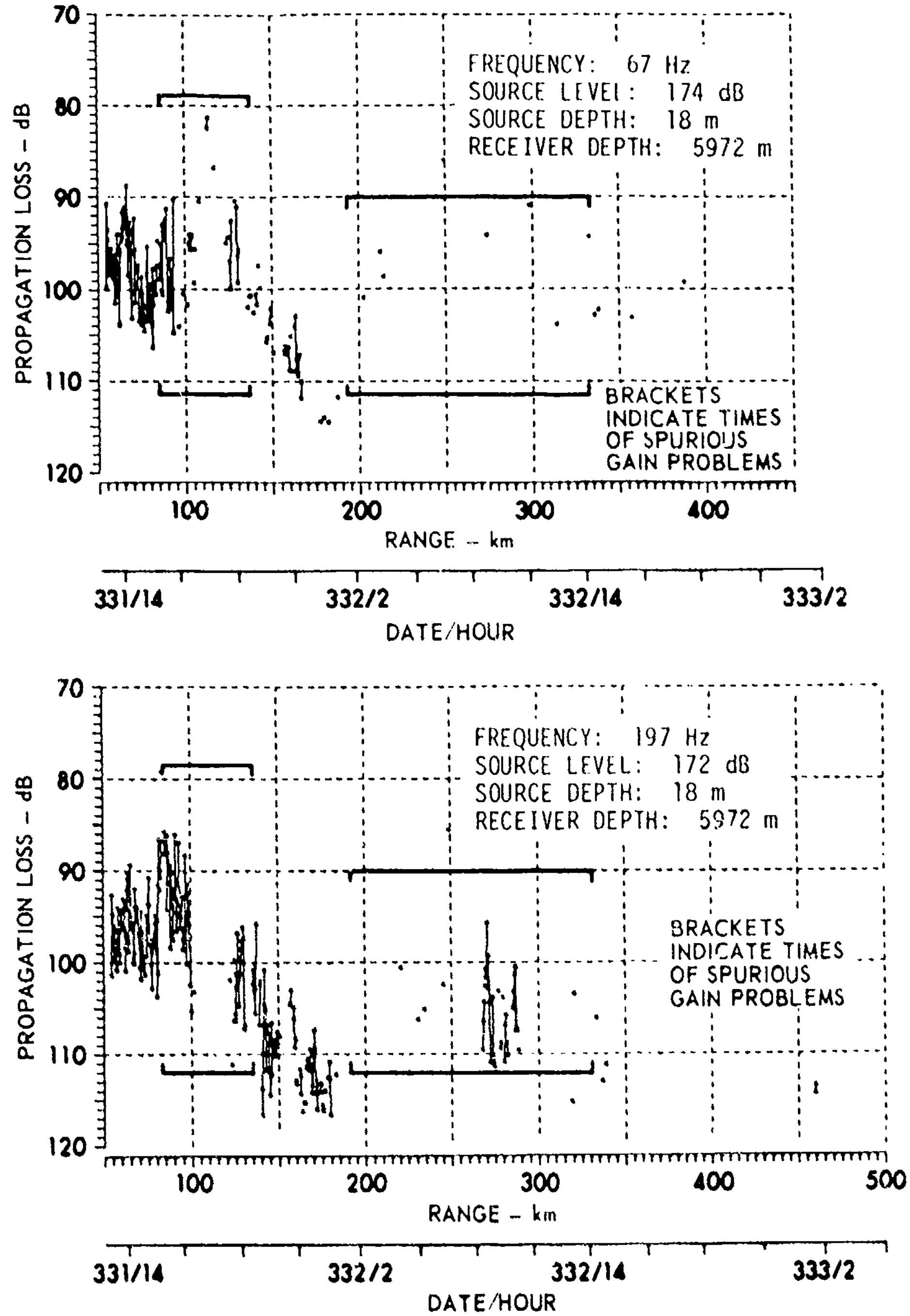

FIGURE 3.14
PROPAGATION LOSS TO 5972 m RECEIVER
CHURCH STROKE II - PHASE 2 SITE EN (U)
SOURCE DEPTH: 18 m

ARL:UT
AS-78-1792
KCF-GA
11-30-78

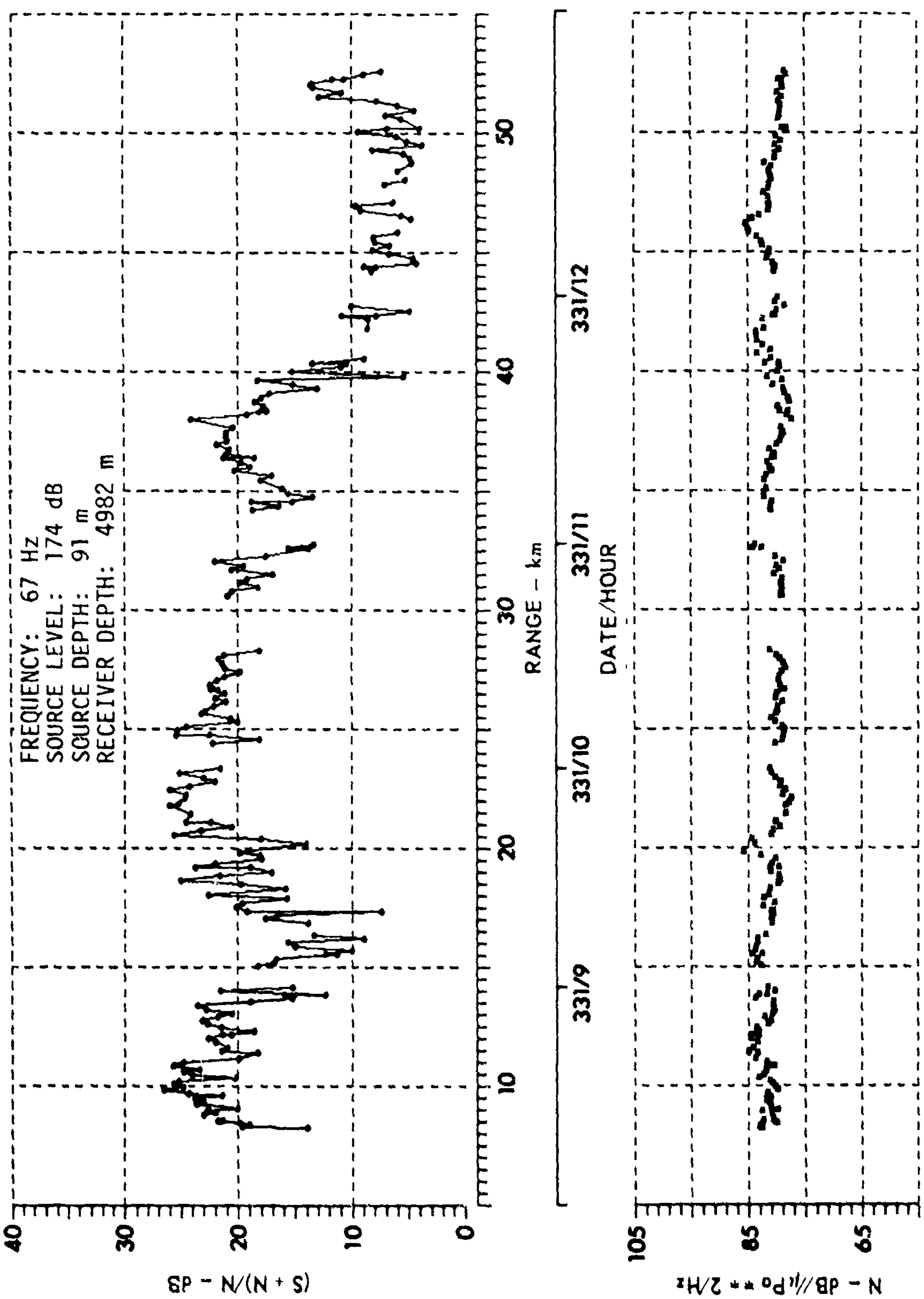

FIGURE 3.15
NOISE AND SIGNAL EXCESS FOR 4982 m RECEIVER AT 67 Hz
CHURCH STROKE II - PHASE 2 SITE EN (U)

ARL:UT
AS-78-1795
KCF-GA
11-30-78

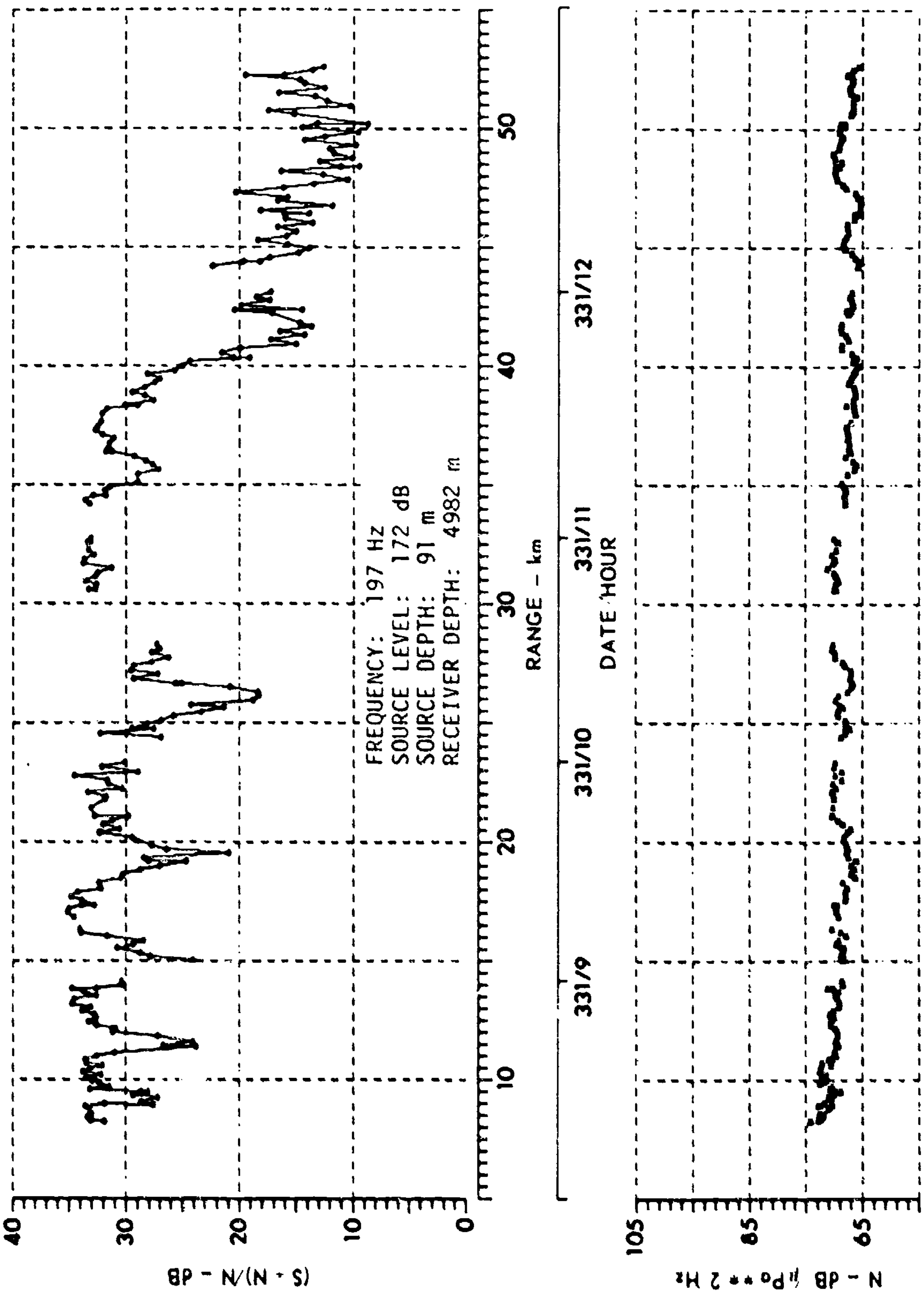

FIGURE 3.16
NOISE AND SIGNAL EXCESS FOR 4982 m RECEIVER AT 197 Hz
CHURCH STROKE II - PHASE 2 SITE EN (U)

ARL:UT
AS-78-1797
KCF-GA
11-30-78

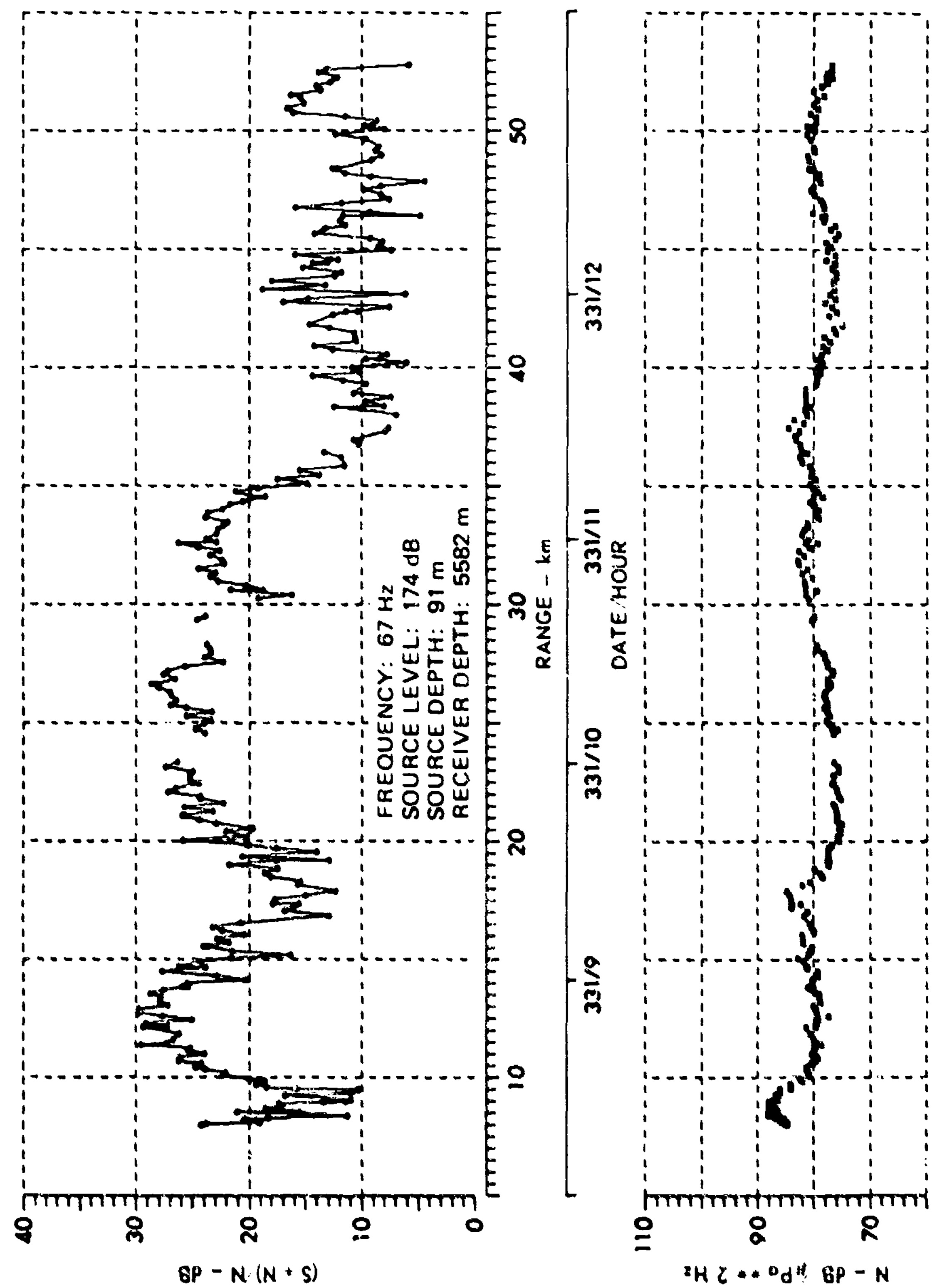

FIGURE 3.17
NOISE AND SIGNAL EXCESS FOR 5582 m RECEIVER AT 67 Hz
CHURCH STROKE II - PHASE 2 SITE EN (U)

ARL:UT
AS-78-1799
KCF - GA
11-30-78

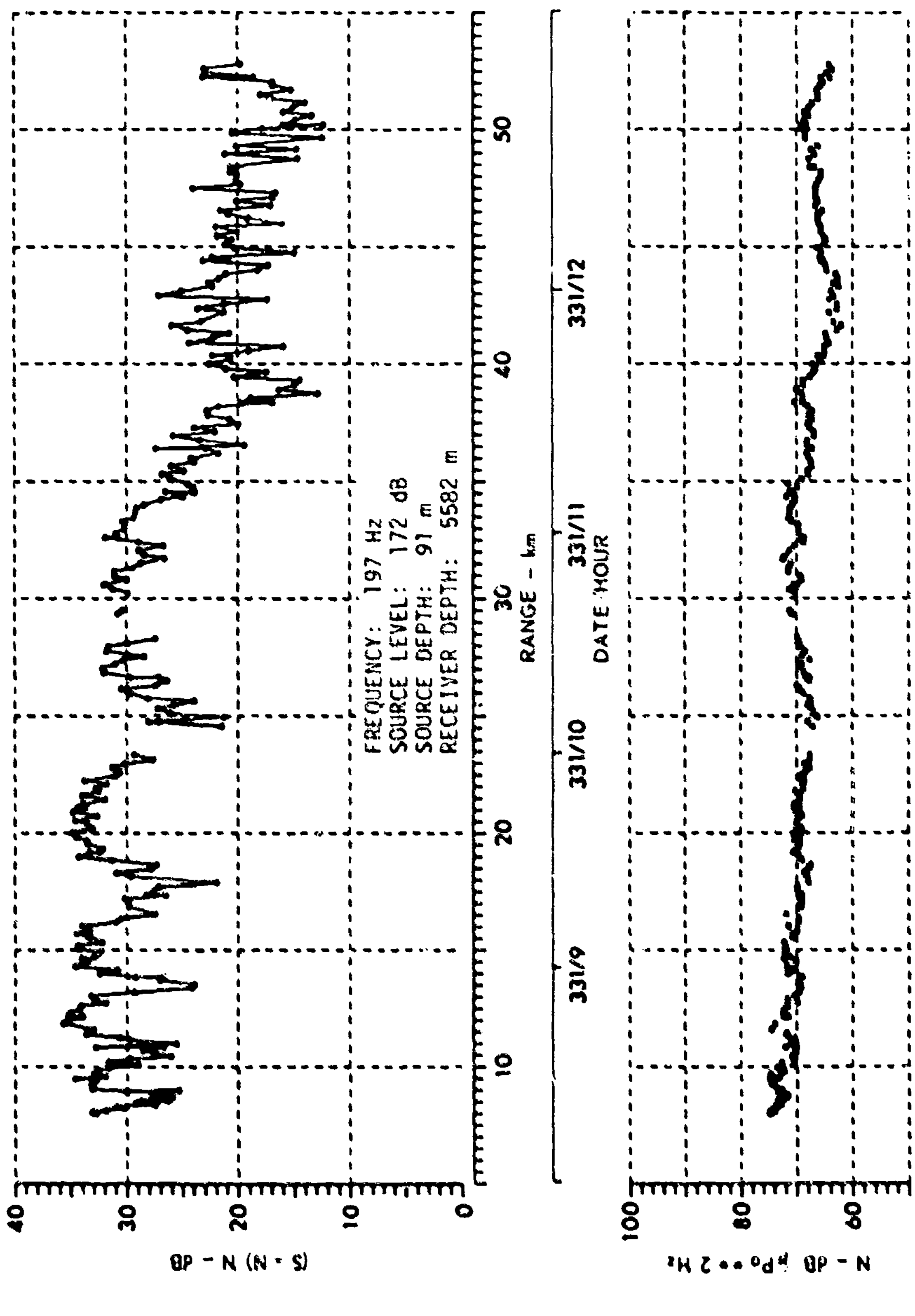

FIGURE 3.18
NOISE AND SIGNAL EXCESS FOR 5582 m RECEIVER AT 197 Hz
CHURCH STROKE II · PHASE 2 SITE EN (U)

ARL·UT
AS-78-1801
KCF · GA
11-30-78

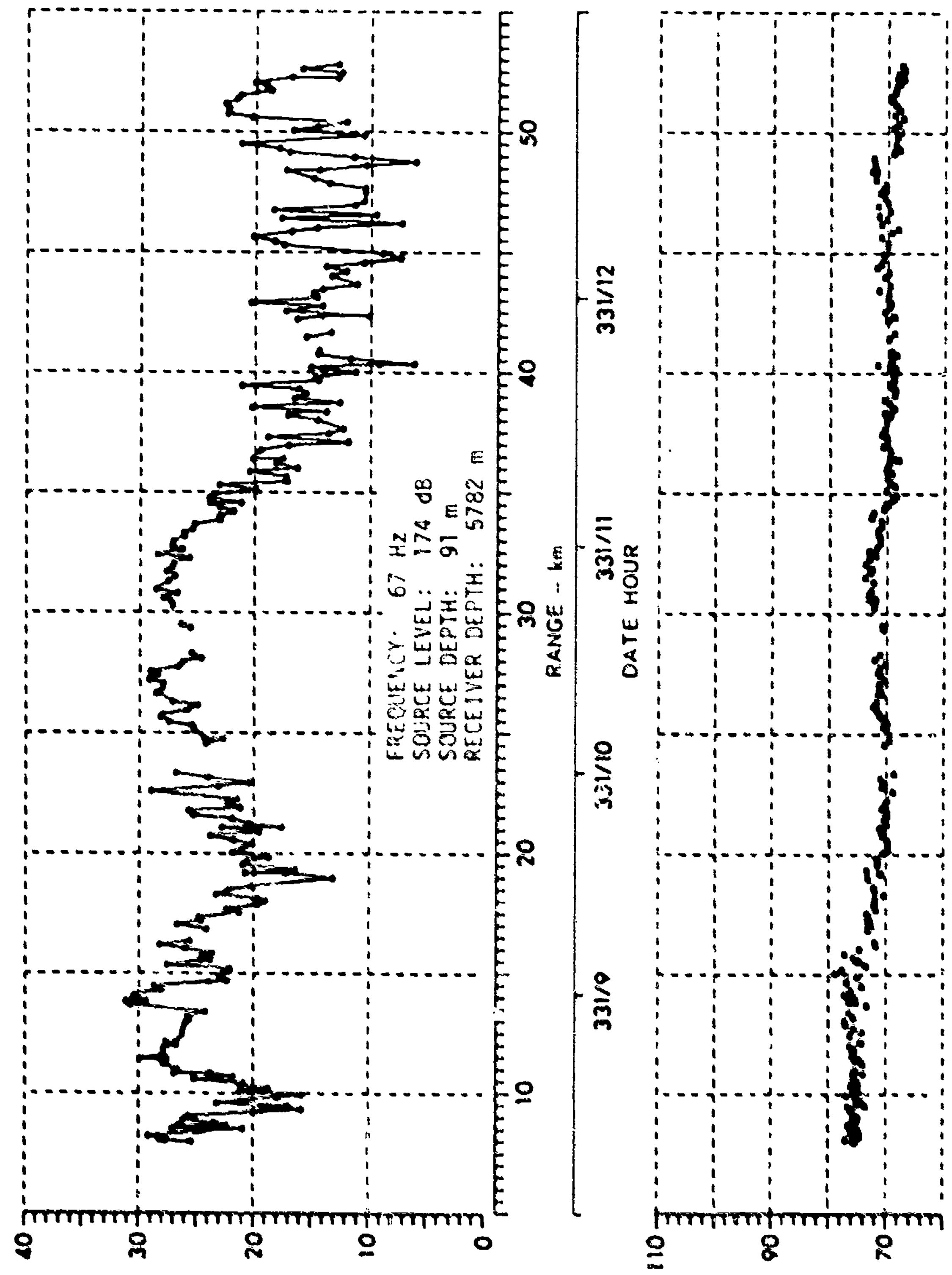

FIGURE 3.19
NOISE AND SIGNAL EXCESS FOR 5782 m RECEIVER AT 67 Hz
CHURCH STROKE II - PHASE 2 SITE EN (U)

ARL UT
AS-78-1803
KCF-GA
11-30-78

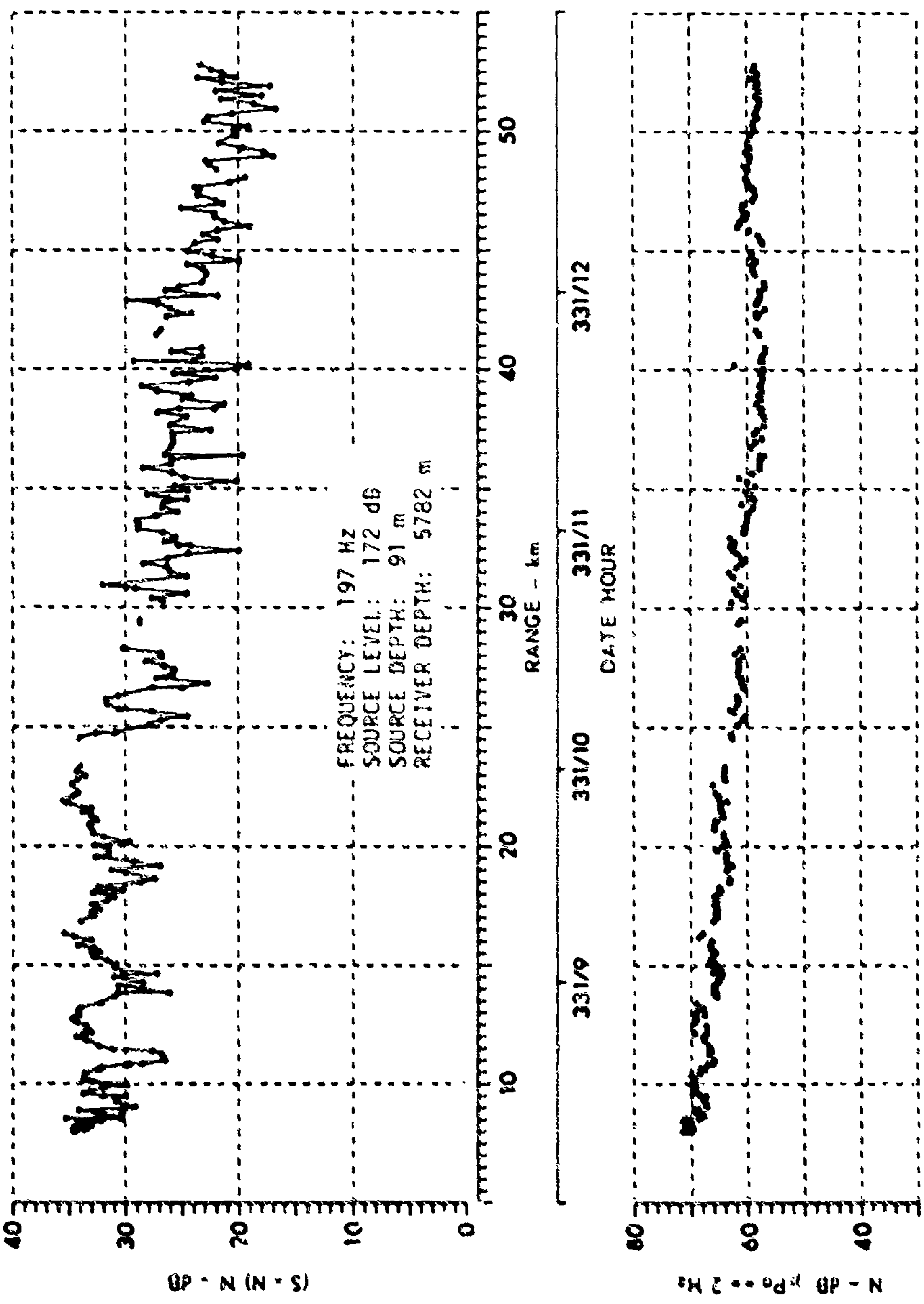

FIGURE 3.20
NOISE AND SIGNAL EXCESS FOR 5782 m RECEIVER AT 197 Hz
CHURCH STROKE II · PHASE 2 SITE EN (U)

ARL UT
AS-78-1805
KCF-GA
11-30-78

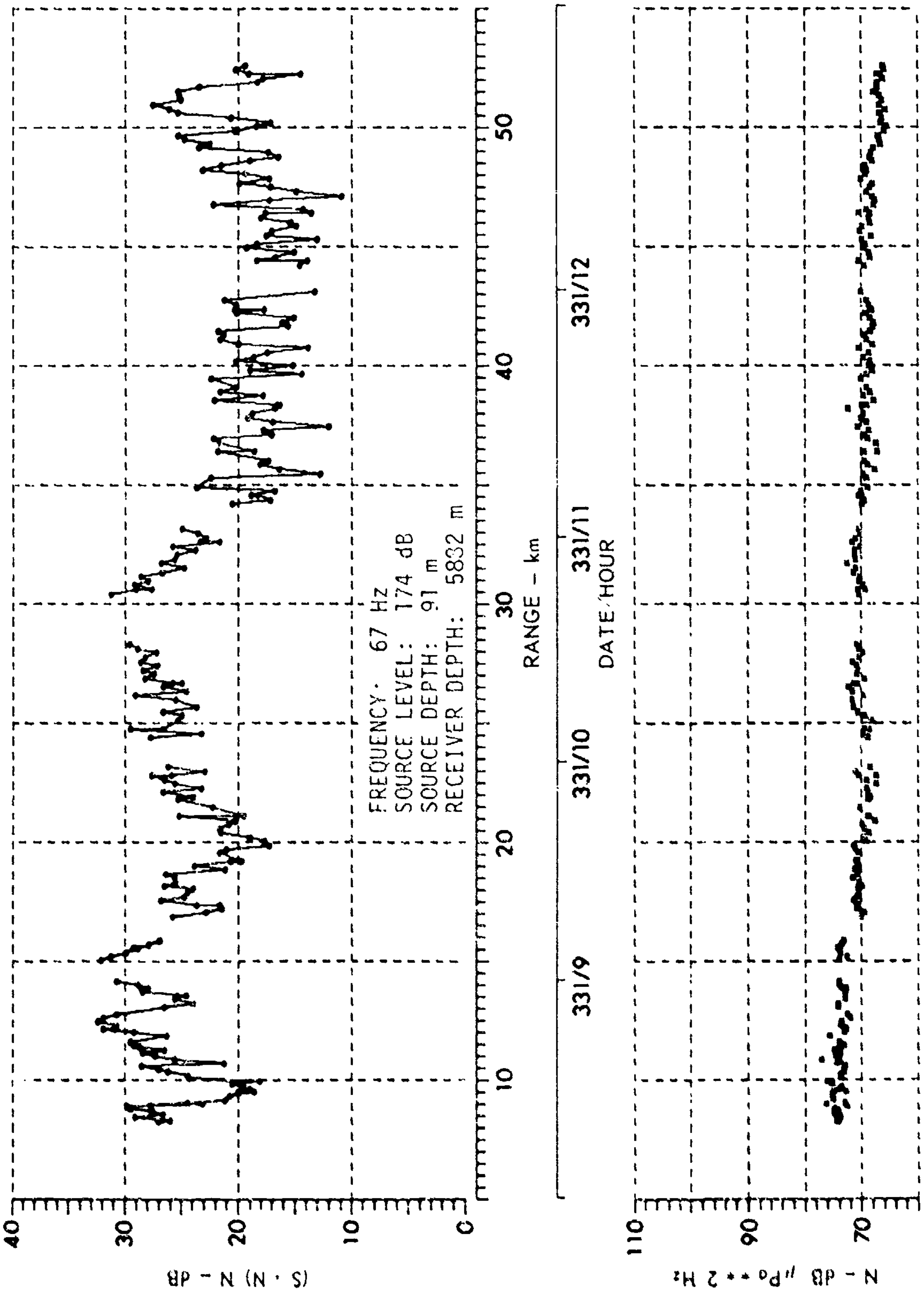

FIGURE 3.21
NOISE AND SIGNAL EXCESS FOR 5882 m RECEIVER AT 67 Hz
CHURCH STROKE II - PHASE 2 SITE EN (U)

ARL:UT
AS-78-1811
KCF-GA
11-30-78

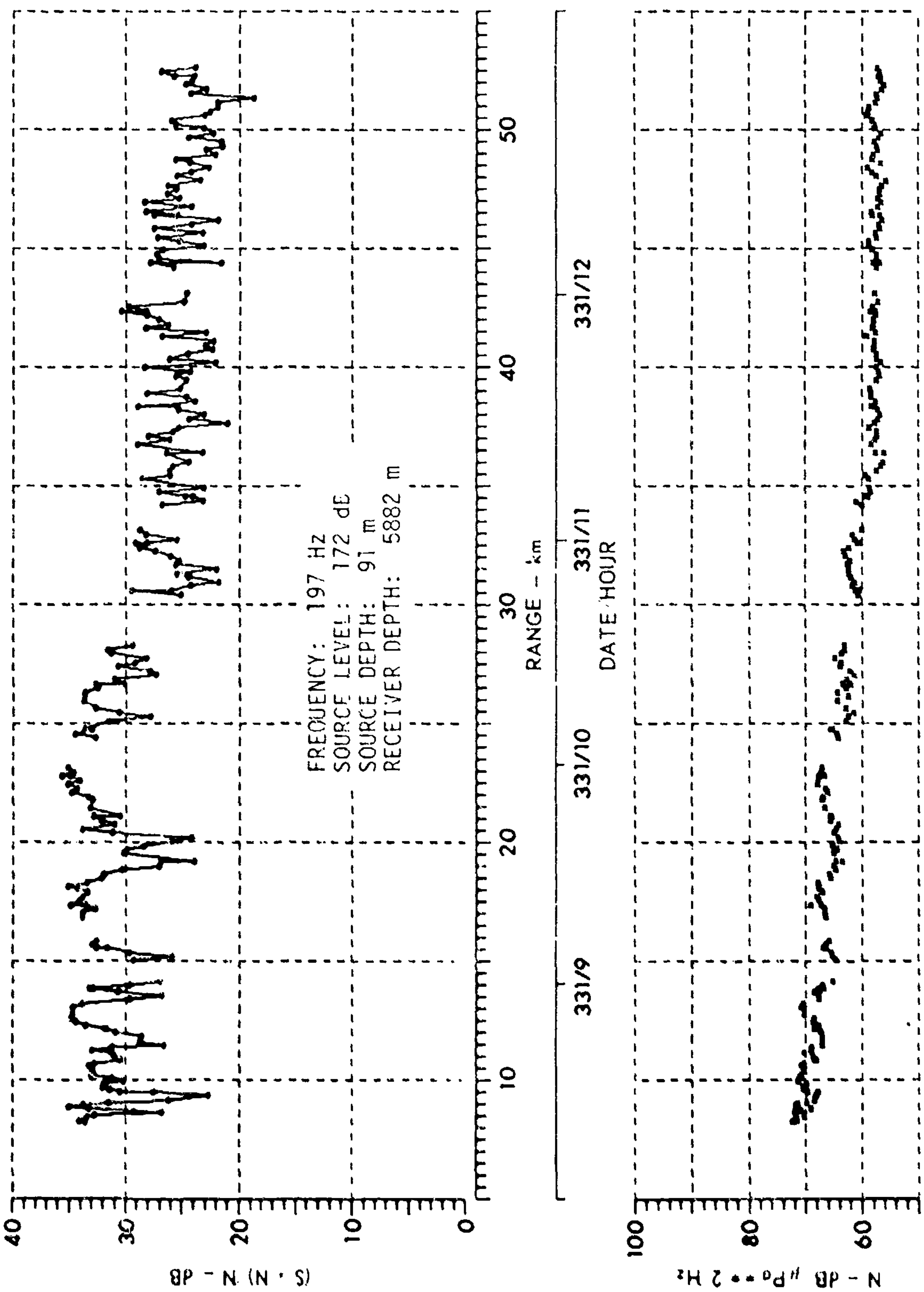

FIGURE 3.22
NOISE AND SIGNAL EXCESS FOR 5882 m RECEIVER AT 197 Hz
CHURCH STROKE II - PHASE 2 SITE EN (U)

ARL:UT
AS-78-1813
KCF - GA
11-30-78

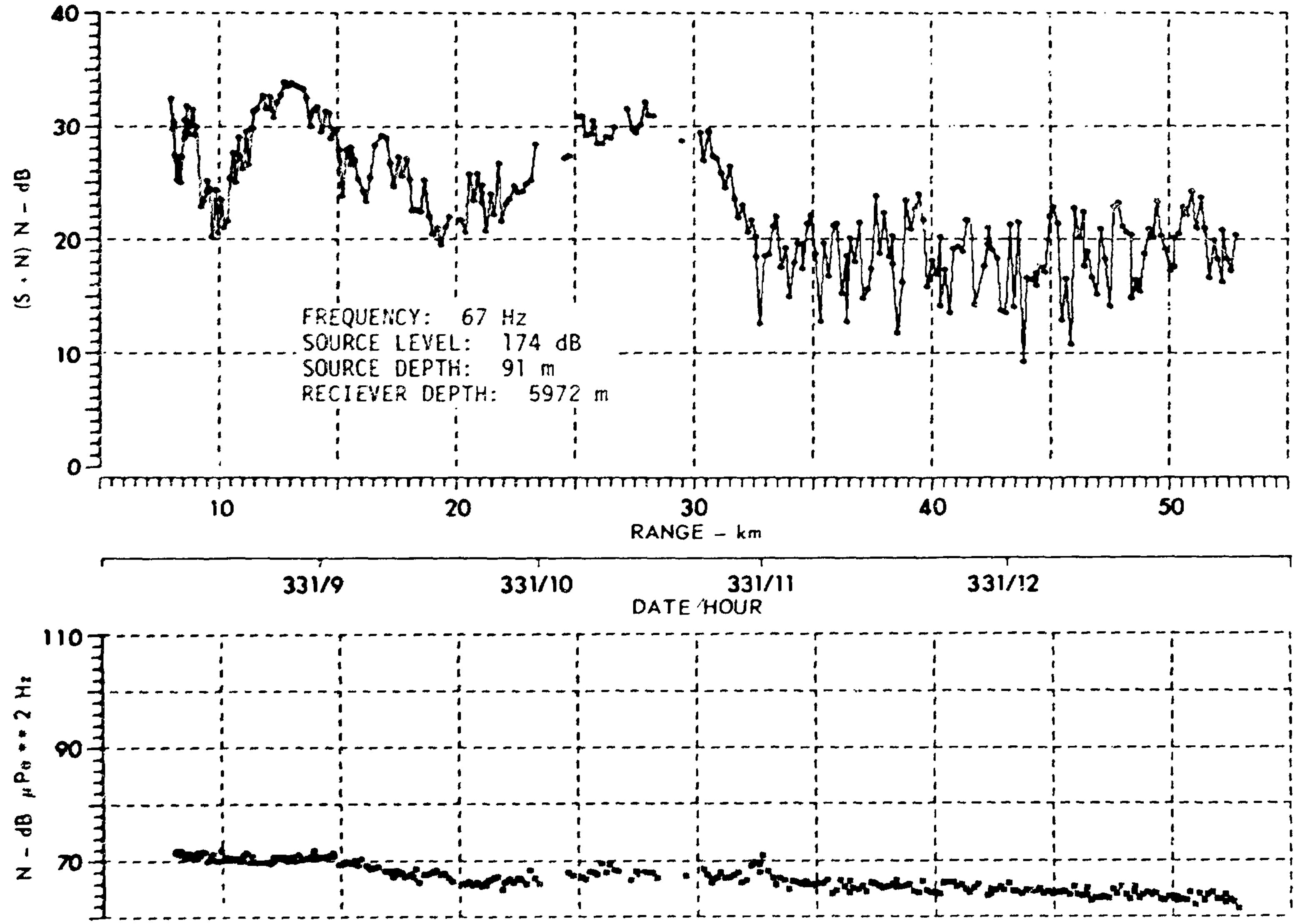

FIGURE 3.23
NOISE AND SIGNAL EXCESS FOR 5972 m RECEIVER AT 67 Hz
CHURCH STROKE II - PHASE 2 SITE EN (U)

ARL:UT
AS-78-1807
KCF-GA
11-30-78

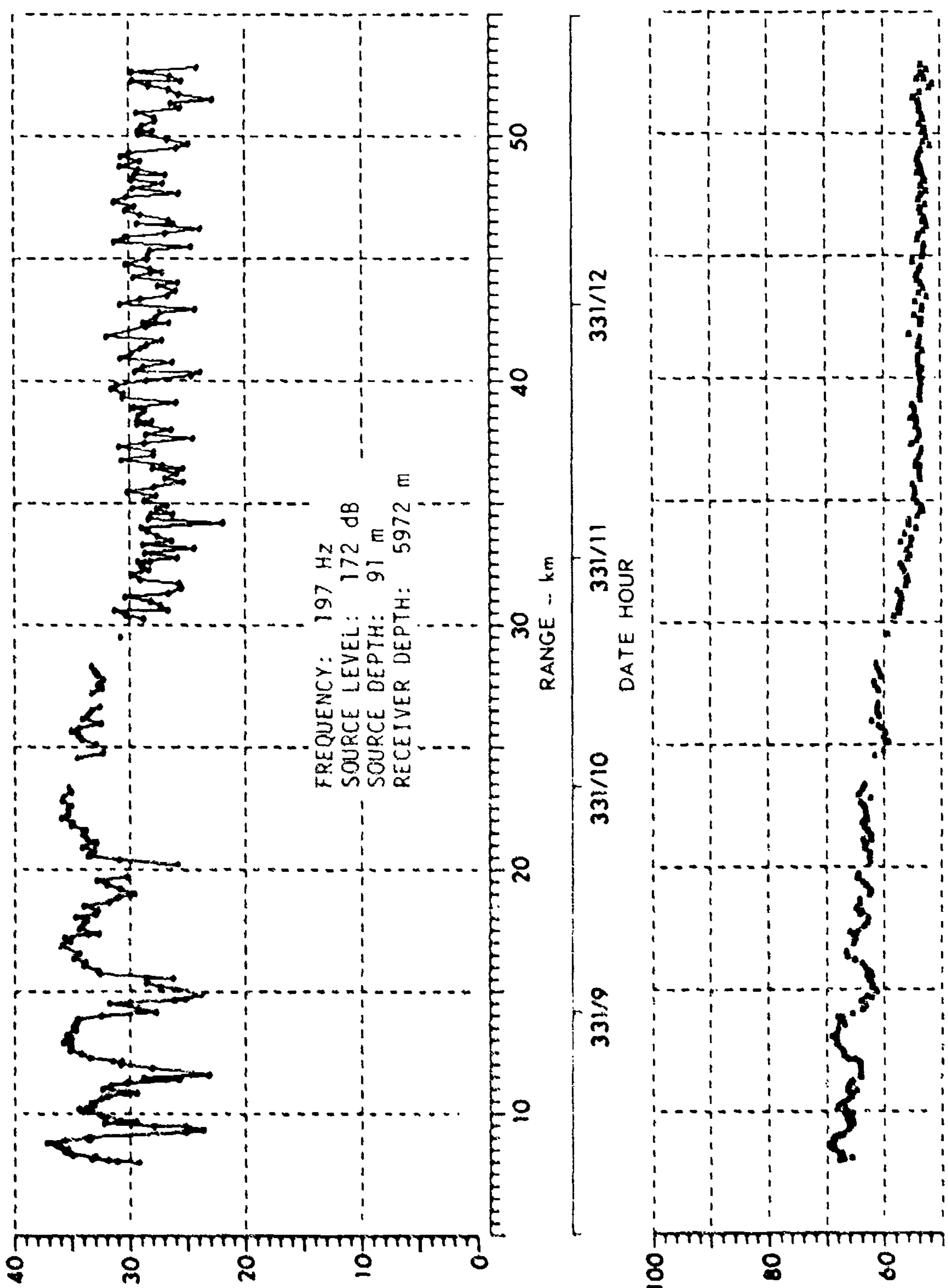

FIGURE 3.24
NOISE AND SIGNAL EXCESS FOR 5972 m RECEIVER AT 197 Hz
CHURCH STROKE II - PHASE 2 SITE EN (U)

ARL UT
AS-78-1809
KCF - GA
11-30-78

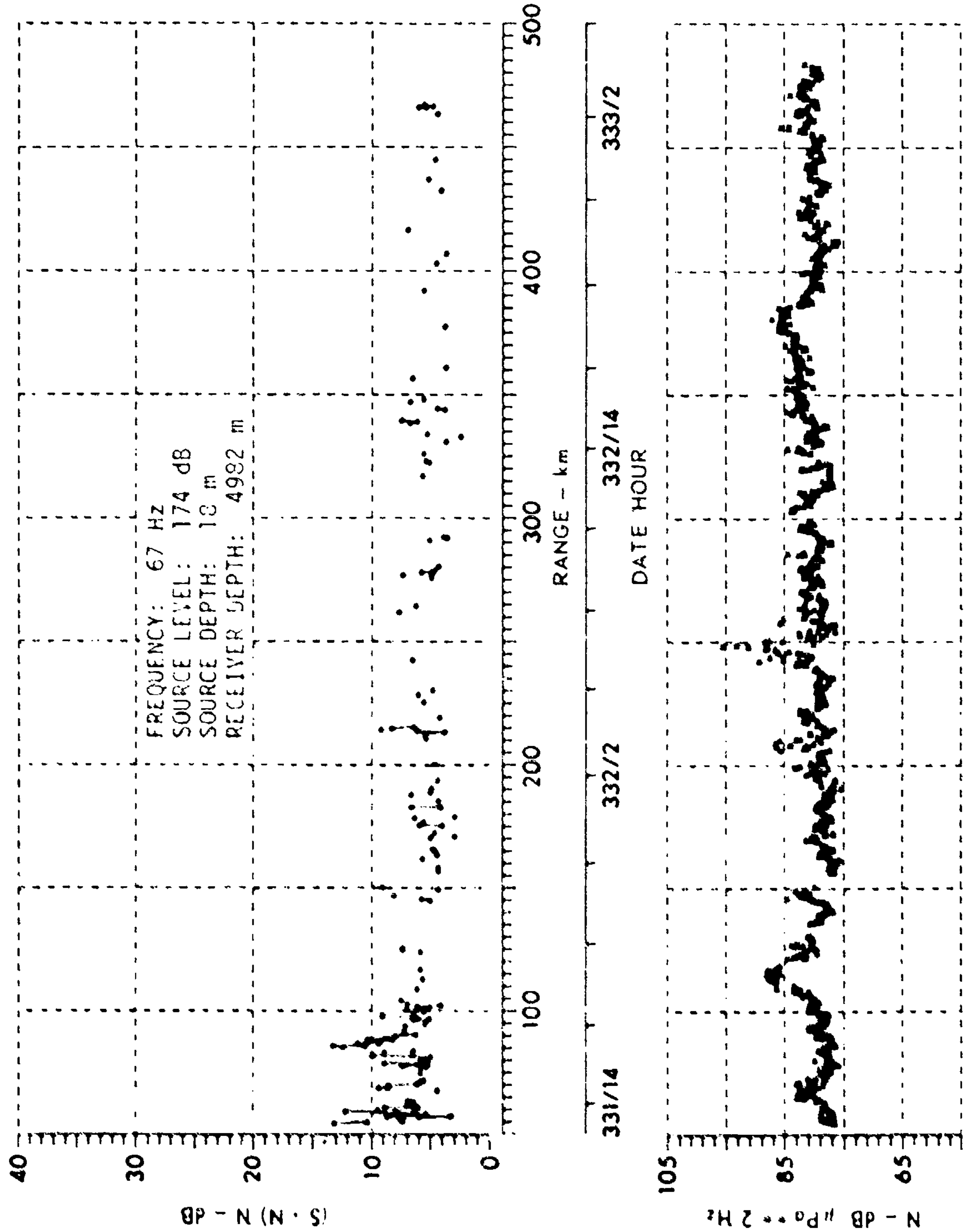

FIGURE 3.25
NOISE AND SIGNAL EXCESS FOR 4982 m RECEIVER AT 67 Hz
CHURCH STROKE II - PHASE 2 SITE EN (U)

ARL UT
AS-78-1796
KCF-GA
11-30-78

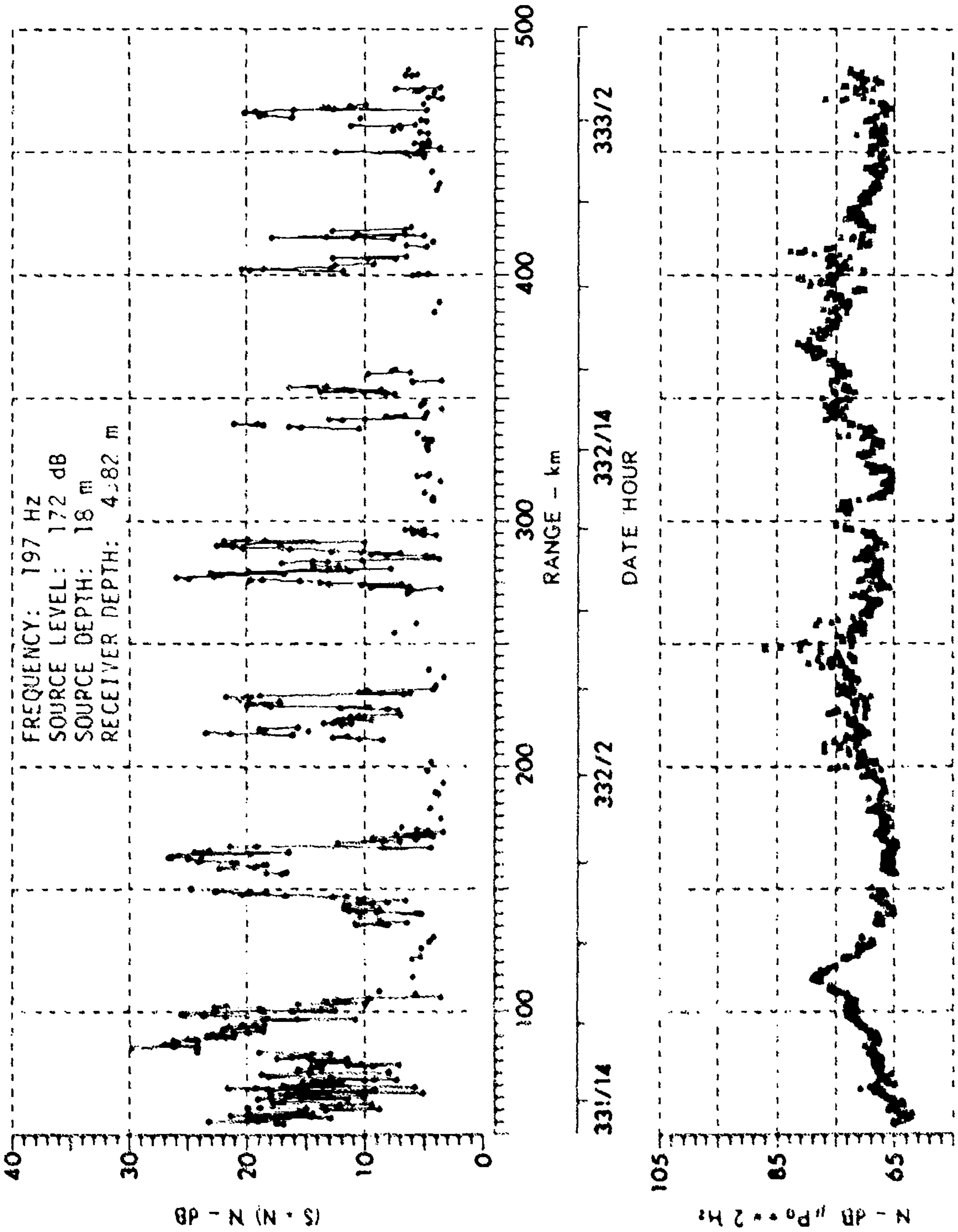

FIGURE 3.26
NOISE AND SIGNAL EXCESS FOR 4982 m RECEIVER AT 197 Hz
CHURCH STROKE II - PHASE 2 SITE EN (U)

ARL:UT
AS-78-1798
KCF - GA
11-30-78

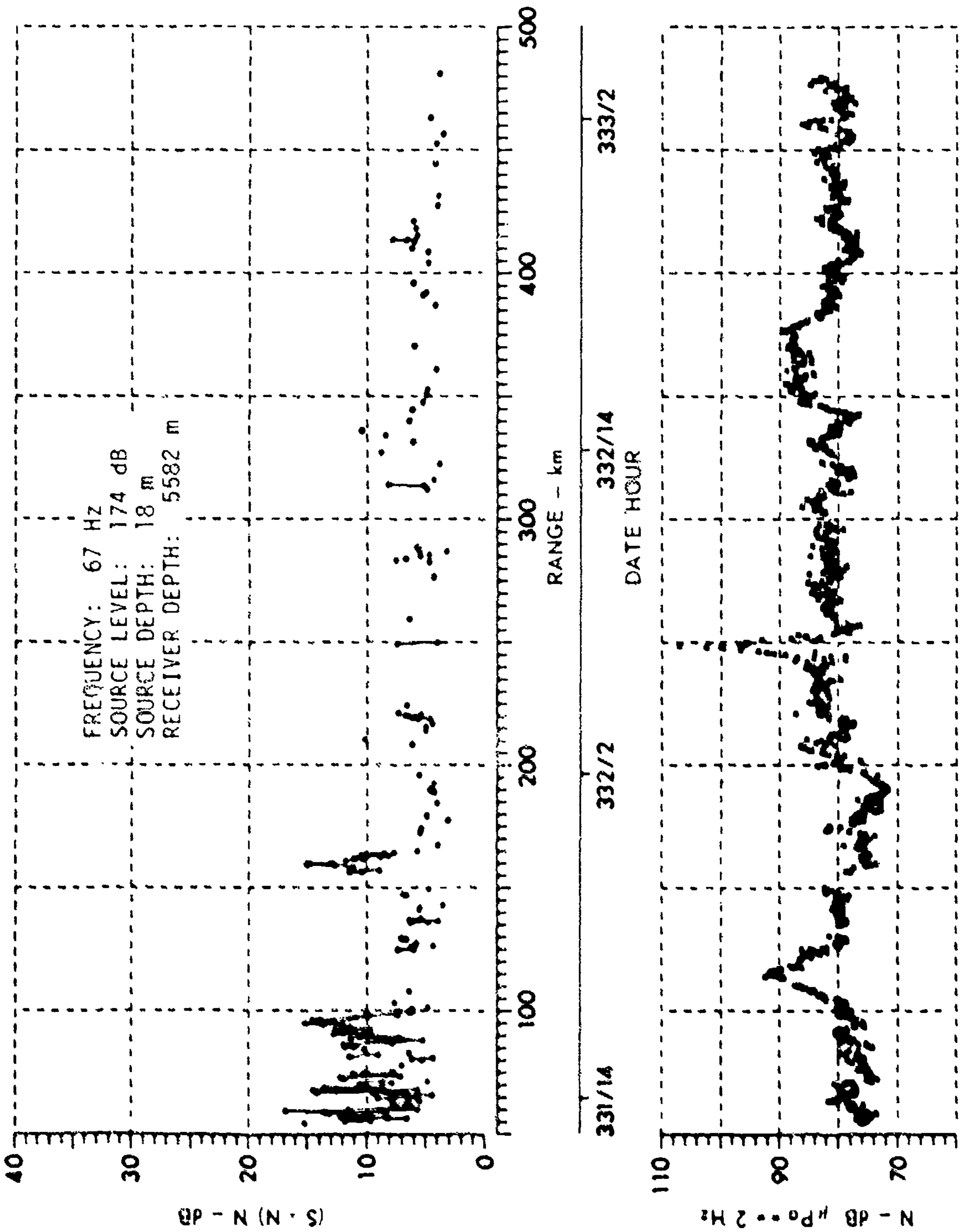

FIGURE 3.27
NOISE AND SIGNAL EXCESS FOR 5582 m RECEIVER AT 67 Hz
CHURCH STROKE II - PHASE 2 SITE EN (U)

ARL:UT
AS-78-1800
KCF-GA
11-30-78

CONFIDENTIAL

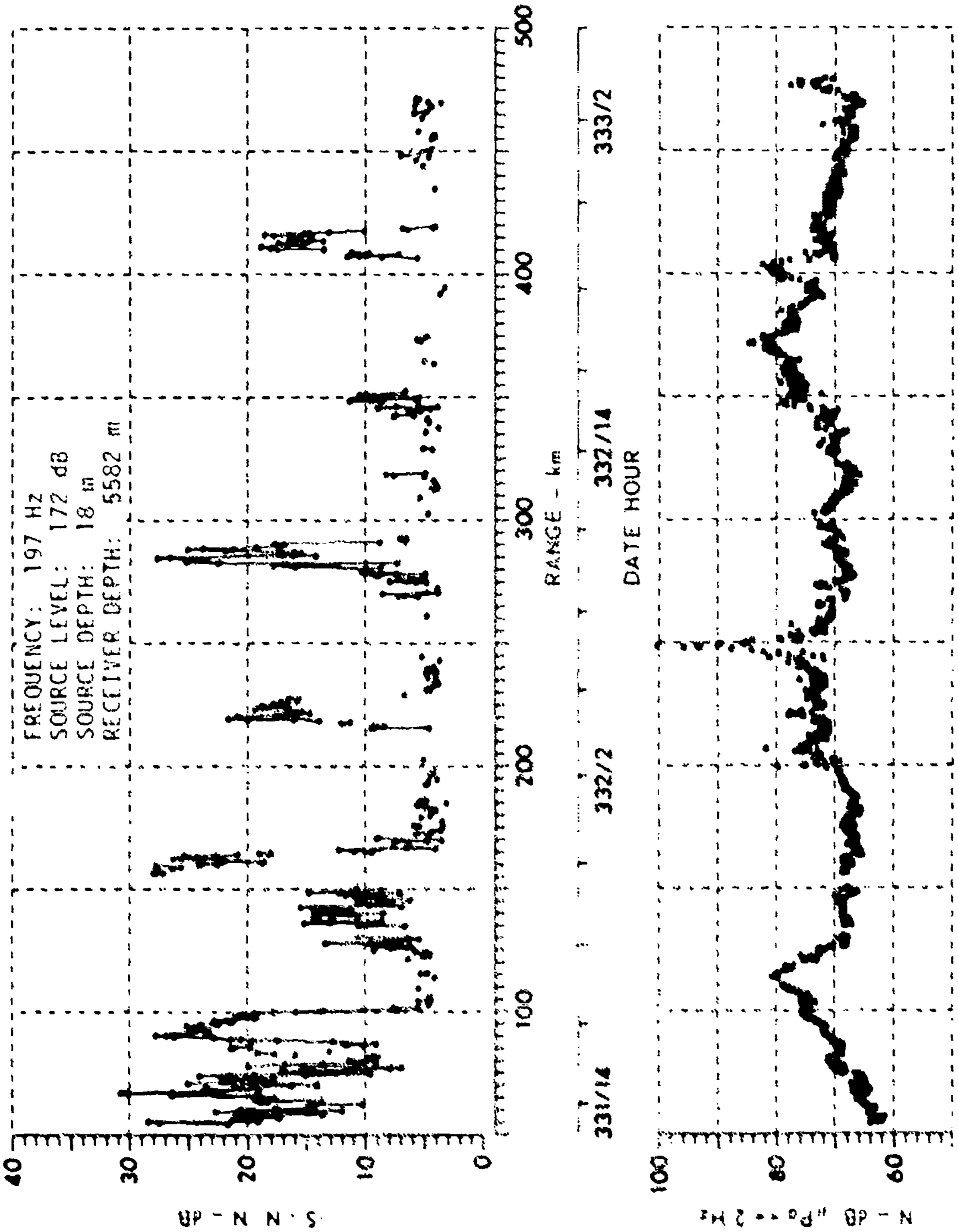

FIGURE 3.28
NOISE AND SIGNAL EXCESS FOR 5582 m RECEIVER AT 197 Hz
CHURCH STROKE II - PHASE 2 SITE EN (U)

ARL UT
AS-76-1802
KCF-GA
11-30-76

CONFIDENTIAL

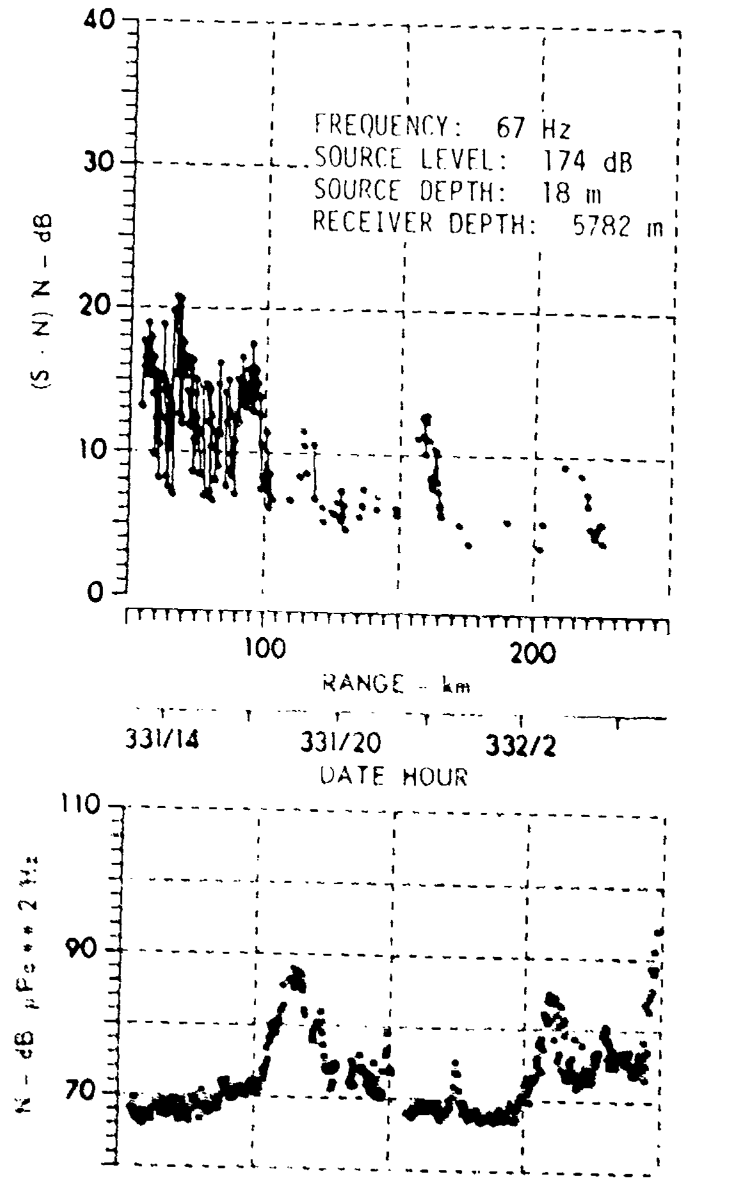

FIGURE 3.29
NOISE AND SIGNAL EXCESS FOR 5782 m RECEIVER AT 67 Hz
CHURCH STROKE II - PHASE 2 SITE EN (U)

ARL UT
AS-78-1804
KCF-GA
11-30-78

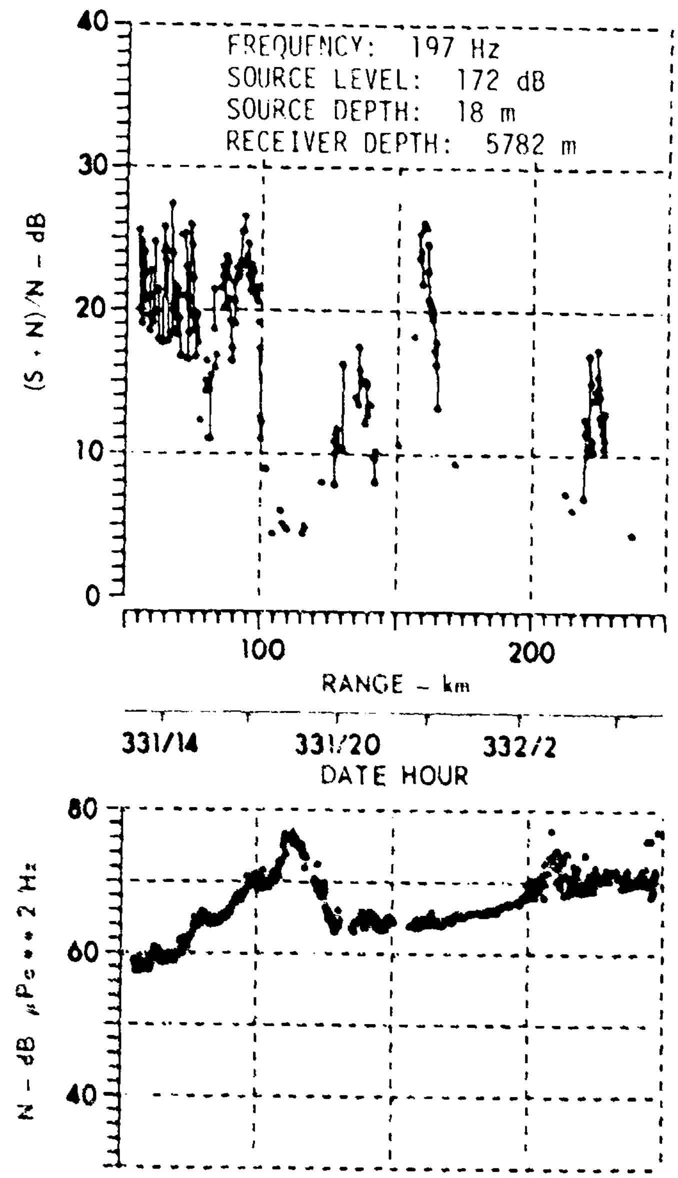

FIGURE 3.30
NOISE AND SIGNAL EXCESS FOR 5782 m RECEIVER AT 197 Hz
CHURCH STROKE II · PHASE 2 SITE EN (U)

ARL UT
AS-78-1806
KCF - GA
11-30-78

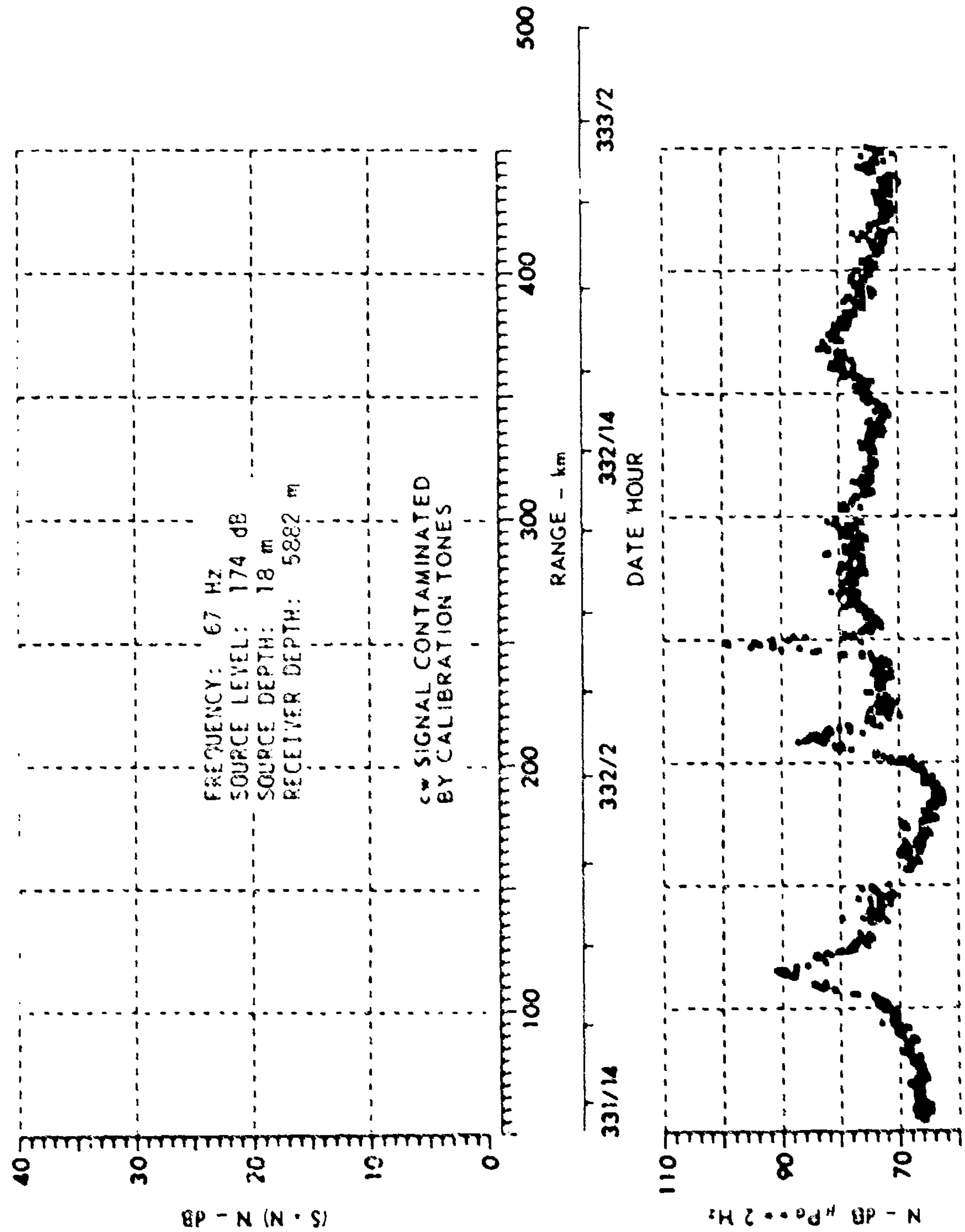

FIGURE 3.31
NOISE AND SIGNAL EXCESS FOR 5882 m RECEIVER AT 67 Hz
CHURCH STROKE II - PHASE 2 SITE EN (U)

ARL UT
AS-78-1812
KCF - GA
11-30-78

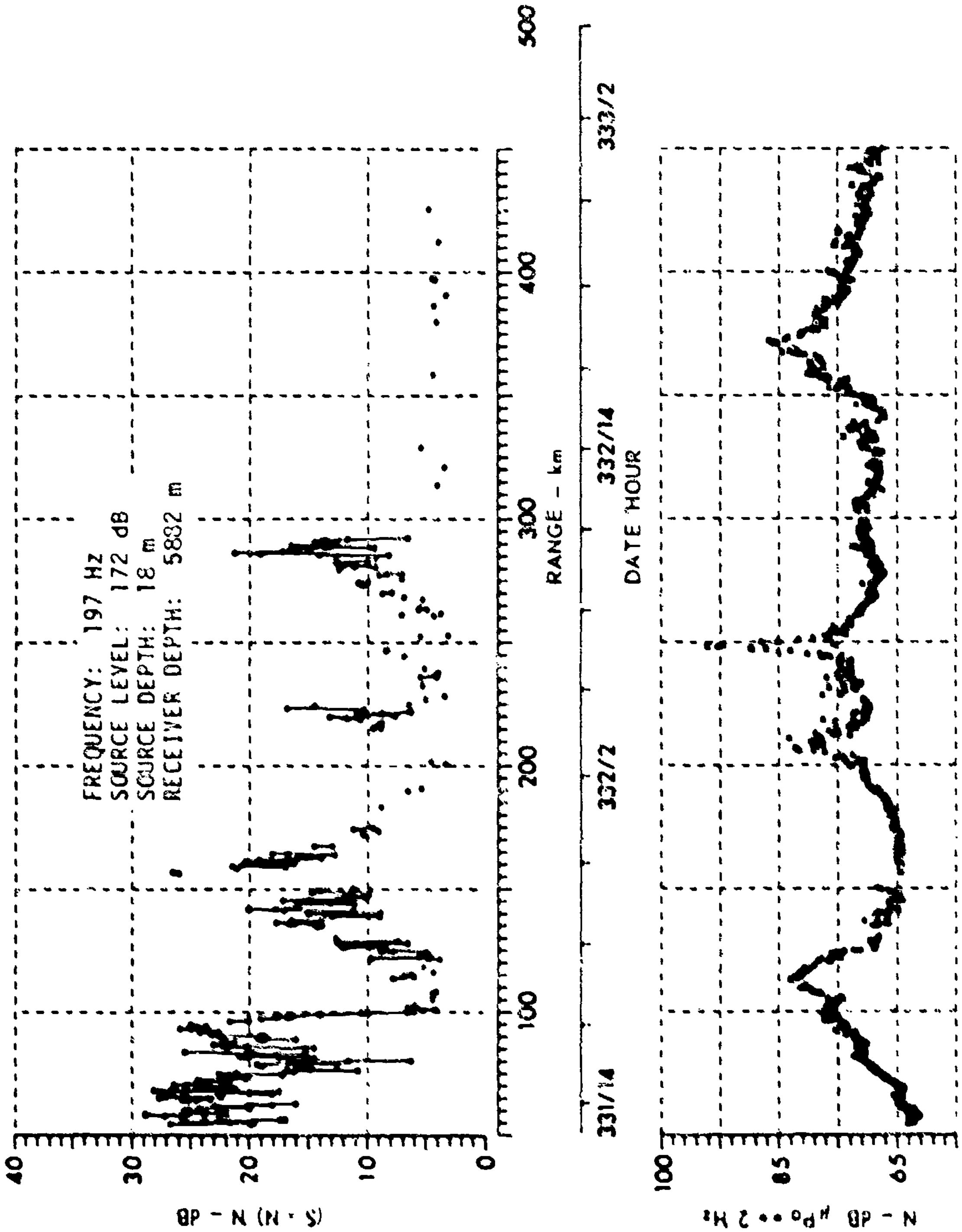

FIGURE 3.32
NOISE AND SIGNAL EXCESS FOR 5882 m RECEIVER AT 197 Hz
CHURCH STROKE II - PHASE 2 SITE EN (U)

ARL UT
AS-78-1814
KCF - GA
11-30-78

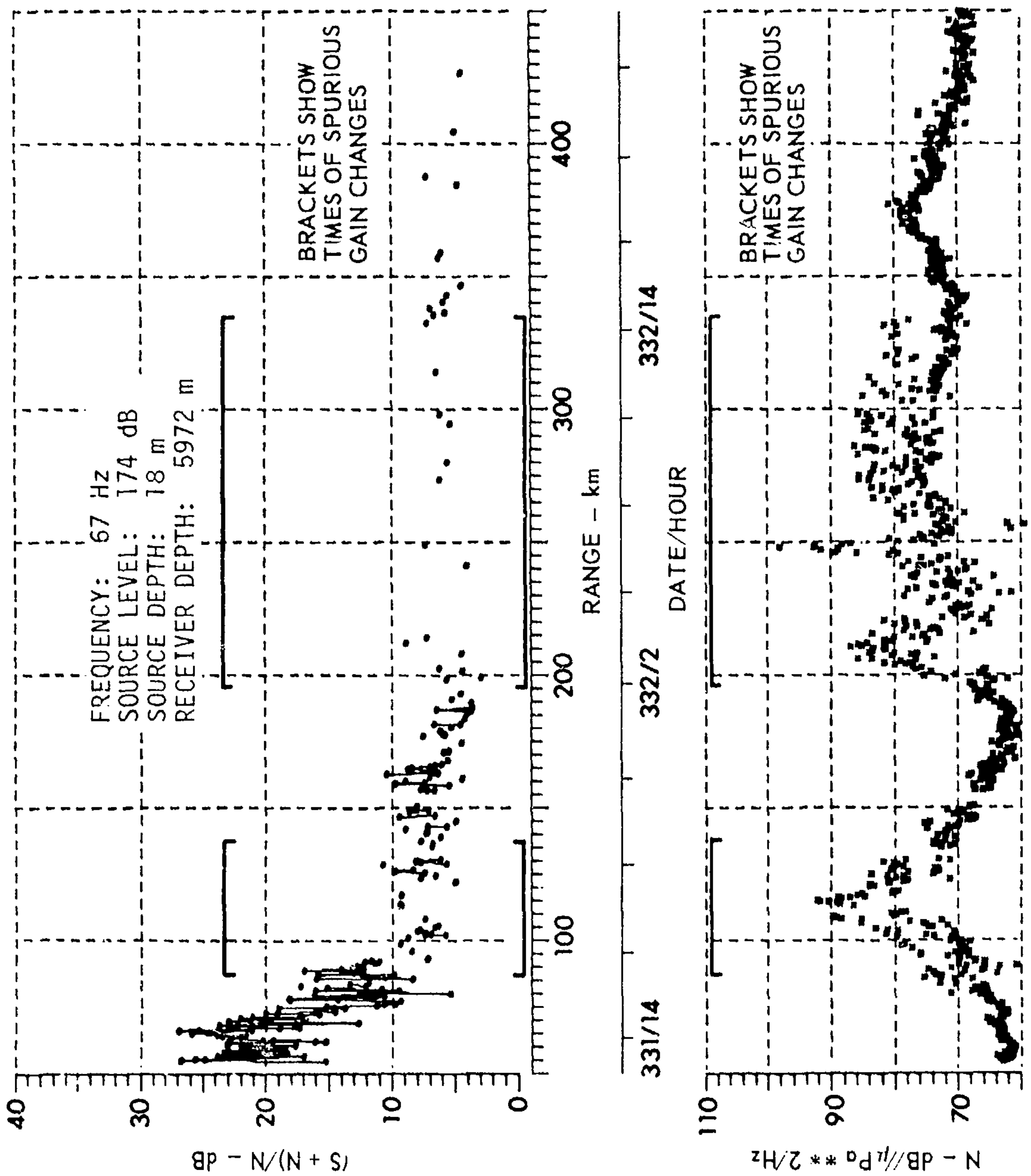

FIGURE 3.33
NOISE AND SIGNAL EXCESS FOR 5972 m RECEIVER AT 67 Hz
CHURCH STROKE II - PHASE 2 SITE EN (U)

ARL:UT
AS-78-1808
KCF - GA
11-30-78

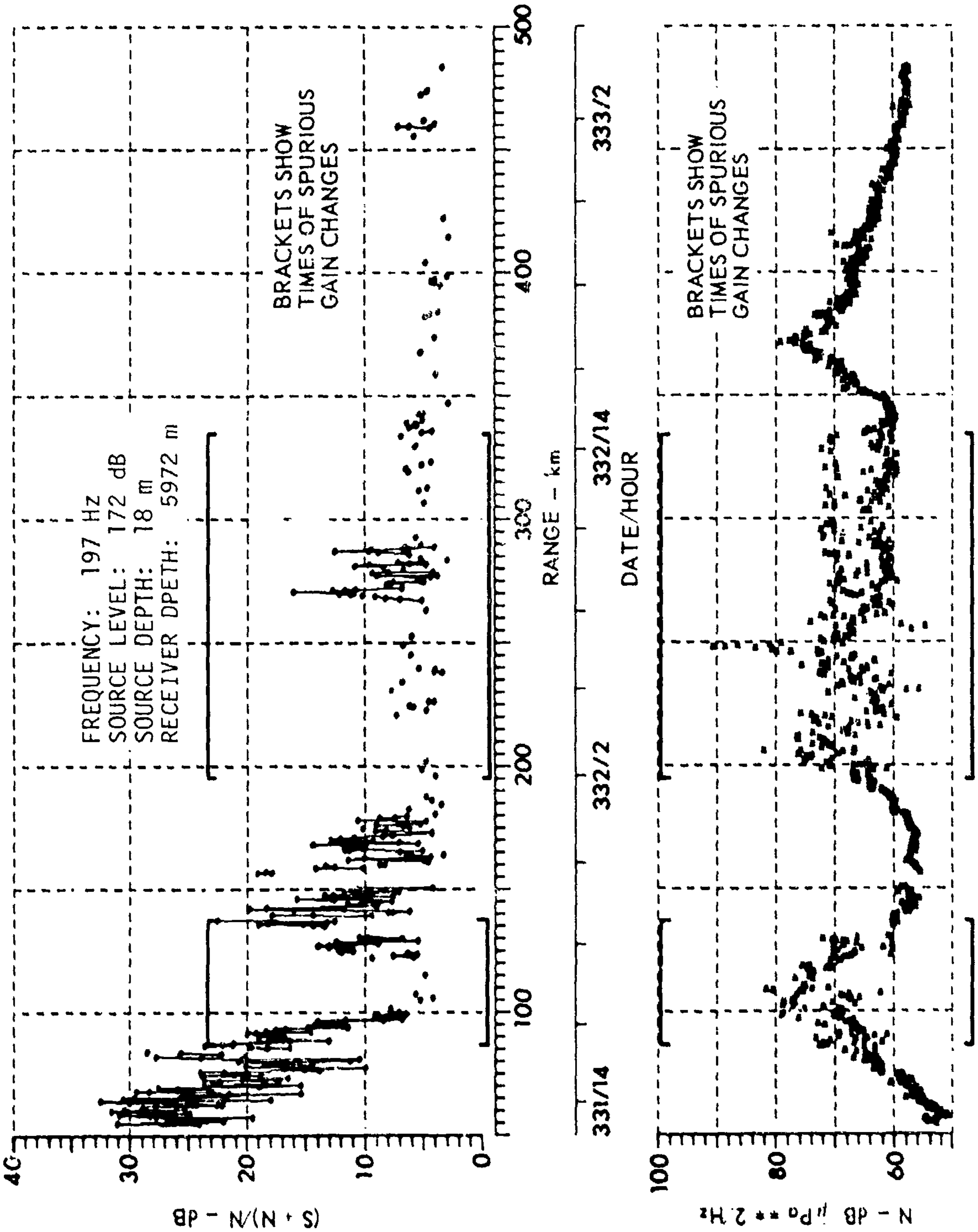

FIGURE 3.34
NOISE AND SIGNAL EXCESS FOR 5972 m RECEIVER AT 197 Hz
CHURCH STROKE II - PHASE 2 SITE EN (U)

ARL:UT
AS-78-1810
KCF-GA
11-30-78

(U) Propagation loss at 50, 100, and 200 Hz from SUS run 3 are shown in Figs. 3.35, 3.36, and 3.37, respectively; the southern leg of that run is along the cw projector track. Results from runs 1 and 2 at the same frequencies are shown in Figs. 3.38 through 3.40.

(C) Remember that "S" means that some of the signal saturated the ACODAC; the cw propagation loss data of Figs. 3.5 through 3.14 provide a better estimate of propagation in the basin near Site EN. However, note in Fig. 3.1 that runs 2 and 3 cross from the basin into a more irregular region at approximately 400 km range from Site EN; run 1 is entirely in that region. The SUS data of Figs. 3.35 through 3.40 show that propagation is abruptly blocked at approximately 420 km on run 3, and at 450 km on run 2. That is, the recorded signals change from saturated to undetected, with perhaps one unsaturated shot in between. No shots from SUS run 1 were detected.

3.3 Ambient Noise at Site EN

(U) Ambient noise recorded by ACODAC during the period 331/6 through 333/6 has been processed and also noise recorded by PAR (see Appendix A) during the period 337/0 through 340/12. Several displays of ambient noise information are presented: noise time series, percentile levels versus frequency, percentile levels during an interval of stable noise, displays of minimum noise level versus depth and frequency, and spectra generated by Typhoon Lucy.

(U) The spectral levels from the ACODAC in 1/10 octave bands versus time at the different receiver depths are shown in Figs. 3.41 through 3.45. The distributions of noise at the receivers over the two-day period are shown by the percentile plots of Figs. 3.46 through 3.50.

(U) In all of the ambient noise data, system electronics noise is present below 10 Hz at least part of the time. Also, the percentile spectra of Fig. 3.49 is corrupted by a 10 Hz square wave calibration signal which inadvertantly turned on during the data perio . The 10 Hz signal and its

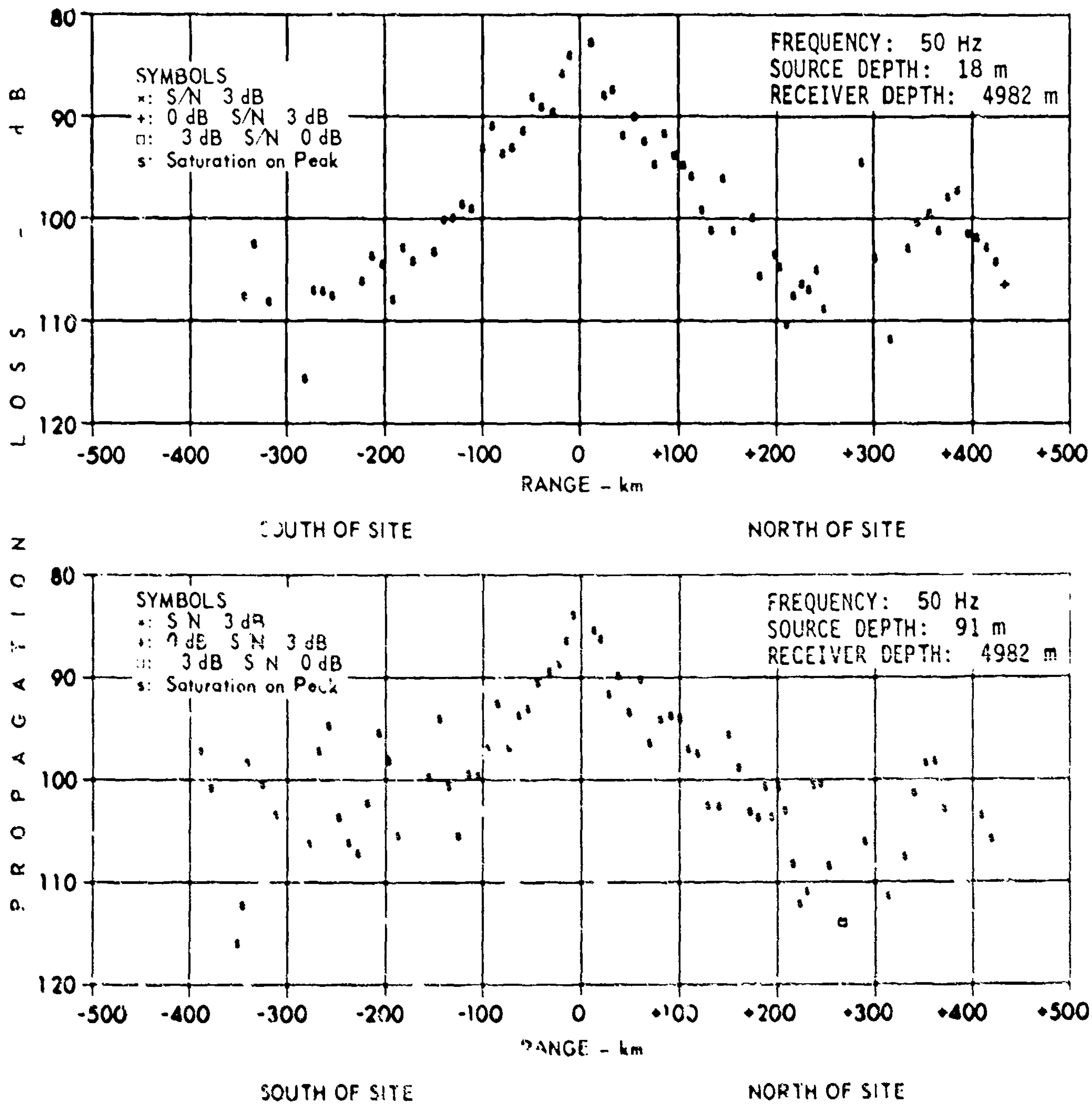

FIGURE 3.35
PROPAGATION LOSS AT 50 Hz*
CHURCH STROKE II - SITE EN (U)
RADIAL RUN 3
18 m AND 91 m SUS

ARL UT
AS-78-1939
KCF - GA
12 - 12 - 78

*SATURATED - SEE TEXT

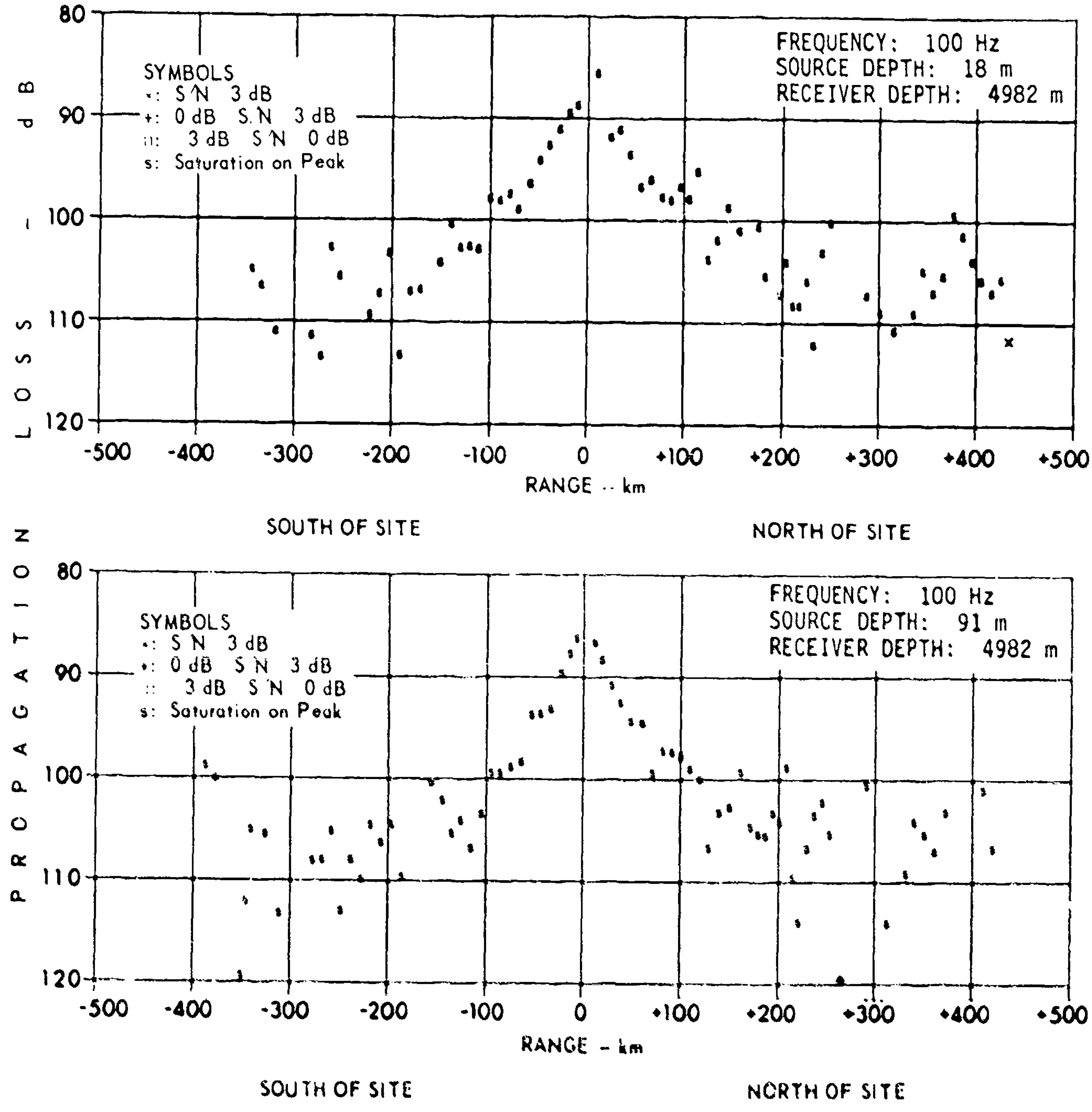

FIGURE 3.36
PROPAGATION LOSS AT 100 Hz*
CHURCH STROKE II - SITE EN (U)
RADIAL RUN 3
18 m AND 91 m SUS

ARL UT
AS-78-1941
KCF - GA
12-12-78

*SATURATED -- SEE TEXT

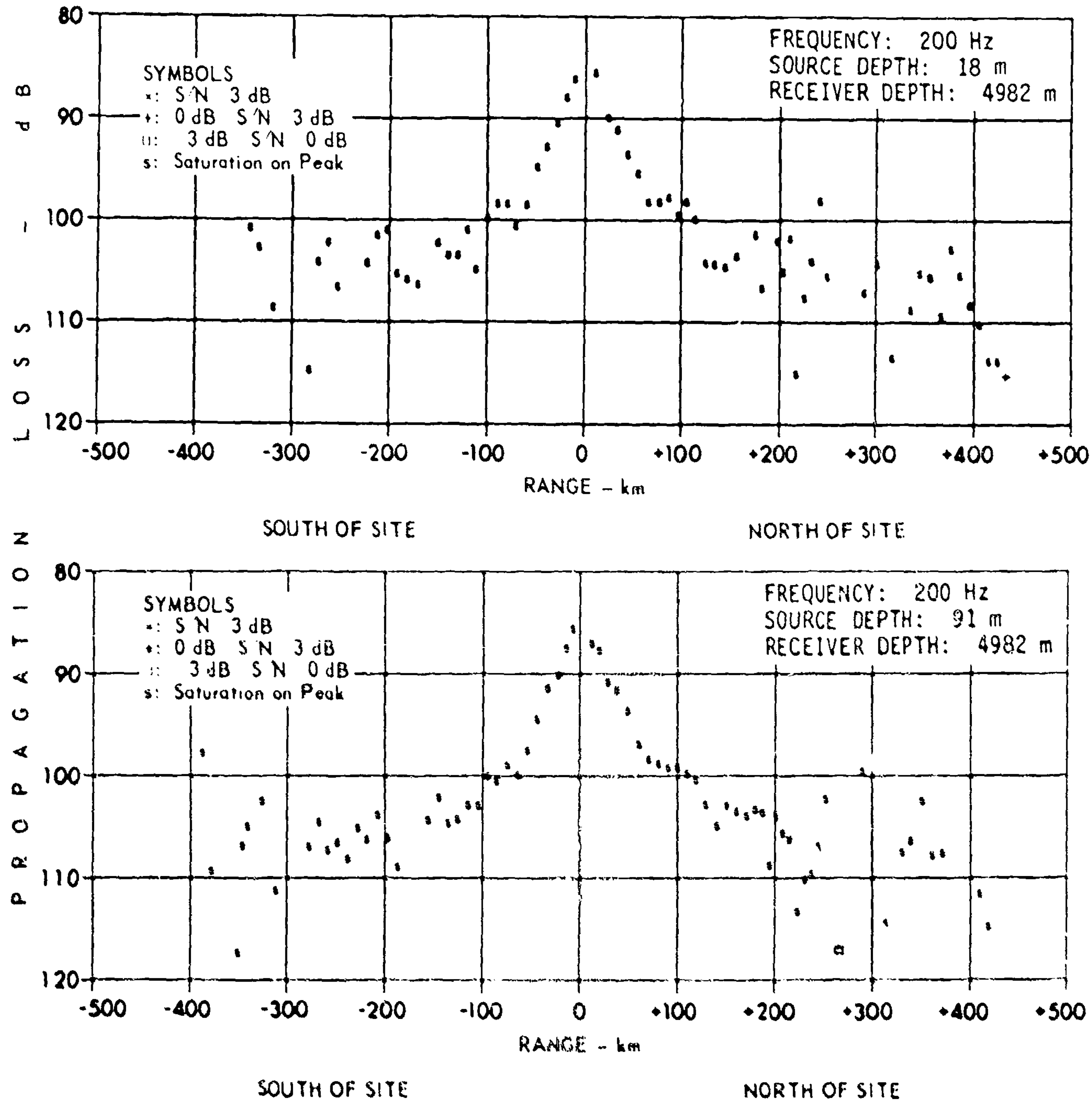

FIGURE 3.37
PROPAGATION LOSS AT 200 Hz*
CHURCH STROKE II-SITE EN (U)
RADIAL RUN 3
18 m AND 91 m SUS

ARL UT
AS-78-1943
KCF - GA
12-12-78

*SATURATED – SEE TEXT

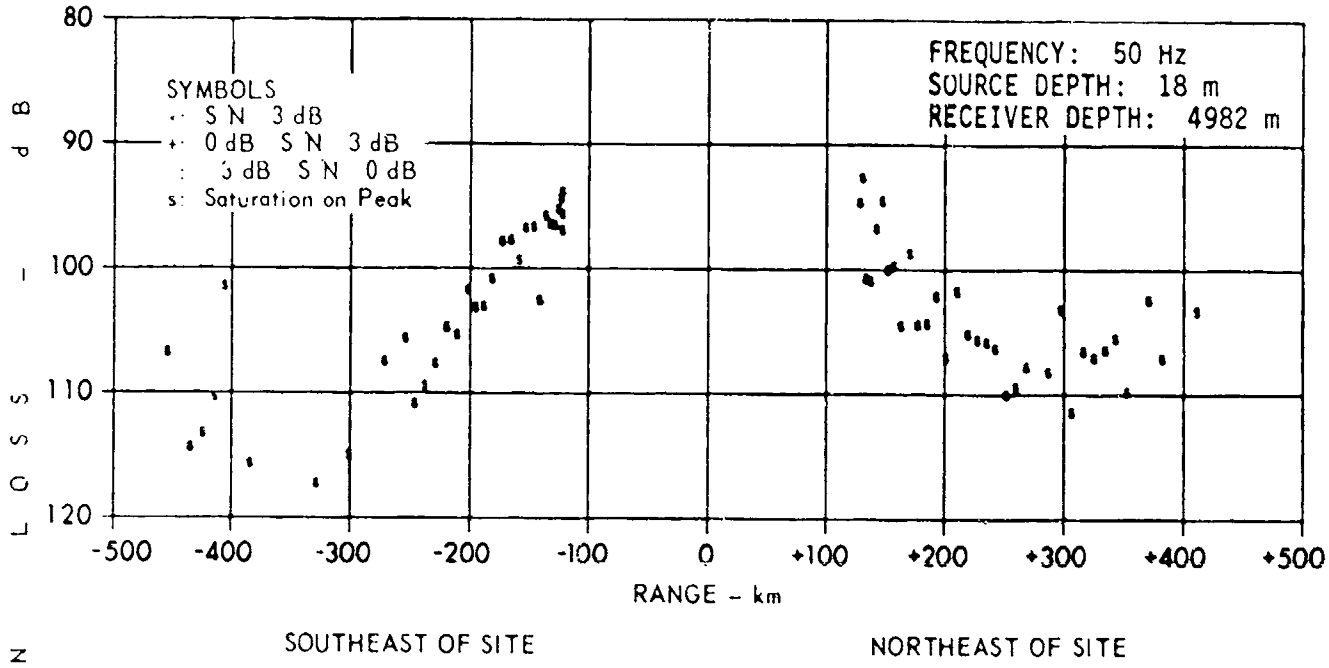

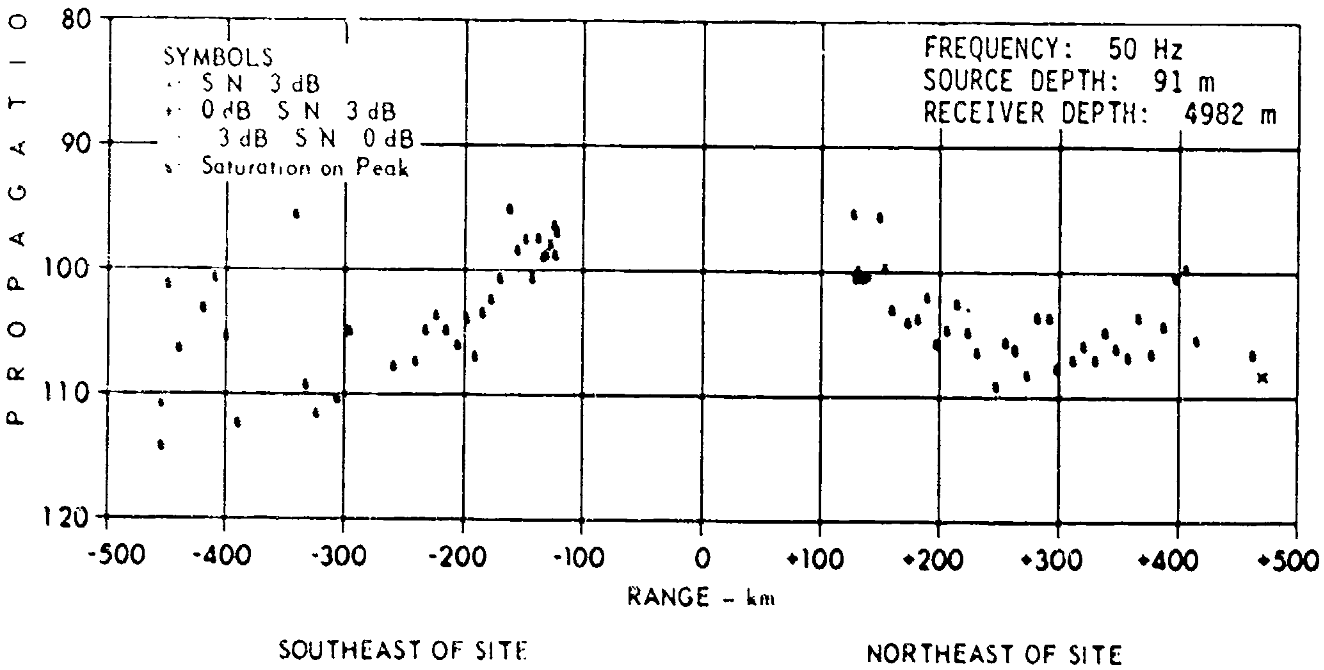

FIGURE 3.38
PROPAGATION LOSS AT 50 Hz*
CHURCH STROKE II · SITE EN (U)
NONRADIAL RUNS 1 AND 2
18 m AND 91 m SUS

ARL UT
AS-78-1947
KCF - GA
12-12-78

*SATURATED – SEE TEXT

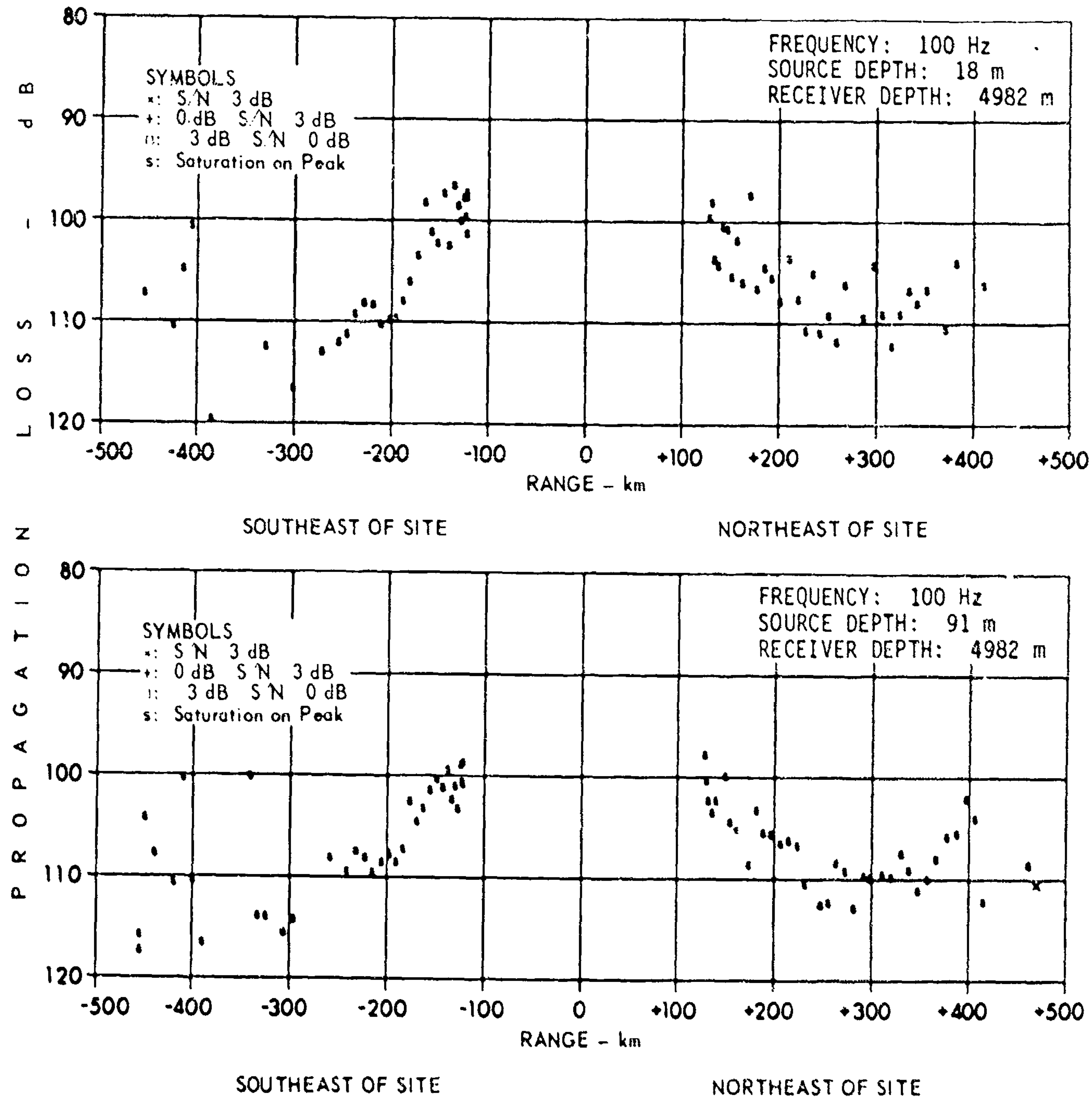

FIGURE 3.39
PROPAGATION LOSS AT 100 Hz*
CHURCH STROKE II - SITE EN (U)
NONRADIAL RUNS 1 AND 2
18 m AND 91 m SUS

ARL UT
AS-78-1949
KCF - GA
12-12-78

*SATURATED – SEE TEXT

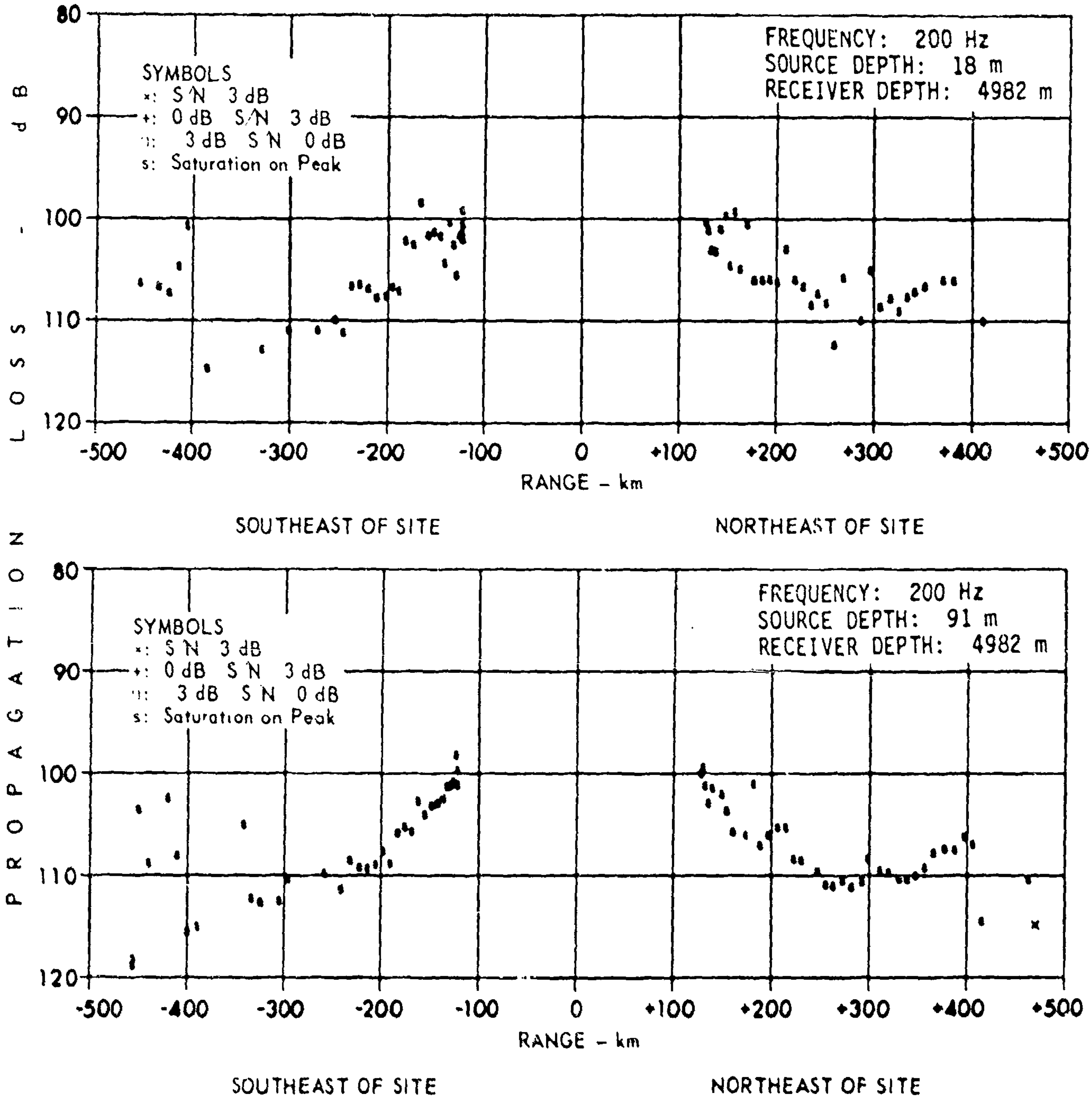

FIGURE 3.40
PROPAGATION LOSS AT 200 Hz*
CHURCH STROKE II - SITE EN (U)
NONRADIAL RUNS 1 AND 2
18 m AND 91 m SUS

ARL UT
AS-78-1951
KCF - GA
12 - 12 - 78

*SATURATED - SEE TEXT

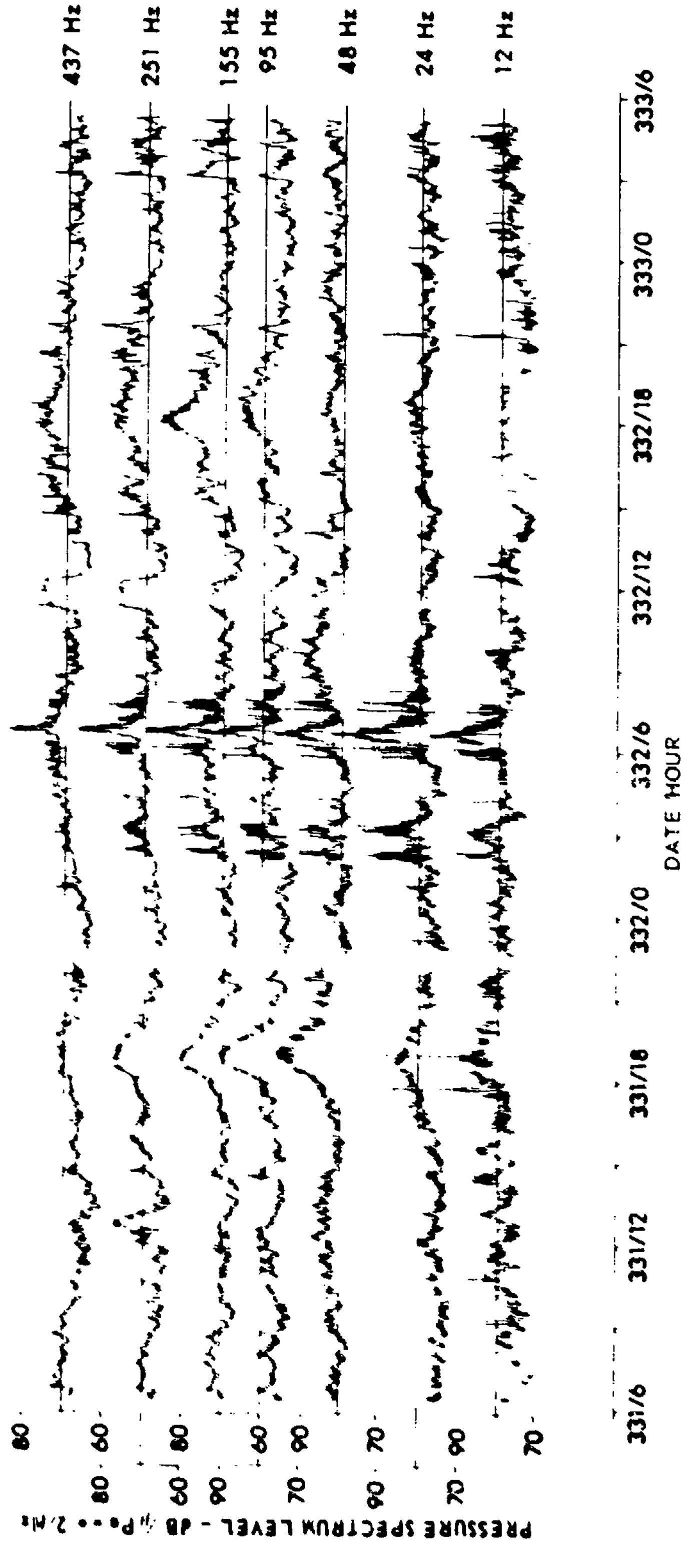

FIGURE 3.41
AMBIENT NOISE TIME SERIES - 4982 m RECEIVER
CHURCH STROKE II - SITE EN (U)

ARL UT
AS-78-1815
KCF - GA
11-30-78

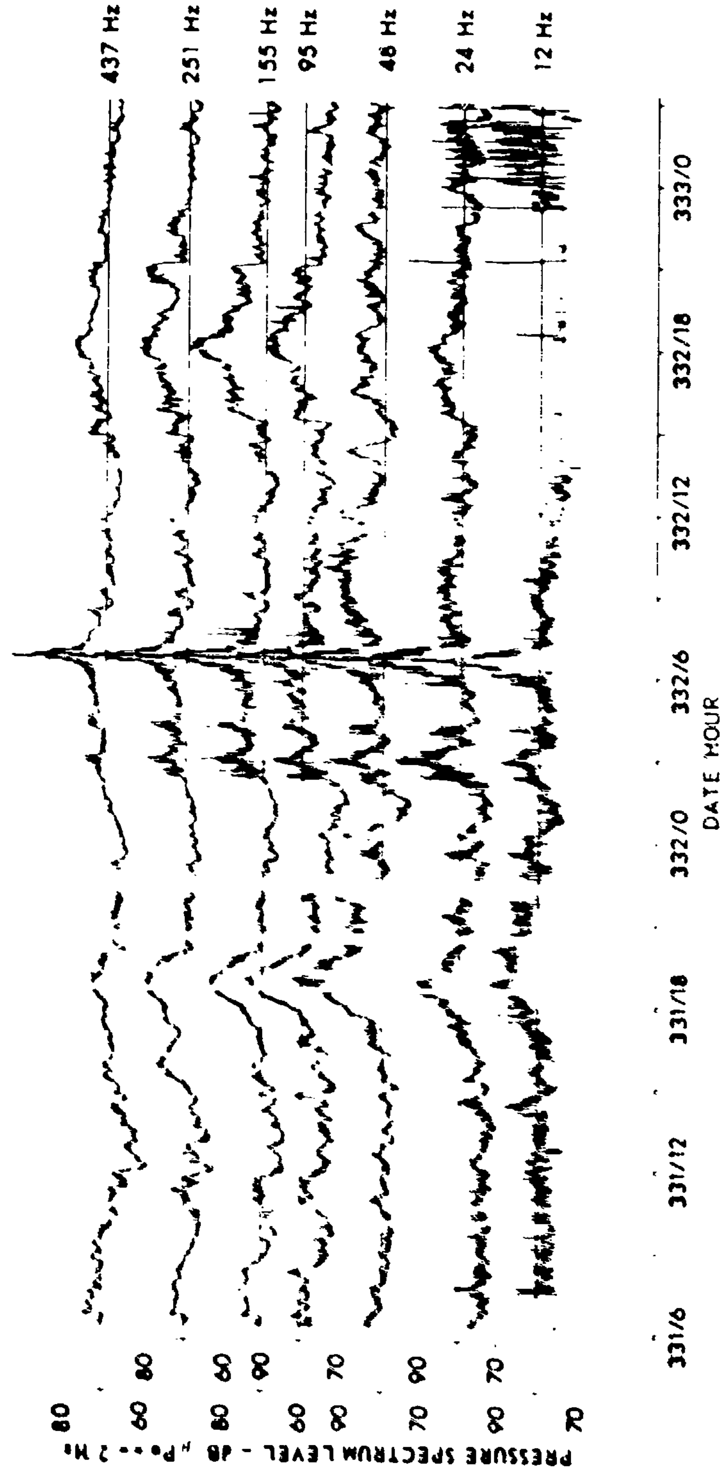

FIGURE 3.42
AMBIENT NOISE TIME SERIES - 5582 m RECEIVER
CHURCH STROKE II - SITE EN (U)

ARL UT
AS-78-1810
KCP-GA
11-30-78

CONFIDENTIAL

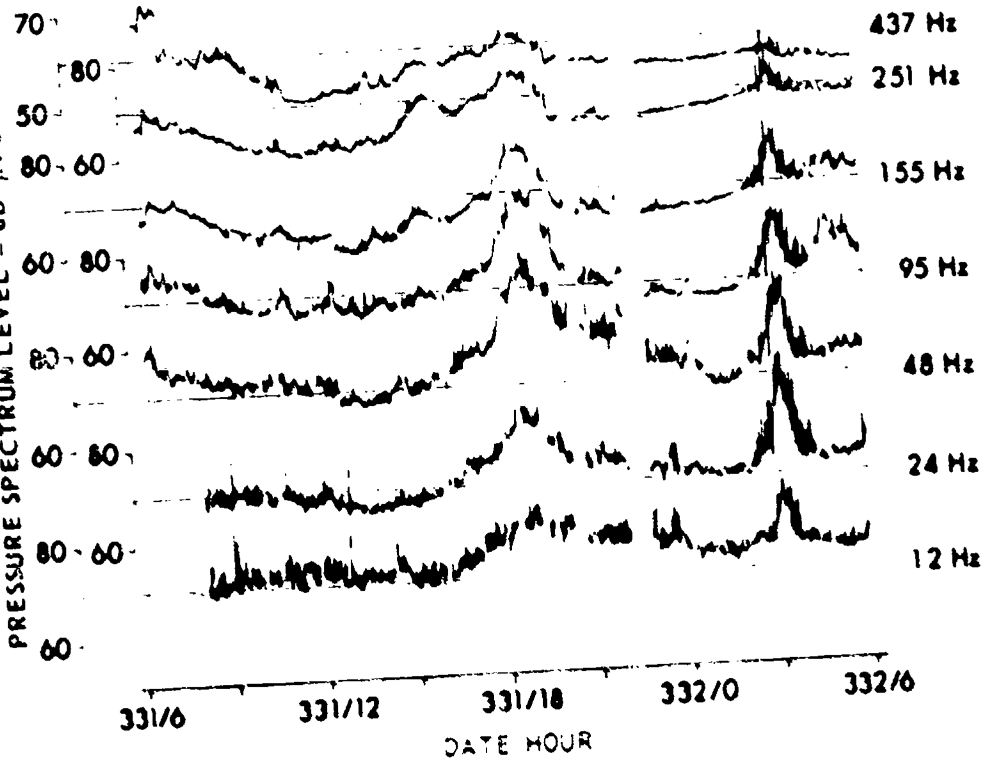

FIGURE 3.43
AMBIENT NOISE TIME SERIES - [illegible] RECEIVER
CHURCH STROKE II - SITE EN [illegible]

CONFIDENTIAL

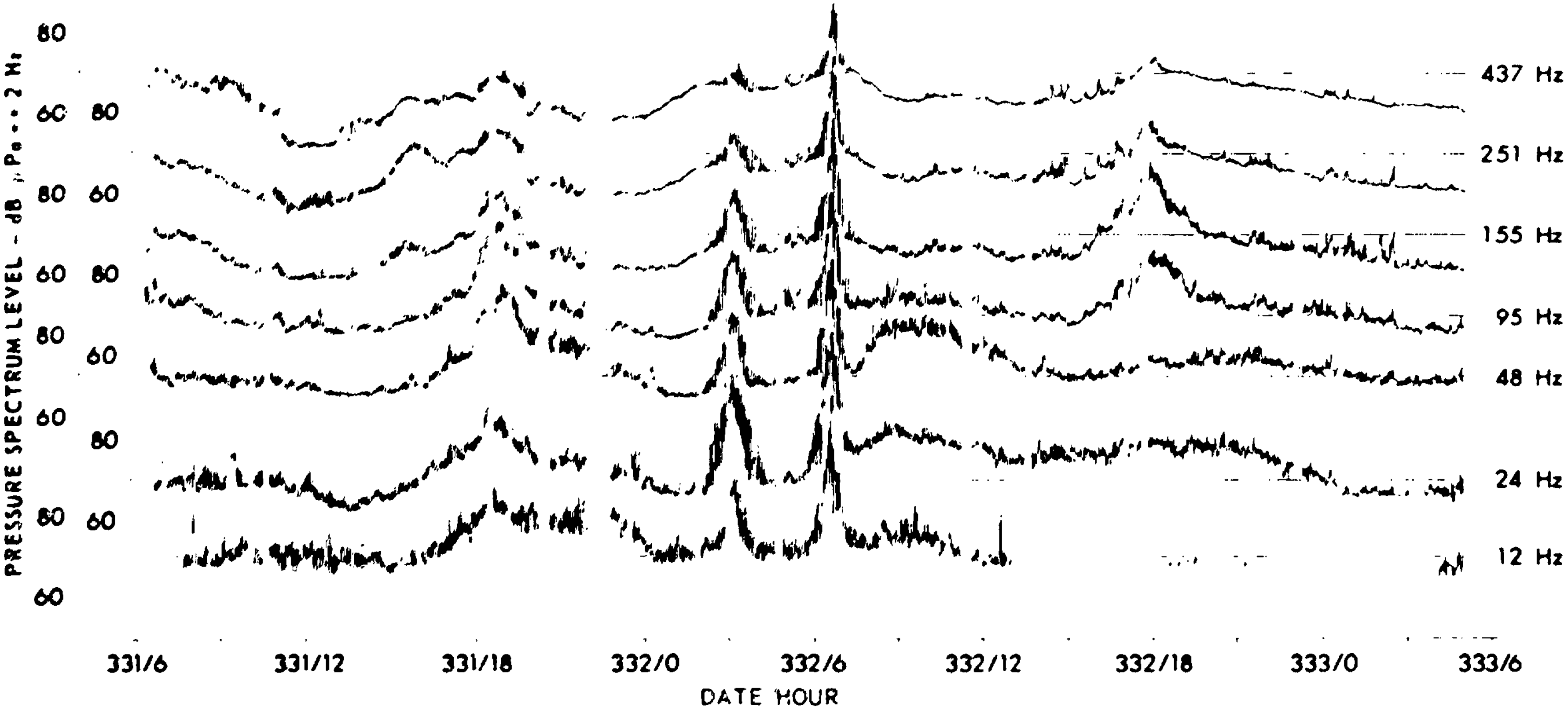

FIGURE 3.44
AMBIENT NOISE TIME SERIES - 5882 m RECEIVER
CHURCH STROKE II - SITE EN (U)

ARL UT
AS-78-1818
KCF - GA
11-30-78

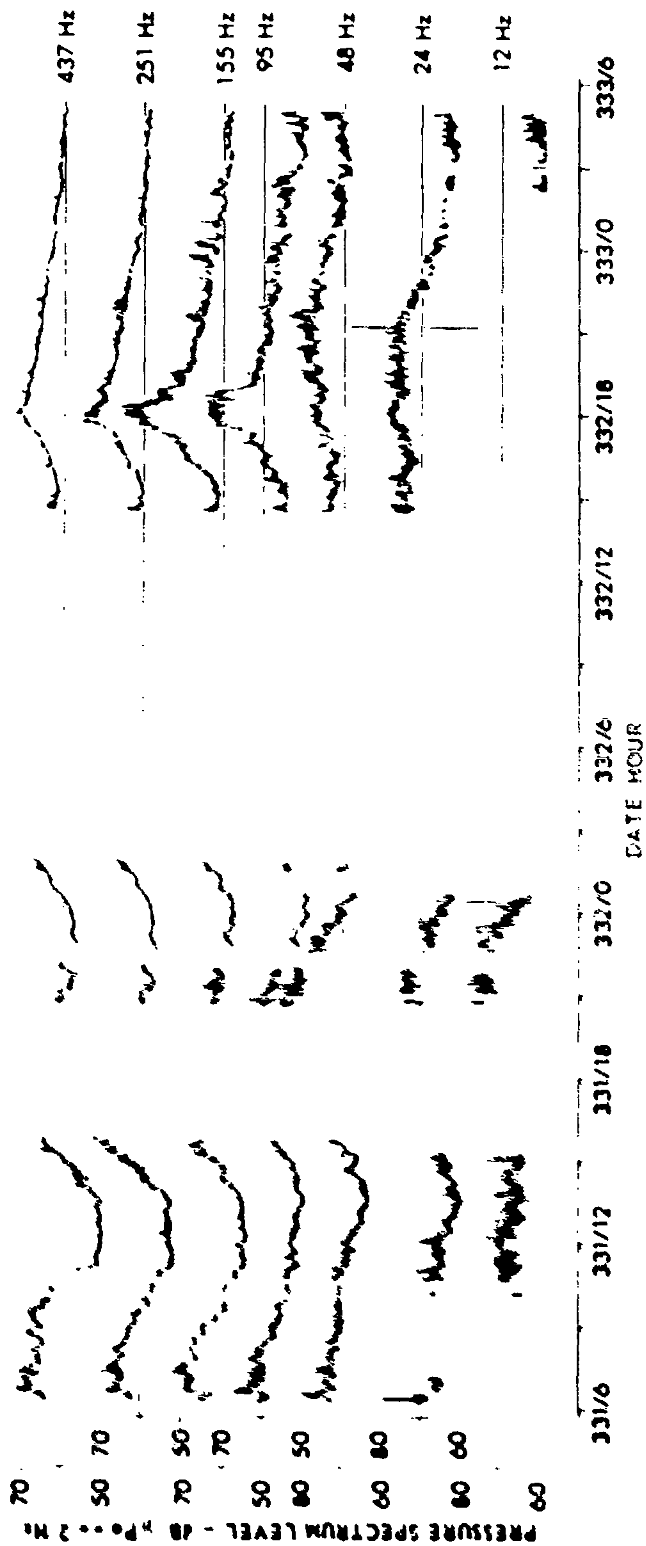

FIGURE 3.45
AMBIENT NOISE TIME SERIES - 5972 m RECEIVER
CHURCH STROKE II - SITE EN (U)

ARL UT
AS-78-1819
ACF-GA
11-30-78

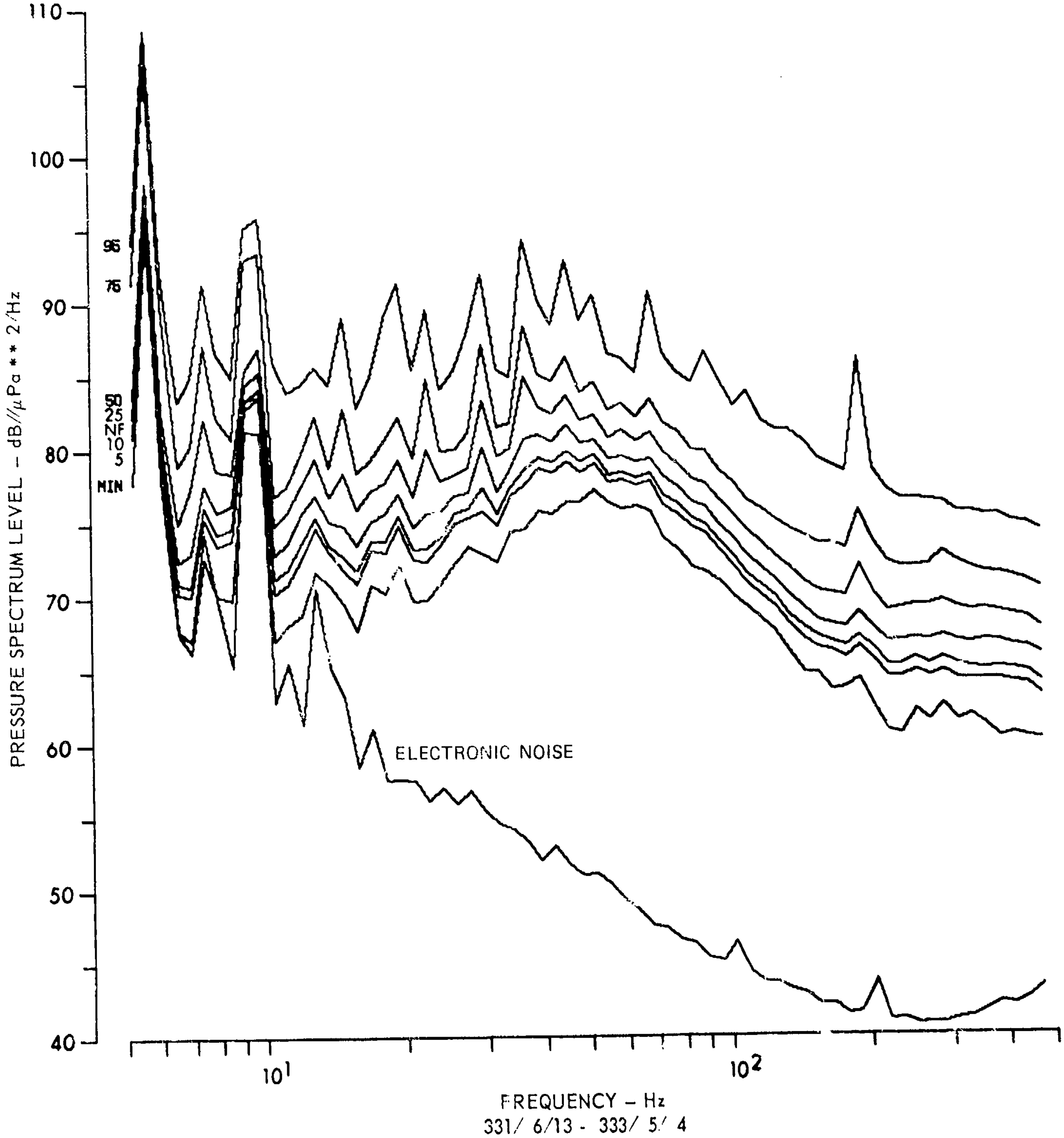

FIGURE 3.46
AMBIENT NOISE PERCENTILE SPECTRUM LEVELS FOR CHURCH STROKE II - SITE EN - 4982 m RECEIVER (U)

ARL:UT
AS-78-1820
KCF - GA
11-30-78

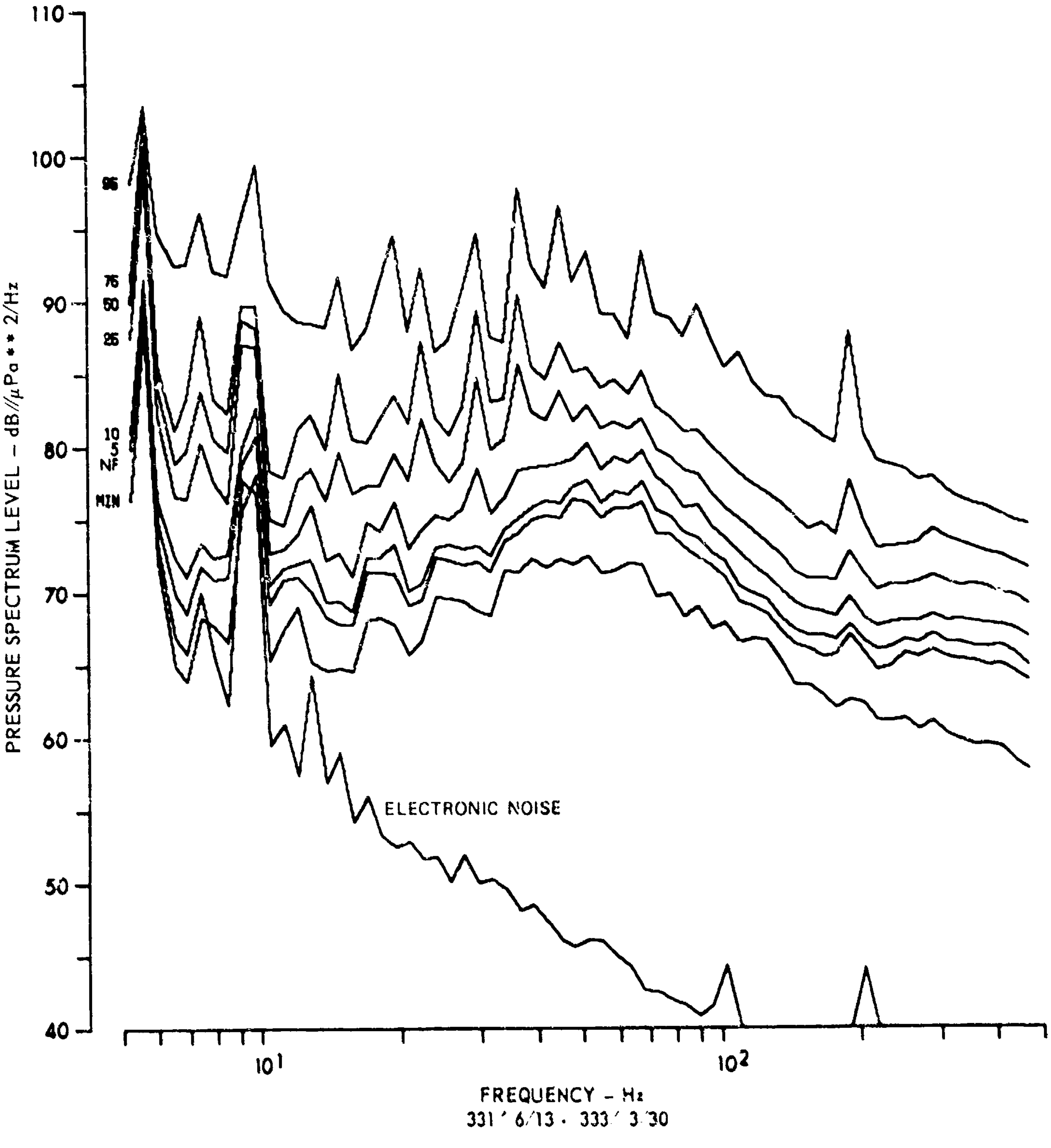

FIGURE 3.47
AMBIENT NOISE PERCENTILE SPECTRUM LEVELS FOR CHURCH STROKE II - SITE EN - 5582 m RECEIVER (U)

ARL:UT
AS-78-1821
KCF - GA
11-30-78

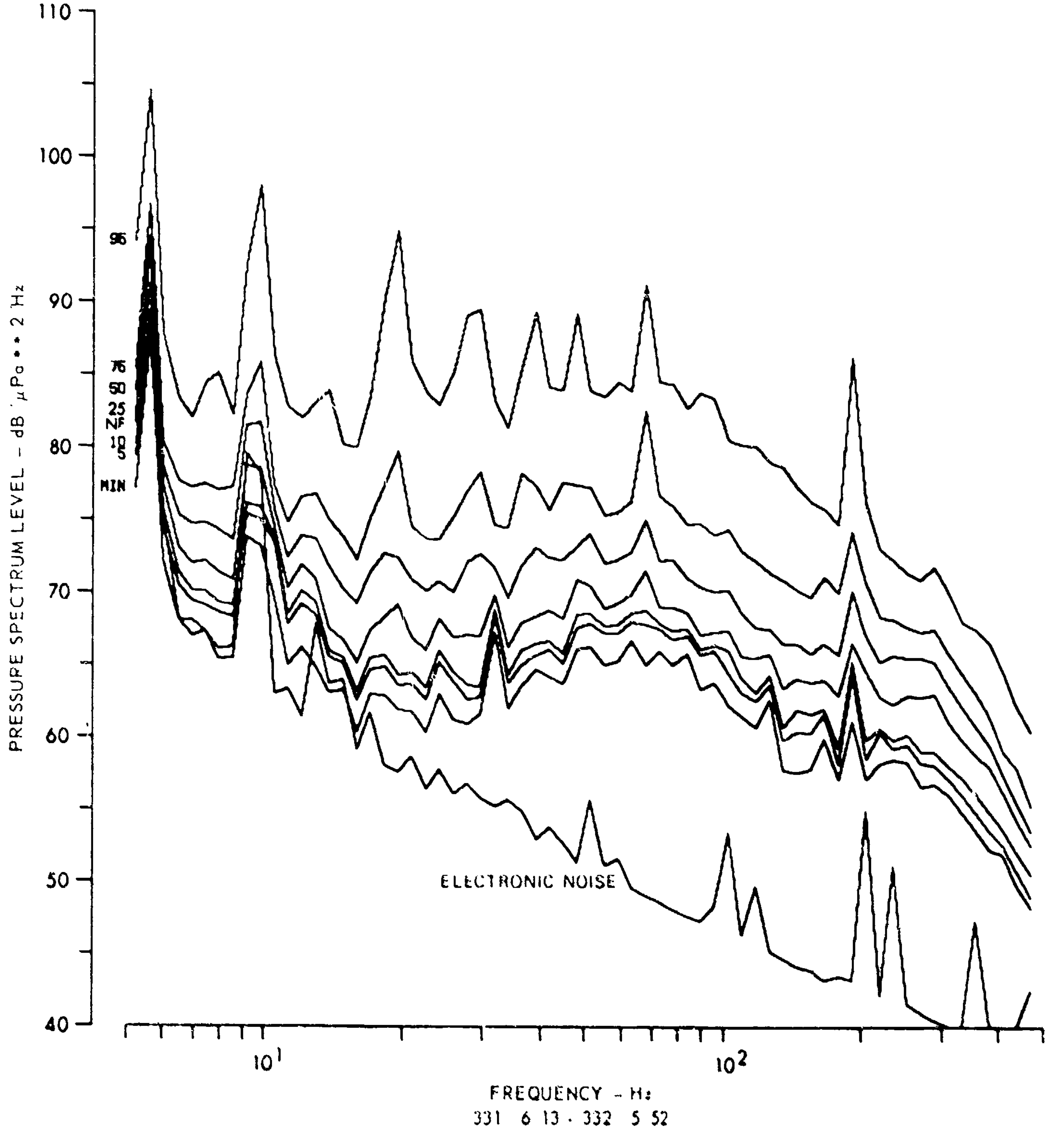

FIGURE 3.48
AMBIENT NOISE PERCENTILE SPECTRUM LEVELS FOR CHURCH STROKE II - SITE EN - 5782 m RECEIVER (U)

ARL:UT
AS-78-1822
KCF - GA
11-30-78

CONFIDENTIAL

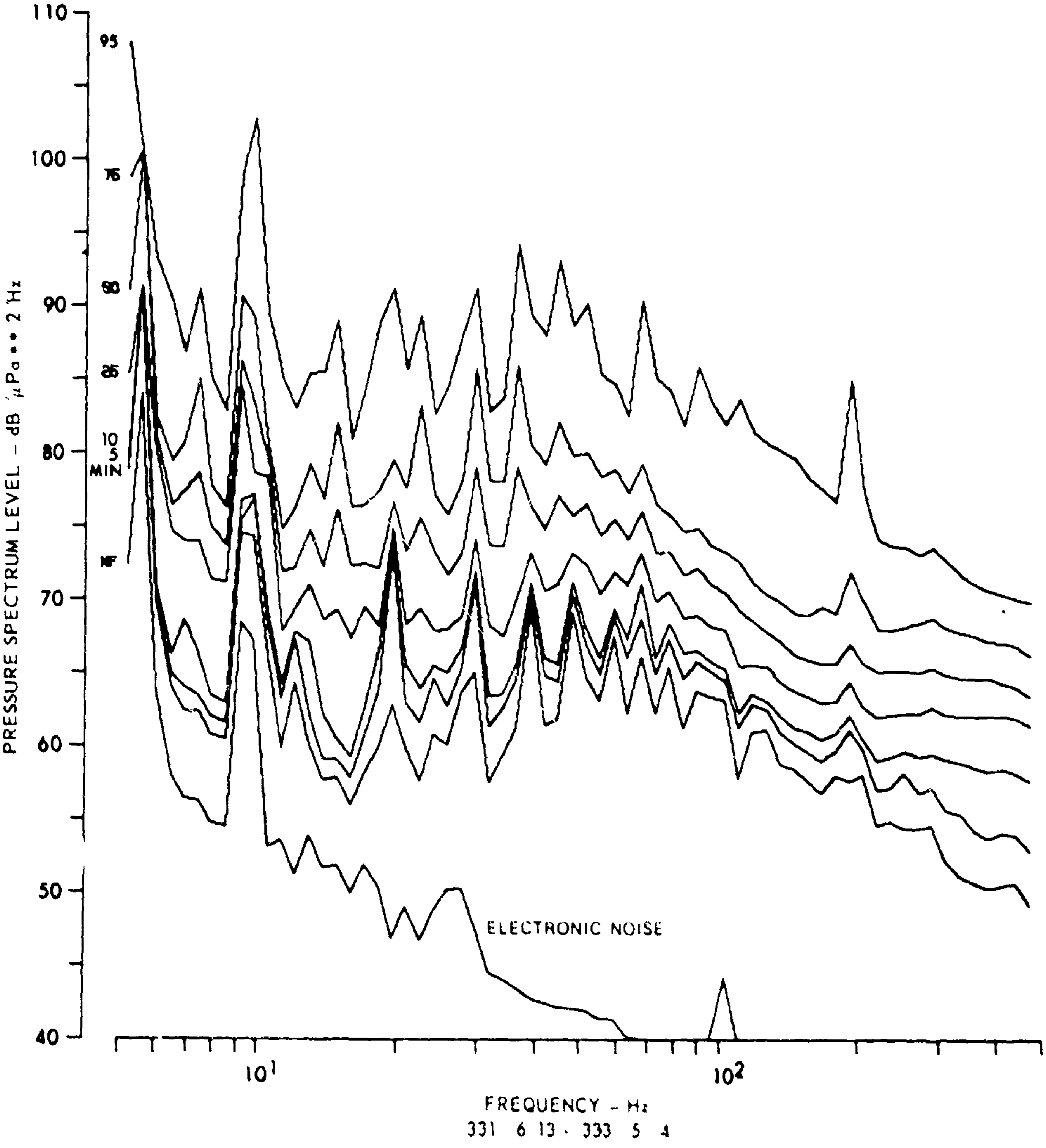

FIGURE 3.49
AMBIENT NOISE PERCENTILE SPECTRUM LEVELS FOR
CHURCH STROKE II · SITE EN · 5882 m RECEIVER (U)

ARL UT
AS-78-1823
KCF · GA
11-30-78

CONFIDENTIAL

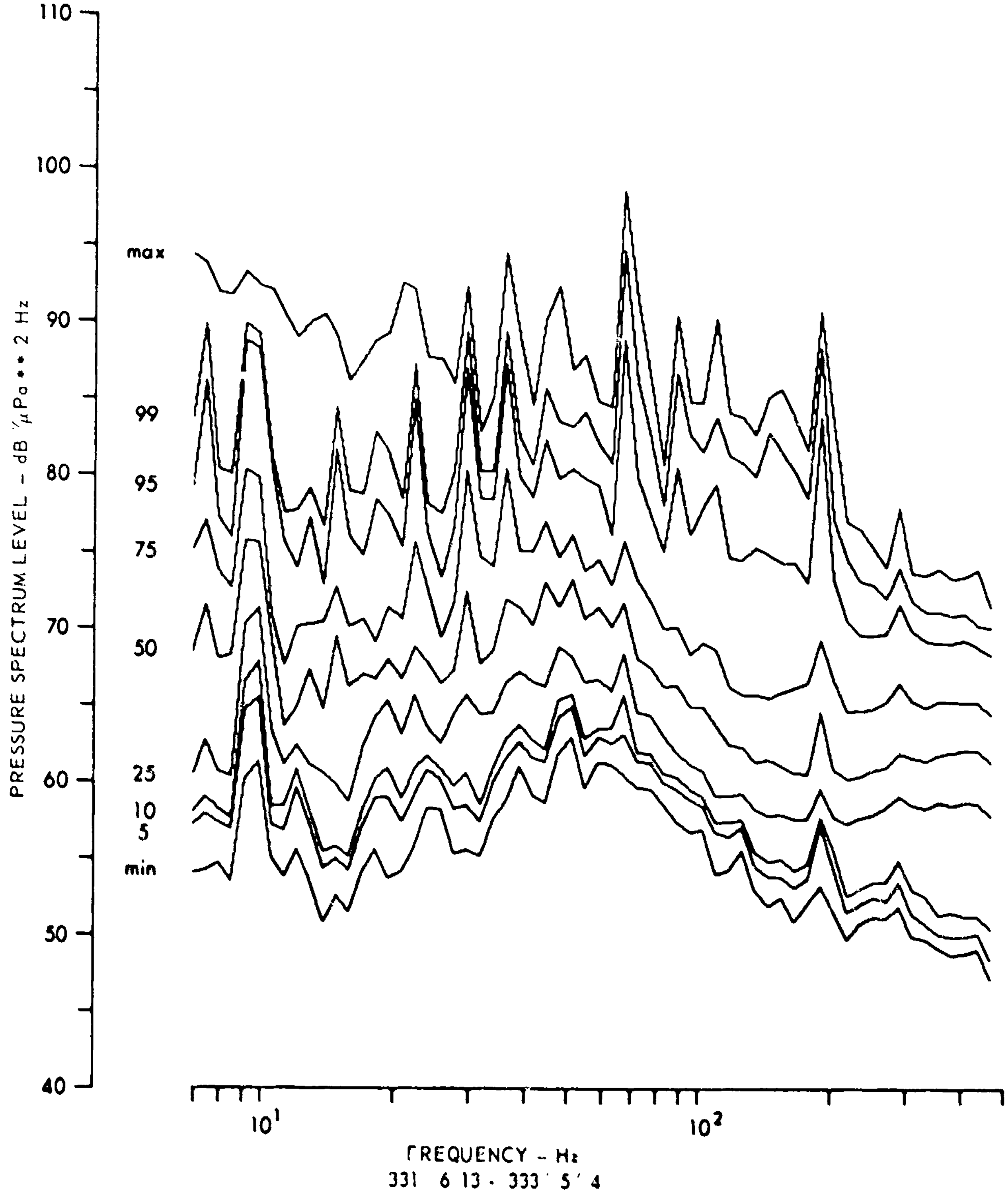

FIGURE 3.50
AMBIENT NOISE PERCENTILE SPECTRUM LEVELS FOR
CHURCH STROKE II - SITE EN - 5972 m RECEIVER (U)

ARL UT
AS-78-1824
KCF - GA
11-30-78

(U) harmonics can be seen in the lower percentiles. As an editorial procedure, the time period covering the aircraft SUS run, 332/0130 through 332/0730, was deleted from the percentile estimates of ambient noise level. In addition, erratic gain ranging on the deepest channel (see Fig. 3.34) could not be accounted for and (the times 331/1530 through 331/2030 and 332/0200 through 332/1430) were deleted as shown in Fig. 3.45.

(U) One goal of CHURCH STROKE II Cruise 5 was to obtain estimates of noise characteristics during a stable relatively quiet period. By examining Figs. 3.41 through 3.45, it can be seen that one such period is centered near hour 12 of day 331. The distribution of noise versus frequency during that period (hour 11 to hour 15 of day 331) is shown by the percentile plots of Figs. 3.51 through 3.55.

(C) Another quantity of interest is the minimum spectrum levels observed. The minimum levels (from Figs. 3.46 through 3.50) are shown versus depth in Fig. 3.56 and versus frequency in Fig. 3.57. Figure 3.56 shows noticeable quieting with depth below the critical depth at 5000 m.

(C) Typhoon Lucy was of course a significant event. The pressure spectrum levels in 1/10 octave bands are shown in Fig. 3.58 as functions of time as the storm is at its closest point of approach (CPA). These data were from the PAR, which recorded the data in short segments. The receiver was 30 m above the bottom. Figures 3.59 and 3.60 show the spectral levels as the storm approaches and then recedes. It should be no surprise that these spectra show no evidence of shipping as the storm approaches the site. The very high values of 85 to 95 dB//μPa^2/Hz pressure spectrum level indicate that rain was an important component of the noise source.

(U) The wind speeds for three sites around Site EN were provided by FNWC and are shown in Fig. 3.61, along with the storm track around Site EN. The eye of the storm approached Site EN to within 50 nmi and diminished rapidly in intensity after passing Site EN. The spectral shapes in Figs. 3.59 and 3.60 show an increasing pressure level with decreasing frequency as the storm approached CPA.

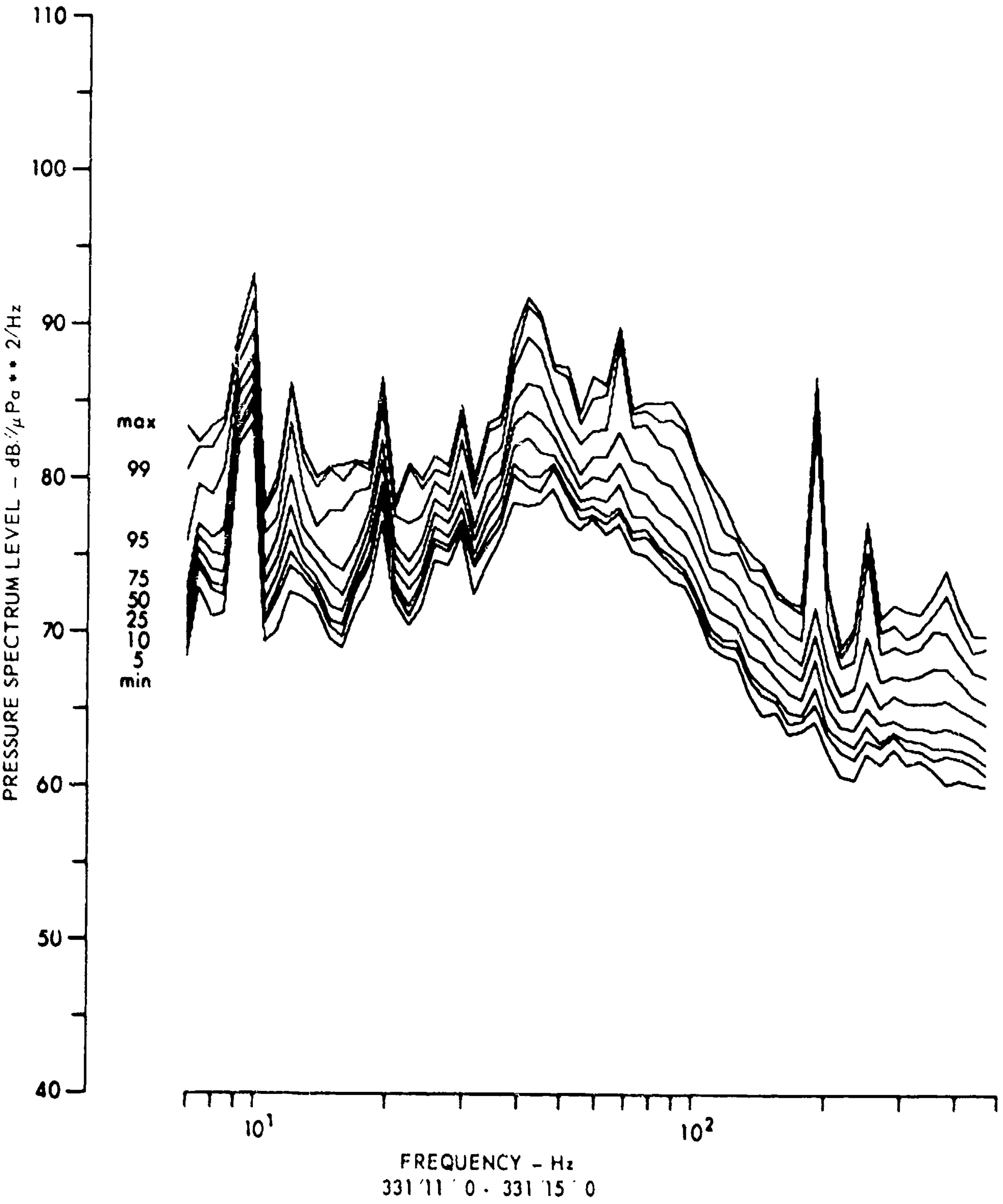

FIGURE 3.51

AMBIENT NOISE PERCENTILE SPECTRUM LEVELS DURING A STABLE TIME PERIOD FOR CHURCH STROKE II - SITE EN - 4982 m RECEIVER (U)

ARL:UT
AS-78-1825
KCF - GA
11-30-78

CONFIDENTIAL

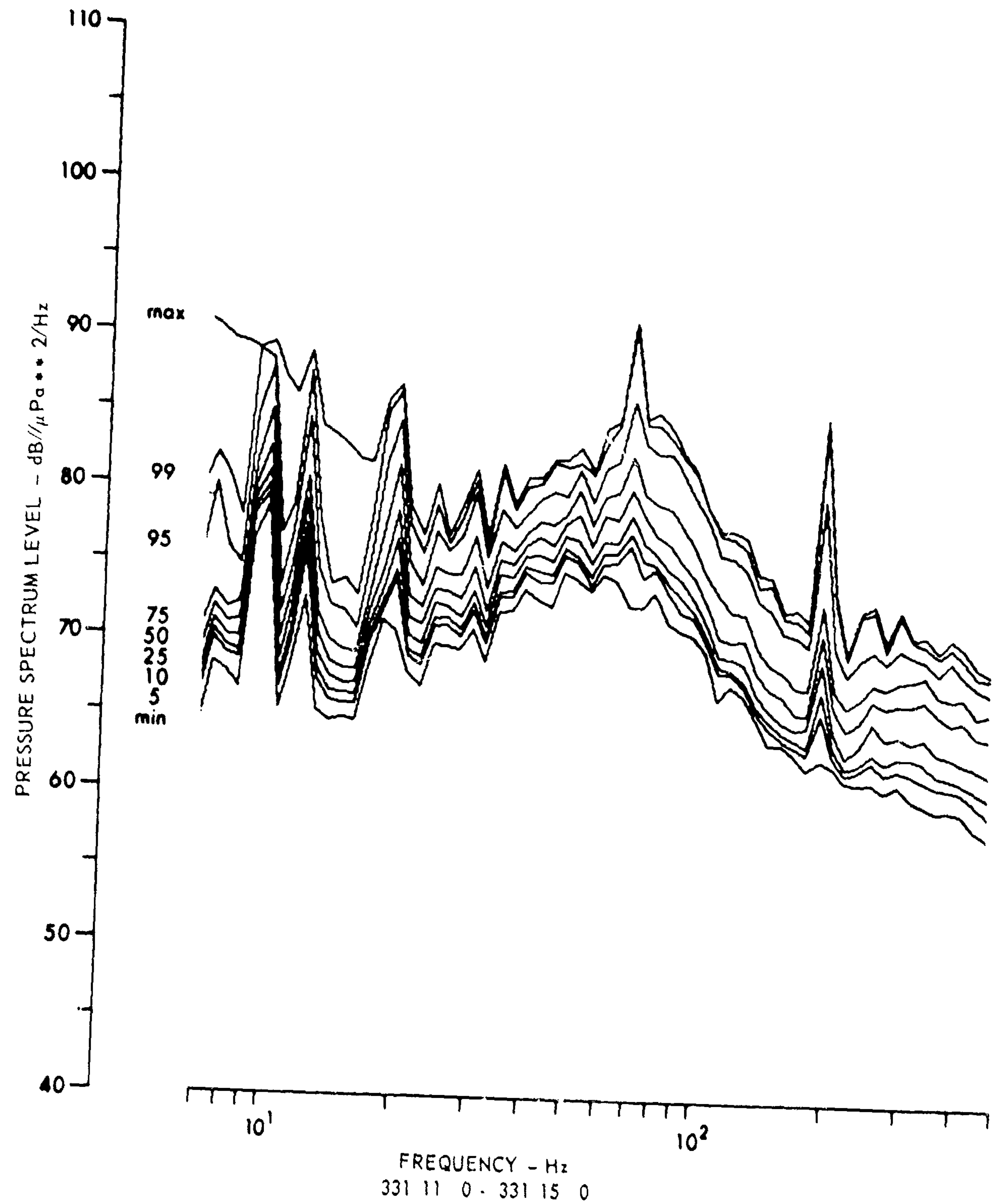

FIGURE 3.52
AMBIENT NOISE PERCENTILE SPECTRUM LEVELS DURING A STABLE TIME PERIOD FOR CHURCH STROKE II - SITE EN - 5582 m RECEIVER (U)

ARL:UT
AS-78-1826
KCF - GA
11-30-78

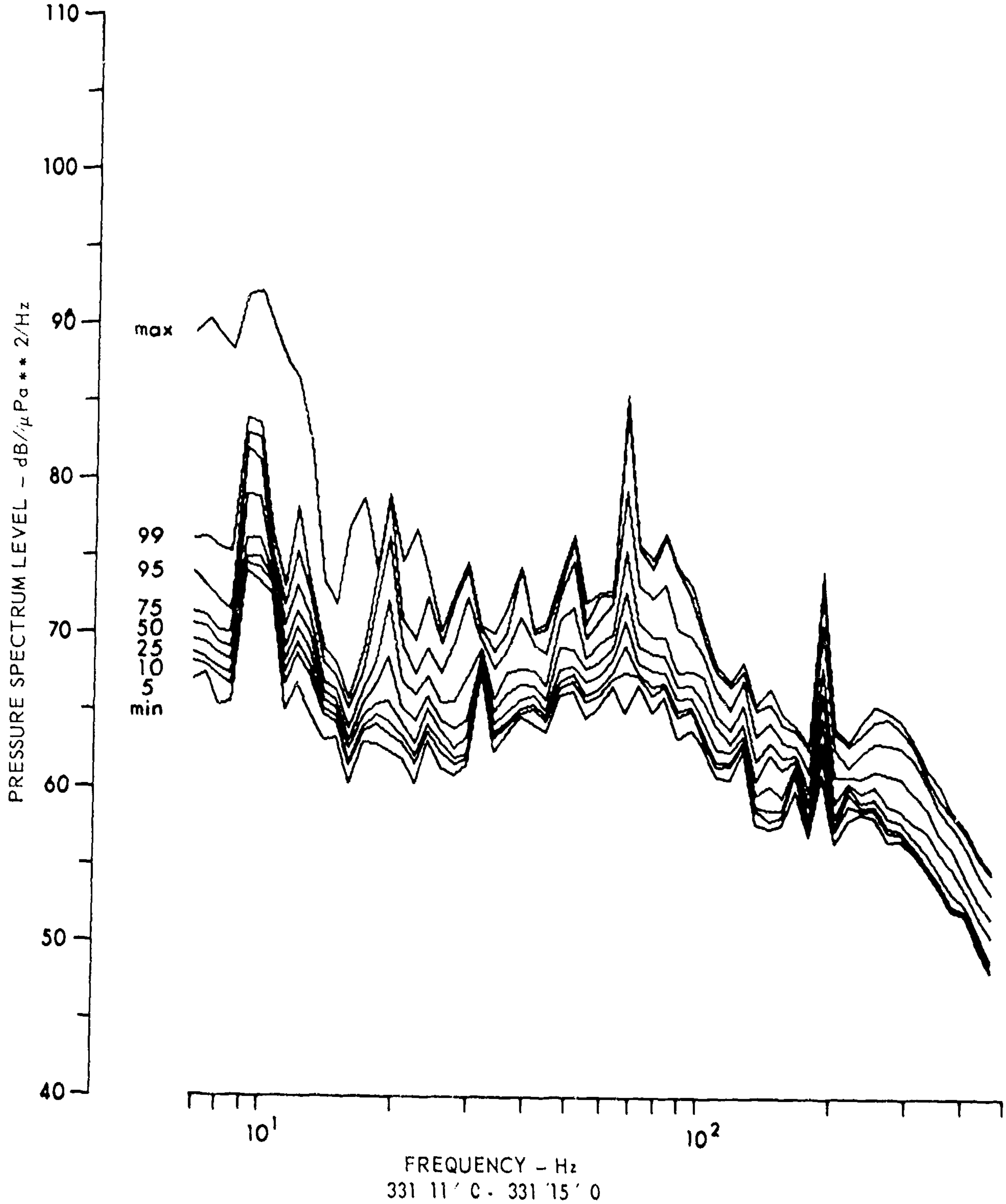

FIGURE 3.53
AMBIENT NOISE PERCENTILE SPECTRUM LEVELS DURING A STABLE TIME PERIOD FOR CHURCH STROKE II - SITE EN - 5782 m RECEIVER (U)

ARL:UT
AS-78-1827
KCF - GA
11-30-78

CONFIDENTIAL

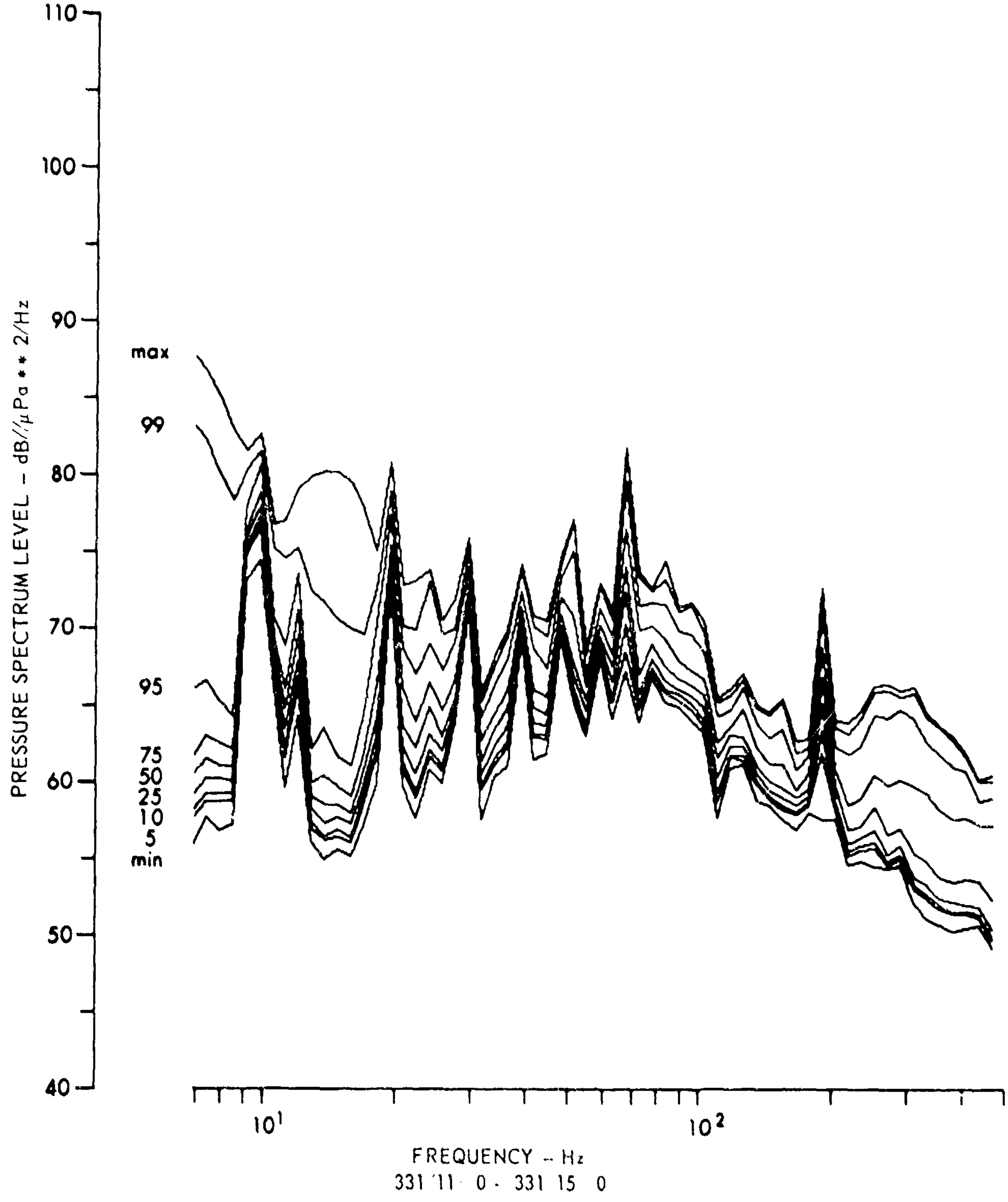

FIGURE 3.54
AMBIENT NOISE PERCENTILE SPECTRUM LEVELS DURING A STABLE TIME PERIOD FOR CHURCH STROKE II - SITE EN - 5882 m RECEIVER (U)

ARL:UT
AS-78-1828
KCF-GA
11-30-78

CONFIDENTIAL

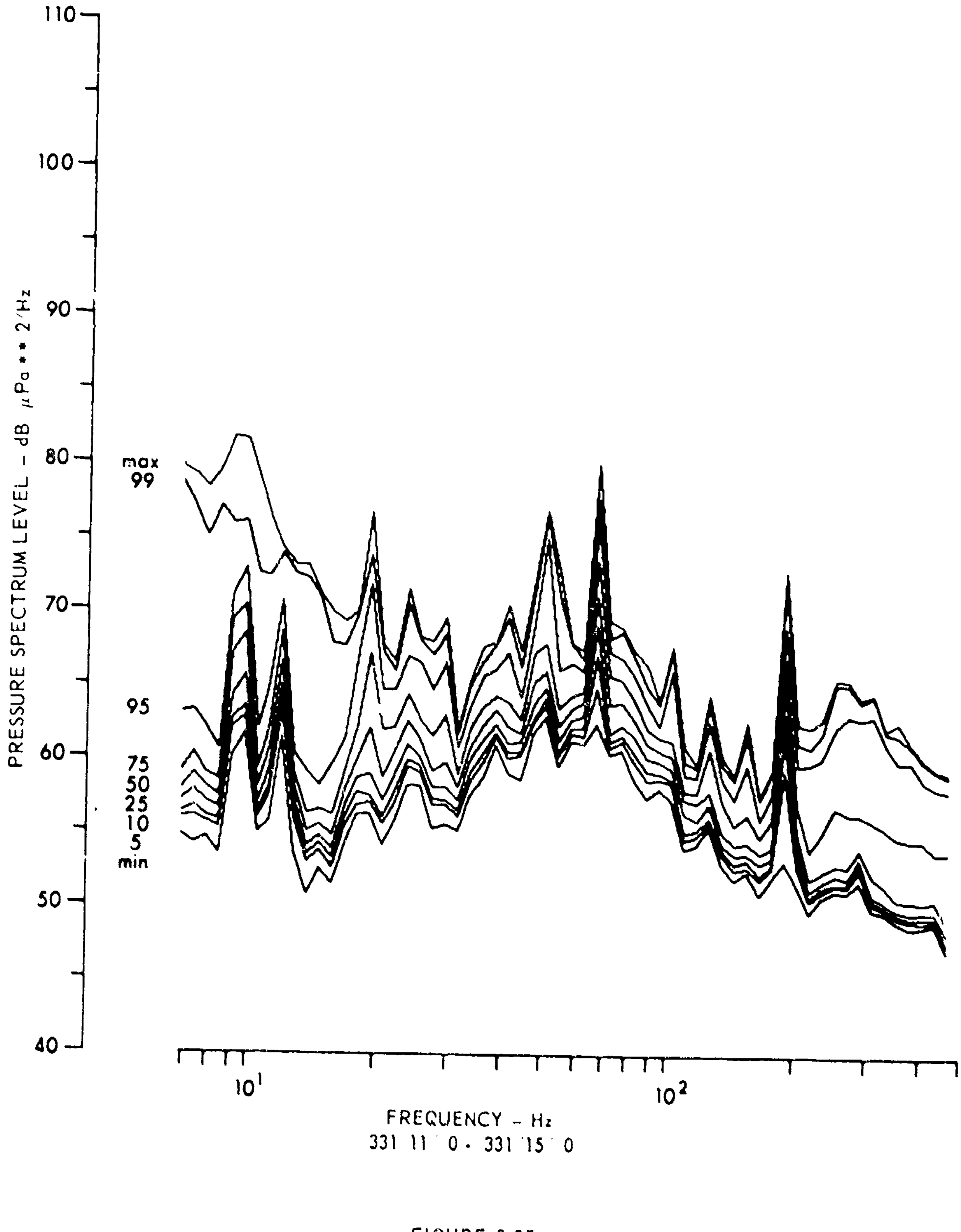

FIGURE 3.55
AMBIENT NOISE PERCENTILE SPECTRUM LEVELS DURING A STABLE TIME PERIOD FOR CHURCH STROKE II - SITE EN - 5972 m RECEIVER (U)

ARL:UT
AS-78-1829
KCF - GA
11-30-78

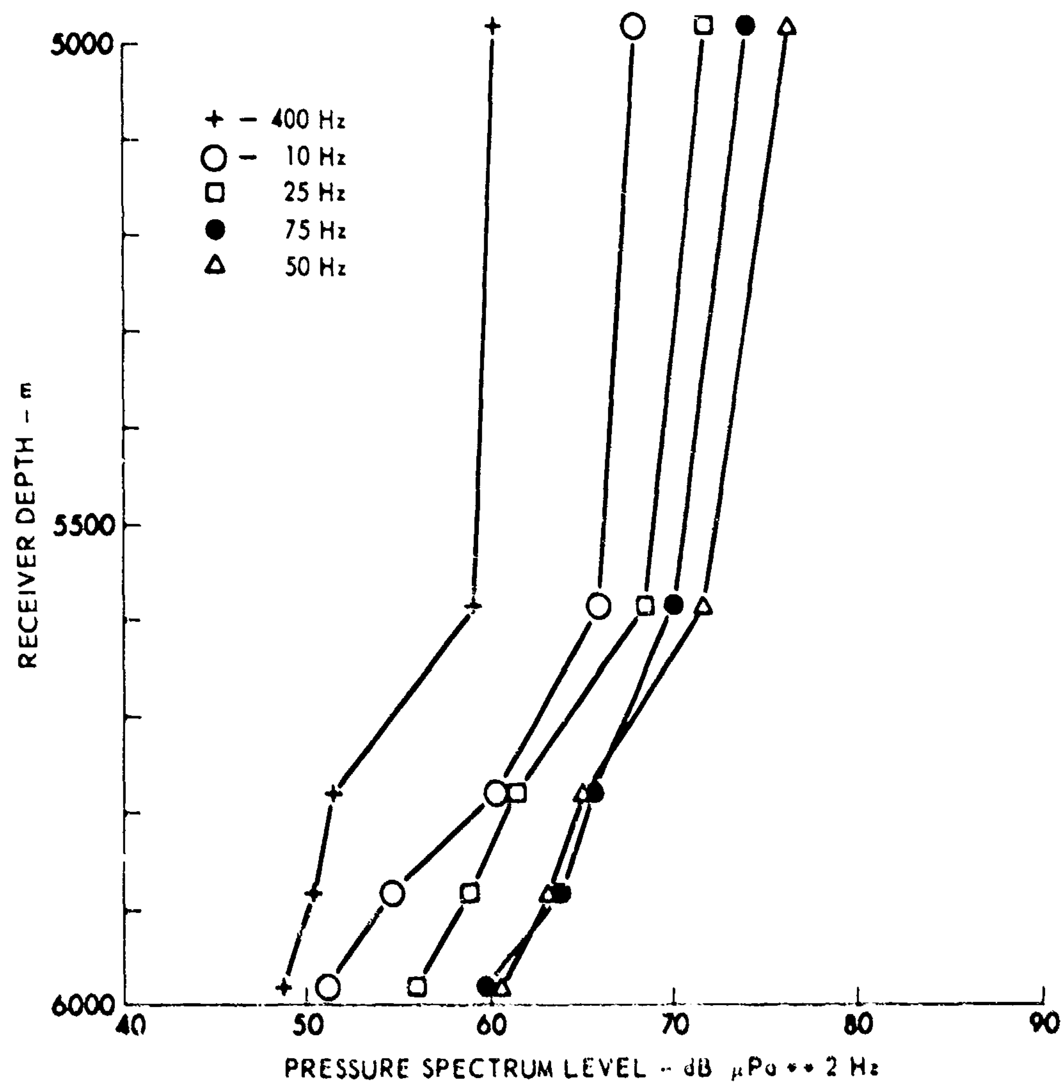

FIGURE 3.56
MINIMUM PRESSURE SPECTRUM LEVEL versus RECEIVER DEPTH
FOR FIVE FREQUENCIES AT CHURCH STROKE II - SITE EN (U)

ARL:UT
AS-78-1831
KCF - GA
11-30-78

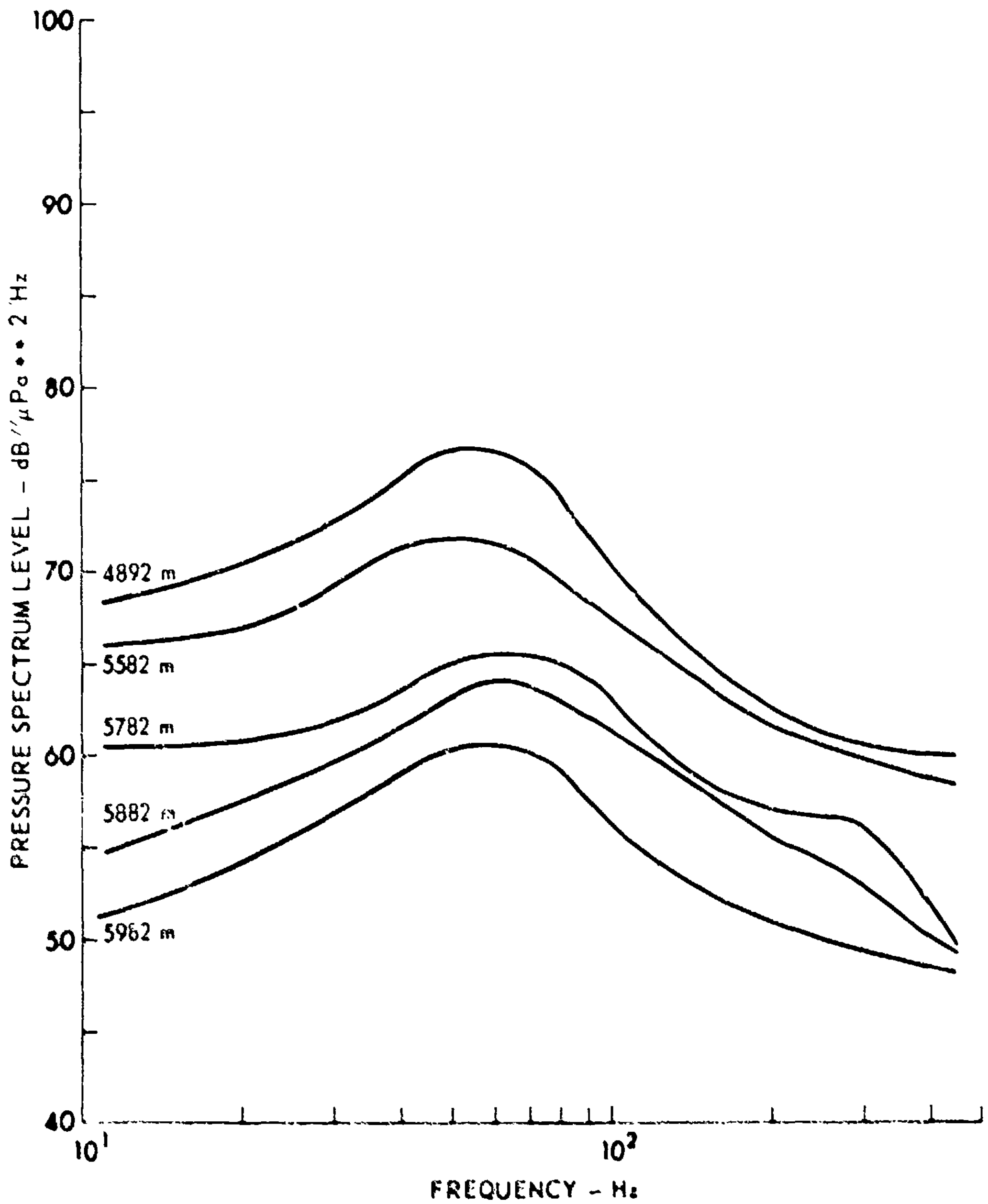

FIGURE 3.57
MINIMUM PRESSURE SPECTRUM LEVEL versus FREQUENCY
FOR FIVE DEPTHS AT CHURCH STROKE II - SITE EN (U)

ARL UT
AS-78-1830
KCF - GA
11-30-78

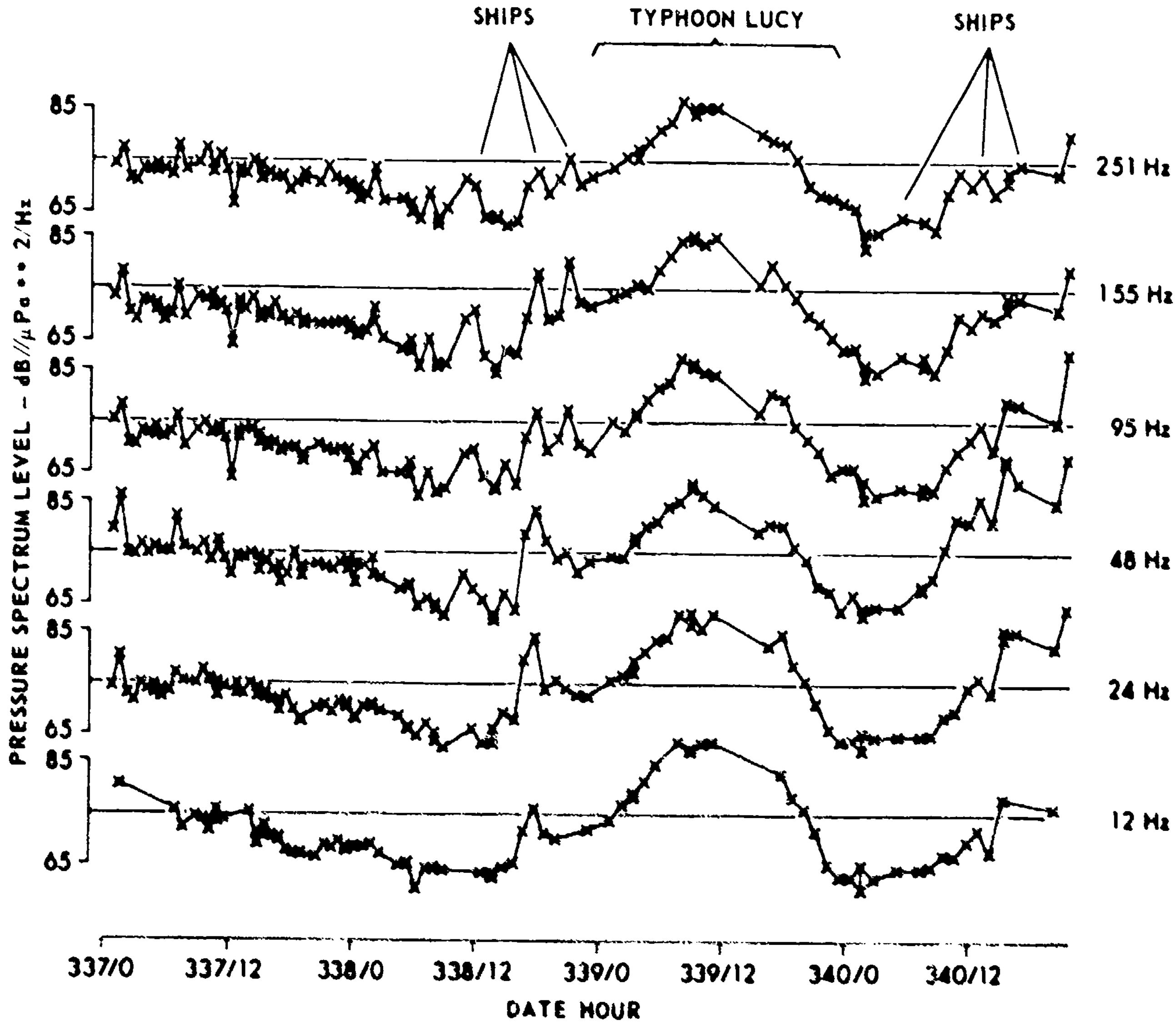

FIGURE 3.58
AMBIENT NOISE TIME SERIES - 4982 m RECEIVER
CHURCH STROKE II - SITE EN PAR (U)

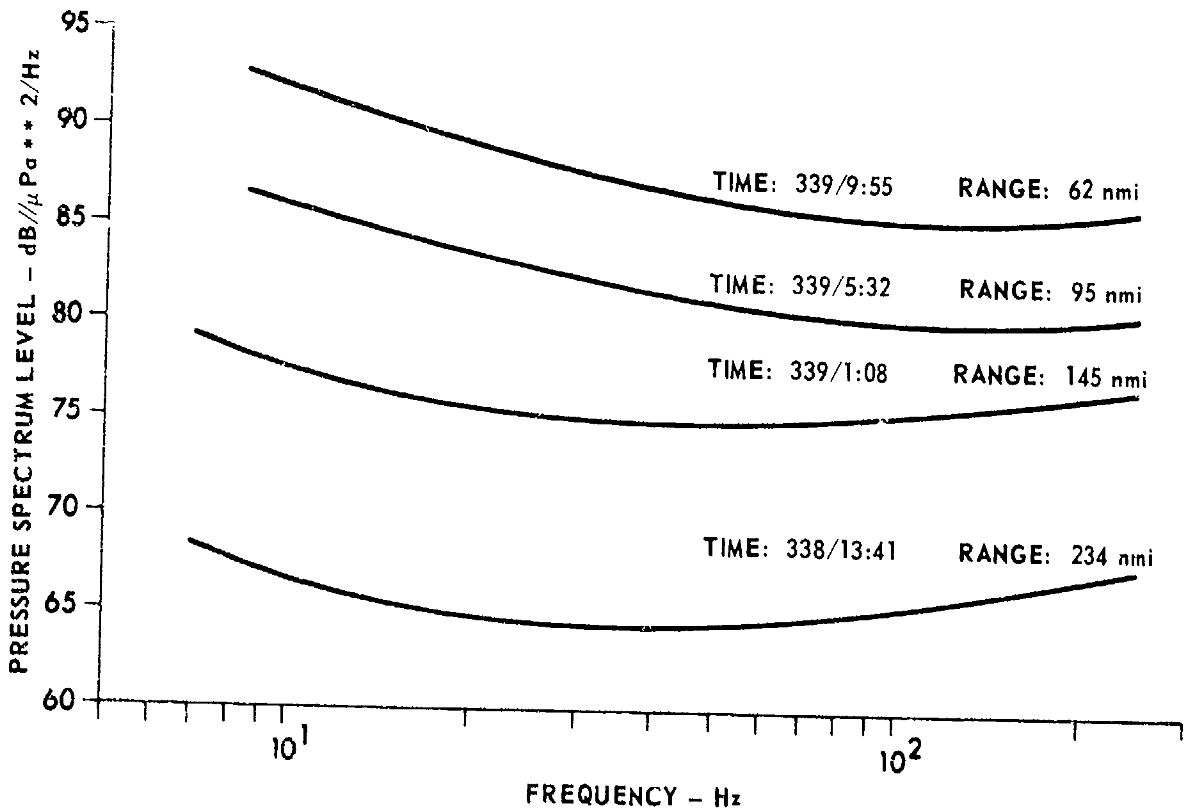

FIGURE 3.59
AMBIENT NOISE SPECTRA WITH TYPHOON LUCY APPROACHING SITE EN

ARL:UT
AS-79-893
KCF-GA
5-1-79

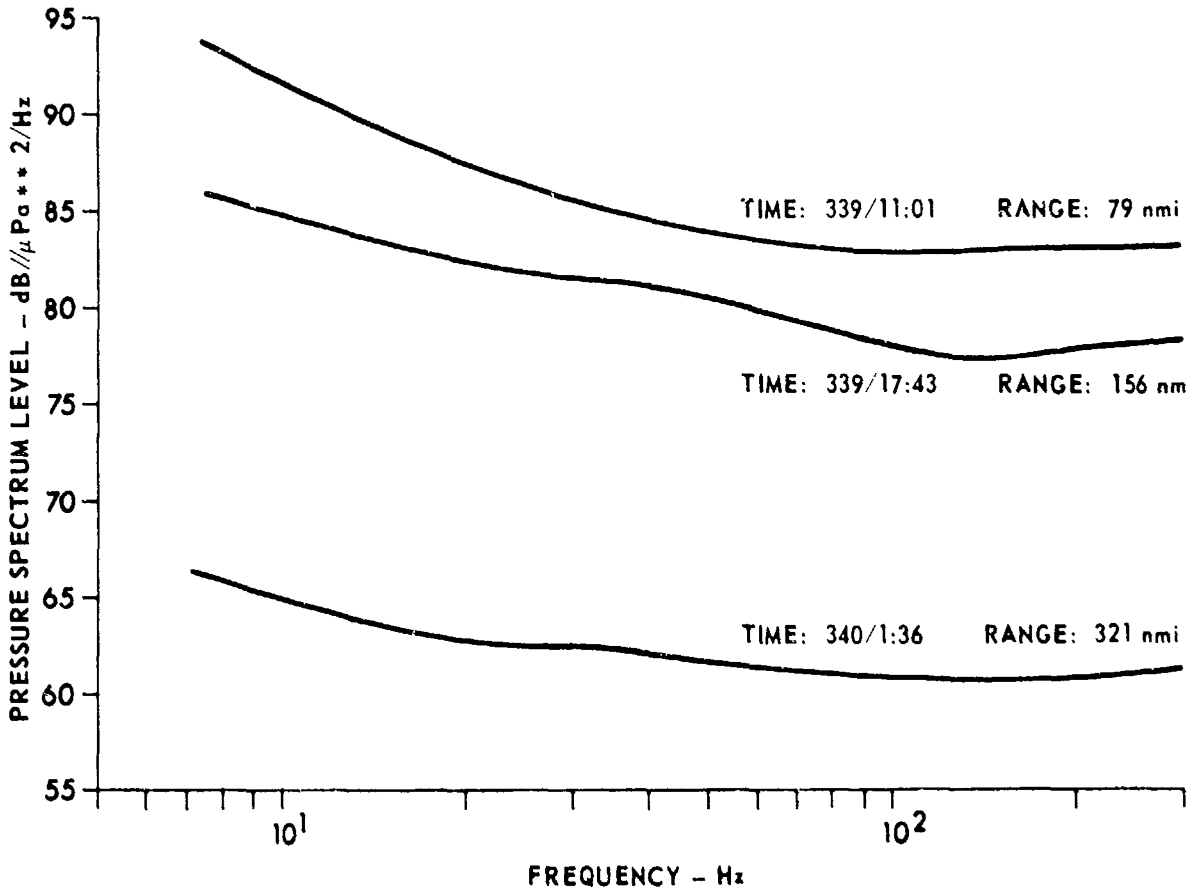

FIGURE 3.60
AMBIENT NOISE SPECTRA WITH TYPHOON LUCY RECEDING FROM SITE EN

ARL UT
AS-79-894
KCF - GA
5 - 1 - 79

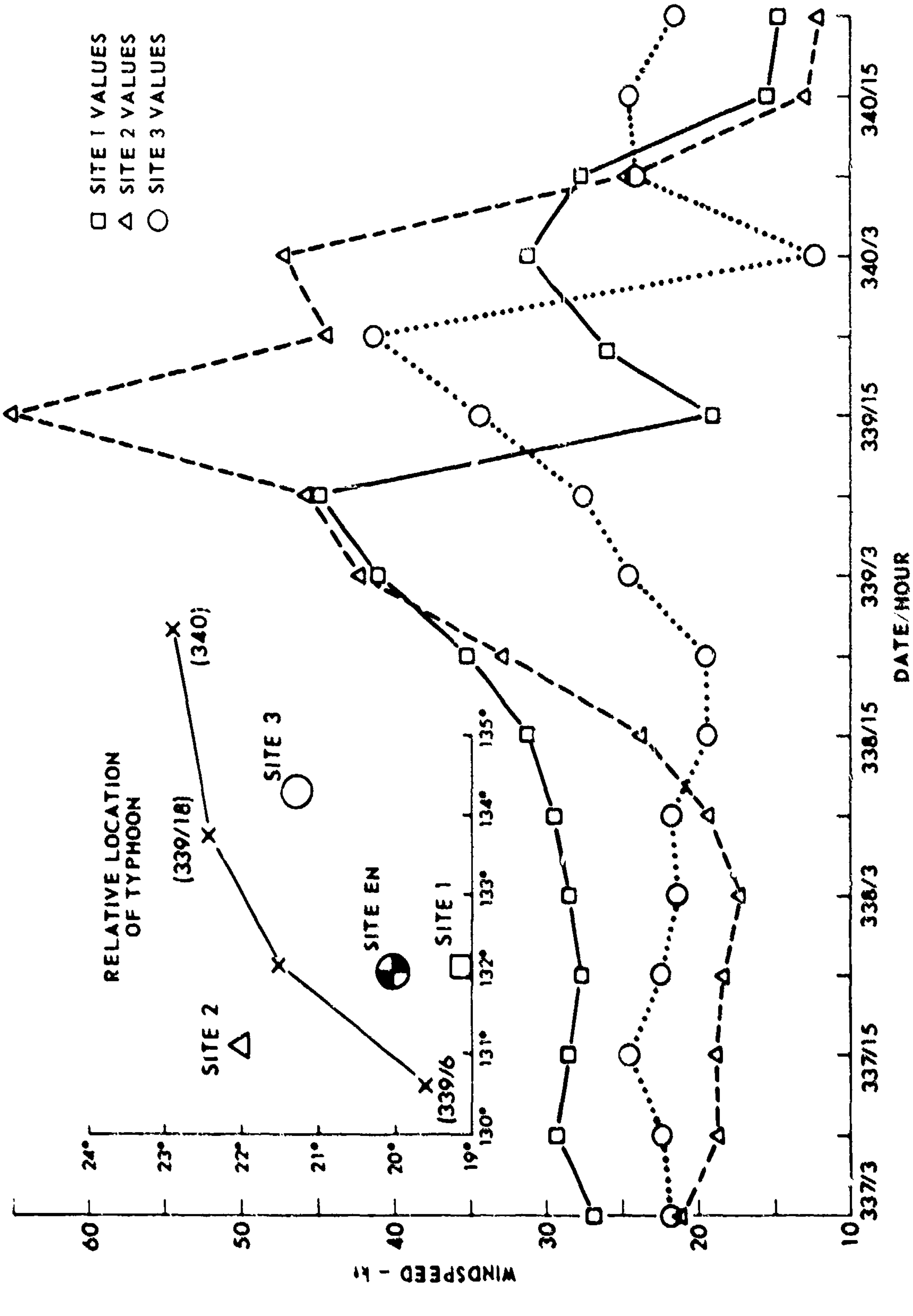

FIGURE 3.61
FNWC REPORTED WINDSPEED FOR CHURCH STROKE II - PHASE II SITE EN (U)

ARL UT
AS-79-892
KCF - GA
5 - 1 - 79

IV. SITE C - ENVIRONMENTAL ACOUSTIC DATA

(C) Figure 4.1 shows the Site C location and the track of the cw source run processed for this site. The site location is 19°41.3' N, 140°7.9' E.[11] The radial source run has a maximum range of approximately 60 km from the site. Delays due to poor weather conditions forced cancellation of longer source runs and limited total recording time to 1.5 days.

(U) A 12 h segment of data from the Site C PAR hydrophone 42 m above bottom (receiver channel 9) was processed. These data were used to estimate cw propagation loss, ambient noise level, and the ship signature of JNXN (to be discussed in Chapter V). Data from the other working hydrophones in the same 40 m array were not processed since they would not add to the omnidirectional data set.

4.1 Propagation Loss at Site C

(C) The cw projector was towed at a depth of 18 m during the entire event processed for Site C. Propagation loss for the 67 Hz and 197 Hz signals received at a depth of 4946 m is shown in Fig. 4.2. These curves provide a look at near-bottom reception of shallow source signals. For those ranges with direct path propagation, less than 30 km, the propagation loss is approximately 75 dB. Between 30 km and the end of the run, 64 km, the propagation loss is approximately 87 dB at 67 Hz and 90 dB at 197 Hz.

(C) Signal excess and ambient noise levels (in an adjacent frequency band) during the projector tow at Site C are presented in Figs. 4.3 and 4.4. The ambient noise levels at both frequencies decrease 14 dB as the tow ship increases range out to 40 km; this is evidence of noise contamination from the tow ship itself. Throughout the entire event signal excess remains high for the 172 dB source levels. Beyond the direct path range,

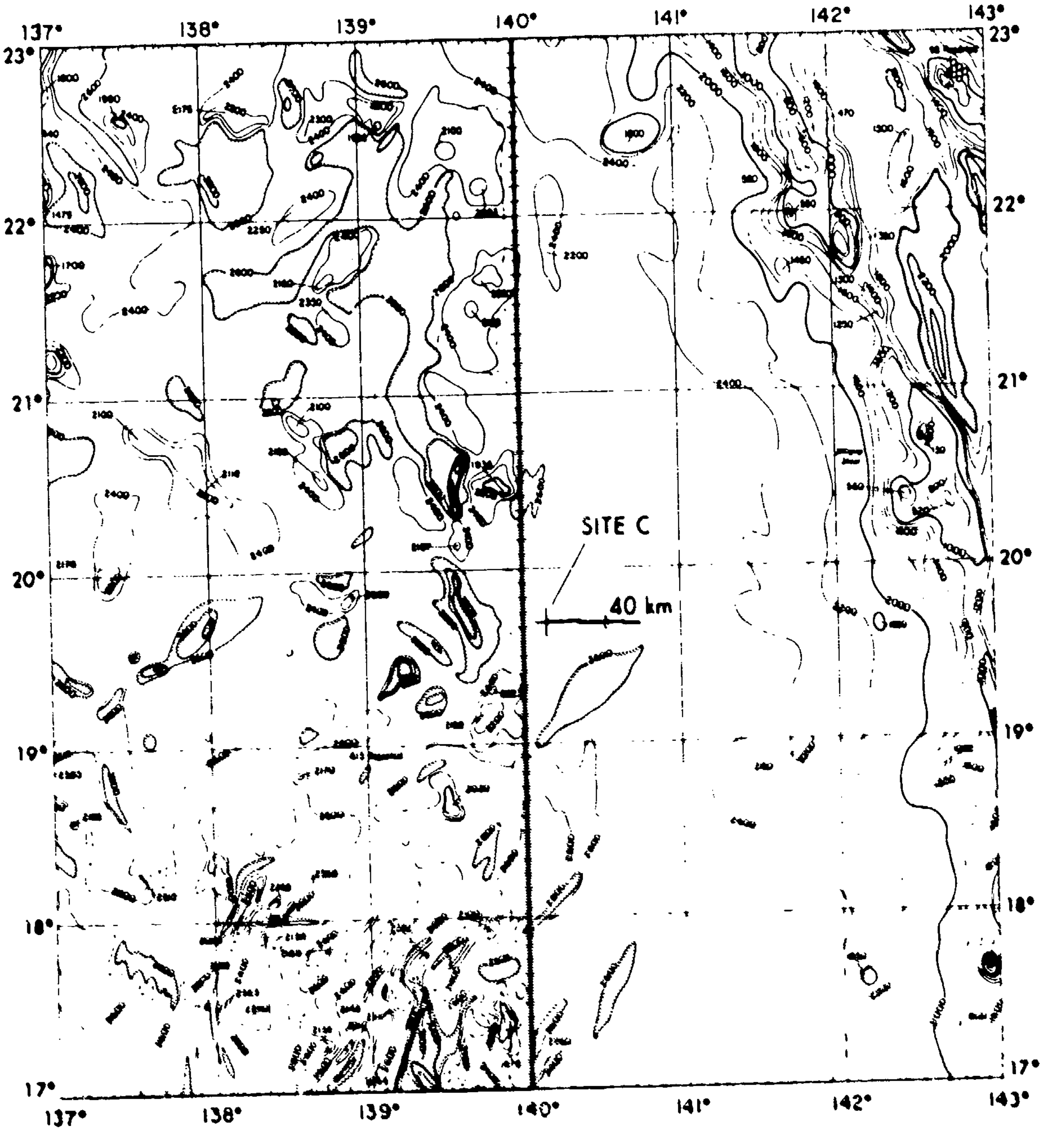

FIGURE 4.1
INDIAN SEAL SOURCE TRACK AT CHURCH STROKE II - SITE C (U)

ARL UT
AS-79-981
KCF - GA
5 - 8 - 79

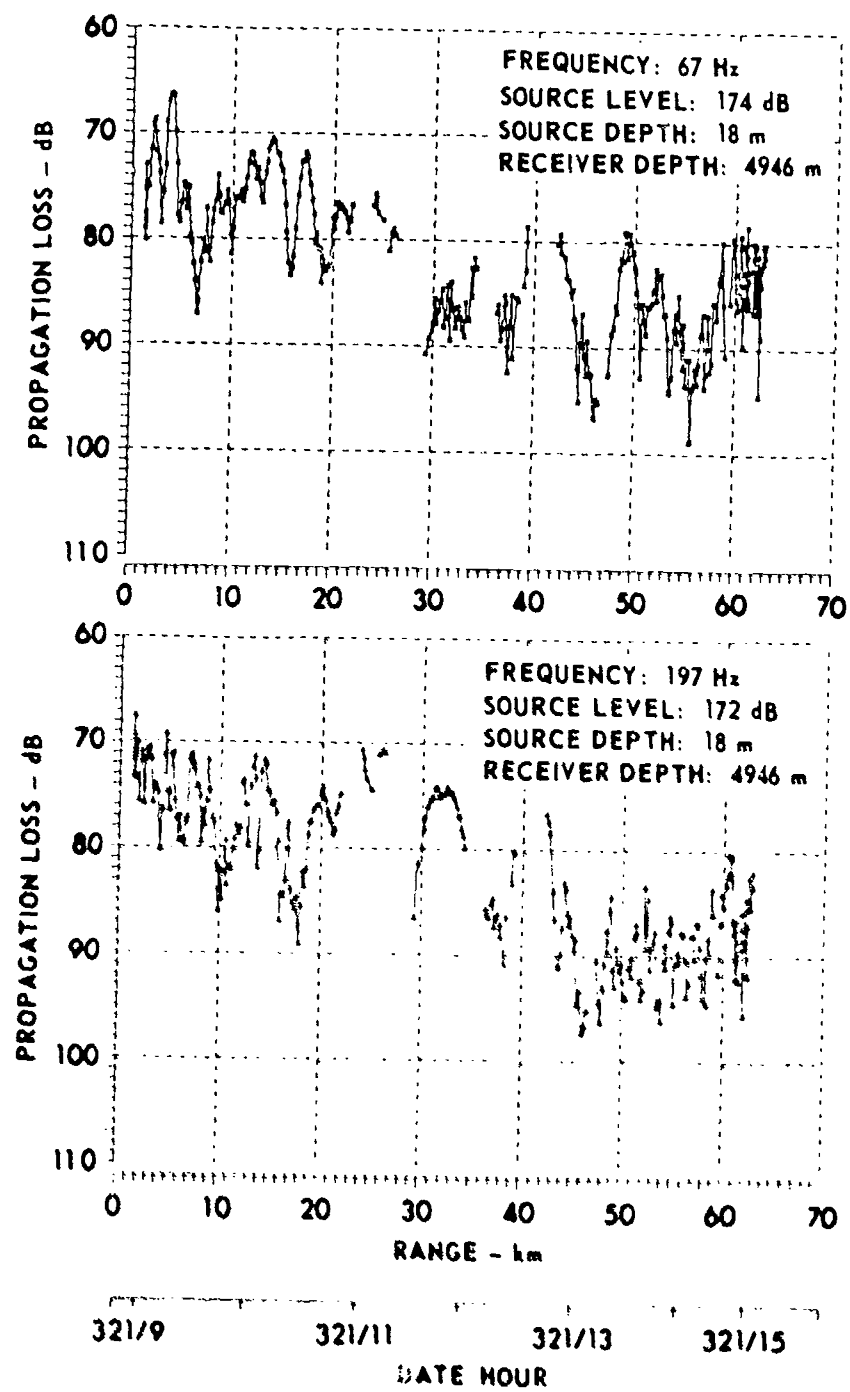

FIGURE 4.2
PROPAGATION LOSS TO 4946 m RECEIVER
CHURCH STROKE II - SITE C PAR (U)

ARL UT
AS-79-855
KCF - GA
4 - 30 - 79

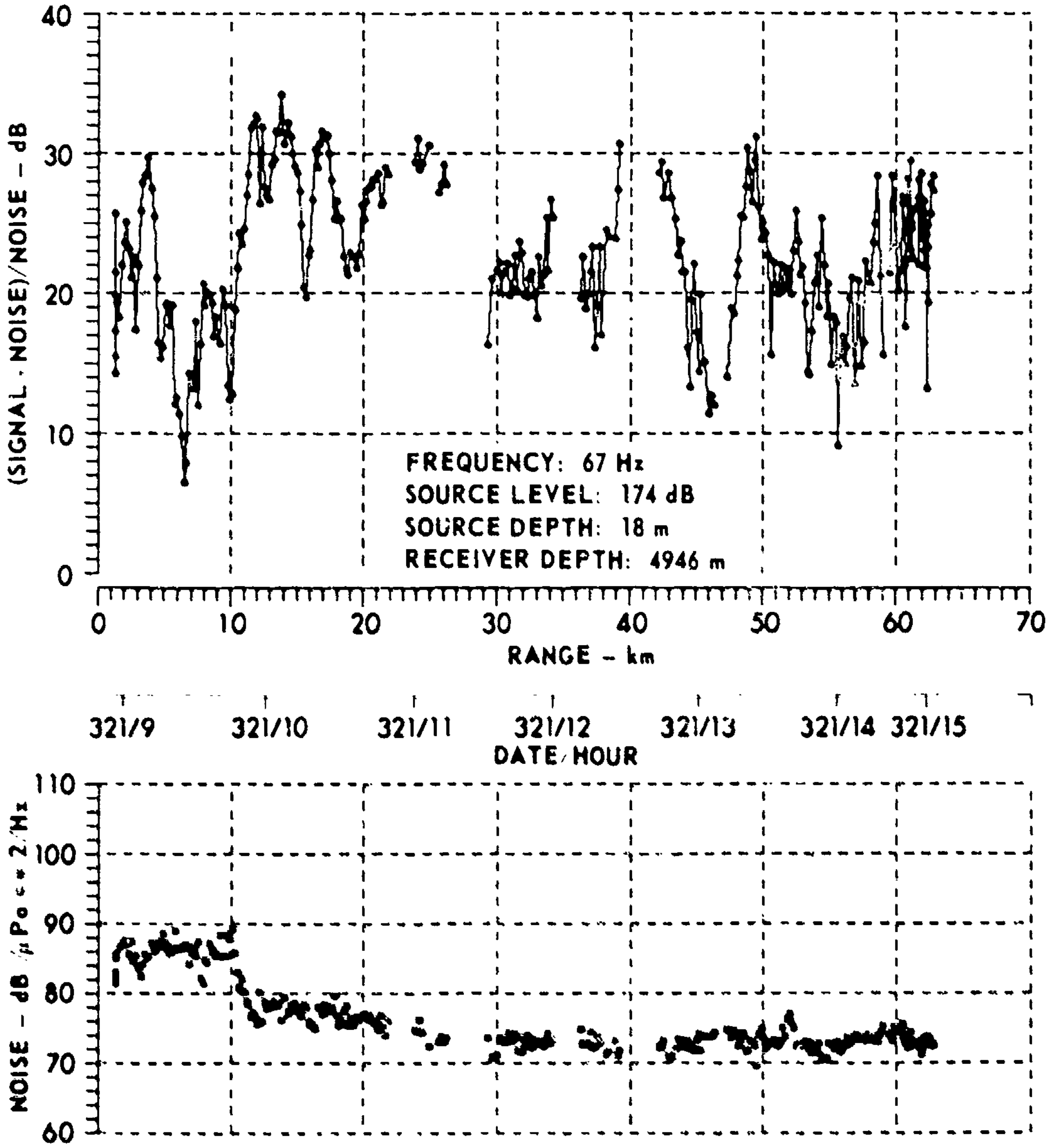

FIGURE 4.3
NOISE AND SIGNAL EXCESS FOR 4946 m RECEIVER
AT 67 Hz CHURCH STROKE II - SITE C PAR (U)

ARL UT
AS-79-859
KCF - GA
4 - 30 - 79

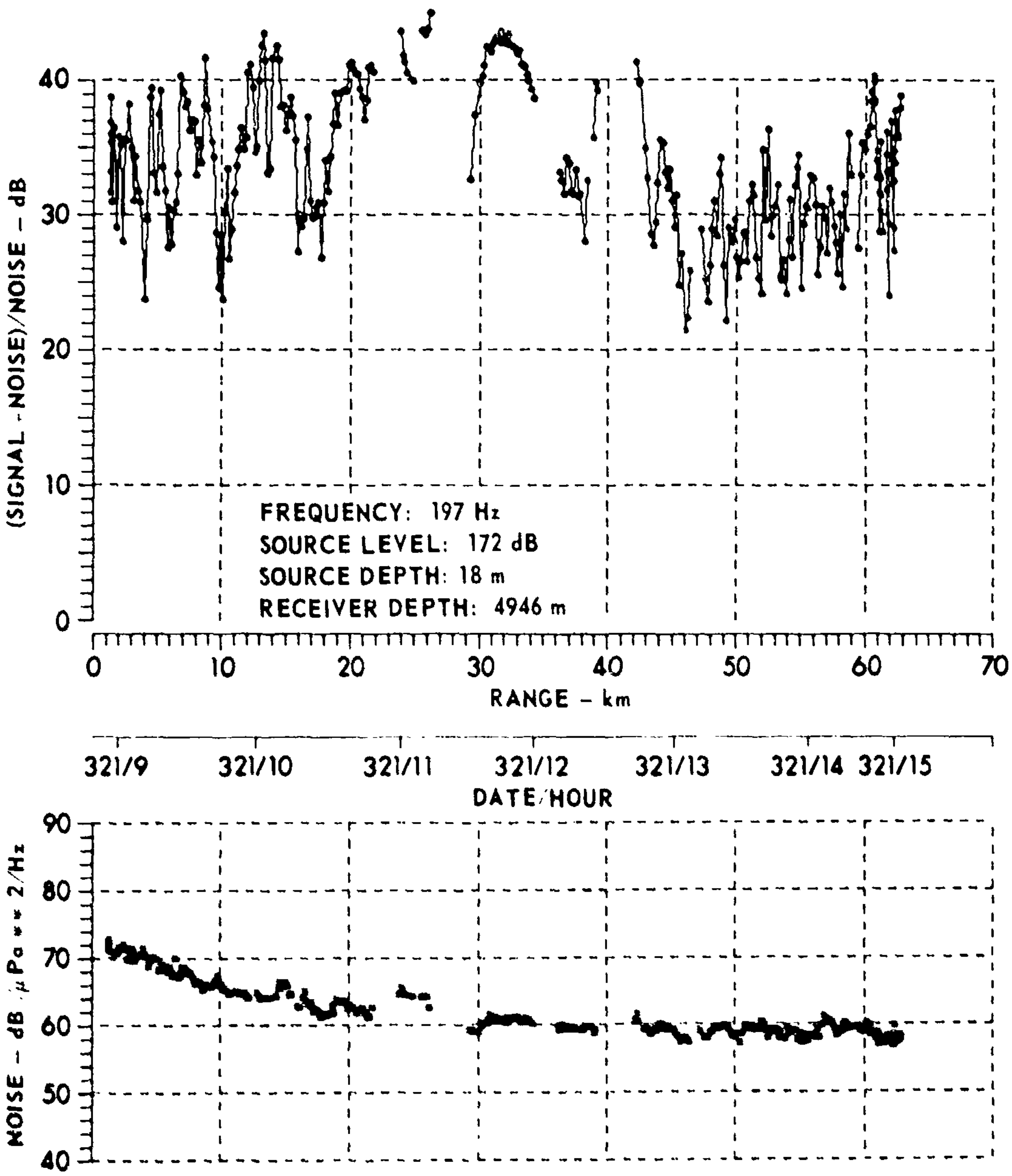

FIGURE 4.4
NOISE AND SIGNAL EXCESS FOR 4946 m RECEIVER
AT 197 Hz CHURCH STROKE II - SITE C PAR (U)

ARL UT
AS-79-860
KCF - GA
4 - 30 - 79

(U) 30 km, the signal excess was generally greater than 20 dB at 67 Hz, and 25 dB at 197 Hz. At Site C sources with levels as low as 150 dB re 1 μPa should therefore be possible under similar noise conditions.

4.2 Ambient Noise at Site C

(C) Selected 1/10 octave bands from the 12 h segment at Site C are shown in Fig. 4.5. The CPA of JNXN occurred at approximately 321/0930; 5 to 8 h later the noise field had settled back down and JNXN was 65 to 100 nmi distant. Three spectra at approximately 3 h intervals are shown in Figs. 4.6 through 4.8; these appear very stable as far as the broadband noise is concerned. Blade rate harmonics from JNXN at 100 nmi can still be clearly seen at frequencies below 30 Hz. The broadband level is near 75 dB around 50 Hz and drops off to near 56 dB around 300 Hz. Since this was such a short time segment, no percentile level displays were computed.

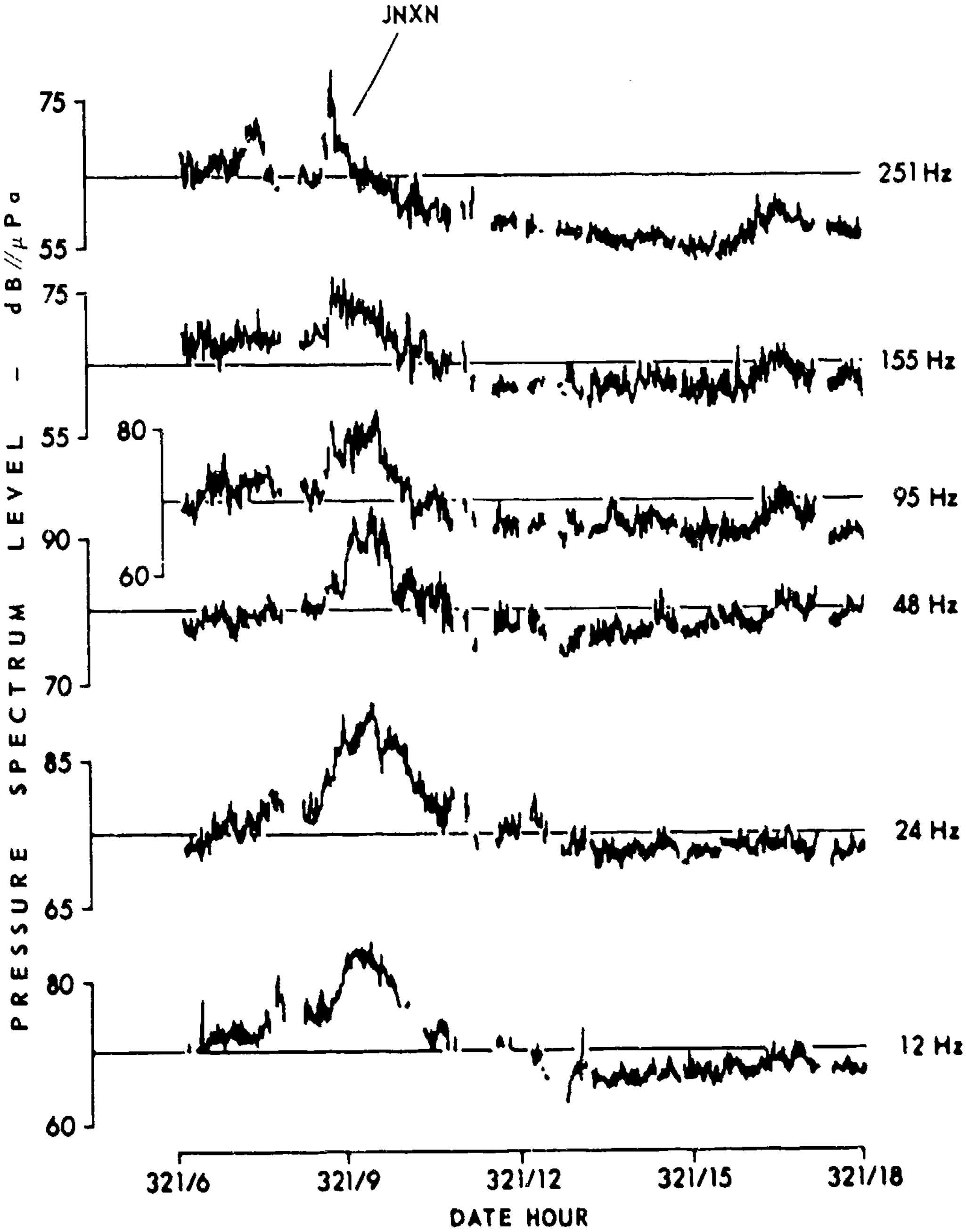

FIGURE 4.5
AMBIENT NOISE TIME SERIES - 4946 m RECEIVER
CHURCH STROKE II - SITE C PAR (U)

ARL UT
AS-79-363
KCF - GA
5 - 1 - 79

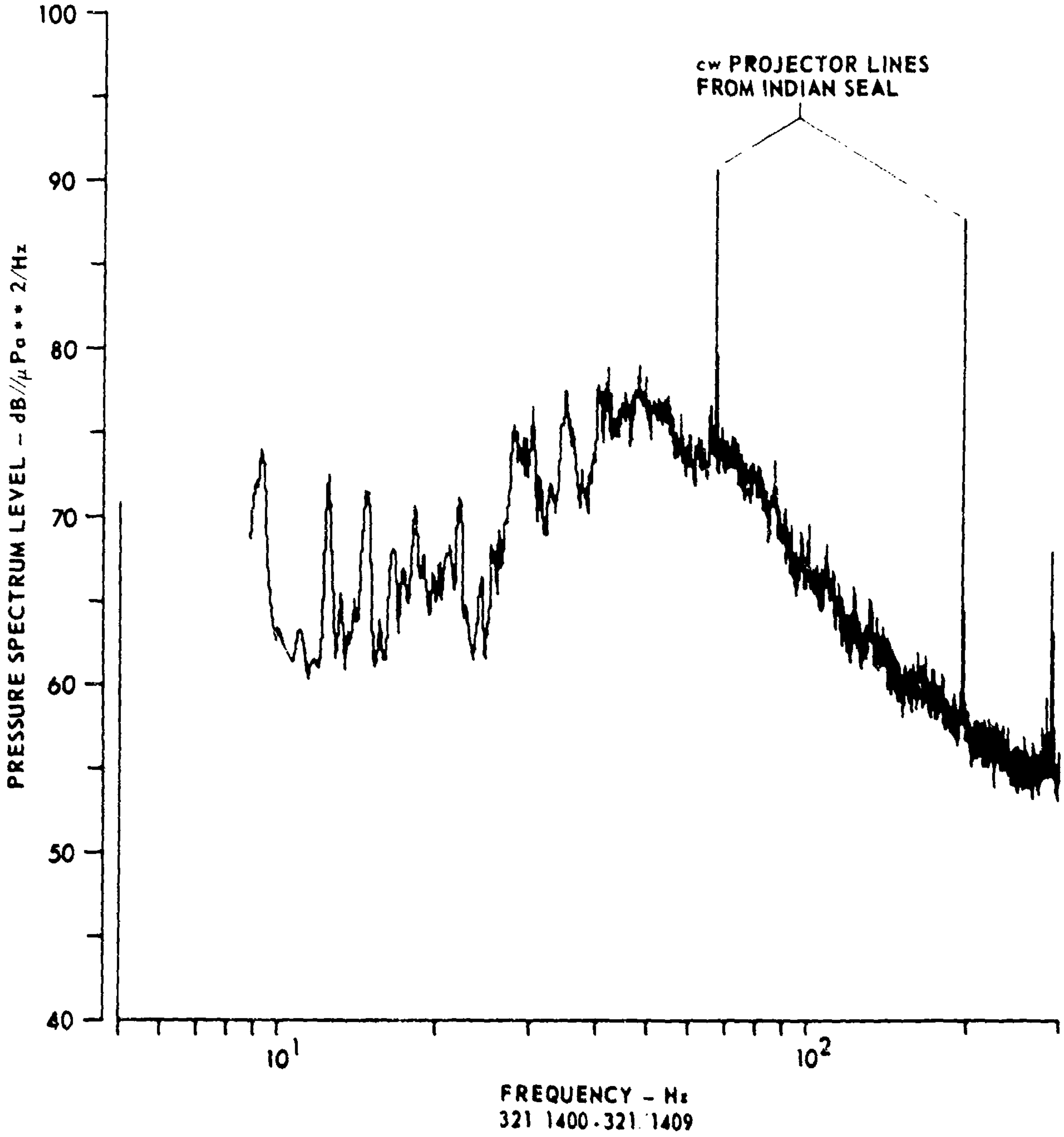

FIGURE 4.6
SITE C AMBIENT NOISE FOLLOWING JNXN
CHURCH STROKE II (U)

ARL UT
AS-79-971
KCF-GA
5-8-79

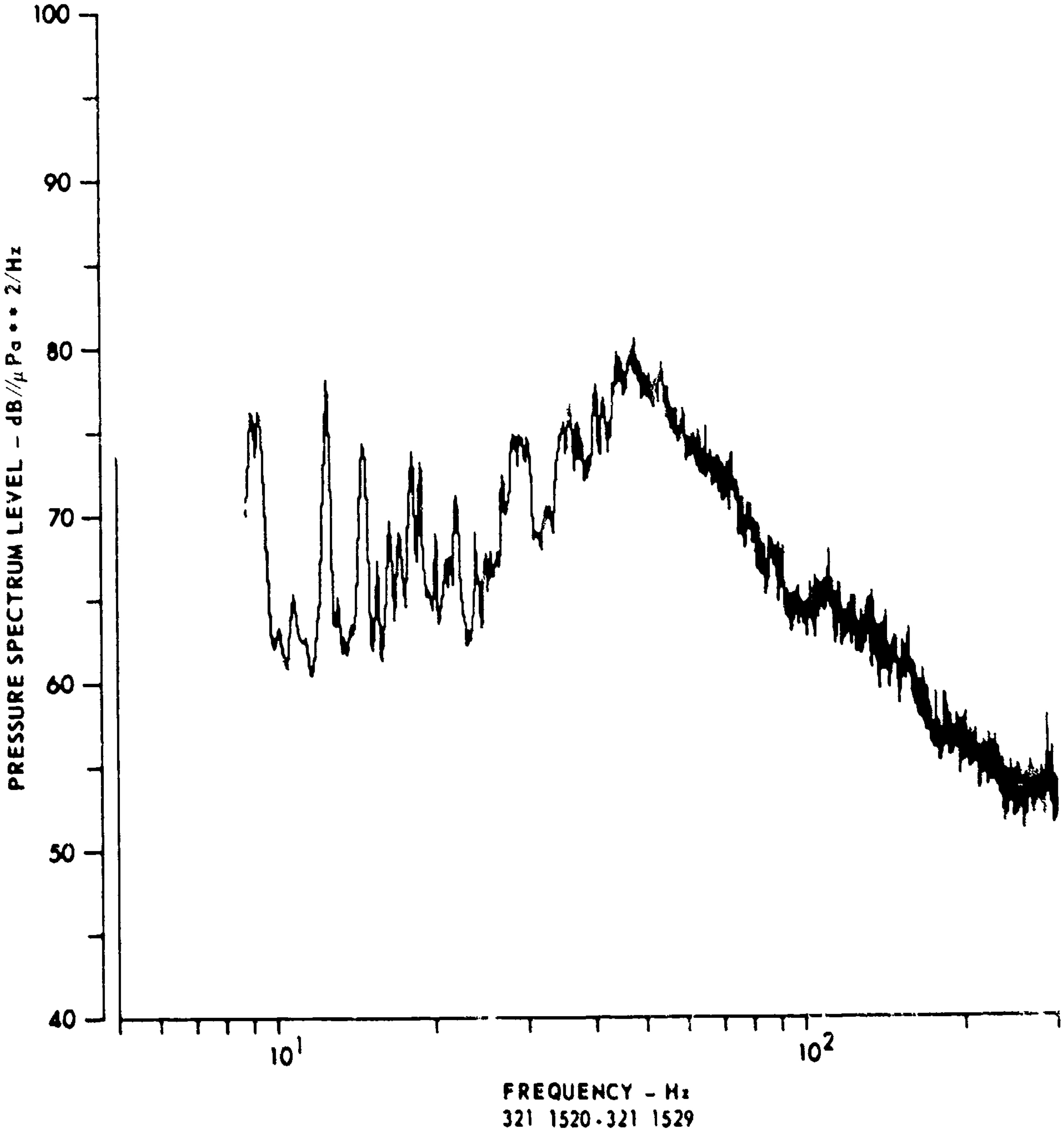

FIGURE 4.7
SITE C AMBIENT NOISE FOLLOWING JNXN
CHURCH STROKE II (U)

ARL UT
AS-79-969
KCF-GA
5-8-79

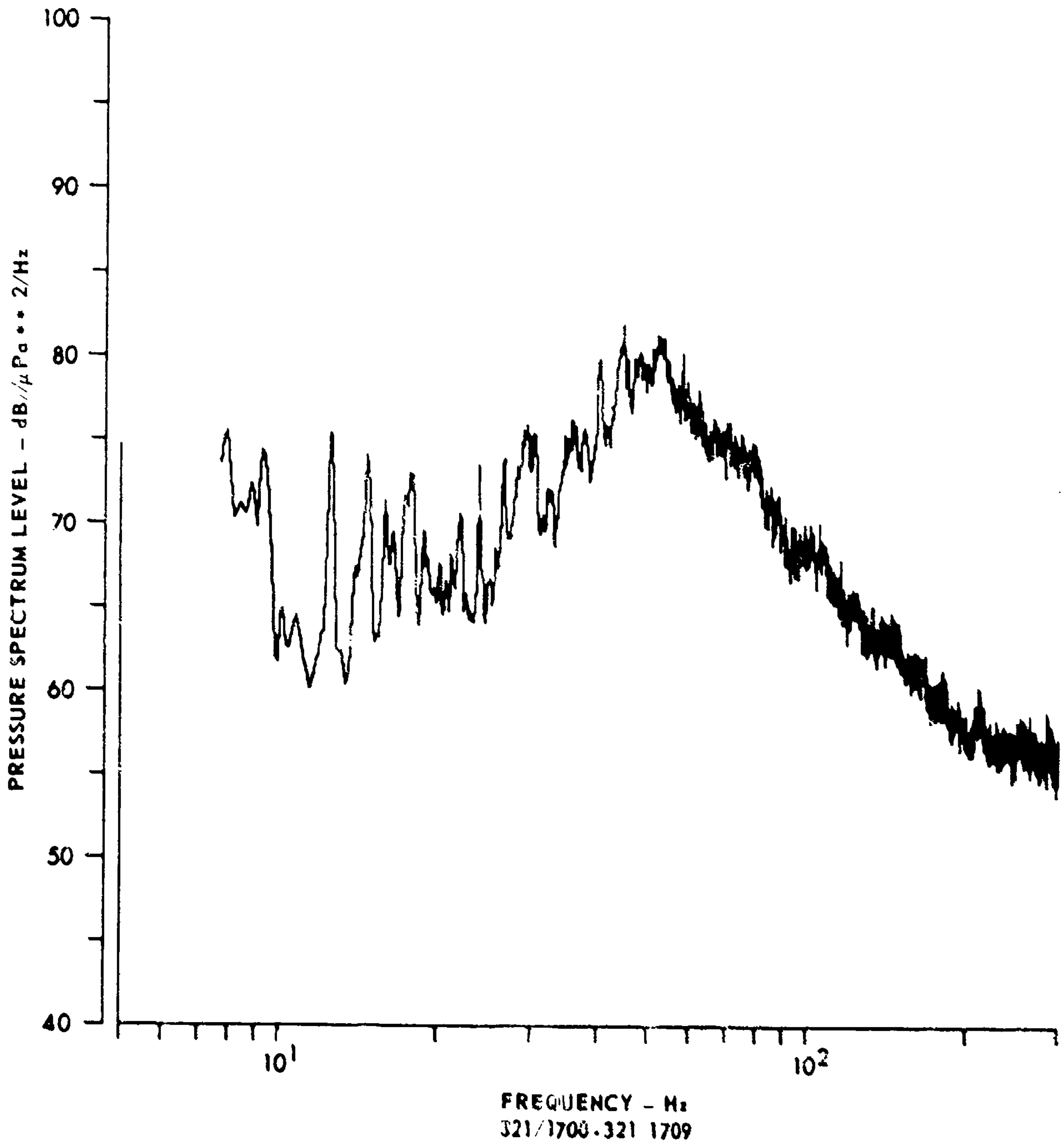

FIGURE 4.8
SITE C AMBIENT NOISE FOLLOWING JNXN
CHURCH STROKE II (U)

ARL UT
AS-79-970
KCF-GA
5-8-79

V. SHIP SIGNATURES

(U) During CHURCH STROKE II several merchant ships passed close to the PAR/ACODAC at Sites B, C, and EN. Two ships were tentatively identified based on reported FNWC position data. This chapter, Sections 1 and 2, presents narrowband spectra generated by these ships; Section 3 presents spectra from three unidentified ships at Sites EN and B; and Section 4 presents spectra from INDIAN SEAL. All of the spectra are in the form of 10 min averages.

(U) The speed of advance (SOA) of the various ships was calculated using Doppler data for each ship. A prominent line component of the ship signature is tracked as the ship steams past the site. The frequency shift of this line between the starting and end points is then measured and assumed to be twice the Doppler shift of this line as the ship approaches CPA. The following equation then yields the SOA of the ship.

$$v = \frac{f_s - f_o}{f_o} c_o \quad ,$$

where f_s is the Doppler shifted frequency, f_o is the actual frequency of the line component, c_o is an average speed of sound in the water, and v is the SOA.

(U) The source levels for the ships discussed below are based on the measured narrowband spectra and the shallow source propagation loss (PL) at the recording sites. At Site C the PL values were obtained from measurements (Fig. 4.2). At Sites B and EN the PL values were obtained from calculations based on incoherently summed eigenrays for an 18 m source (Fig. 5.1) (the measurements at short ranges are for a deeper source). The median PL at 50 Hz for either the measurements or the calculations at the ship-to-receiver range was taken to be the loss incurred by the broadband signature. At Sites B and C, the median broadband PL is approximately

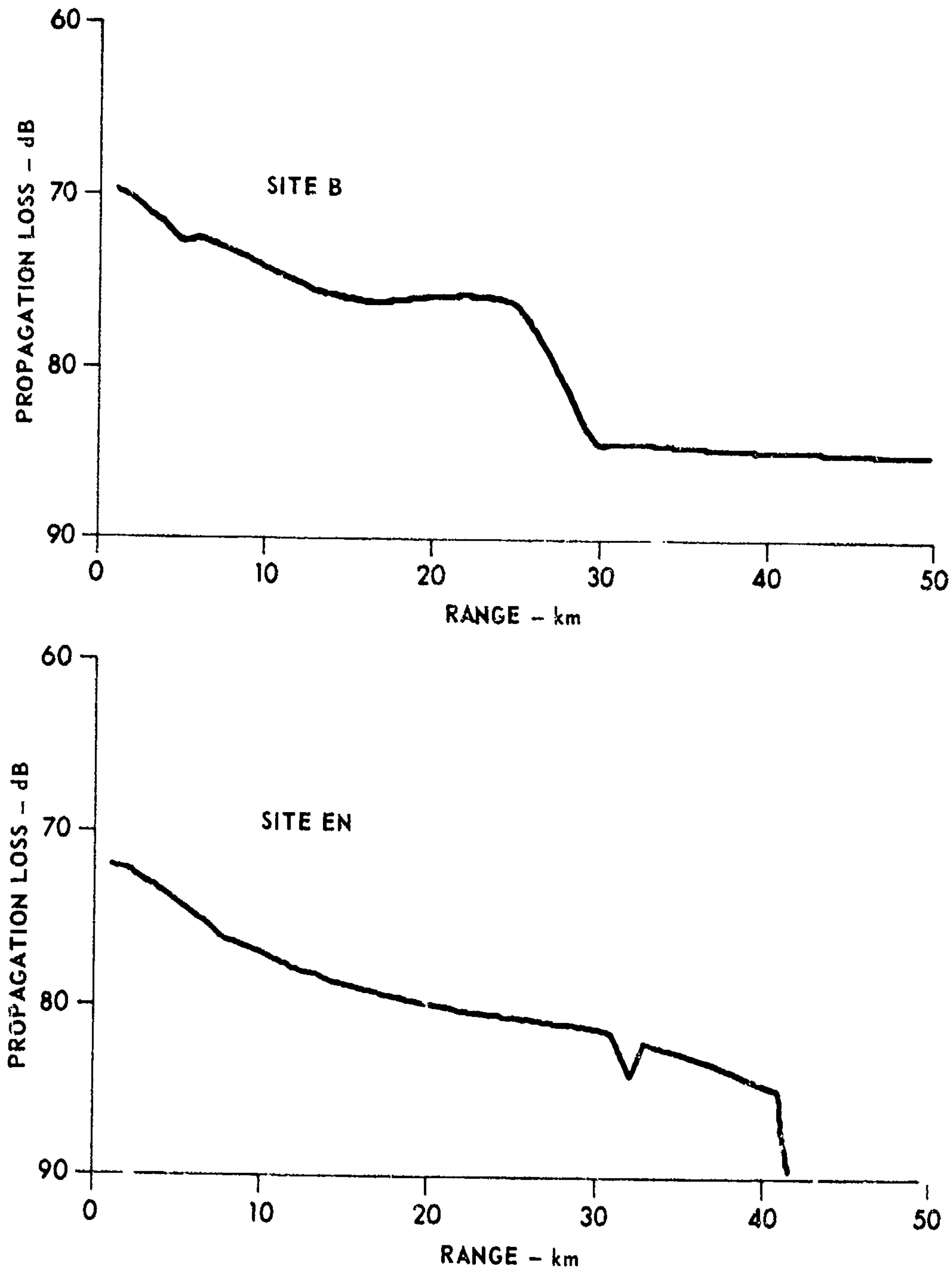

FIGURE 5.1
INCOHERENT RAY THEORY PROPAGATION LOSS
AT 50 Hz FOR 18 m SOURCE
CHURCH STROKE II SITE B AND SITE EN

ARL:UT
AS-79-2077
KCF - GA
10 - 9 - 79

(U) 75 dB between 10 km and 20 km, the range interval used to compute the source levels. At Site EN the PL is around 78 dB at 10 km, which is the range to INDIAN SEAL. These PL values are added to the spectrum levels to obtain the source levels.

(U) Signatures of six different ships are discussed in the following sections of this chapter. The characteristics of the ships' signatures are summarized in Table V-1.

5.1 Unknown or JNXN

(U) On day 321, just before starting a cw radial tow away from Site C, the chief scientist (Dr. A. F. Wittenborn, Ref. 14) on board INDIAN SEAL spotted a "large tanker" bearing down on Site C. The INDIAN SEAL commenced its cw tow at about 321/0830 and tracked the incoming ship on radar to a CPA of 5 nmi from Site C at 321/0910. The acoustic data recorded by the PAR confirm the passage of this ship, as shown in the 1/10 octave band data of Fig. 4.5. The acoustic Doppler data show a CPA at 321/0910 and an approximate SOA of 6 kt.

(U) The ship was possibly the YAMAHATA MARU (radio call sign JNXN), a medium bulk carrier of 186 m length, 27.2 m beam, and 10.5 to 15.5 m draft. The propulsion system given in Lloyd's Register is "Oil 2 SA 7 Cy. 740 x 1600, 8579 kW (11500 bhp)".[15]

(U) The track of JNXN as reported by FNWC is plotted in Fig. 5.2; it shows JNXN approaching Site C to within 5 nmi at 321/0740 at a SOA of 13.73 kt.

(U) There are three inconsistencies in the assumption that this ship is JNXN. JNXN was 1.5 h earlier than measured and was moving too fast, and Dr. Wittenborn reported a "large tanker," not a medium bulk carrier. On the other hand, INDIAN SEAL was practically on the site (within 1 nmi of Site C) for several hours and reported no other ships. In this report,

(C)

TABLE V-1

SHIP SIGNATURE CHARACTERISTICS (U)

Frequencies are the blade rate fundamental and its first three harmonics. Levels are estimated source levels at 1 m.

(Ranges to two of the unknown ships are not available and therefore source levels were not estimated.)

	Blade Rate Lines Frequency Hz and Level - dB//μPa				Broad Band Level dB//μPa²/Hz		
SHIP	F1	F2	F3	F4	50 Hz	100 Hz	200 Hz
"JNXN"	7Hz/-	14/168	21/167	28/174	165	155	140
JJCD	8.7/172	17.4/172	26.1/168	34.8/172	165	162	145
UNKN (unknown) following JJCD	9.7/-	19.4/170	29.1/172	38.8/172	162	150	142
UNKN (unknown) DATE: 331/1900	9.5/-	19/-	28.5/-	38/-	---	---	---
UNKN (unknown) DATE: 332/1810	7.4/-	14.8/-	22.2/-	29.6/-	---	---	---
INDIAN SEAL SPEED: 2.7 kt	7.6/140 9/144	15.2/144 18/143	22.8/143 27/148	30.4/148 36/150	143	135	130
INDIAN SEAL SPEED: 5.25 kt	8.8/-	17.5/152	26.4/151	34.8/153	150	145	139

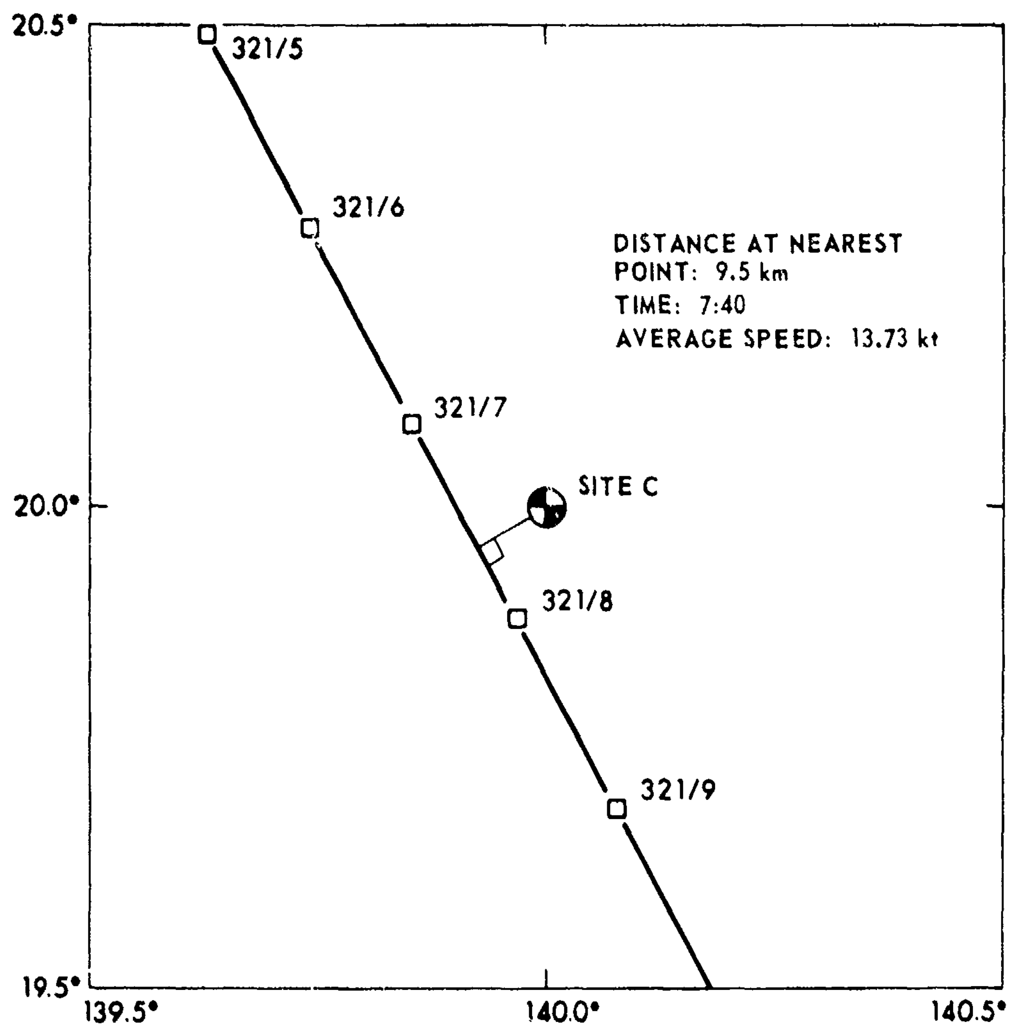

FIGURE 5.2
REPORTED COURSE OF JNXN AT SITE C (U)
CHURCH STROKE II

ARL.UT
AS-79-870
KCF-GA
5-1-79

(U) the ship at 321/0910 is referred to as JNXN with the understanding that these discrepancies do exist.

(C) Spectra from CPA and ±1 h of CPA are shown in Figs. 5.3 through 5.5 on a log frequency scale and in Figs. 5.6 through 5.8 on a linear frequency scale. The spectra at 1 h before CPA, Figs. 5.3 and 5.6, show harmonics of the ship's blade rate and these are almost exact multiples of 7 Hz. The levels in Fig. 5.3 above 50 Hz to 300 Hz were generated by INDIAN SEAL and are discussed in Section 5.4 (see Figs. 5.21 and 5.23). The spectrum at near CPA, Fig. 5.4, shows clear blade rate harmonics up to the 7th harmonic. The cw projector lines from INDIAN SEAL are seen at 67 Hz and 197 Hz. The "lines" for this ship are quite broad as seen in the linear displays of Figs. 5.6 through 5.8.

(C) The source level of the assumed JNXN at CPA can be estimated by adding 75 dB to the spectra in Fig. 5.4 and Fig. 5.7. This 75 dB is for the PL at both 67 Hz and 197 Hz based on an approximate range of 5 nmi (10 km). If 75 dB PL is added to the spectrum, then the broadband level, which peaks near 50 Hz, is 165 dB//μPa^2/Hz and the line peak at 35 Hz is at a level of 178 dB//μPa. The slope of the spectrum between 50 Hz and 200 Hz is 45 dB/decade or 13 dB/octave. This slope is slightly greater than the 10 dB/octave slopes found for some of the ships in the CHURCH OPAL exercise.[16]

5.2 JJCD

(U) On day 322 the ship JJCD (radio call sign) passed near Site B and was recorded by the PAR system. This ship is annotated in the 1/10 octave band time series of Fig. 2.27 and its reported track, plotted from the FNWC position report, is shown in Fig. 5.9. The acoustic estimates at CPA are in fair agreement with this track. The Doppler data shows CPA at 322/0620 and the reported track shows CPA at 322/0710, a 50 min difference. The Doppler data also shows SOA 7.5 kt and the track shows SOA 7.1 kt.

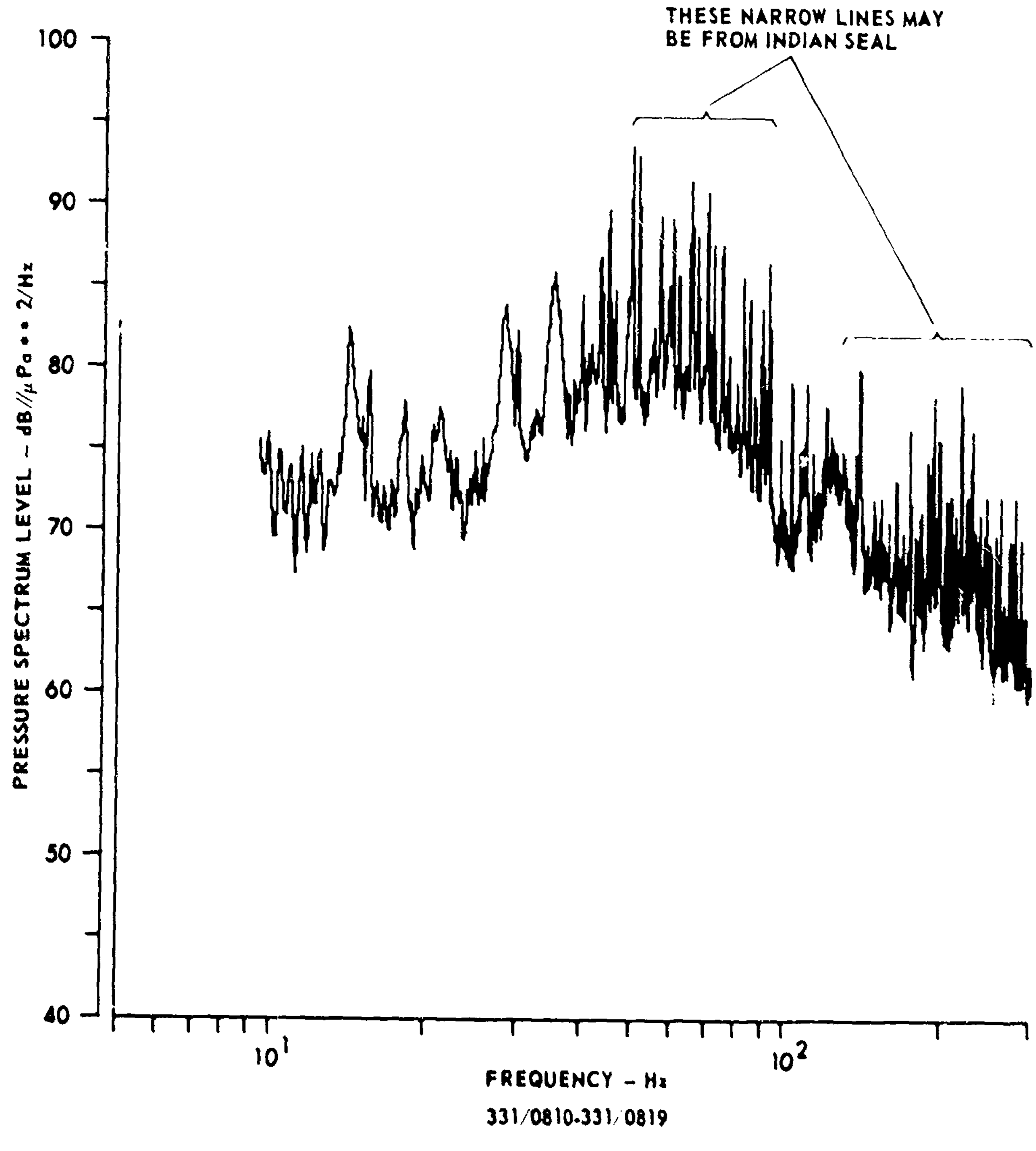

FIGURE 5.3
SIGNATURE OF JNXN APPROACHING SITE C (U)
CHURCH STROKE II

ARL UT
AS-79-880
KCF - GA
5 - 1 - 79

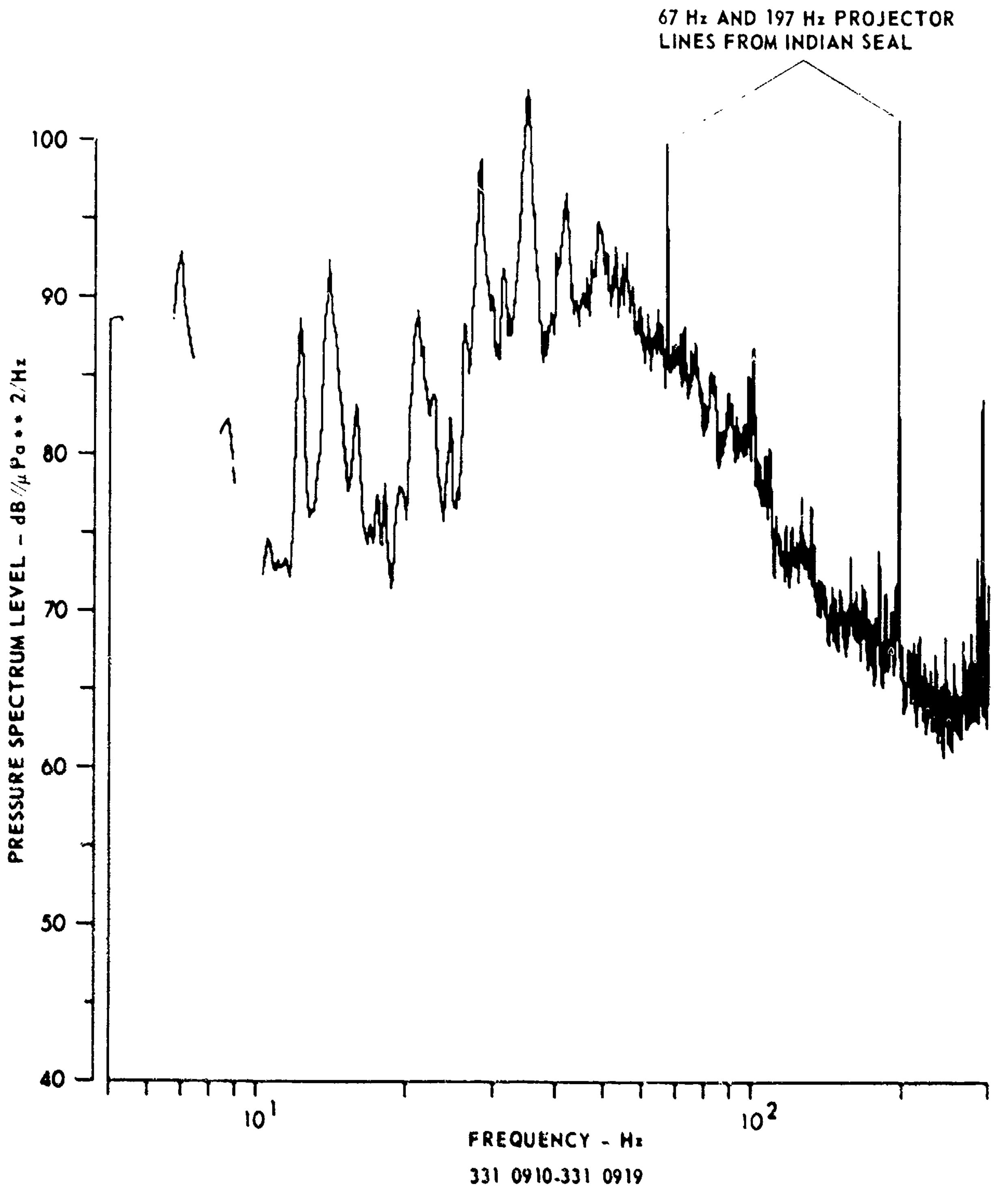

FIGURE 5.4
SIGNATURE OF JNXN NEAR CPA OF SITE C (U)
CHURCH STROKE II

ARL UT
AS-79-881
KCF-GA
5-1-79

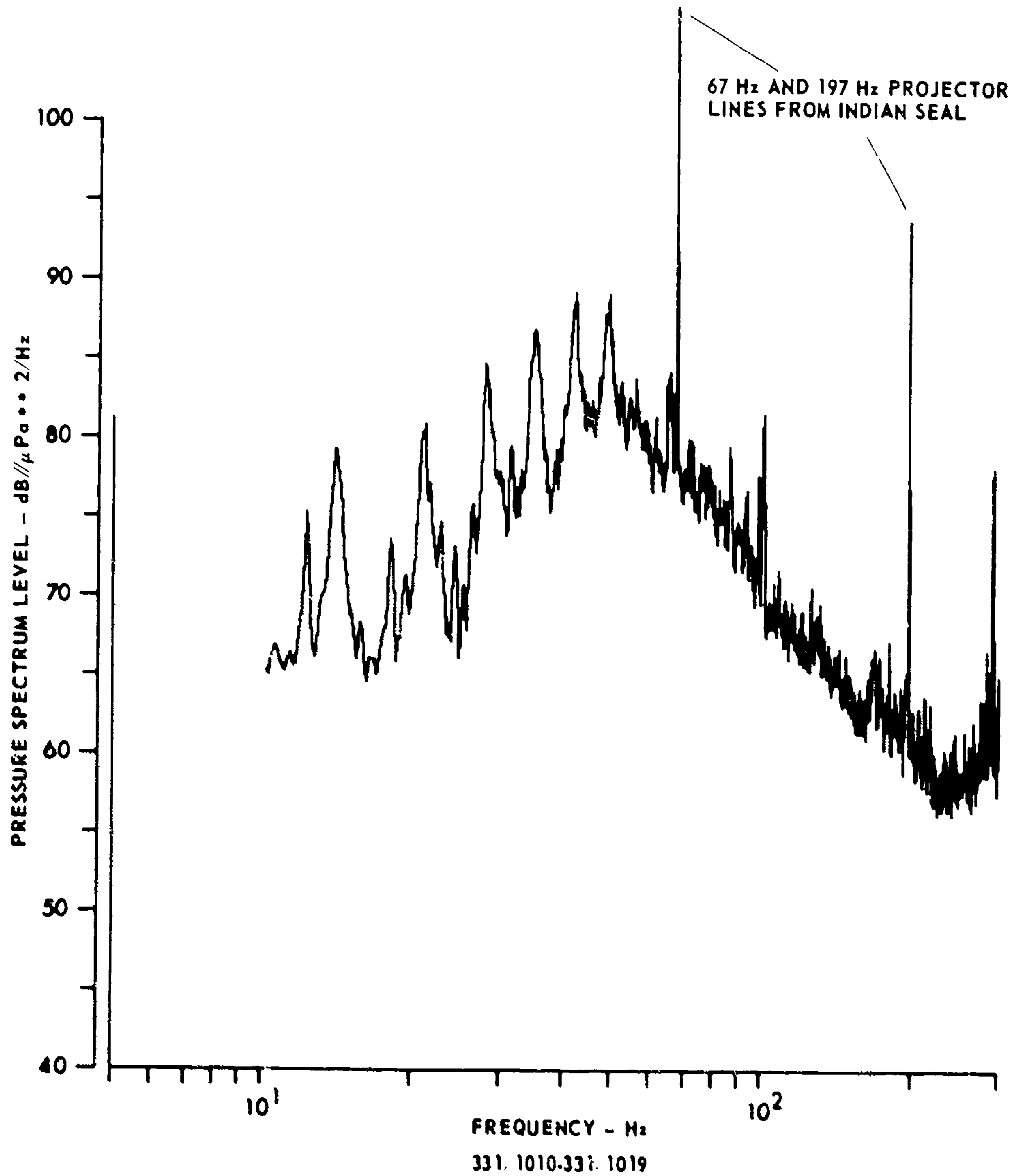

FIGURE 5.5
SIGNATURE OF JNXN DEPARTING FROM SITE C (U)
CHURCH STROKE II

ARL UT
AS-79-882
KCF-GA
5-1-79

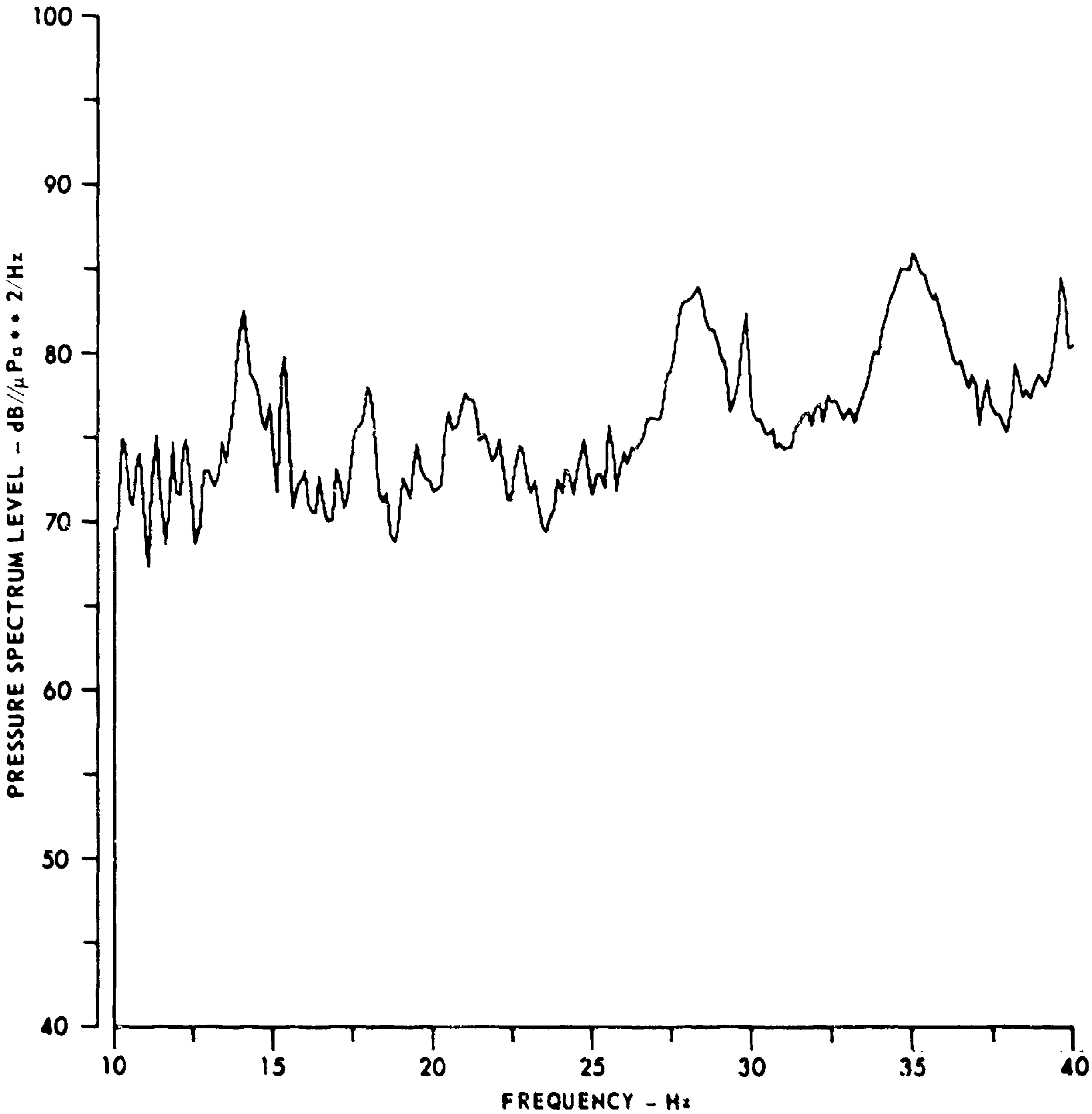

331 0810-331 0819

FIGURE 5.6
SIGNATURE OF JNXN APPROACHING SITE C (U)
CHURCH STROKE II

ARL UT
AS-79-883
KCF - GA
5 - 1 - 79

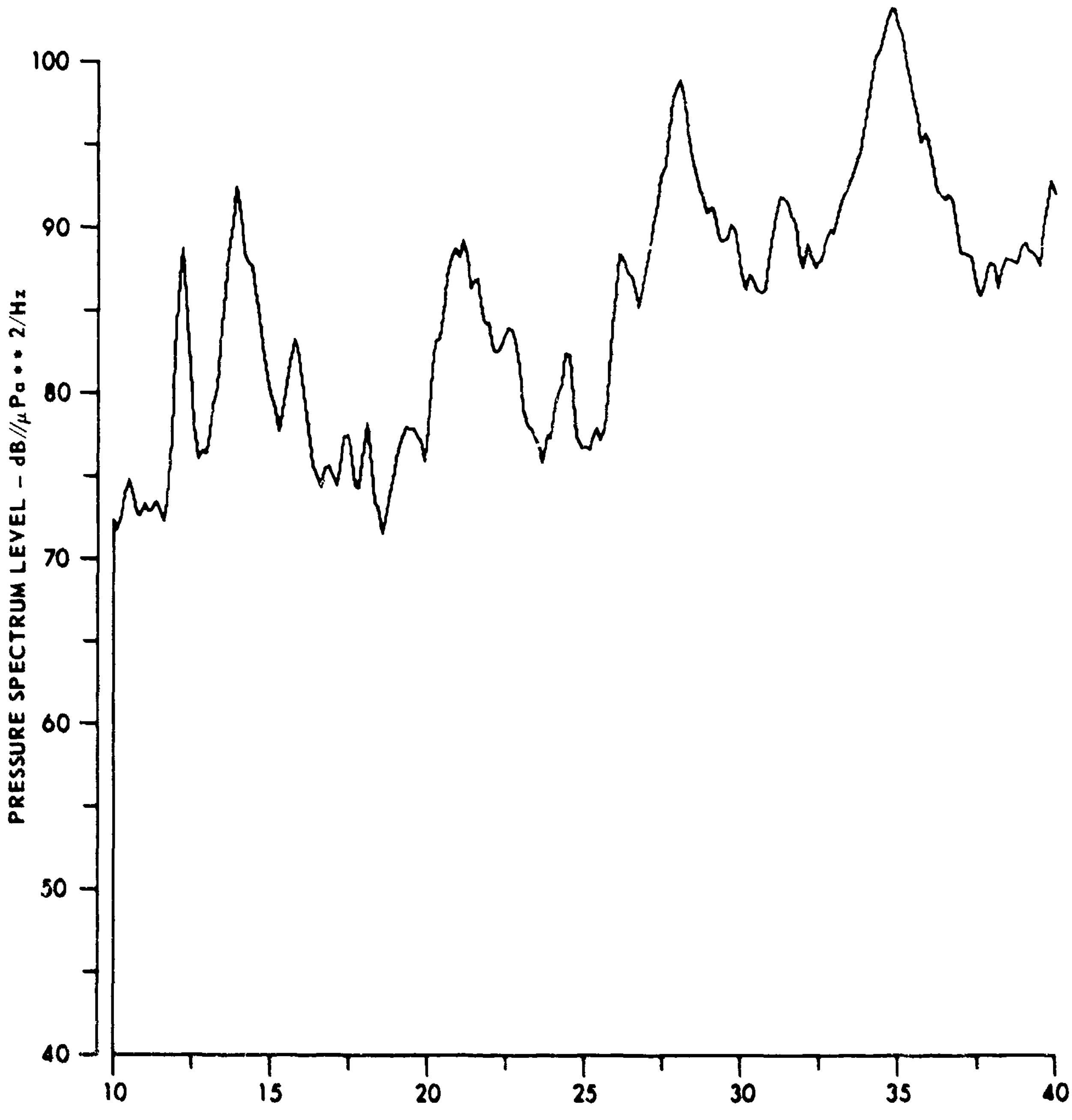

331/0910-331/0919

FIGURE 5.7
SIGNATURE OF JNXN NEAR CPA AT SITE C (U)
CHURCH STROKE II

ARL UT
AS-79-884
KCF - GA
5 - 1 - 79

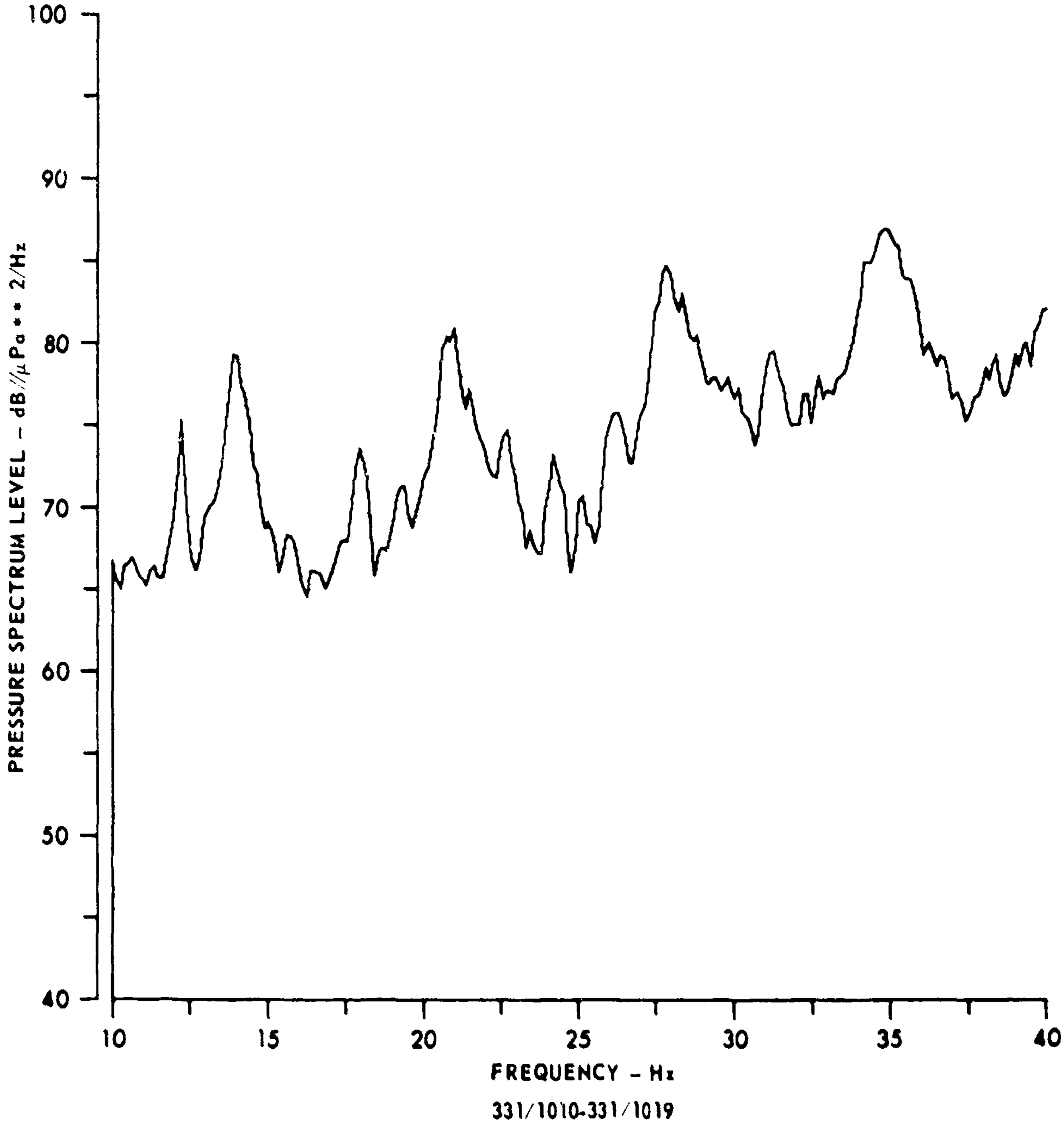

FIGURE 5.8
SIGNATURE OF JNXN DEPARTING FROM SITE C (U)
CHURCH STROKE II

ARL:UT
AS-79-885
KCF-GA
5-1-79

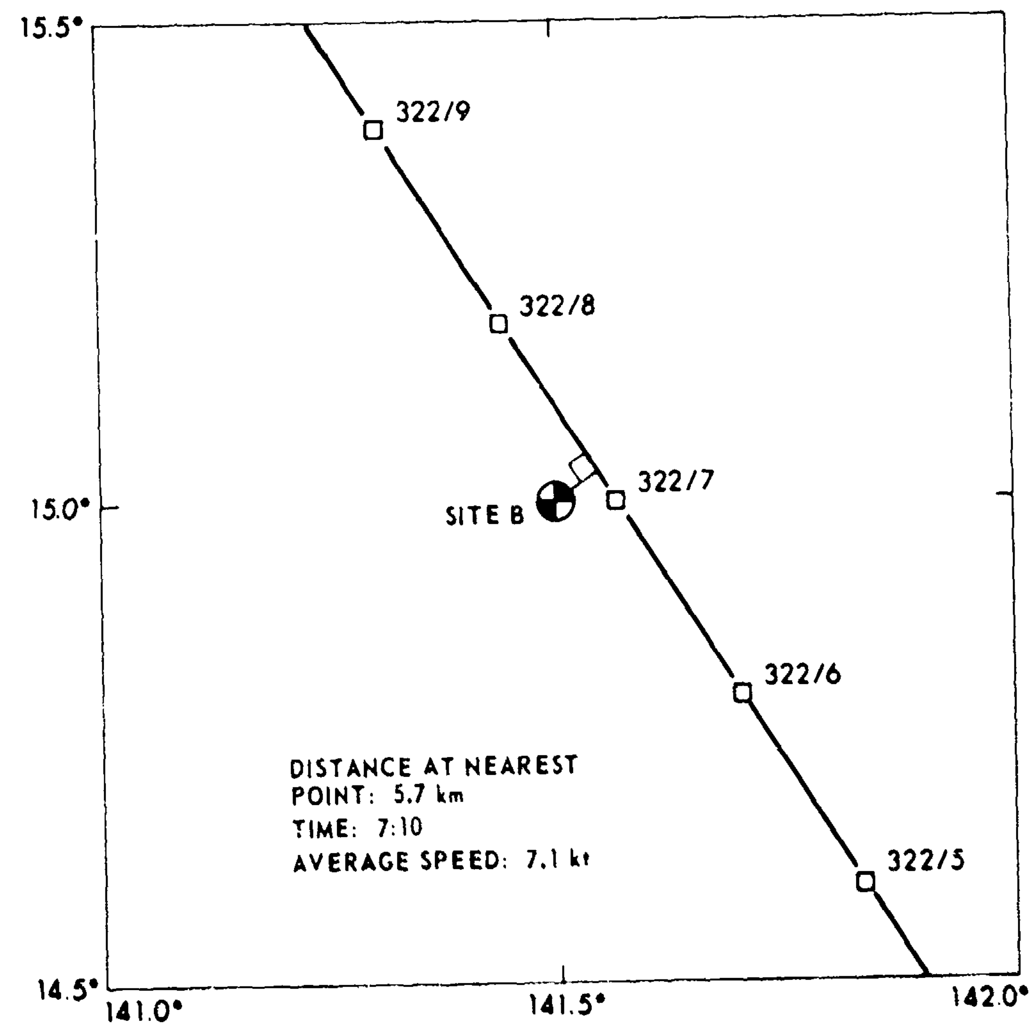

FIGURE 5.9
REPORTED COURSE OF JJCD AT SITE B (U)
CHURCH STROKE II

ARL UT
AS-79-871
KCF-GA
5-1-79

(C) The spectra before, during, and after CPA are shown on a log frequency scale in Figs. 5.10 through 5.13. The spectrum near CPA on a linear frequency scale is shown in Fig. 5.14. The blade rate "lines" of this ship are narrower than those of JNXN in Section 5.1. The blade rate frequency is 8.7 Hz; the level at this frequency is about the same as or greater than the levels of the rest of the blade rate harmonics. This can be contrasted with the tanker in Section 5.1, which had its 7 Hz blade rate fundamental 10 dB below its 5th harmonic at 35 Hz. All of the CHURCH OPAL signatures had their blade rate fundamental frequency levels several decibels below their harmonics.[16]

(U) The source level of JJCD can be estimated by adding 75 dB to the spectra near CPA, which was at a reported (FNWC) range of 5 to 10 km. The uncertainty in PL due to a range error over the interval 5 km to 25 km amounts to only 3 to 5 dB. For ranges less than 25 km the PL is direct path dominated. The spectra 1 h before and after CPA are 12 dB lower than the CPA spectra. This change in level is also seen in the cw PL of Fig. 2.21 between the direct path region and the shadow zone. Based on the reported positions, the range at CPA is no less than 10 km.

(C) Based on the 75 dB PL, the peak source level is 175 dB//μPa; the broadband source level peaks at 165 dB//μPa^2/Hz at 50 Hz. The spectral rolloff at CPA beyond 100 Hz is 65 dB/decade or 20 dB/octave. Beyond direct path the slope changes to 55 dB/decade or 17 dB/octave. In either case this is a steep rolloff of the spectrum.

5.3 Three Unknown Ships

(C) Close behind JJCD an unknown ship also approached Site B, as annotated in the 1/10 octave band time series of Fig. 2.27. The spectrum of this ship is shown in Figs. 5.15 and 5.16; it appears from the time series to have approached Site B within 20 km. Thus a PL of 75 dB should be added to the spectrum to estimate source level. From the appearance of the overall spectrum, the blade rate was 9.7 Hz, but the level at this frequency was below the electronics noise level and was not detected.

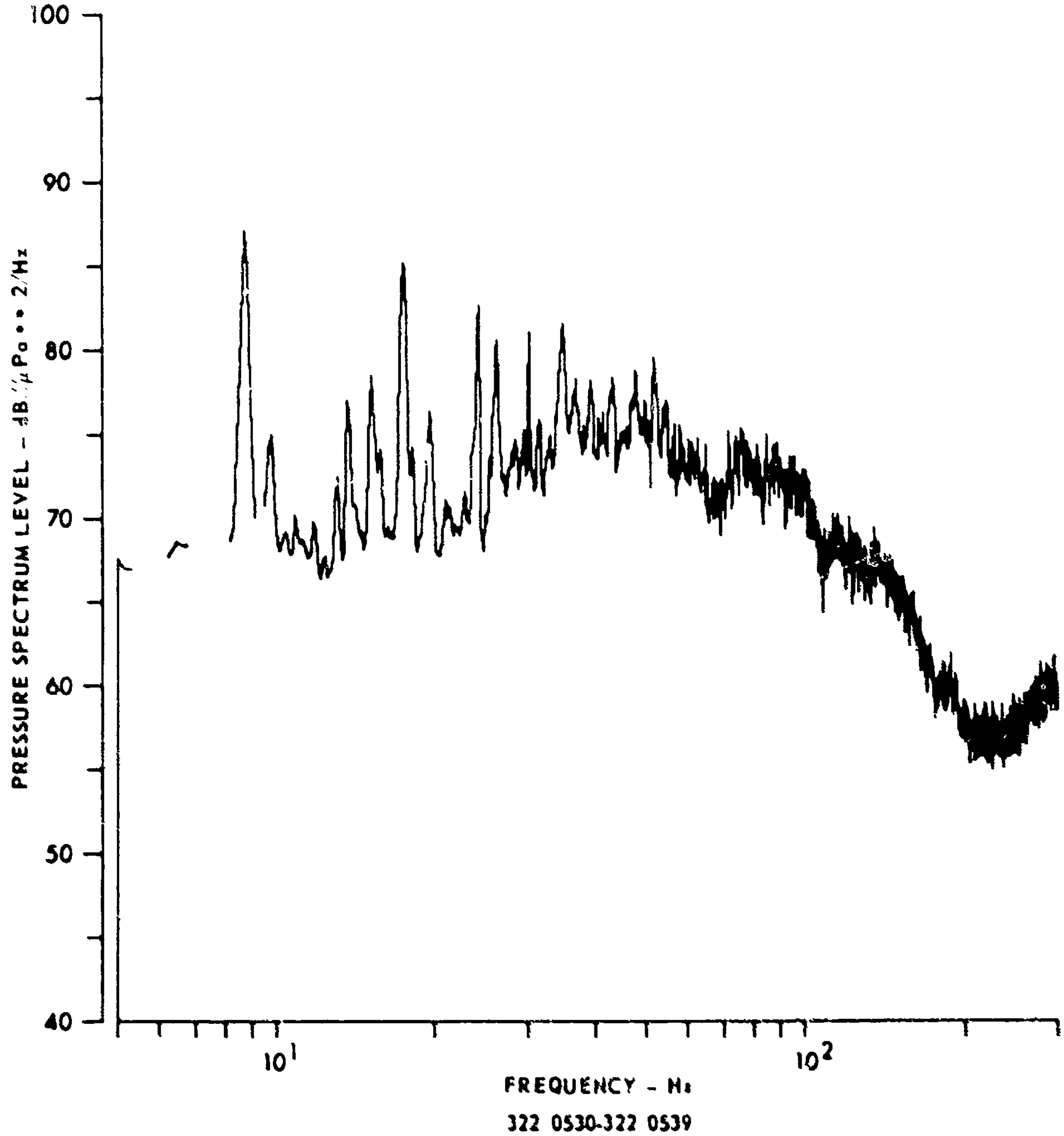

FIGURE 5.10
SIGNATURE OF JJCD APPROACHING SITE B (U)
CHURCH STROKE II

ARL UT
AS-79-886
KCF-UA
5-1-79

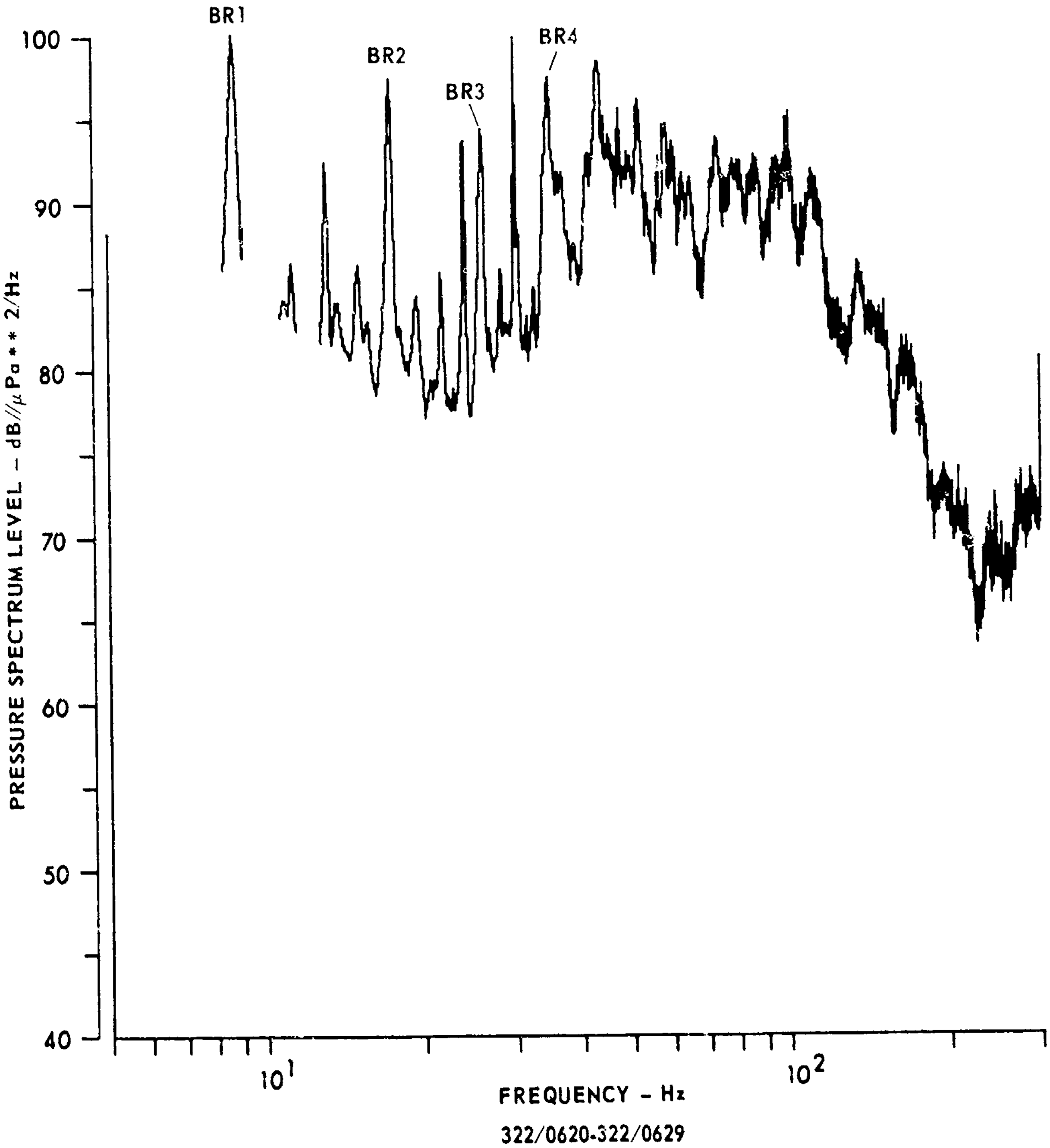

FIGURE 5.11
SIGNATURE OF JJCD NEAR CPA OF SITE B (U)
CHURCH STROKE II

ARL:UT
AS-79-887
KCF-GA
5-1-79

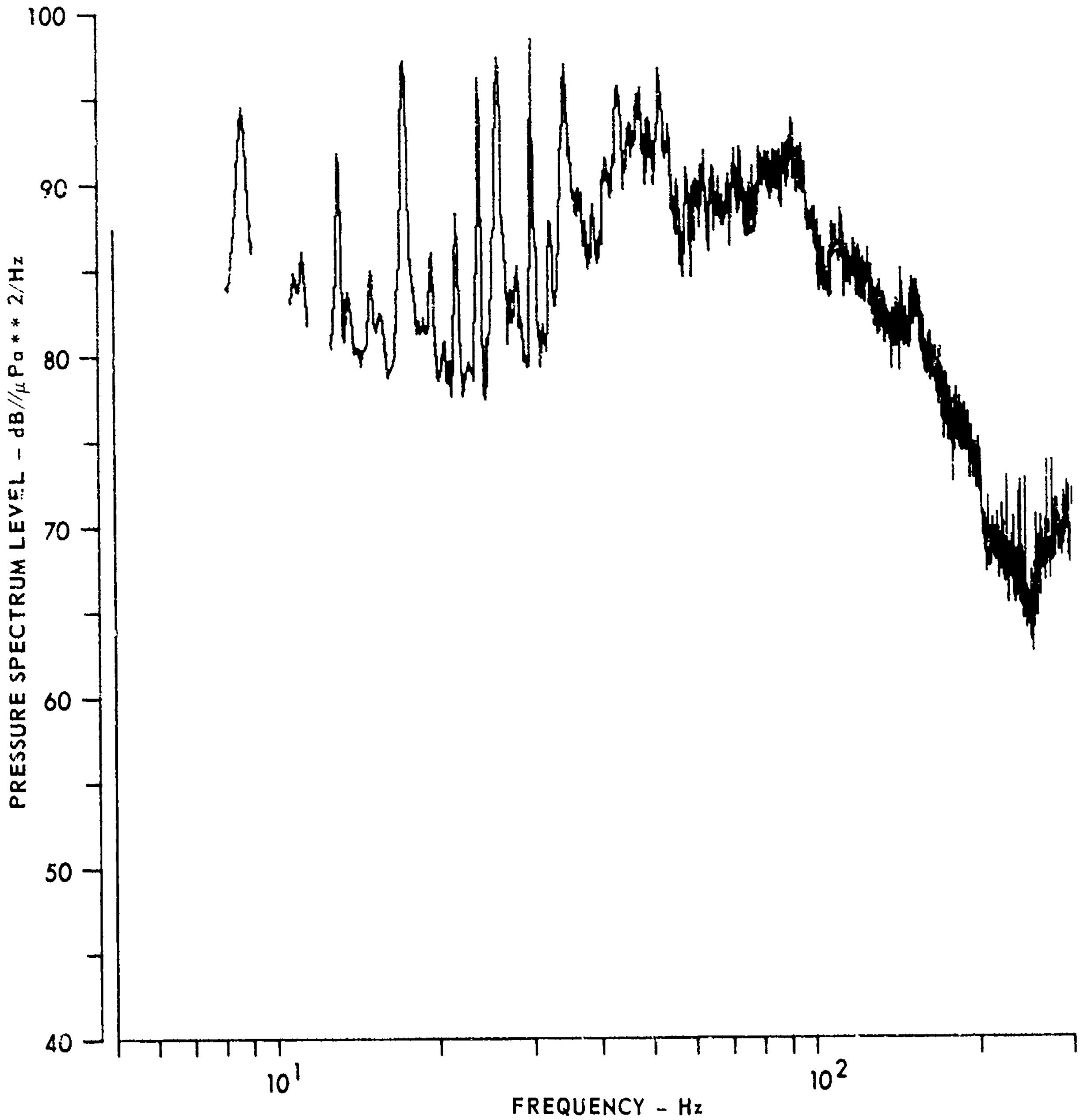

322/0630-322/0639

FIGURE 5.12
SIGNATURE OF JJCD NEAR CPA OF SITE B (U)
CHURCH STROKE II

ARL:UT
AS-79-888
KCF-GA
5-1-79

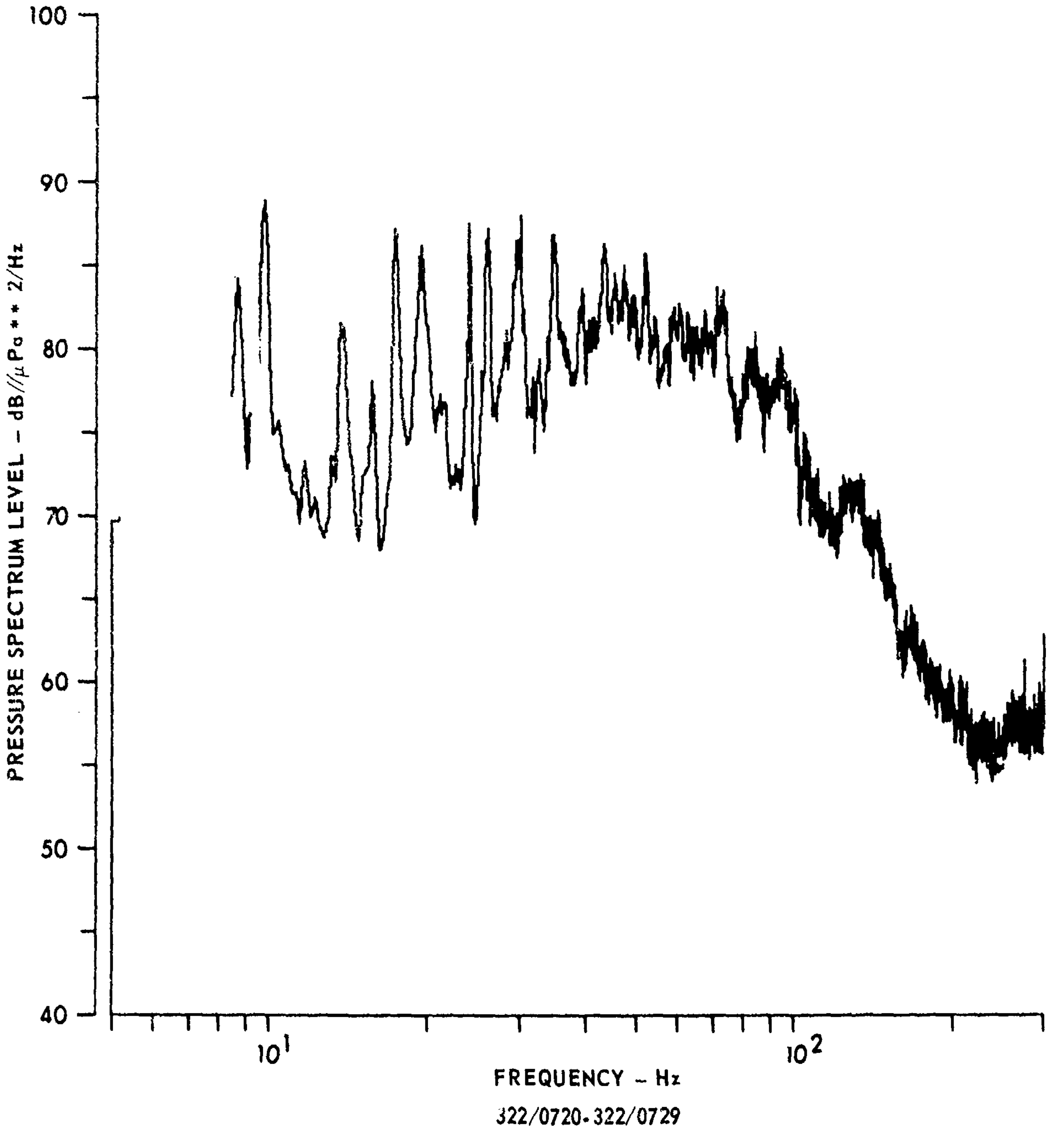

FIGURE 5.13
SIGNATURE OF JJCD DEPARTING FROM SITE B (U)
CHURCH STROKE II

ARL:UT
AS-79-889
KCF-GA
5-1-79

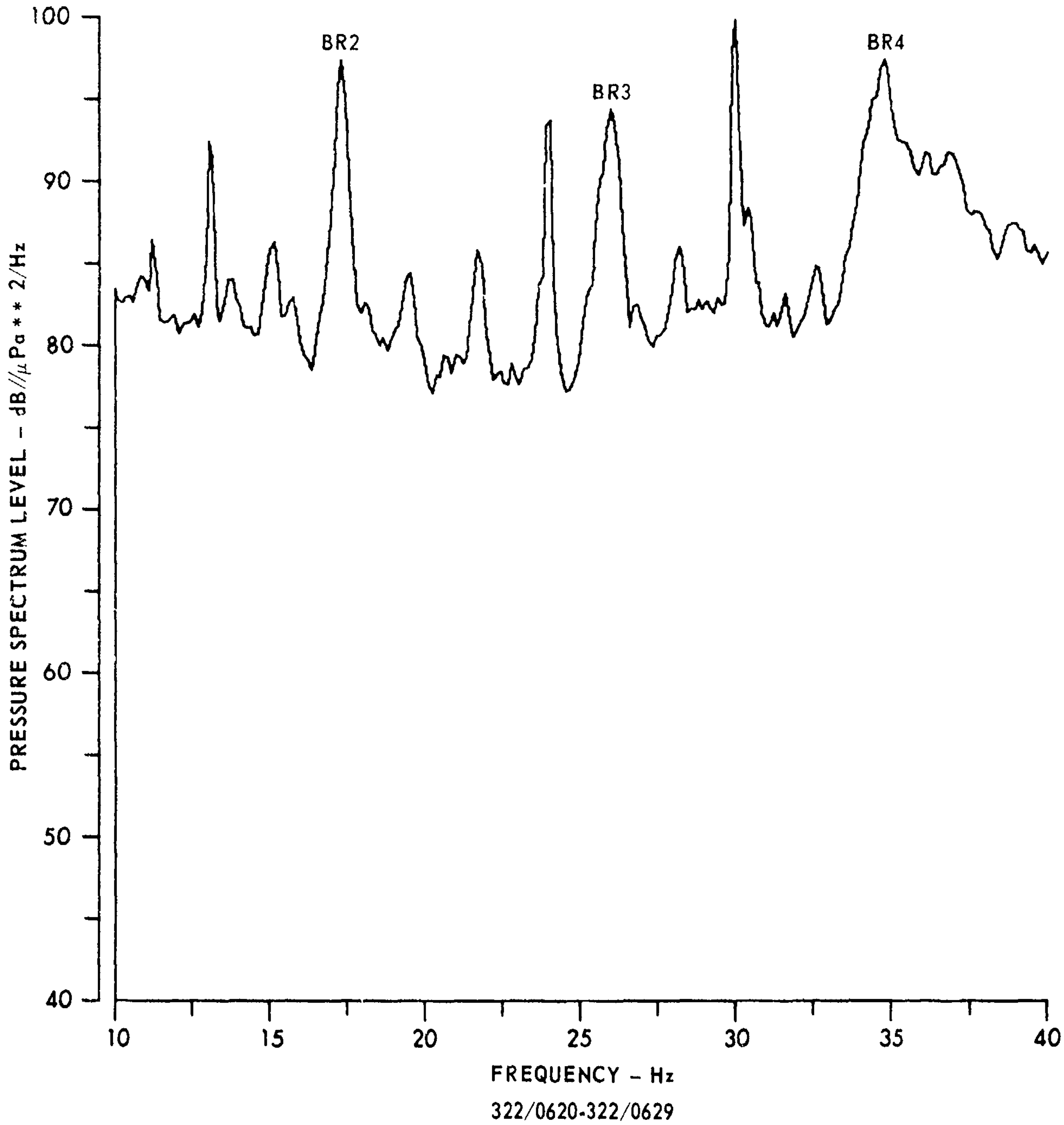

FIGURE 5.14
SIGNATURE OF JJCD NEAR CPA OF SITE B (U)
CHURCH STROKE II

ARL:UT
AS-79-890
KCF-GA
5-1-79

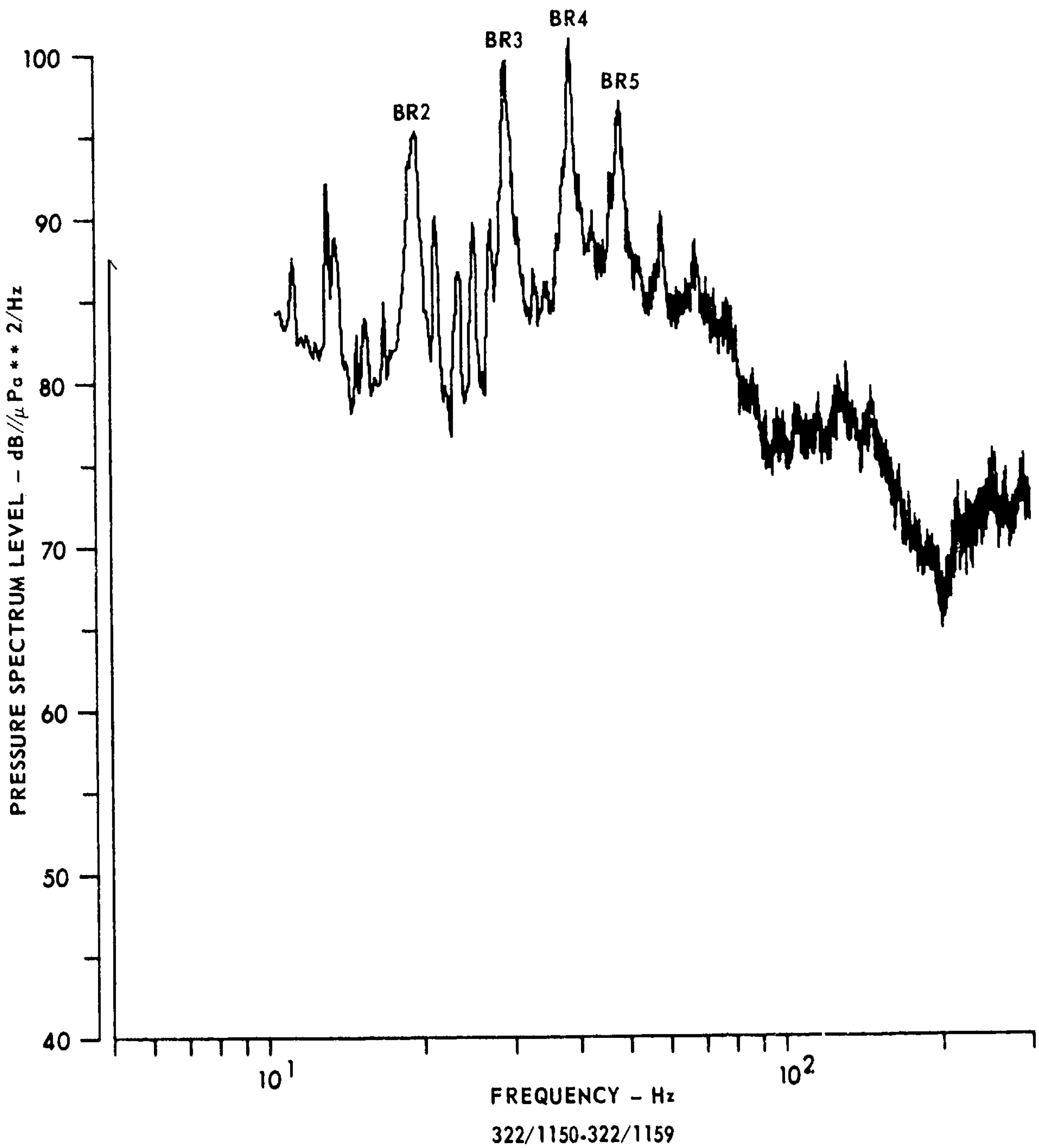

FIGURE 5.15
SIGNATURE OF UNKNOWN SHIP FOLLOWING JJCD (U)

ARL:UT
AS-79-878
KCF - GA
5 - 1 - 79

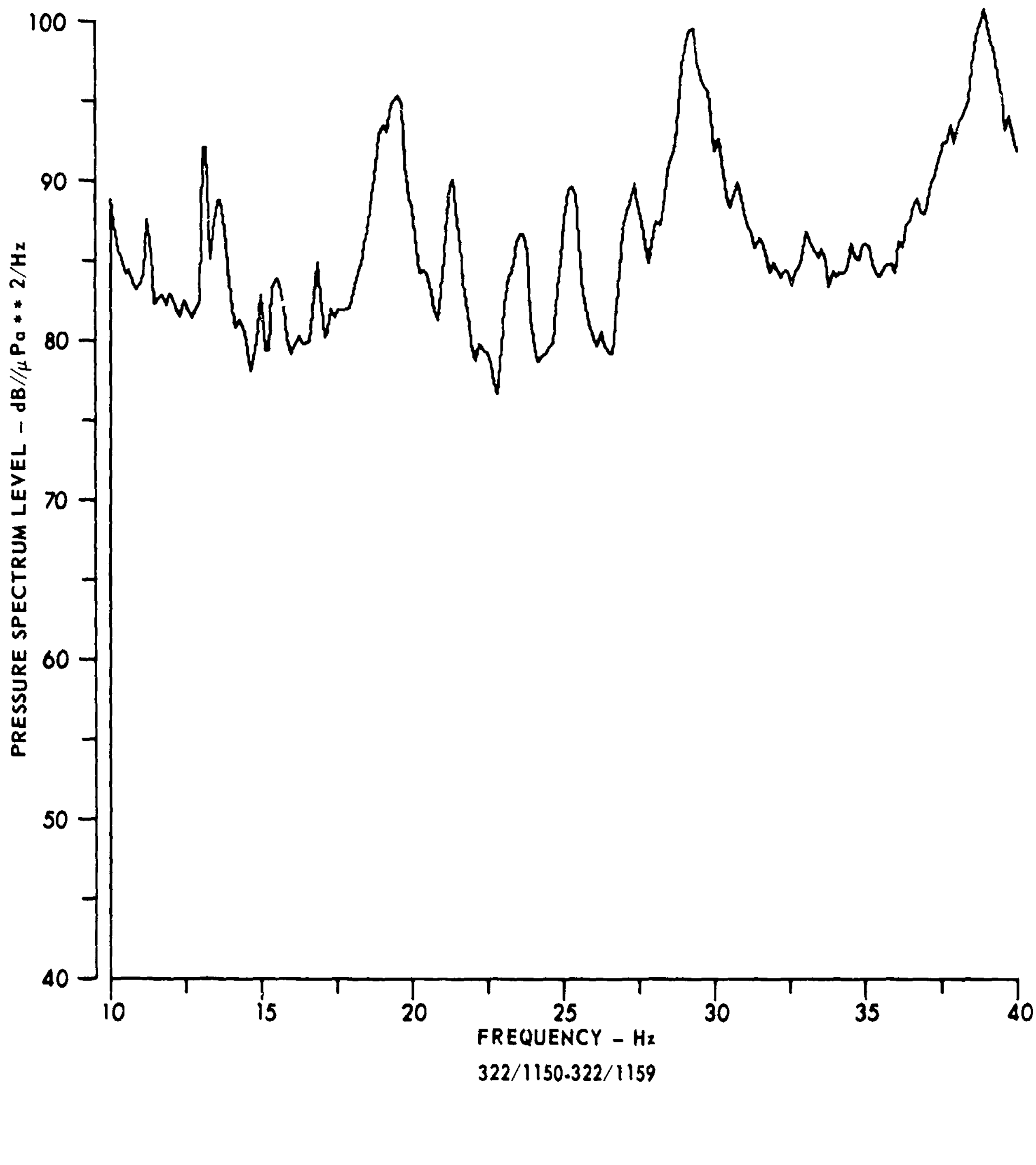

FIGURE 5.16
SIGNATURE OF UNKNOWN SHIP FOLLOWING JJCD (U)

ARL:UT
AS-79-879
KCF-GA
5-1-79

(C) At Site EN the ACODAC and PAR were deployed early because of the weather. Consequently, no ship track information was collected during the first 48 h of recording time for the ACODAC, from which two ship signatures were extracted. The ship at 331/1900 was detected at all depths by the ACODAC as seen in Figs. 3.41 through 3.45. The spectrum in Fig. 5.17 shows a high level blade rate at 9.5 Hz, and its harmonics can be seen up to the 10th order. The "lines" are very broad as seen in the linear frequency plot of Fig. 5.18.

(C) One day later at 332/1810 another ship passed by Site EN and its spectrum is shown in Figs. 5.19 and 5.20. The blade rate was 7.4 Hz and the "lines" are narrower.

5.4 INDIAN SEAL

(U) The best documented signature is from INDIAN SEAL, which was the deployment ship for the PAR/ACODAC systems. This ship is 62.5 m (205 ft) long with a beam of 12.2 m (40 ft) and a draft of 4.3 m (14 ft) forward and 4.6 m (15 ft) aft. The displacement is 270 gross tons.[17] The propulsion system is twin screw direct drive, 3 blades/screw, variable pitch. The engines are ALCO 12V251 - 5250 hp (2 each). The design cruise speed is 10 kt. Signature data were taken at 2.7 kt and 5 kt while the ship was towing a cw source.

(C) The first signature is from Site B, time 323/1020, using channel 4 of the PAR system 30 m above the bottom. Possible blade rate lines are at 7.6 Hz and 9.0 Hz, as seen in Figs. 5.21 and 5.22. These correspond to engine speeds of 150 rpm and 180 rpm. The large number of narrow lines seen above 50 Hz in the logarithmic spectrum of Fig. 5.21 are shown on a linear scale in Fig. 5.23. The 67 Hz projector line is identified; the source of the other lines is unknown. The ship was approaching Site B at 2.7 kt at a range of 11 km and the estimated PL, as in the case of the other ship signatures for Site B, is 75 dB. The broadband noise level is then 143 dB//μPa^2/Hz at 50 Hz; blade rate harmonics go as high as

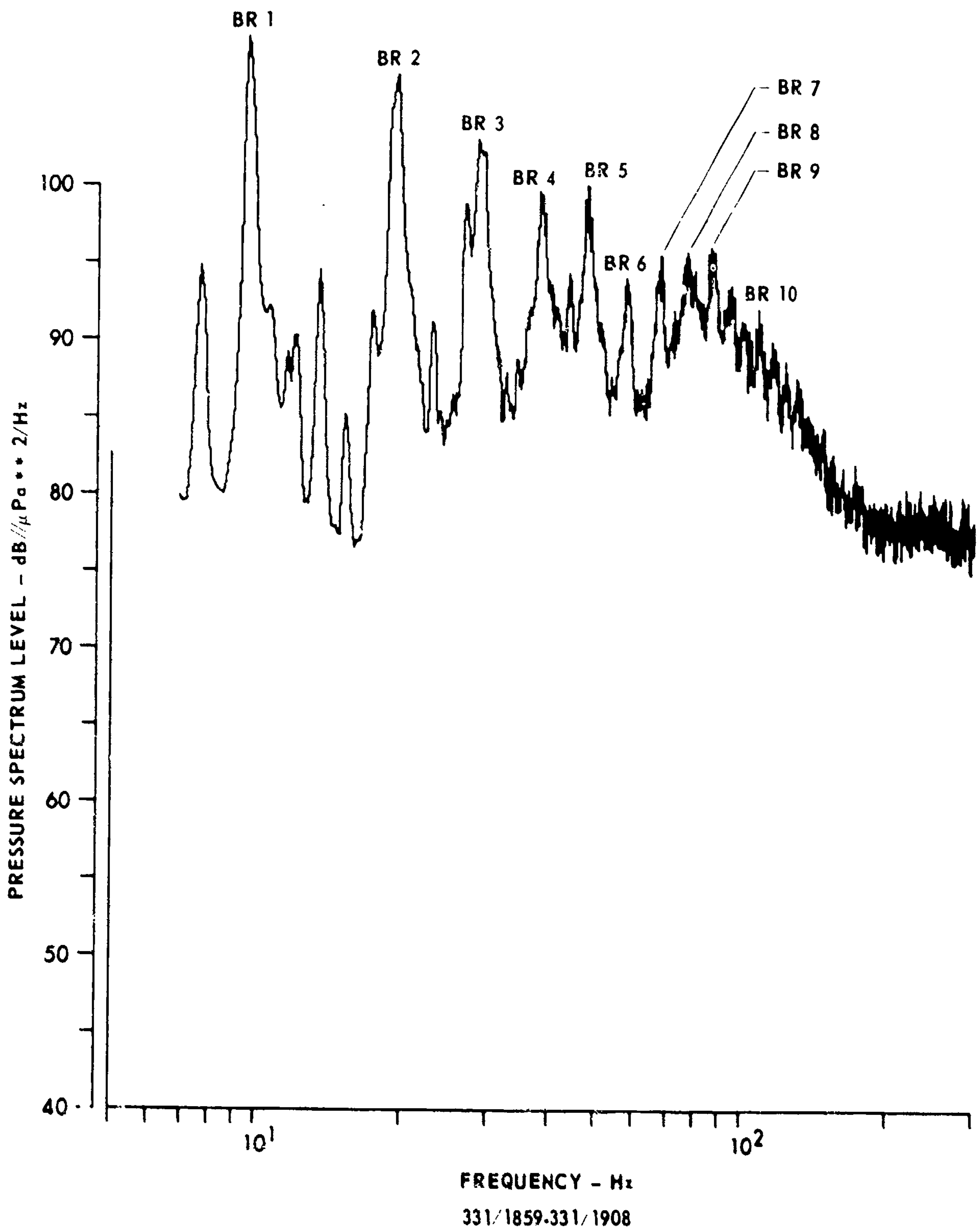

FIGURE 5.17
SIGNATURE OF UNKNOWN SHIP AT CHURCH STROKE II - SITE EN (U)

ARL:UT
AS-79-979
KCF-GA
5-8-79

CONFIDENTIAL

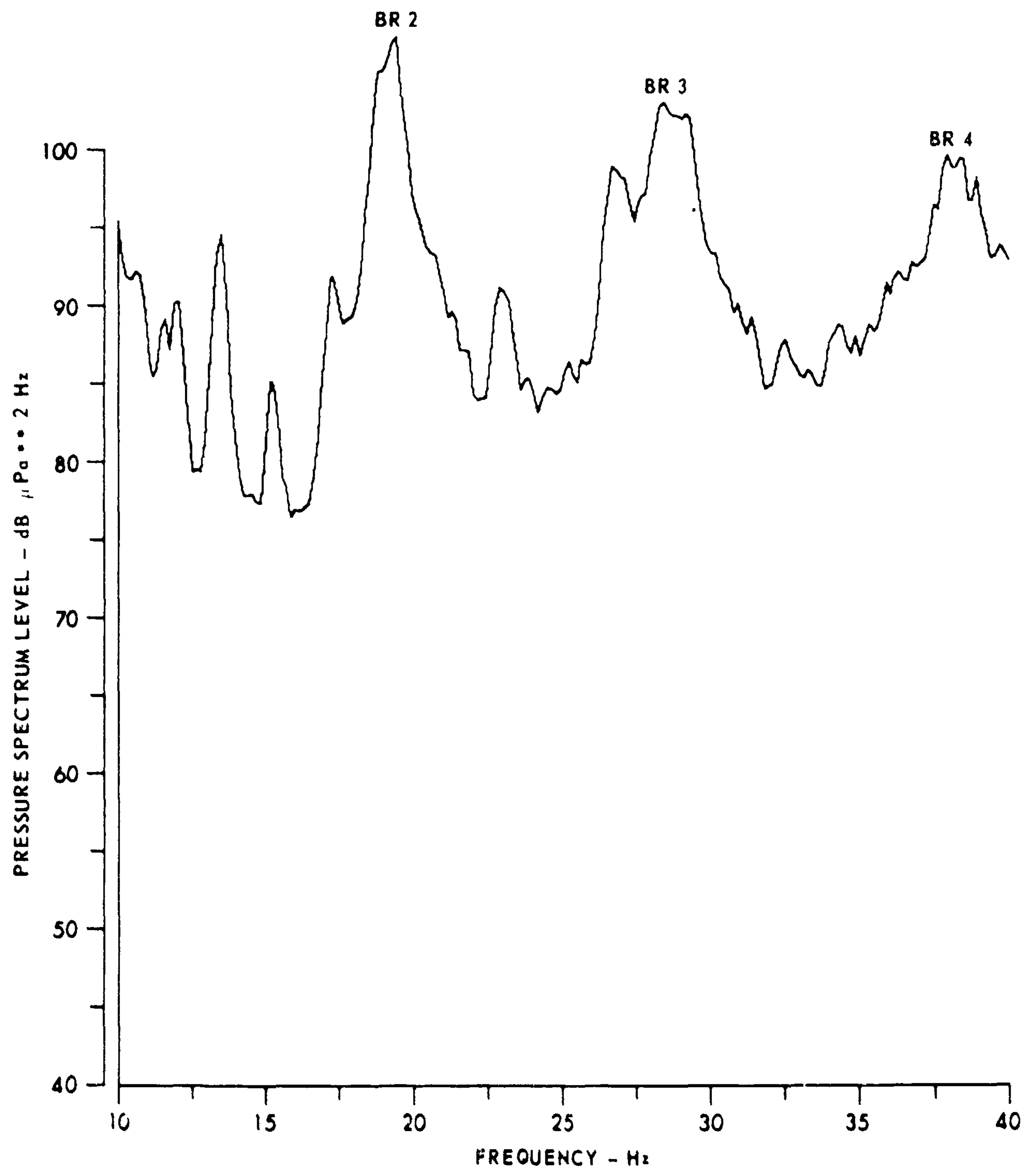

331 1859-331 1908

FIGURE 5.18
SIGNATURE OF UNKNOWN SHIP NEAR CHURCH STROKE II - SITE EN (U)

ARL UT
AS-79-980
KCF - GA
5 - 8 - 79

CONFIDENTIAL

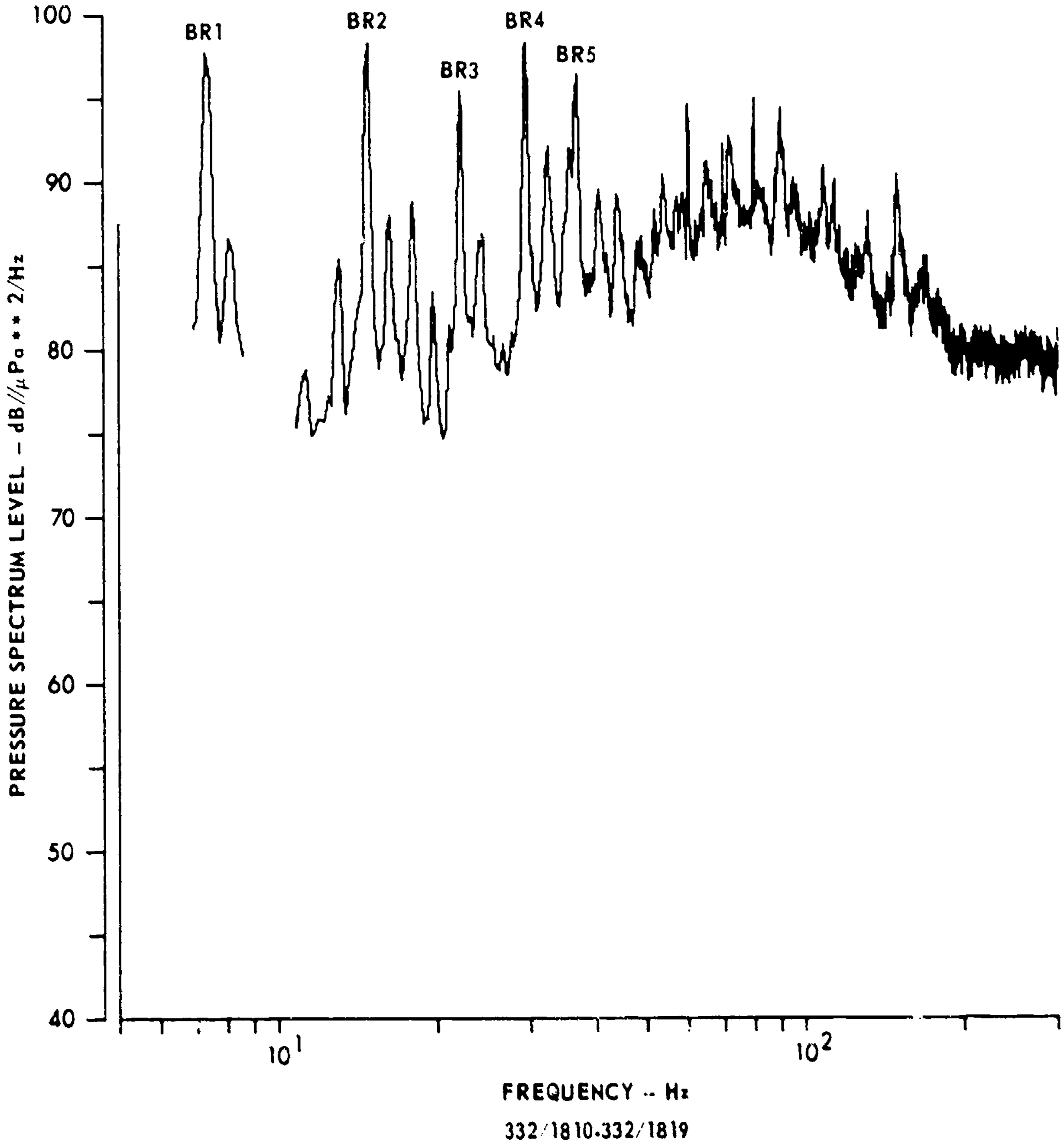

FIGURE 5.19
SIGNATURE OF UNKNOWN SHIP AT CHURCH STROKE II - SITE EN (U)

ARL UT
AS-79-976
KCF - GA
5 - 8 - 79

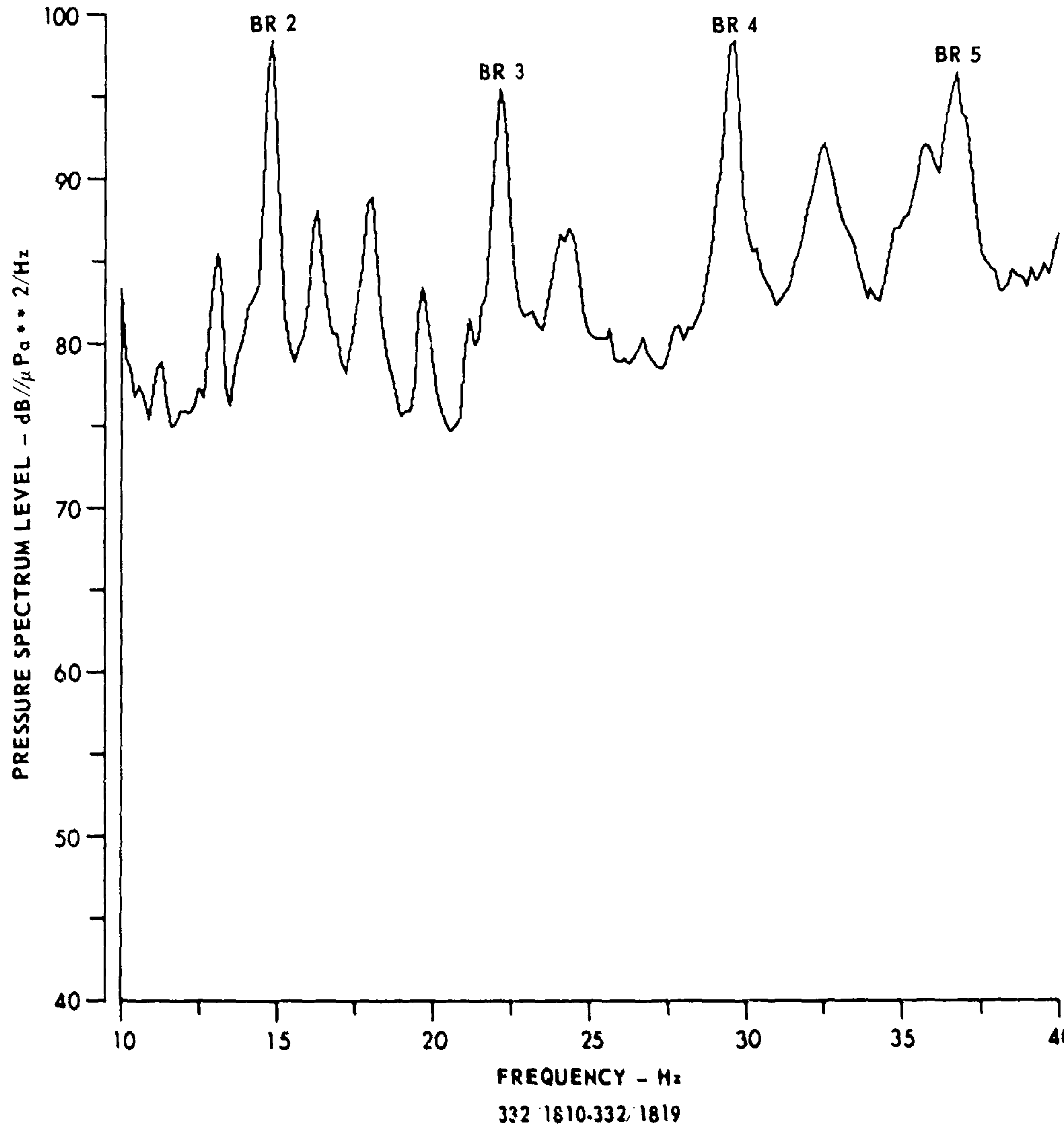

FIGURE 5.20
SIGNATURE OF UNKNOWN SHIP AT CHURCH STROKE II -SITE EN (U)

ARL:UT
AS-79-978
KCF-GA
5-8-79

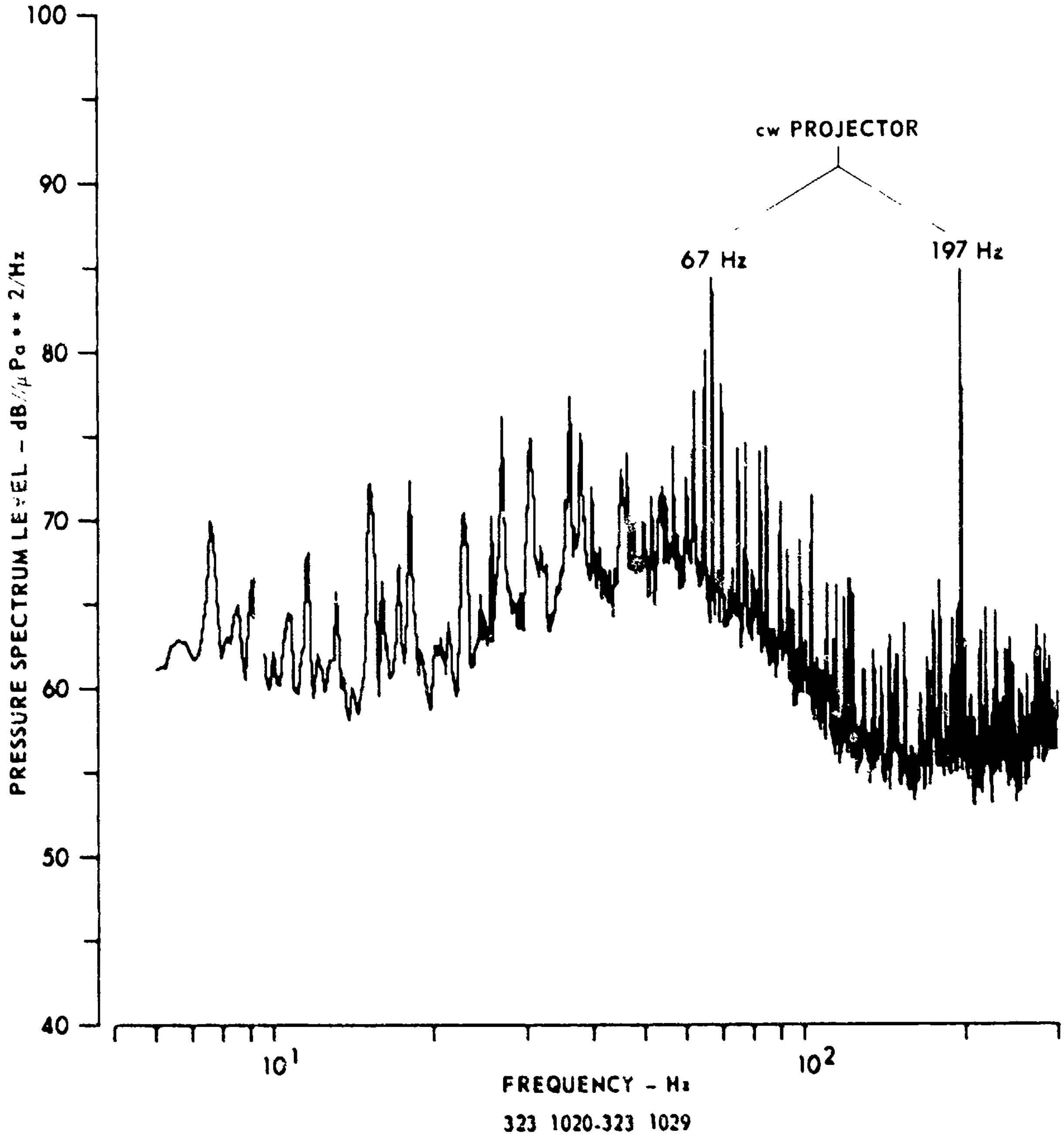

FIGURE 5.21
SIGNATURE OF INDIAN SEAL AT CHURCH STROKE II - SITE B (U)

SPEED: 5 km h (2.7 kt)
RANGE: 11.5 km
ESTIMATED PROPAGATION LOSS: 75 dB
WIND SPEED: 11 kt at 10 m ABOVE WATER

ARL UT
AS-79-872
KCP - GA
5 - 1 - 79

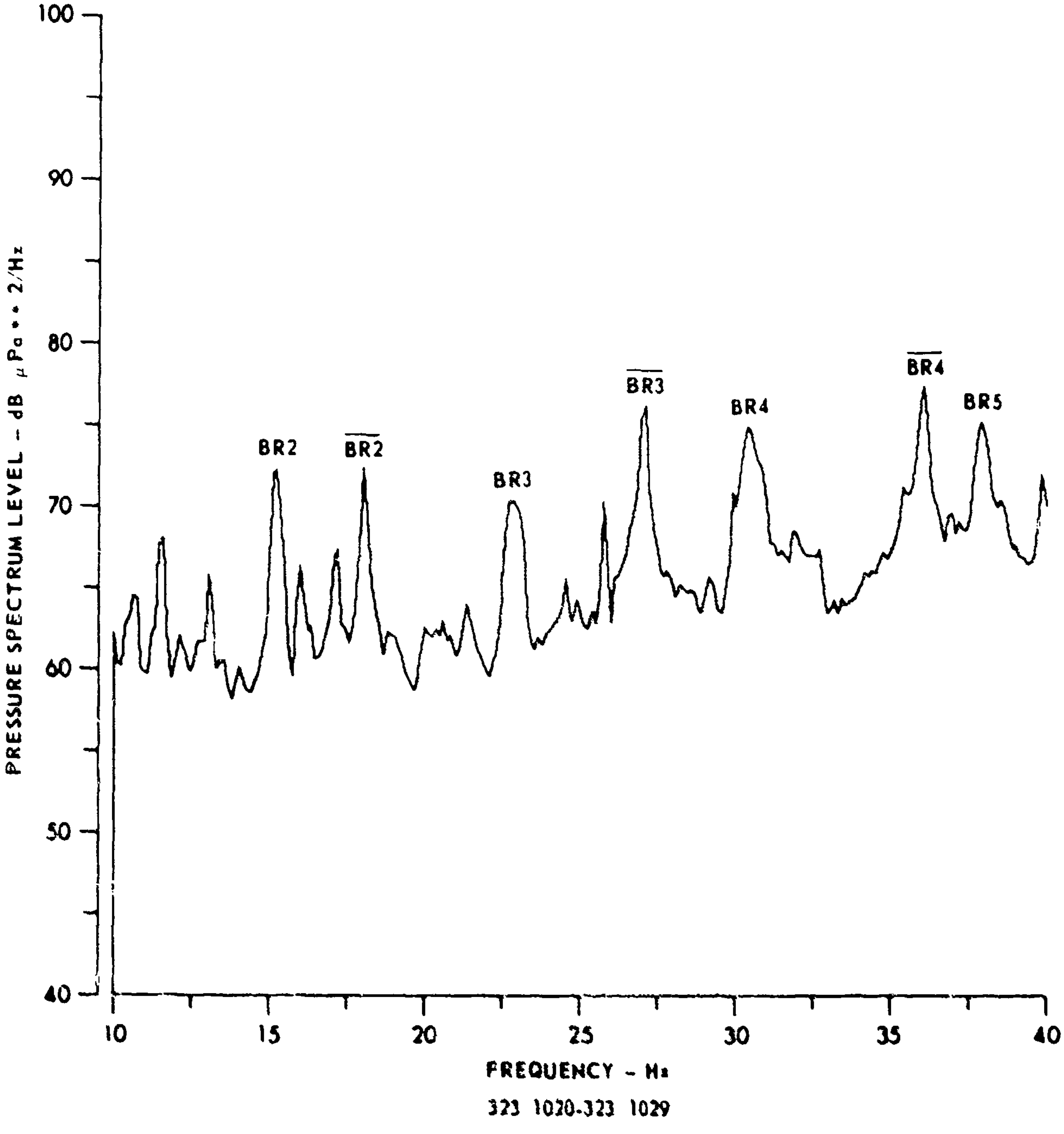

FIGURE 5.22
SIGNATURE OF INDIAN SEAL AT CHURCH STROKE II-SITE B (U)

ARL UT
AS-79-96?
KCF - GA
5 - 8 - 79

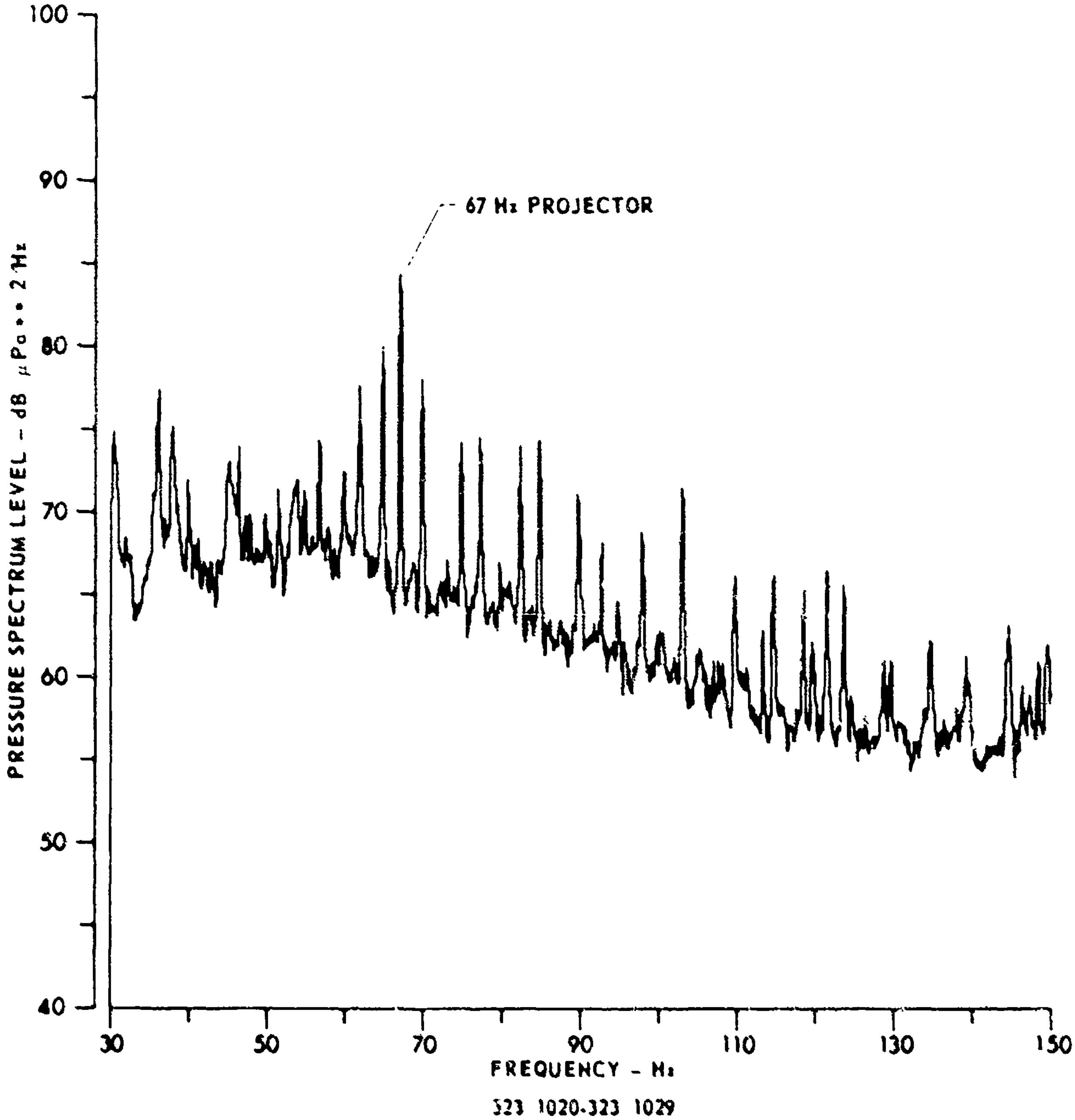

FIGURE 5.23
SPURIOUS LINES FROM INDIAN SEAL (U)

(C) 150 dB//μPa at 1 m. The wind speed was 12 kt as given by an anemometer 10 m above the surface.

(C) The INDIAN SEAL signature from Site EN is shown in Figs. 5.24 and 5.25. Harmonics of the frequency 8.8 Hz, which is a probable blade rate based on the line width, can be seen in the linear spectrum (Fig. 5.25). The data above 50 Hz are dominated by the cw projector, which appears to be putting out prominent lines at 100 and 300 Hz in addition to the nominal 67 Hz and 197 Hz lines. At the time, the ship was advancing at a speed of 5.25 kt away from Site EN at a range of 10 km. The nominal PL is 78 dB, which can be added to the spectrum to estimate source level. This gives the broadband noise around 50 Hz a source level of 150 dB//μPa^2/Hz; the peak noise levels equal 158 dB//μPa at 1 m.

(U) The INDIAN SEAL signatures and the signatures of the other five ships discussed above are summarized in Table V-1. For each ship the fundamental blade rate is given in column F1; columns F2, F3, and F4 give the next three harmonic lines of the fundamental. Accompanying these line frequencies are estimates of their source level, for those ships with known ship-to-receiver ranges. Also presented are estimates of the broadband source levels at 50 Hz, 100 Hz, and 200 Hz.

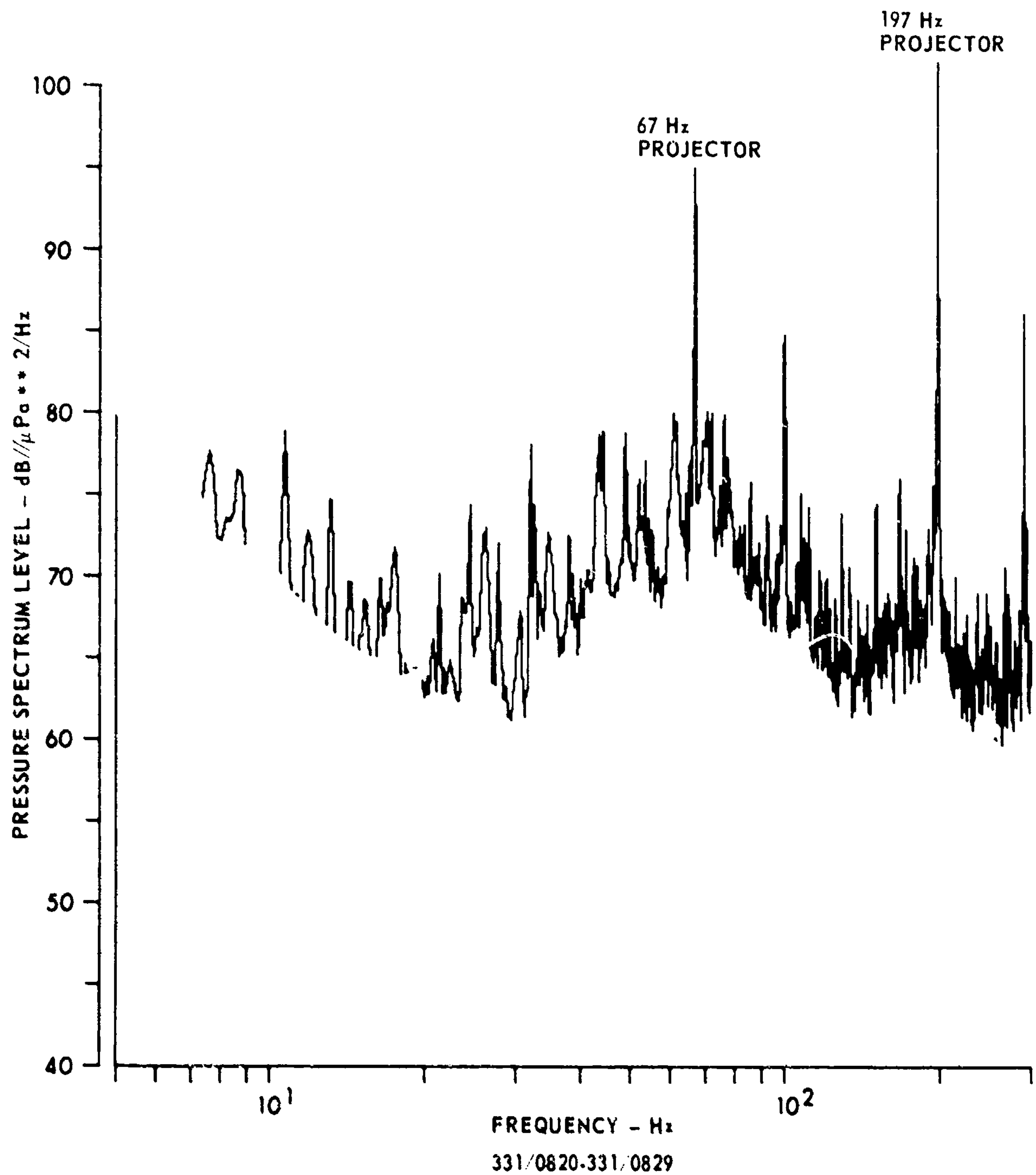

FIGURE 5.24
SIGNATURE OF INDIAN SEAL AT CHURCH STROKE II - SITE EN (U)
SPEED: 9.7 km h (5.25 kt)
RANGE: 10 km
ESTIMATED PROPAGATION LOSS: 78 dB

ARL UT
AS-79-876
KCF - GA
5 - 1 - 79

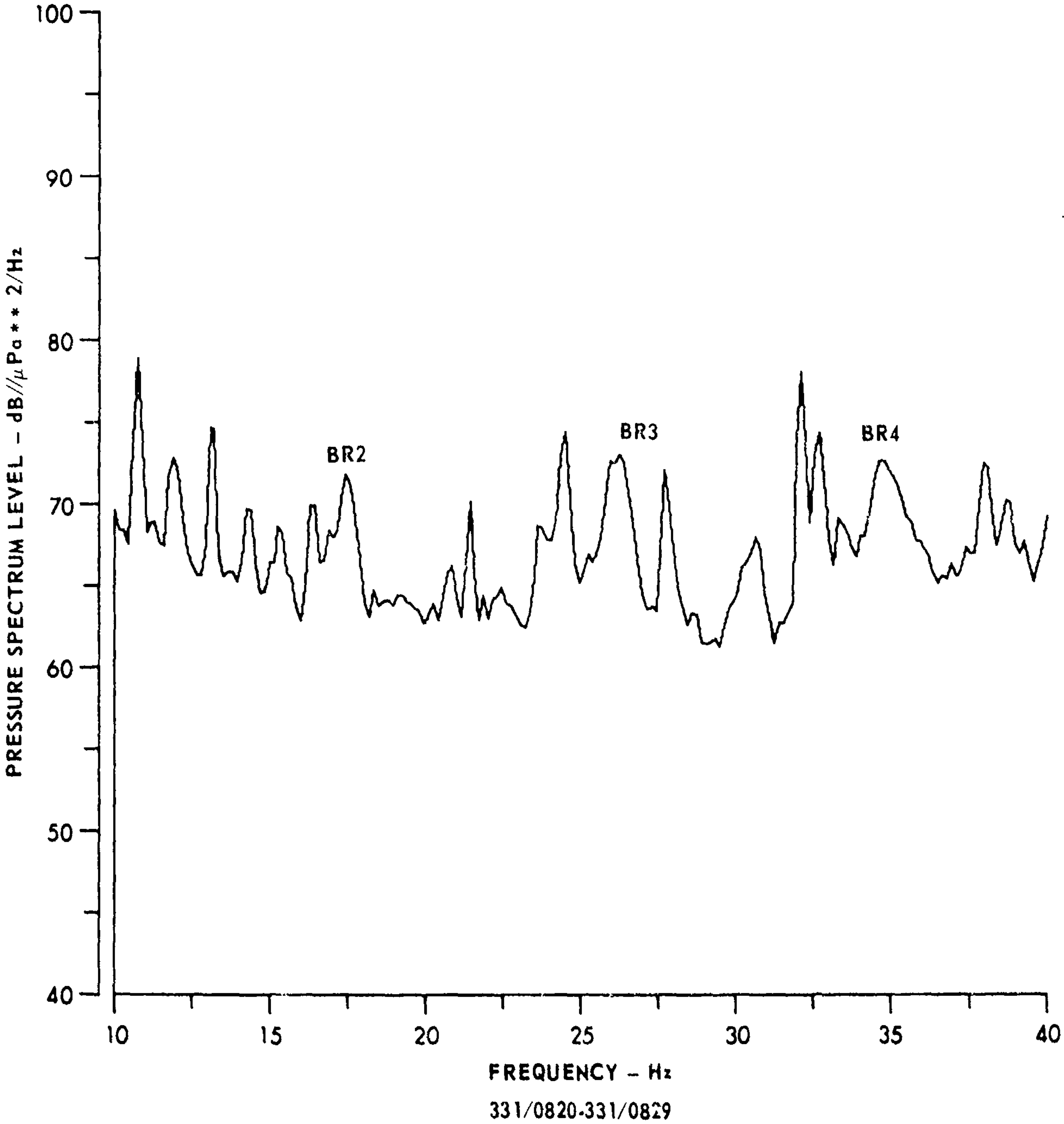

FIGURE 5.25
SIGNATURE OF INDIAN SEAL AT CHURCH STROKE II-SITE EN (U)

ARL:UT
AS-79-968
KCF-GA
5-8-79

CONFIDENTIAL

VI. DATA SUMMARY AND ANALYSIS

(U) This chapter will present an analysis of the CHURCH STROKE II data in terms of acoustic mechanisms and will compare the results with results of other exercises. Section 6.1 will deal with bottom loss, Section 6.2 with propagation loss, and Section 6.3 with ambient noise. Each section will summarize the data and the environmental factors affecting the data, and make comparisons with other exercises and preexercise predictions.

(C) The exercises chosen for comparison are based on environmental considerations. The CHURCH STROKE II area has two basins, the Parece Vela Basin and the Western Philippine Basin. Sound speed profiles, Figs 6.1 and 6.2, from the Parece Vela Basin, containing Sites B and C, demonstrate the bottom limited character of this basin. The BEARING STAKE exercise,[18] Fig. 6.3, was also conducted in a bottom limited region. Comparisons between the BEARING STAKE data and the CHURCH STROKE II bottom loss data from Sites B and C will be presented in Sections 6.1 through 6.3.

(C) The sound speed profile from Site EN in the Western Philippine Basin, Fig. 6.4, exhibits the 1000 m depth excess found in this basin. The PARKA II, CHURCH ANCHOR, and CHURCH OPAL exercises,[19-21] Fig. 6.5, were all conducted in regions of the Northeast Pacific with depth excess. PARKA II data will be presented in Section 6.2 on PL. Ambient noise and PL data from CHURCH STROKE II and CHURCH ANCHOR will be compared in Sections 6.2 and 6.3; comparisons with the CHURCH OPAL ambient noise will be presented in Section 6.3.

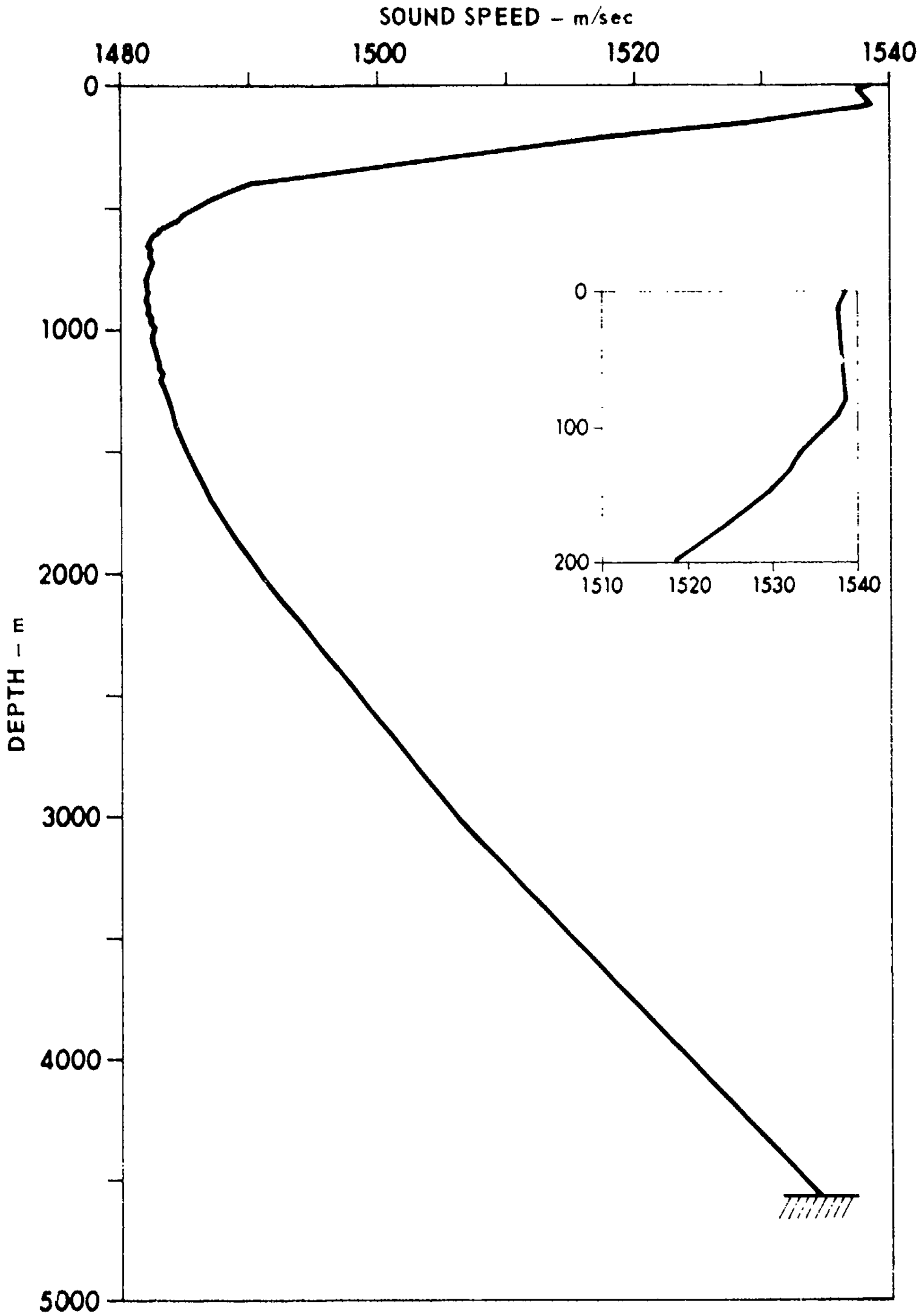

FIGURE 6.1

SOUND SPEED PROFILE
CHURCH STROKE II-SITE B

ARL:UT
AS-79-1307
KCF - GA
7 - 11 - 79

UNCLASSIFIED

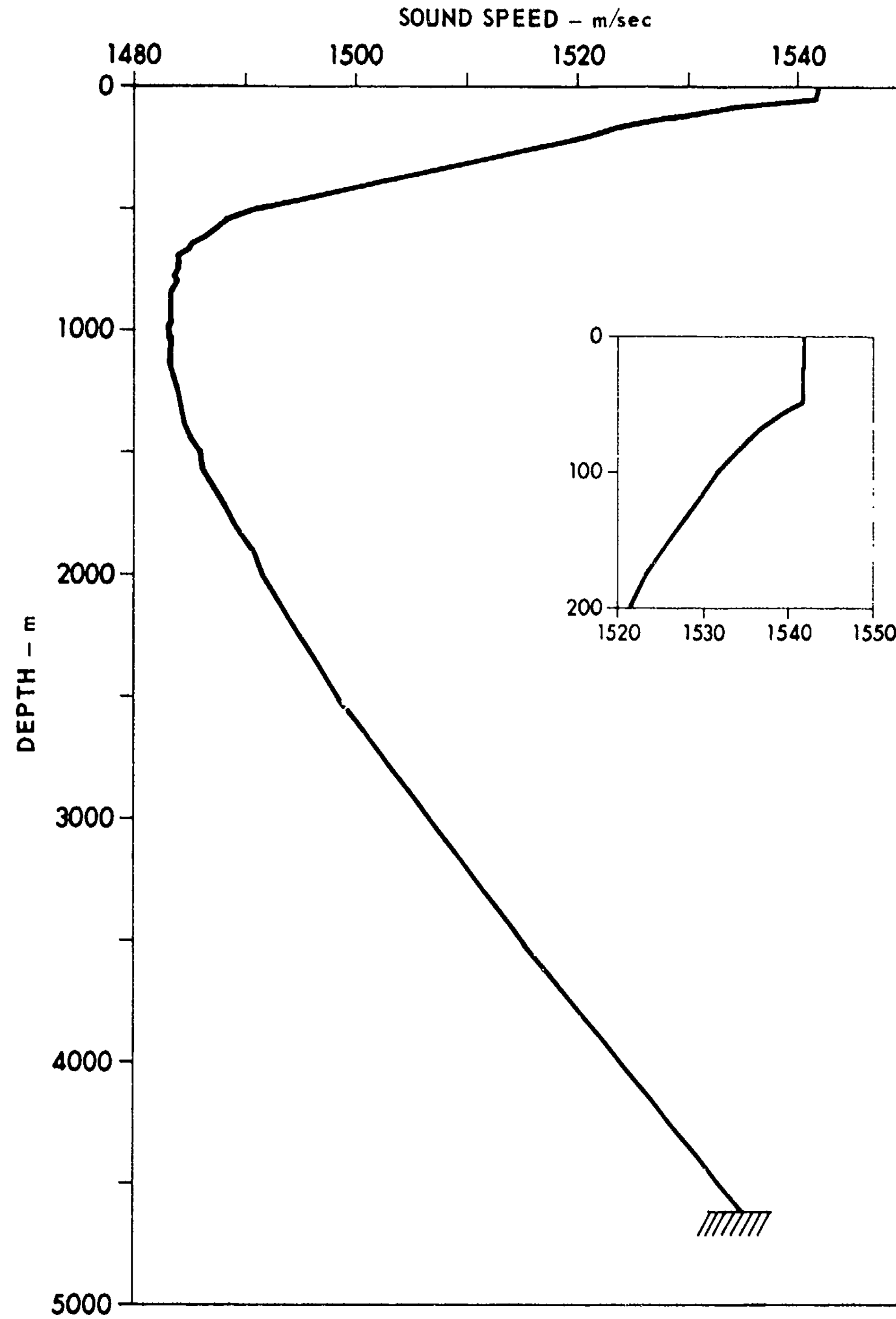

FIGURE 6.2
SOUND SPEED PROFILE
CHURCH STROKE II - SITE C

ARL:UT
AS-79-1308
KCF - GA
7 - 11 - 79

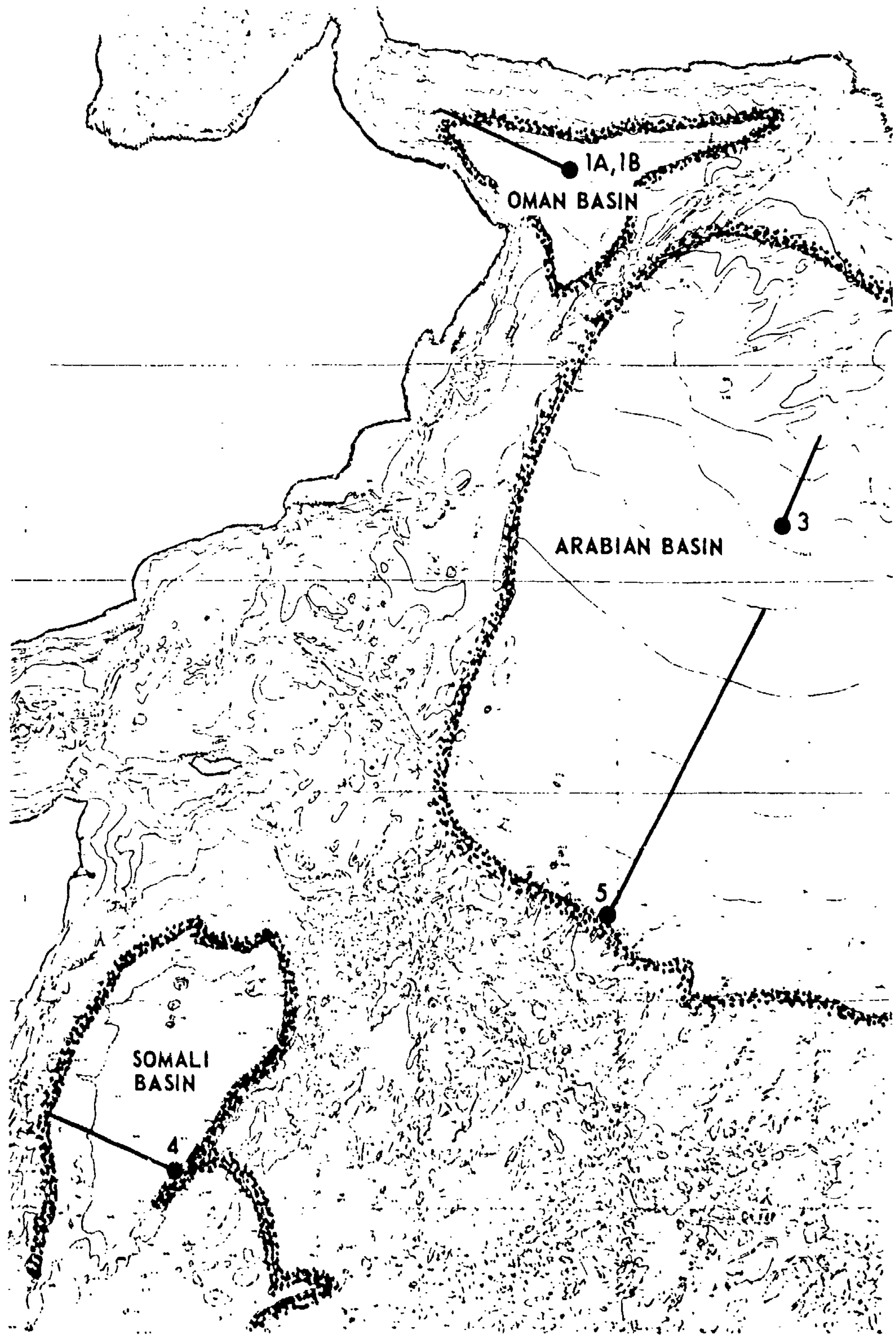

FIGURE 6.3
BEARING STAKE RECEIVER SITE LOCATIONS (U)

ARL:UT
AS-78-1239
KCF-GA
7-20-78

From Ref. 18

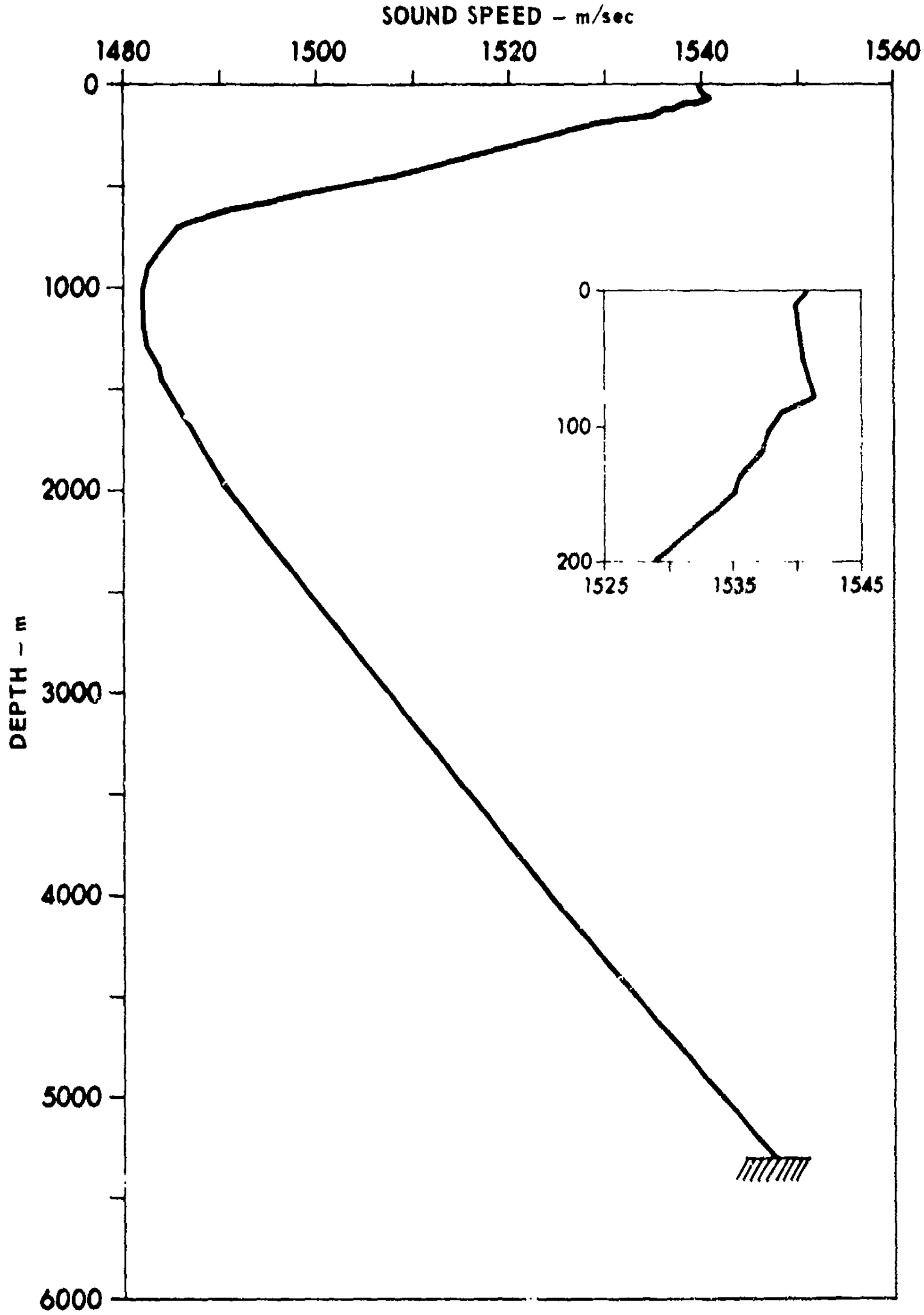

FIGURE 6.4
SOUND SPEED PROFILE
CHURCH STROKE II -SITE EN

ARL:UT
AS-79-1306
KCF - GA
7 - 11 - 79

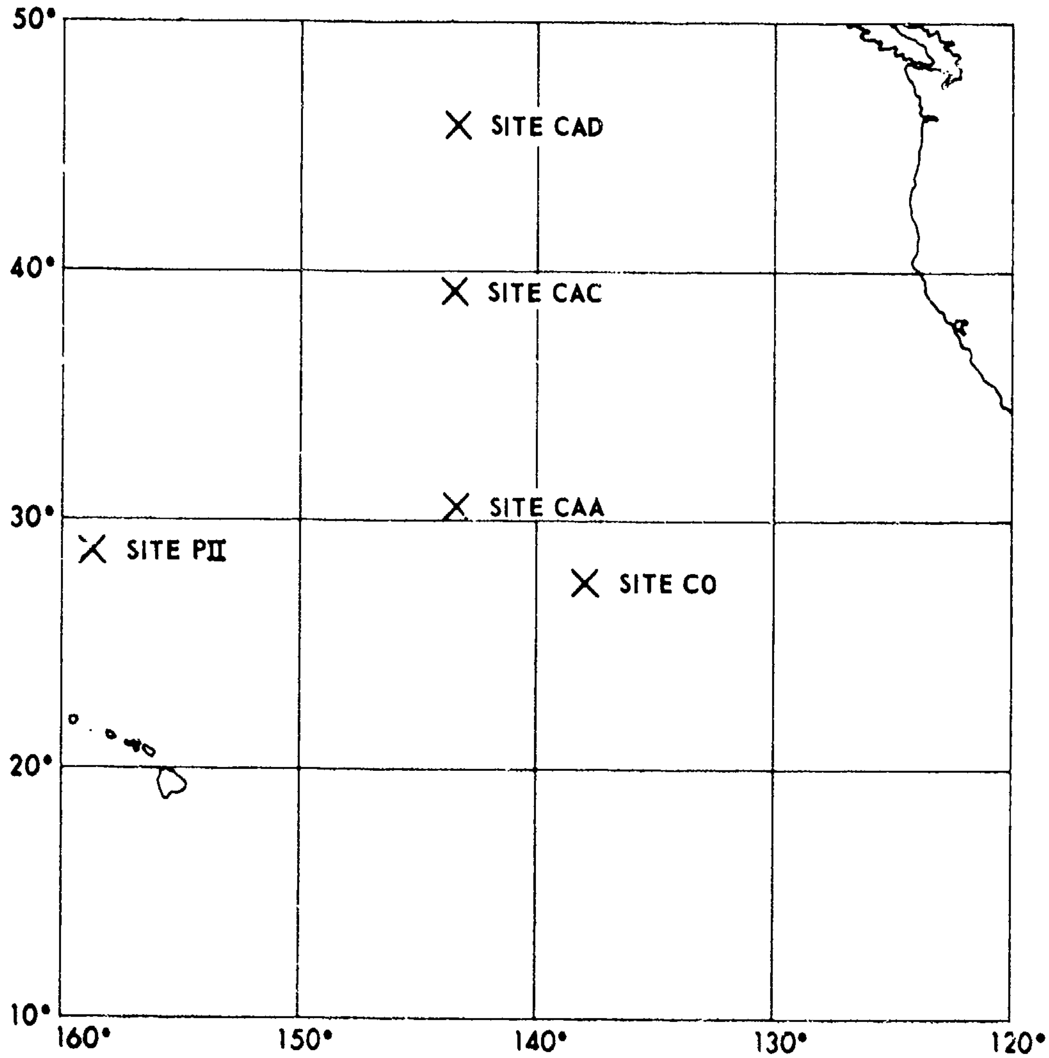

FIGURE 6.5
NORTHEAST PACIFIC SITES FROM CHURCH ANCHOR
PARKA II AND CHURCH OPAL (U)

ARL:UT
AS-79-2078
KCF - GA
10 - 9 - 79

CONFIDENTIAL

6.1 Bottom Loss Analysis

(C) Bottom loss was measured in both the Parece Vela Basin and the Western Philippine Basin. The low bottom loss measured in the Parece Vela Basin will be compared to the bottom loss measured in a similar region. The bottom loss measured for the two CHURCH STROKE II basins will then be compared to one another. Finally, a geoacoustic model for the bottom sediment of the Parece Vela Basin will be shown, with bottom loss values calculated from this geoacoustic model.

(C) The bottom loss measurements at Site B compare well with the measurements from the BEARING STAKE sites in the Oman and Somali Basins. The bottom loss measured in the Oman Basin is low while the Somali Basin bottom loss is somewhat higher.

(C) Bottom loss measured at Site B in the Parece Vela Basin was presented in Fig. 2.6. Below 30° the losses are approximately 0.5 dB at 25 Hz and 1.2 dB at 50 Hz. Figure 6.6 presents a comparison of these losses at Site B with those measured during BEARING STAKE in the Oman Basin. The Site B loss is slightly higher. At 200 Hz, the two curves differ by approximately 1.2 dB at all angles below 32°; below 200 Hz the differences are nearly linear with frequency. Site B bottom loss at 100 Hz is 0.6 dB greater than the Oman Basin data.

(C) Further comparisons can be made between Site B and regions of somewhat higher bottom loss, such as the Somali Basin, Fig. 6.7; the Site B losses are significantly less. At the lower frequencies the Site B losses increase very little below 30°, while the increase with angle is almost uniform in the Somali Basin. At the higher frequencies the Site B losses increase with angle at approximately half the rate of the measurements for the Somali Basin.

(C) Site EN in the Western Philippine Basin is another region where high bottom loss has been measured. These losses, presented in Fig. 3.4, are significantly higher than those in the neighboring basin at Site B.

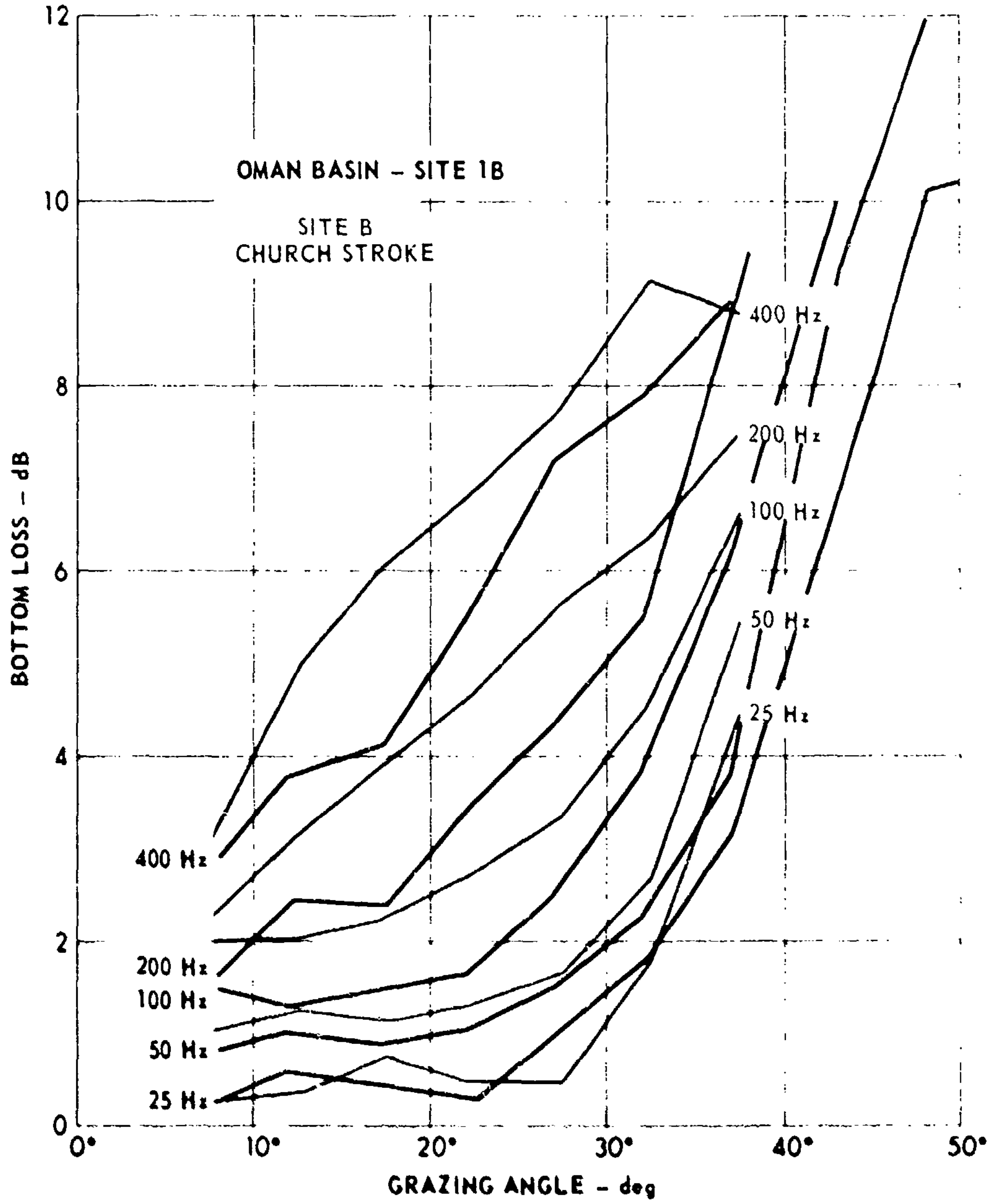

FIGURE 6.6
COMPARISON OF BOTTOM LOSS FOR BEARING STAKE
SITE 1B AND CHURCH STROKE II - SITE B (U)

ARL UT
AS-79-2081
KCF - GA
10 - 9 - 79

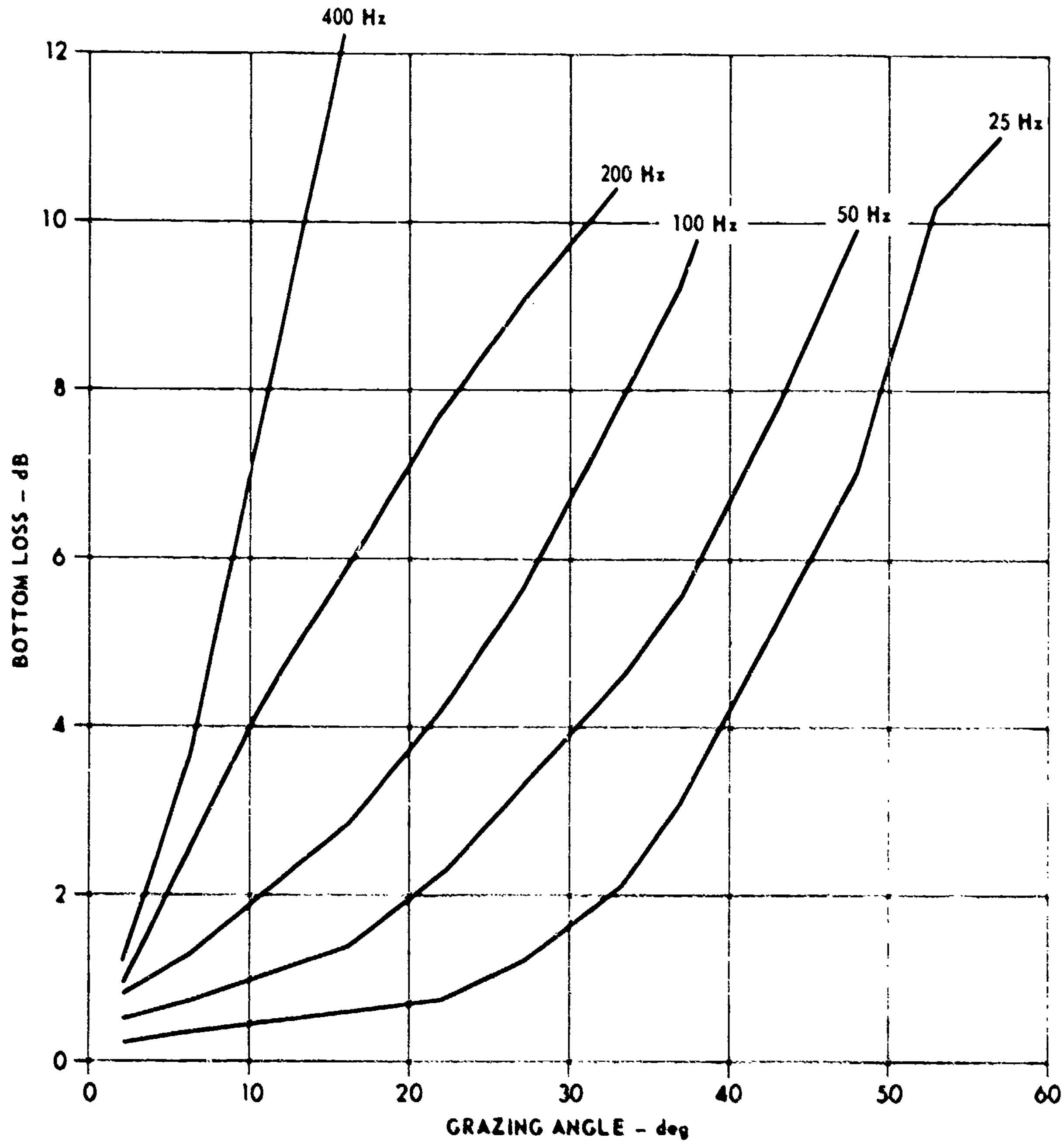

FIGURE 6.7
BOTTOM LOSS FOR THE SOMALI BASIN (U)

ARL UT
AS-79-2087
KCF - GA
10 - 9 - 79

(U) The bottom loss curves for Sites B and EN have one characteristic in common. At the higher angles the slope of the bottom loss curves changes rapidly. For Site EN this break occurs between 20° and 25°, while at Site B it occurs between 30° and 35°. The Deep Sea Drilling Project reports[13,22] indicate that the Western Philippine Basin has approximately 100 m of sediment overlying an acoustic basement, while the Parece Vela Basin has 300 to 400 m of sediment. If one assumes a sound speed profile based on Hamilton's 13 area average velocity gradients,[23] then it may be shown that sound incident on the bottom at angles above 22° for Site EN, and above approximately 27° to 33° for Site B, interacts with the acoustical basement. Therefore, the nature of the sediment basement interface can dominate the reflected field at steeper angles. The presence of a rough basement will introduce scattering and increase the losses at the higher angles, as seen in the bottom loss curves; it is reasonable to assume that this is the case in the CHURCH STROKE II data.

(U) A geoacoustic model for a 400 m thick sediment has been derived for the Parece Vela Basin, Fig. 6.8. The derivation of this model is described in detail in Ref. 24. A summary of the derivation follows. A sound speed profile for the Oman Basin, based on Hamilton's average velocity gradients, was used for Site B. It was modified slightly by using a 0.987 ratio of surface sediment velocity to bottom water velocity so that calculated bottom losses were similar to the observed nearly constant losses at the smaller angles. (This ratio is near Hamilton's world average of 0.985.) The attenuation profile was derived from measured bottom loss using the method outlined in Ref. 25. The density contrast at the water-sediment interface was based on the measured density of the sediment interface at Deep Sea Drilling Project Sites 53 and 54,[13] with the remaining density profile extracted from the Oman Basin geoacoustic model.[26] The sound speed and attenuation for the basement were derived artificially to account for the high losses at the high angles actually resulting from the rough boundary effects.

(U) Before the model calculations and the measurements are compared, the effects of recording system limitations on the measurements should be

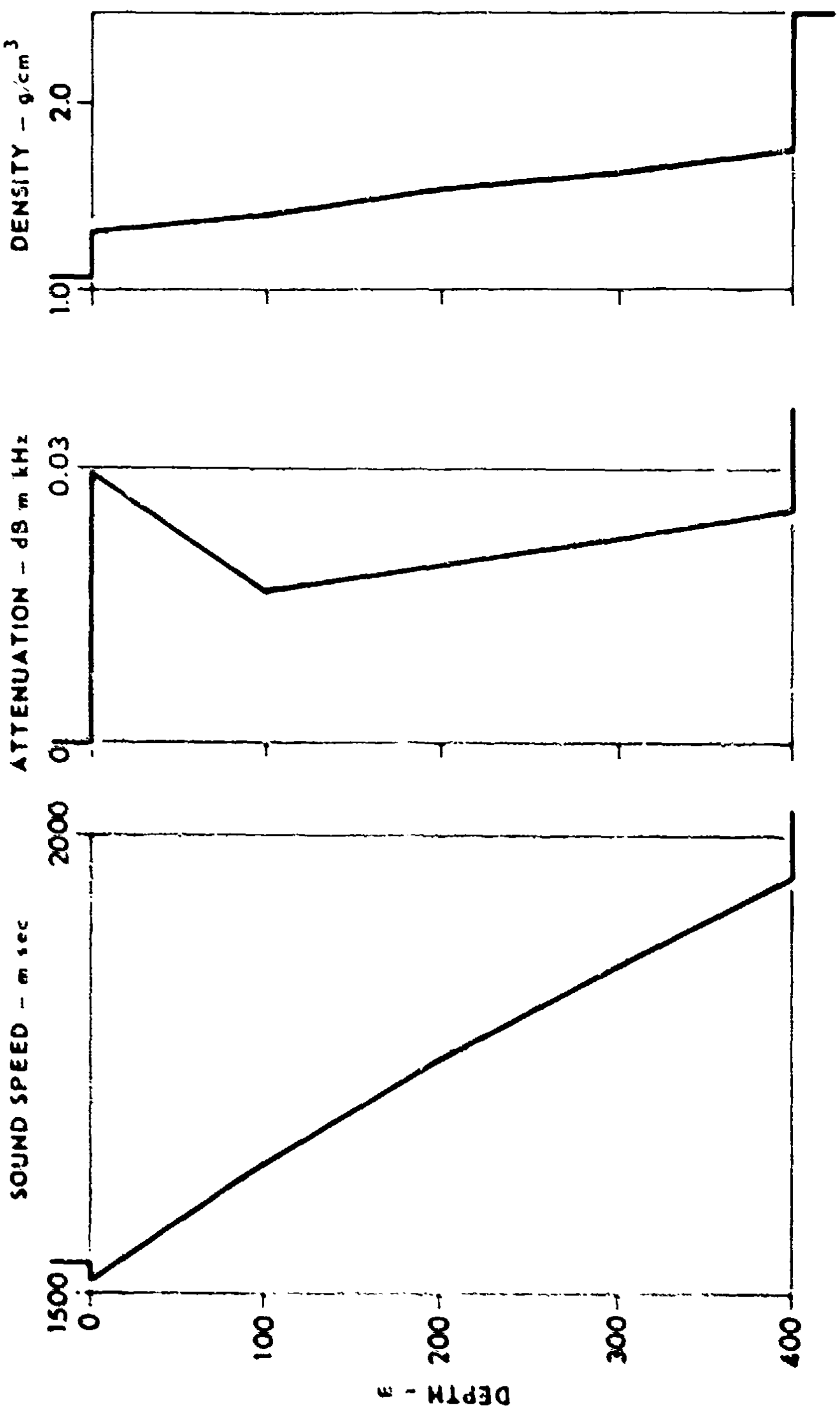

FIGURE 6.8
GEOACOUSTIC MODEL FOR CHURCH STROKE II - SITE B (U)

ARL UT
AS-79-1313
KCF - GA
7 - 11 - 79

(U) noted. The bottom loss measurements are based on multibounce data, permitting proper measurement of the low losses. At higher losses, the higher frequency signal components of arrivals which reflect several times can experience 30 dB more loss than the lower frequencies. Due to the harmonic distortion of the recording system, the level of the third harmonic component is approximately 30 dB below the level of the fundamental. Thus, bottom loss measurements which should show high loss can be biased towards lower values by harmonic distortion.

(U) The geoacoustic model of Fig. 6.8 has been used to calculate bottom loss at 25, 50, 100, 200, and 400 Hz. These curves are compared with measurements in Fig. 6.9. At losses less than 5 dB, where the measurements are not biased by problems of measuring high losses from multibounce data, the two sets of curves are within 0.2 dB of each other. Based on this favorable agreement, the geoacoustic model can be used to extend the bottom loss values into higher loss regions, i.e., to other frequencies and/or other angles. It is recommended that calculated values of bottom loss be used to avoid the measurement problem mentioned above.

(C) The bottom loss measured at Site B has been seen to be relatively low, just slightly higher than the low loss measurements in the Indian Ocean. These measurements have been used to obtain a geoacoustic model for the Parece Vela Basin and to extend the frequency and angular coverage of the measurements. The Western Philippine Basin, when compared to the Parece Vela Basin, is seen to have higher bottom losses at all frequencies.

6.2 Propagation Loss

(U) In this section PL for short ranges and for the long ranges will be discussed separately. A comparison between the CHURCH STROKE II sites will be made using the short range data (less than 35 km); minimum detectable source level estimates are based on these data. Comparisons with other exercise areas are based on the long range data (greater than 35 km). Where appropriate, comparisons are also made with computer model runs.

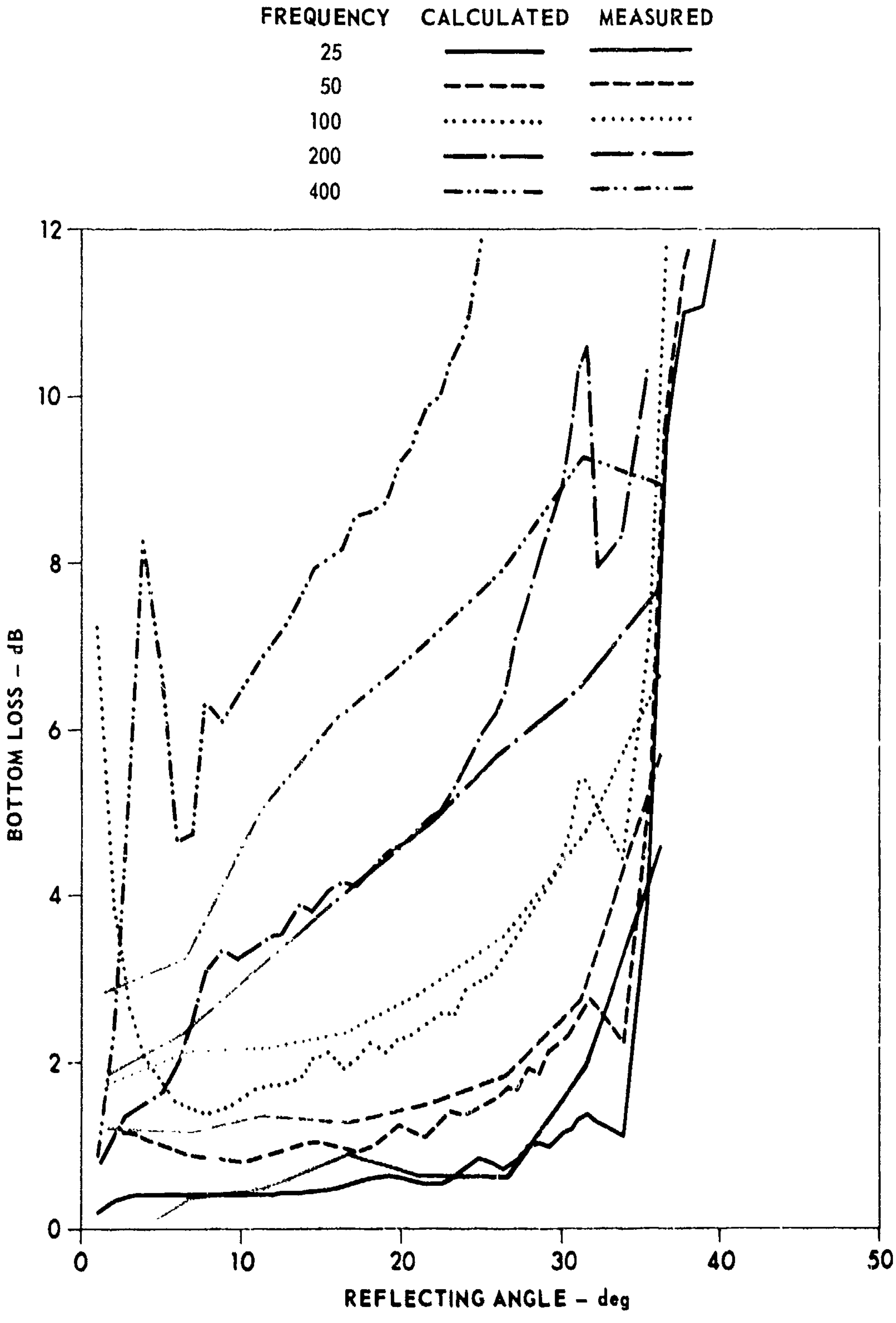

FIGURE 6.9
COMPARISON OF MEASURED BOTTOM LOSS AND
COMPUTED BOTTOM LOSS USING Fig. 6.8
CHURCH STROKE II - SITE B (U)

ARL:UT
AS-79-1309
KCF - GA
7 - 11 - 79

(U) The 91 m source depth cw data from Site B, Fig. 6.10, displays an unusual propagation effect around 25 km; the PL decreases approximately 10 dB and then increases rapidly again in less than 2 km. Figure 6.11 presents range versus source angle curves for this case. These curves were obtained by tracing rays from the 91 m source to a depth of 4542 m. The ranges at which a ray reaches 4542 m is plotted versus the ray angle at the source. Since ray angles are either upgoing or downgoing at the source and at the receiver there are four curves in Fig. 6.11. According to ray theory, intensity at a given range is proportional to the inverse slope of the curve at that range. For the 91 m source, located within the thermocline, the rays which refract near the surface (0° to 2°) have slopes near zero, indicating the formation of a caustic at 25 km. The ray trace diagram in Fig. 6.12 also shows the formation of this caustic near the bottom by the increased density of the rays, which were launched with uniform spacing in angle. The high signal level at 25 km in Fig. 6.10 is the result of this caustic formation. At 67 Hz, Fig. 2.21, a similar decrease in the loss is also seen at 25 km; however, the range interval is about 4 km, demonstrating the low frequency spreading of the caustic. This effect was not seen at the other two sites due to differences in the shapes of the profiles near the source depth.

(C) The short range PLs for the two sites within the Parece Vela Basin are shown in Fig. 2.1 and in Fig. 4.1. Comparisons are based on PL for shallow sources, 18 m at Site C (Fig. 4.2) and 91 m at Site B (Fig. 2.21). The average PL between 10 km and 25 km for the two sites are within 3 dB of each other at both 67 Hz and 197 Hz. At both frequencies the loss at Site B averages 78 dB, and at Site C, 75 dB. Beyond the direct path range (25 to 30 km), PL increases to 90 dB at both sites.

(C) The direct path PL at Site EN (Figs. 3.8 and 3.9) in the Western Philippine Basin is similar to the PL at Site B. Between 10 km and 25 km the PL at Site EN averages 78 dB at both 67 Hz and 197 Hz. The PL also drops below 90 dB beyond the direct path range of Site EN (30 km to 35 km).

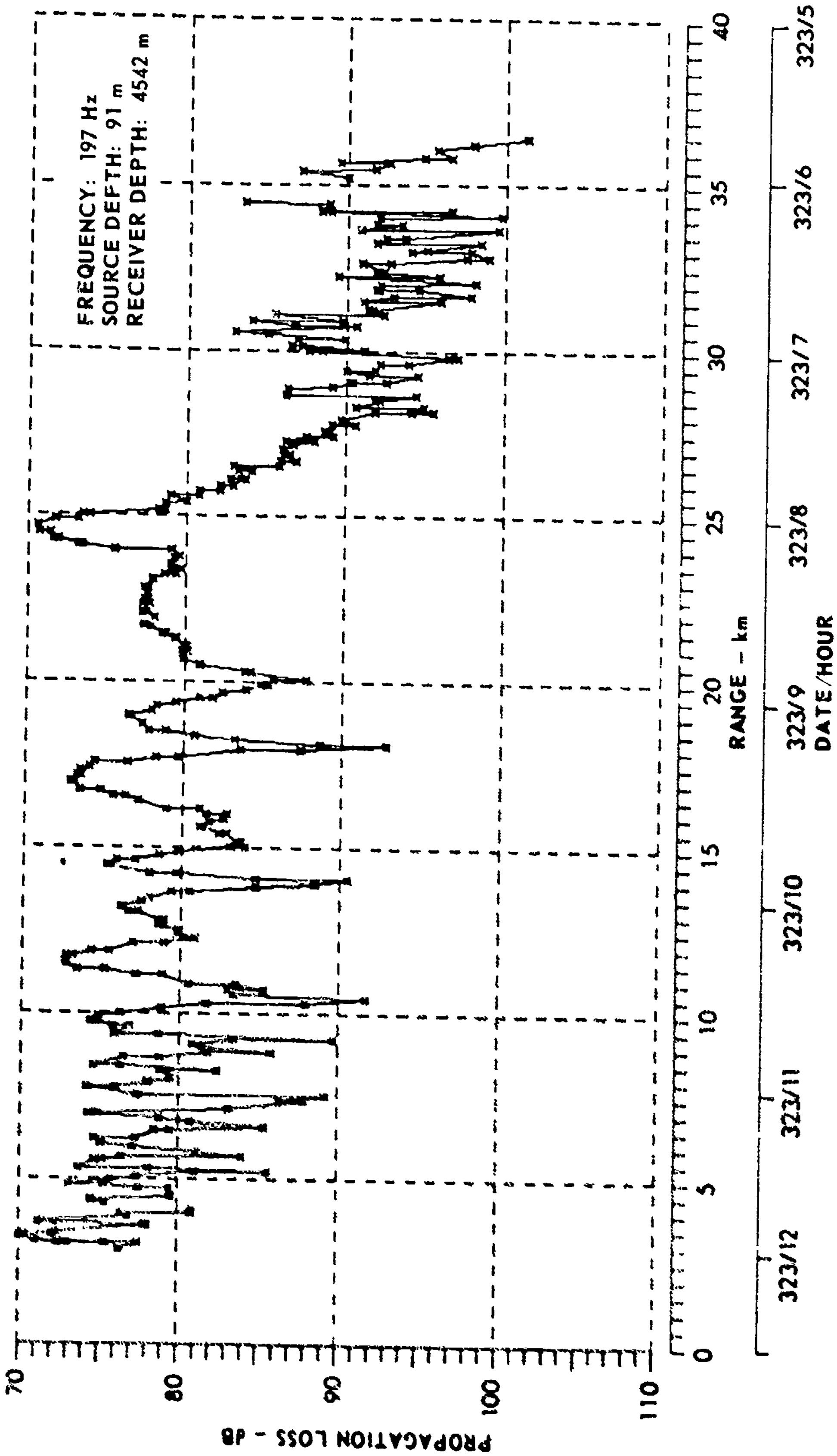

FIGURE 6.10
PROPAGATION LOSS WITH CAUSTIC FORMATION AT 25 km (U)
CHURCH STROKE II - SITE B

ARL UT
AS-79-2086
KCF - GA
10 - 9 - 79

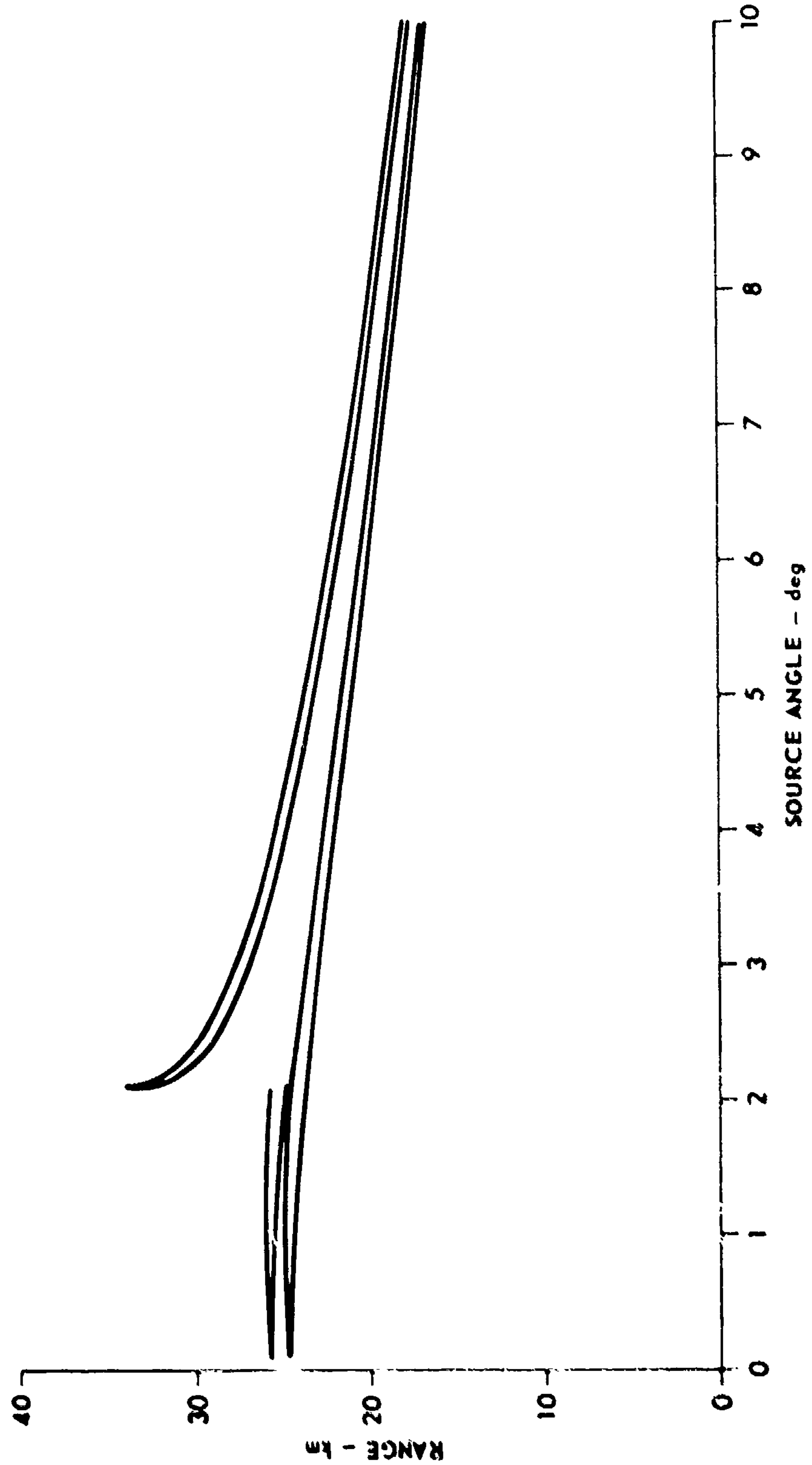

FIGURE 6.11
RANGE versus SOURCE ANGLE
CHURCH STROKE II - SITE B
SOURCE DEPTH: 91 m
RECEIVER DEPTH: 4542 m

ARL UT
AS-79-2079
KCF - GA
10 - 9 - 79

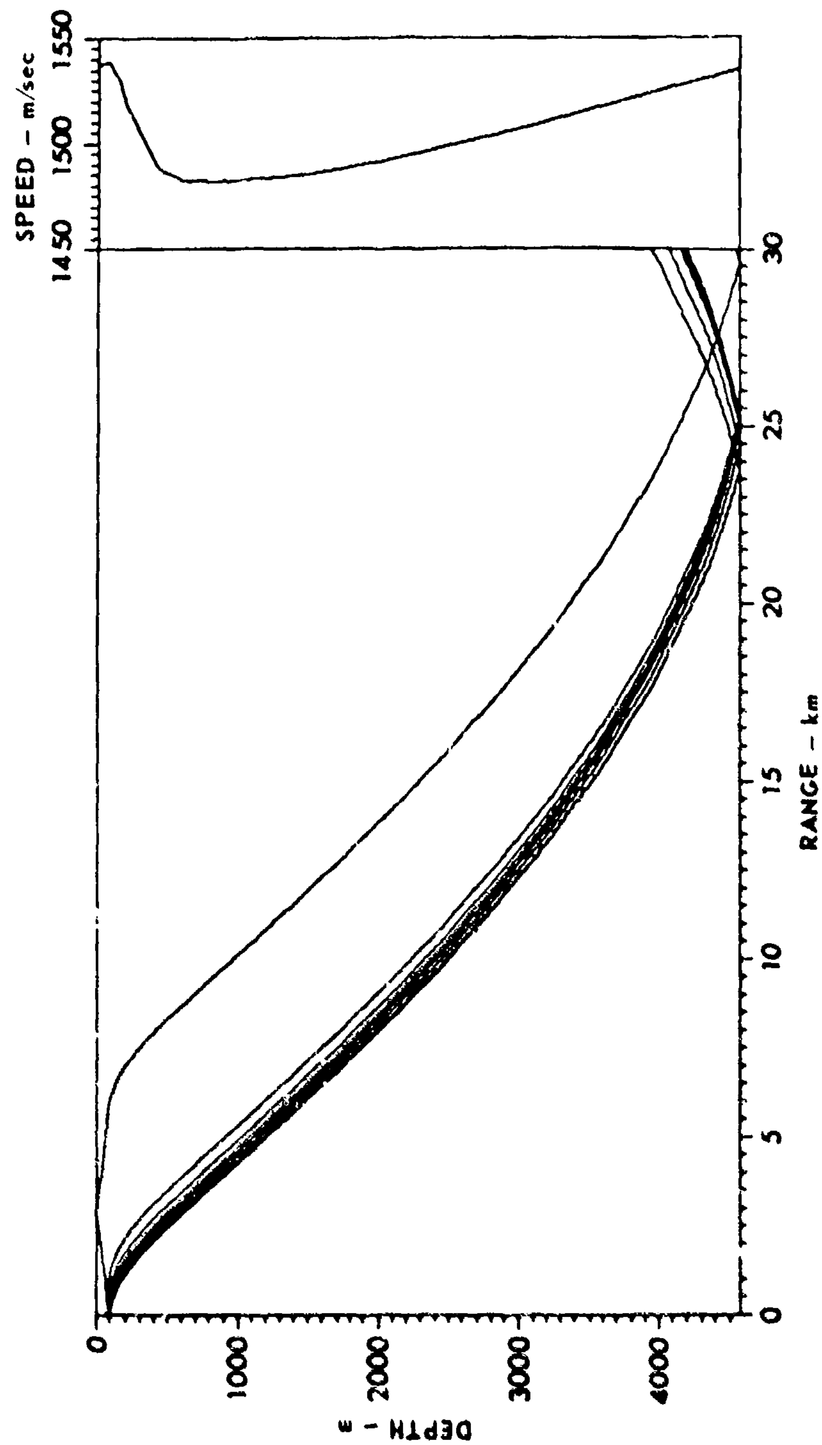

FIGURE 6.12
RAY TRACE FOR CHURCH STROKE II - SITE B
SOURCE DEPTH – 91 m

ARL UT
AS-79-2082
KCF - GA
10 - 9 - 79

(C) Signal excess was also measured during CHURCH STROKE II. The processing bandwidth for the measurements was 147 mHz. A 155 dB//μPa source level at Site B (Figs. 2.23 and 2.24) results in 16 to 17 dB signal excess at 67 Hz and 25 to 26 dB signal excess at 197 Hz for ranges less than 25 km. Beyond 25 km, a 165 dB source level yields 14 to 15 dB signal excess at 67 Hz and 20 dB at 197 Hz. At Site C, within 25 km a 174 dB source level produces 25 dB signal excess at 67 Hz and 35 dB at 197 Hz (Fig. 4.3 and 4.4). At Site EN a 174 dB level results in 25 to 27 dB excess at 67 Hz and 33 dB at 197 Hz.

(C) A minimum source level with 50% probability of detection can be estimated from the signal excess measurements. If the ambient noise is assumed to be white Gaussian, a minimum required signal-to-noise ratio (S/N) can be computed based on a specified false alarm rate and the number of equivalent degrees of freedom. The ambient noise measurements have approximately 14 to 16 equivalent degrees of freedom. For a false alarm rate of 0.001, a 50% probability of detection requires a minimum of 3 dB S/N in the analysis bandwidth. Based on 15 dB of signal excess for a 155 dB source level and this minimum 3 dB S/N, 143 dB is the minimum source level with a 50% probability of detection.

(C) Based on the signal excess presented above, estimates of minimum detectable source levels have been computed. A 151 dB source at 67 Hz has a 50% chance of being detected in a 147 mHz band at ranges less than 25 km from any of the three sites. A 142 dB source can be detected at Site B. At 197 Hz the estimated minimum detectable source levels are approximately 10 dB below the 67 Hz levels, or 142 dB at all sites, and 133 dB at Site B. These results have been summarized in Table VI-1.

(C) The long range PL data from Site B has been compared to BEARING STAKE data.[18] Both areas are bottom limited regions. Propagation to Site B, Figs. 2.8 through 2.13, is characteristic of a bottom limited region. The long range PL for a 91 m depth source, Fig. 6.13, increases with increasing range at a rate greater than that of cylindrical spreading, because of losses in the bottom. As the range increases from 100 km to

(C) TABLE VI-1

Signal Excess Summary and

Estimated Minimum Detectable Source

Levels for CHURCH STROKE II Sites (U)

147 mHz Processing Bandwidth

25 km Maximum Range

SITE	B		C		EN	
Frequency (Hz)	67	197	67	197	67	197
Source Level - dB//μPa	155	155	174	174	174	172
Noise Level - dB//μPa²/Hz	66	58	74	62	68	64
Signal Excess - dB//μPa	16	25	27	35	25	33
Estimated Minimum Detectable Level - dB//μPa	142	133	150	142	151	142

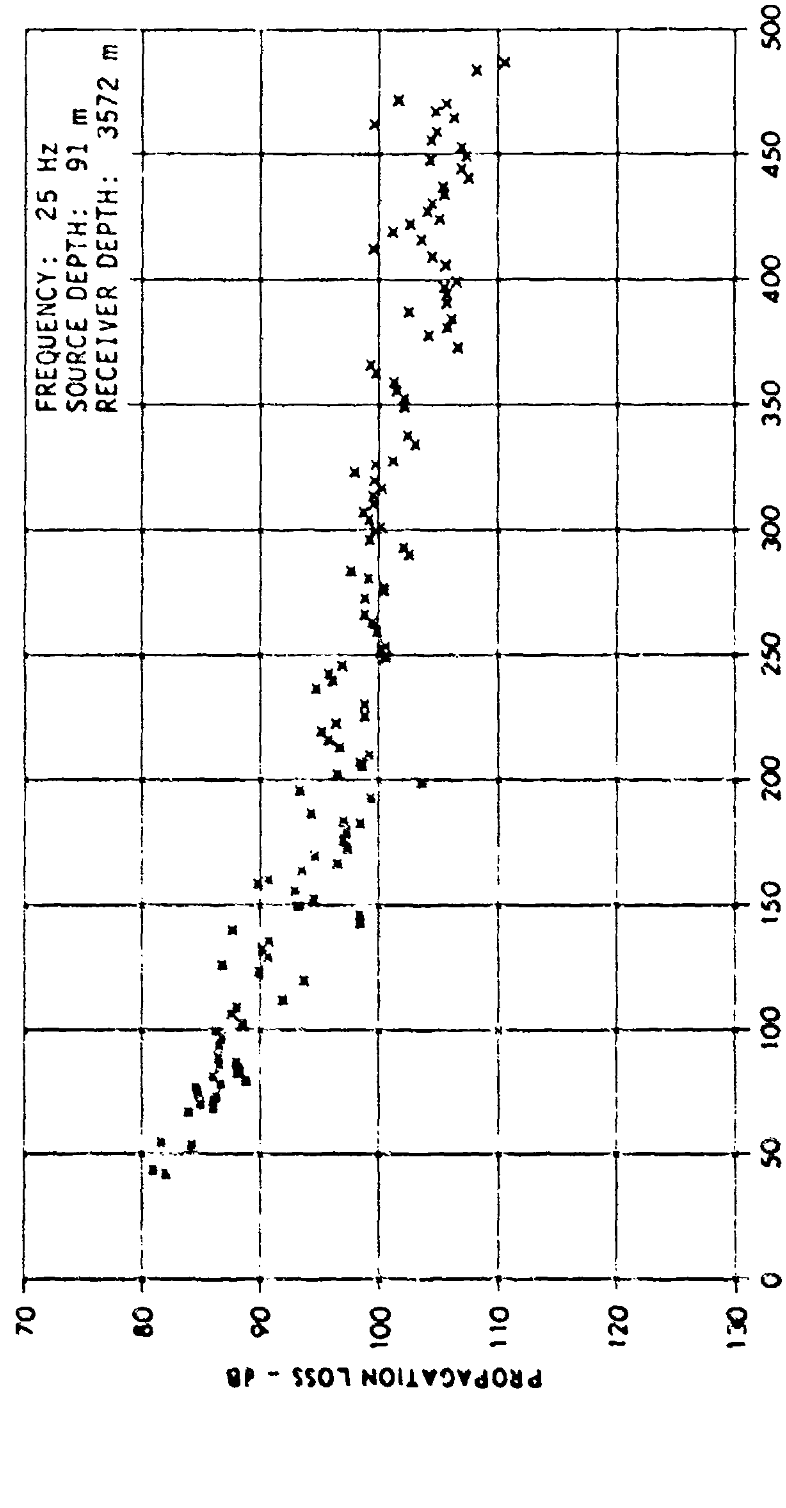

FIGURE 6.13
PROPAGATION LOSS
CHURCH STROKE II - SITE B (U)
SOURCE DEPTH: 91 m

ARL:UT
AS-79-2084
KCF - GA
10 - 5 - 79

(C) 300 km the 25 Hz losses increase from 87 dB to 100 dB. This general increase of loss with range was also seen in the BEARING STAKE area, Fig. 6.14. However, at BEARING STAKE Site 1B, the losses increased from about 90 dB to about 95 dB over the same range interval. Propagation to CHURCH STROKE II Site B therefore presents a slightly higher increase in loss with range. This is consistent with the higher bottom loss values at Site B, as discussed in Section 6.1.

(C) As source depth increases below the bottom conjugate depth (the depth where the sound speed equals the sound speed at the bottom), the character of the Site B propagation changes. Convergence zone propagation is seen for the 244 m source, Fig. 6.15. Propagation loss varies as much as 15 dB between the convergence zones and the shadow zones. Similar effects were not seen in the BEARING STAKE data because no sources were below the bottom conjugate depth.

(C) Spectra from the SUS data at Site B were averaged at 100 km intervals; these are plotted in Figs. 6.16 and 6.17. For both the 91 m and 244 m source depths, the PL generally increases with increasing frequency. Between 0 km and 100 km, PL at both source depths increases about 6 dB/octave, which is more rapid than was seen in BEARING STAKE Site 1B.[18] This characteristic changes, however, with increases in range. Between 200 km and 300 km, at a source depth of 91 m, the low frequency falloff is 7.6 dB/octave; it is slightly less between 300 km and 400 km. For the 244 m source the PL at high frequencies falls off at 6 dB/octave, while the low frequencies fall off less rapidly. The BEARING STAKE data from Site 1B showed this same characteristic for both 244 m and 91 m sources.

(C) At Site EN, in the Western Philippine Basin where depth excess exists, convergence zone propagation predominates for all source depths, Fig. 6.18 and Figs. 3.10 through 3.14. Other areas of depth excess, such as the CHURCH ANCHOR and PARKA II areas, also exhibit convergence zone structure. In these three areas the difference between convergence zone and shadow zone PL is at least 7 to 15 dB. At mid-water depths, the convergence zone propagation is approximately the same for the two regions. Beyond 180 km

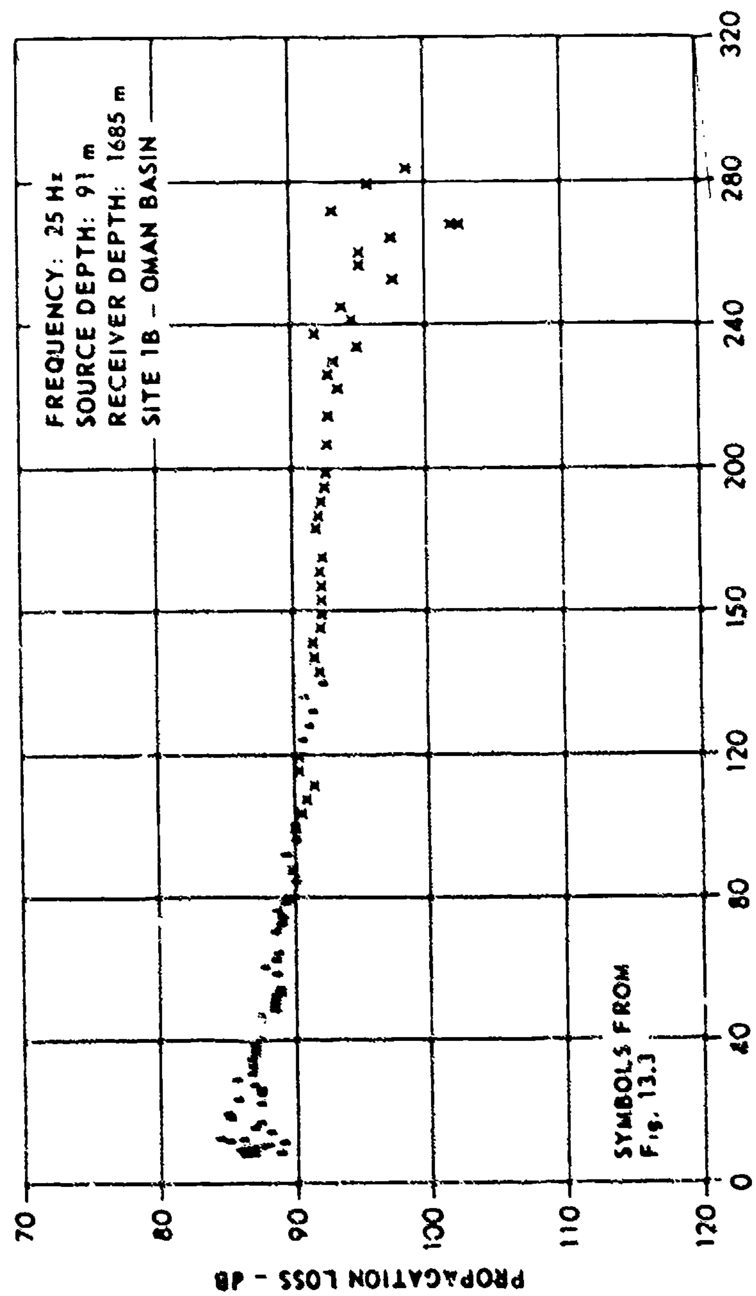

FIGURE 6.14
PROPAGATION LOSS MEASURED DURING BEARING STAKE (U)
FROM Ref 18

ARL UT
AS-79-2080
KCF - GA
10 - 9 - 79

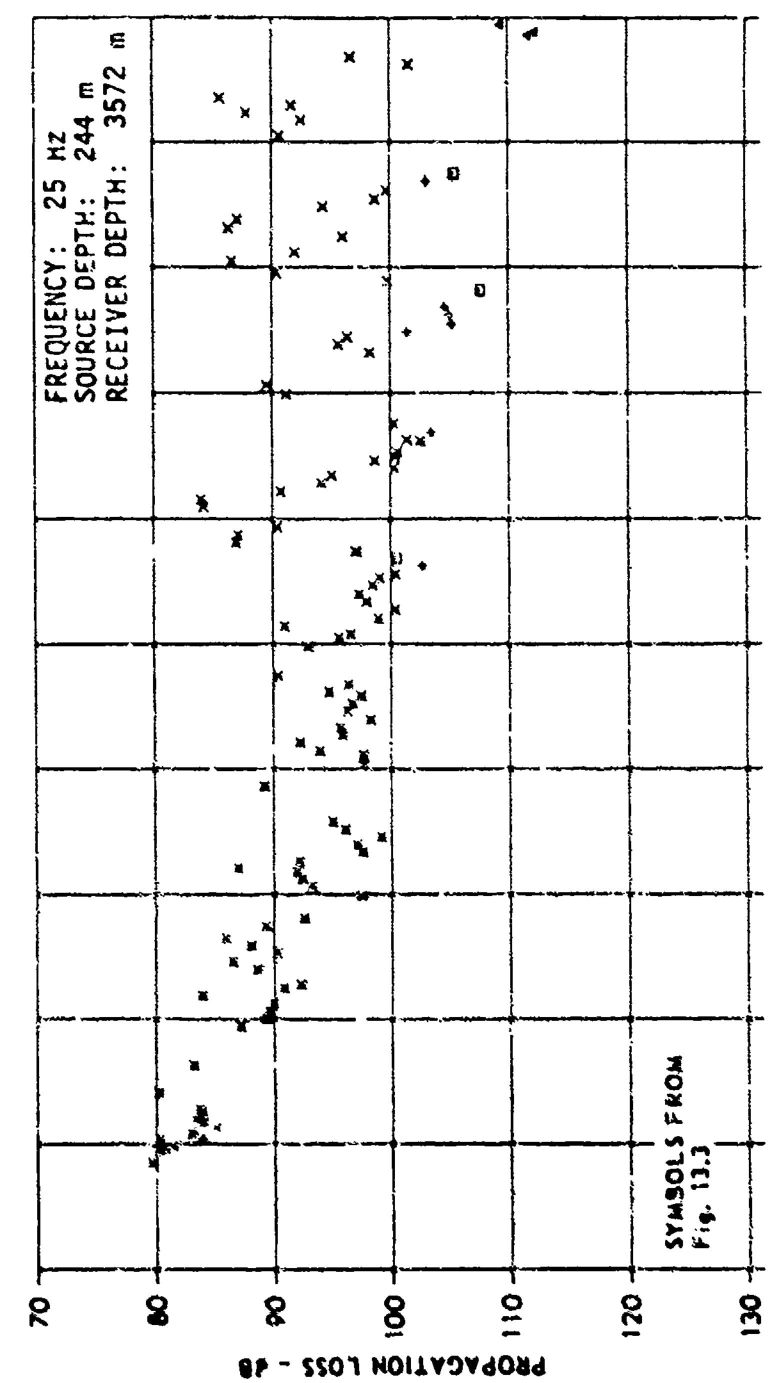

FIGURE 6.15
PROPAGATION LOSS -
CHURCH STROKE II - SITE B (U)
SOURCE DEPTH: 244 m

ARL UT
KCF - GA
10-9-79

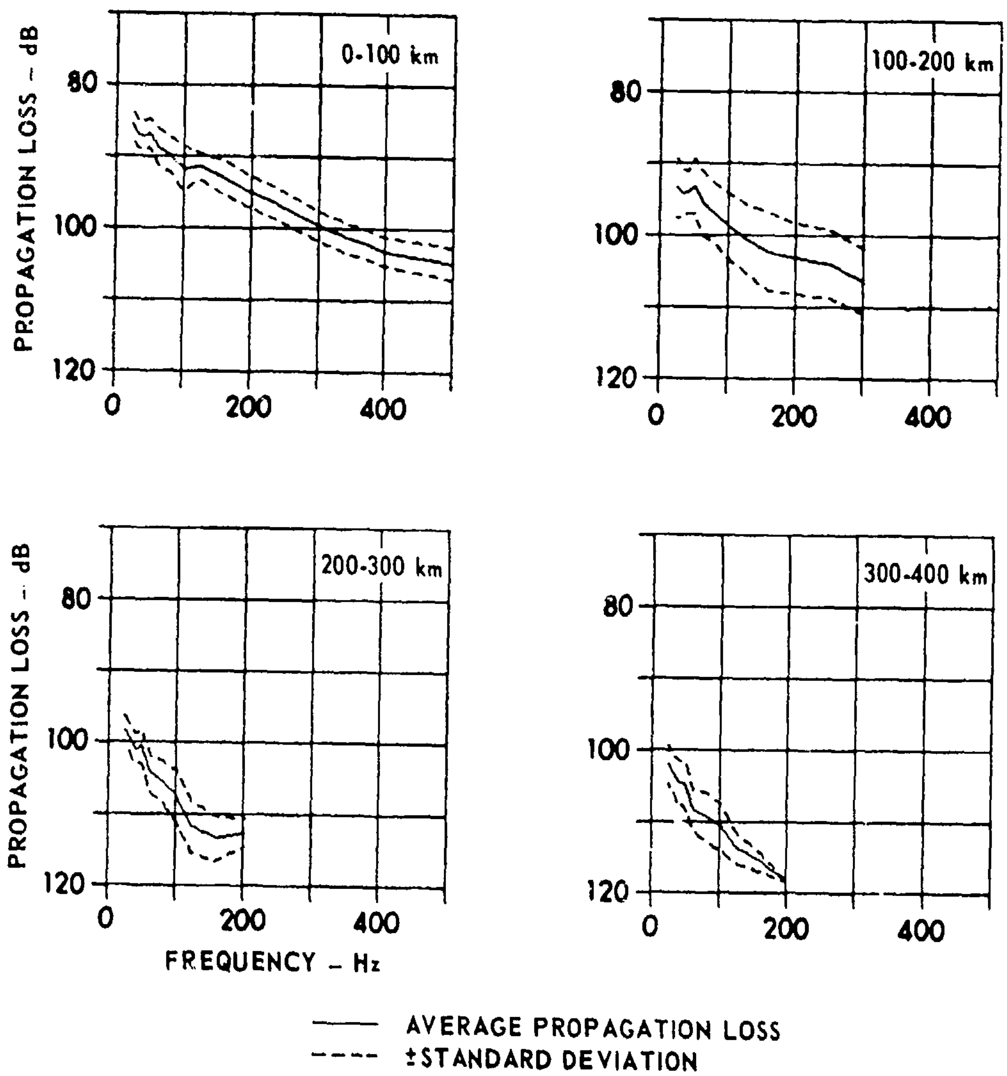

FIGURE 6.16
RANGE AVERAGED SHOT SPECTRA
CHURCH STROKE II - SITE B 91 m SOURCE (U)

ARL:UT
AS-79-1310
KCF - GA
7 - 11 - 79

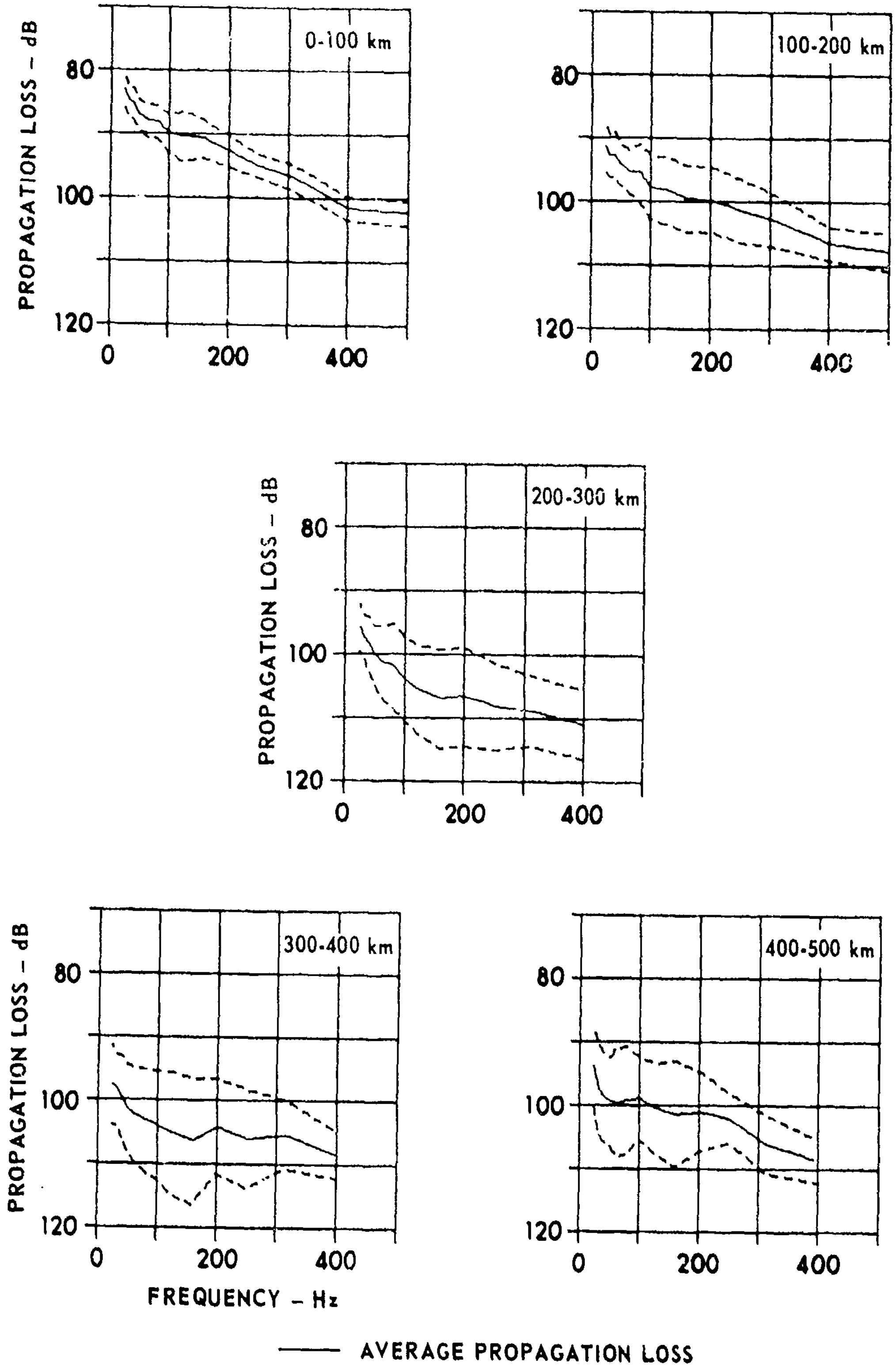

FIGURE 6.17
RANGE AVERAGED SHOT SPECTRA
CHURCH STROKE II - SITE B 244 m SOURCE (U)

ARL:UT
AS-79-1311
KCF - GA
7 - 11 - 79

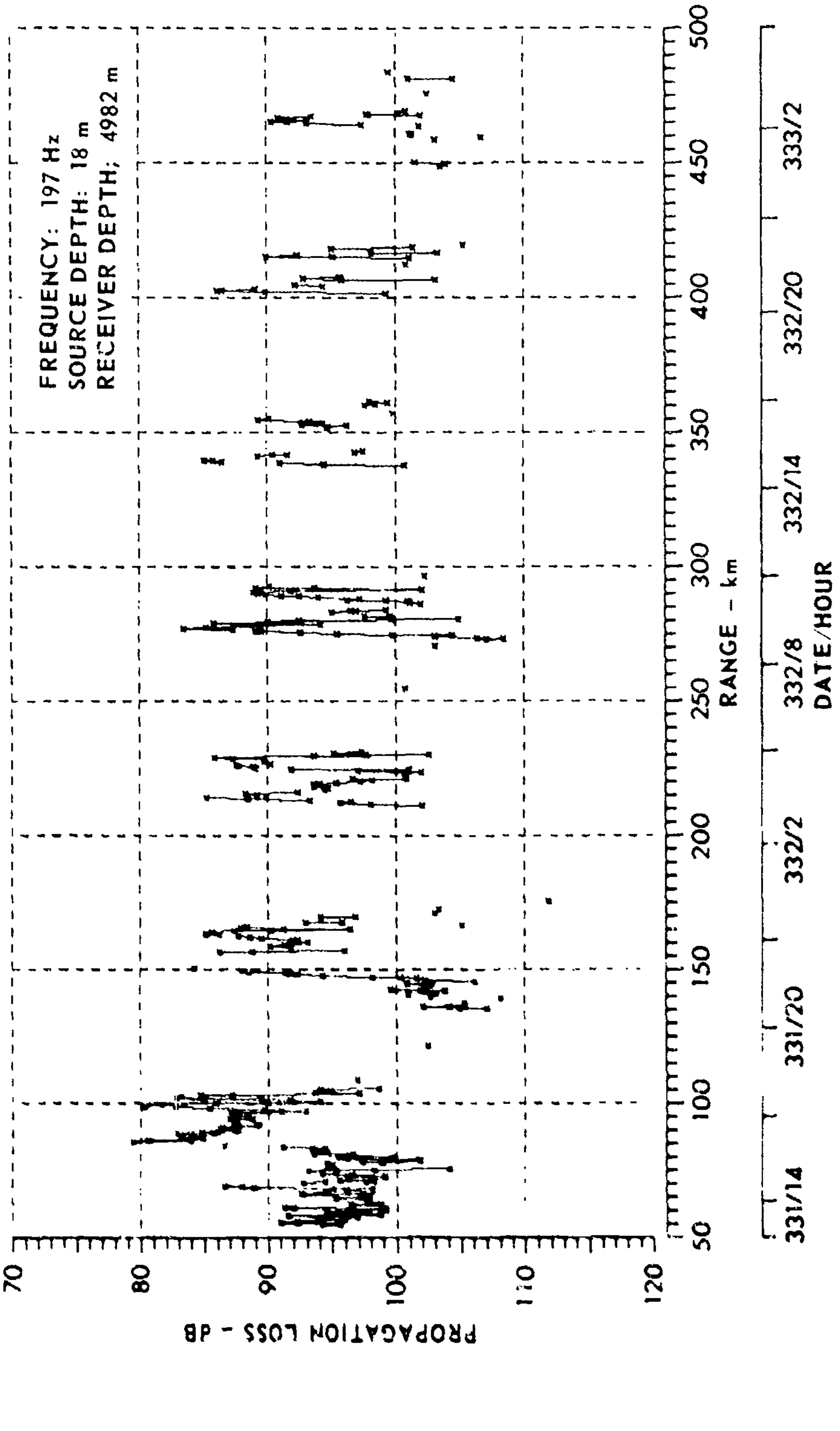

FIGURE 6.18
CONVERGENCE ZONE PROPAGATION LOSS AT 197 Hz
CHURCH STROKE II - SITE EN (U)

ARL UT
AS-79-2085
KCF-GA
10-9-79

(C) (100 nmi), the PL to Site EN from sources within the convergence zone is approximately 88 dB at 197 Hz, while in the Northeast Pacific it is approximately 90 dB at 180 Hz.

(C) Figure 6.19 presents the losses to Site EN from sources within the convergence zone at 180 km as a function of receiver depth. In the bottom 400 m of the water column the losses increase with depth by as much as 15 dB. When compared to data from CHURCH ANCHOR (also in Fig. 6.19) this increase at Site EN is more rapid and occurs over a smaller depth interval; the increase in the CHURCH ANCHOR data begins at least 1000 m off the bottom.

(C) Thus far all the data discussed have been taken with the source within the basin. An acoustic model study conducted prior to the exercise[27] predicted complete acoustic blockage by the bathymetric ridge along the northern boundary of the Western Philippine Basin. Although the model runs were for a site 400 km to the south of Site EN, the blockage would also be predicted for Site EN.

(U) The aircraft SUS event at Site EN extended out beyond the Oki Daito Ridge, the northern boundary of the basin. When the shots were detonated within the basin, the received signals saturated the recording system (Figs. 3.35 through 3.40). At a range of 400 km, the source passed over the Oki Daito Ridge (Fig. 3.1). Shots detonated beyond this range were not detected at the receiver location: the ridge does effectively block acoustic propagation from shallow sources outside the basin, as predicted.

(C) In summary, the PL within the CHURCH STROKE II area from sources at short ranges (10 to 25 km) averages 78 dB. The signal excess measured during the short range events gives an estimated minimum detectable source level of 150 dB//μPa at 67 Hz and 140 dB at 197 Hz at all three sites for noise levels similar to those during the exercise. Long range PL characteristics in the bottom limited Parece Vela Basin are similar to those seen in the Indian Ocean, and are noted for their low losses. The losses however, are approximately 5 dB greater in the Parece Vela Basin. The PL

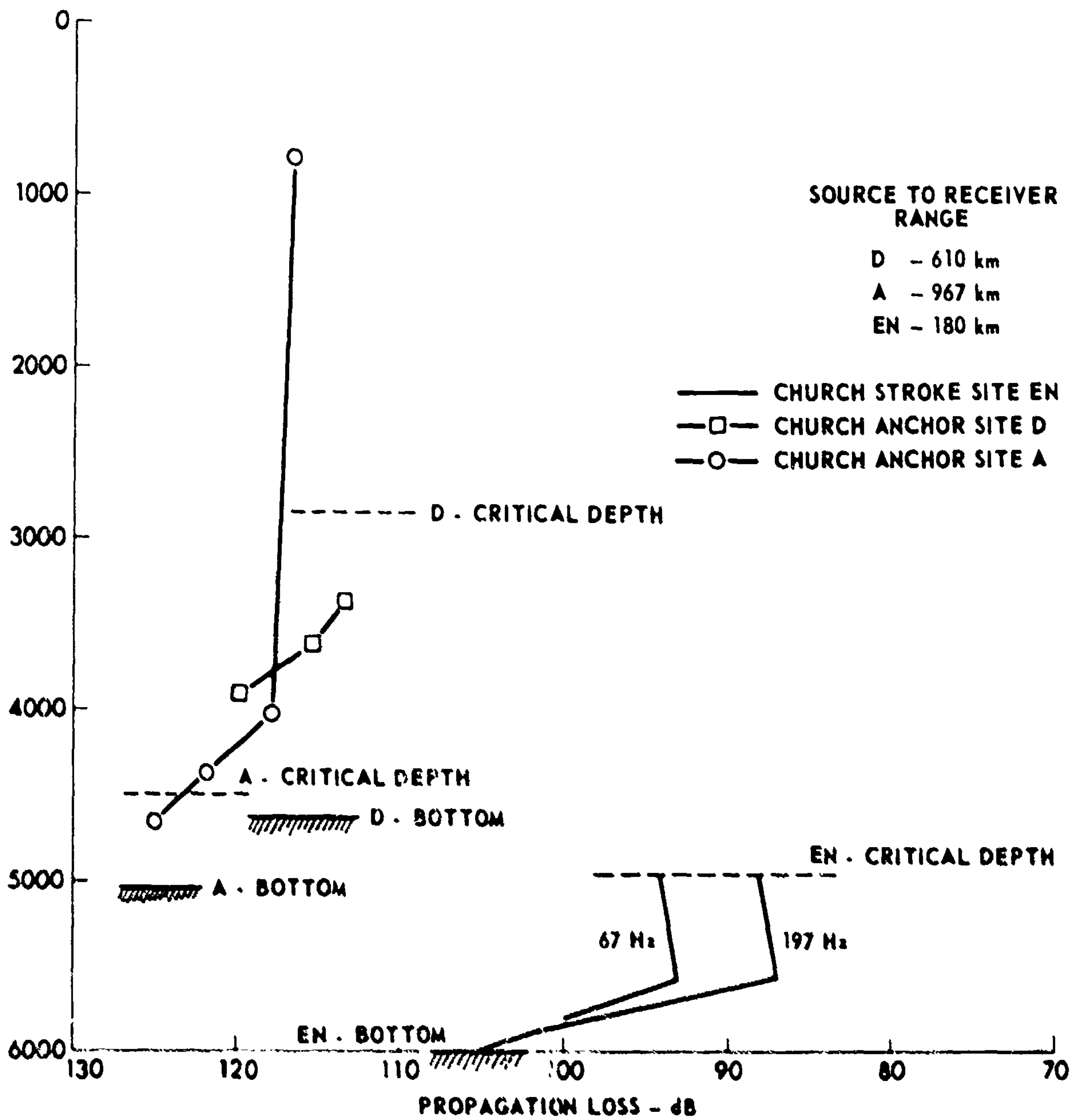

FIGURE 6.19
AVERAGE PROPAGATION LOSS FOR CHURCH STROKE II - SITE EN AND CHURCH ANCHOR SITES (U)

ARL UT
AS-79-1312
KCF - GA
7 - 11 - 79

(C) in the Western Philippine Basin is approximately equal to measurements from the north Pacific. Other characteristics of those regions, such as convergence zone structure and depth dependence, are similar. Finally, propagation to the sites from outside the CHURCH STROKE II basin was not detectable.

6.3 Ambient Noise

(U) This section compares the background ambient noise levels from the Northeast Pacific (CHURCH ANCHOR, CHURCH OPAL) with the levels at Sites B, C, and EN of CHURCH STROKE II. The levels at critical depth and near the bottom are examined separately. The data from Site C were obtained from a short deep array, i.e., no measurements were made at critical depth. The PAR and anemometer data at Site B were examined carefully to estimate wind generated noise. The low signal level PAR data (at lower wind speeds) were rejected, however, because of quality problems due to data compression in the tape recorder.

(C) The critical depth noise levels for the Northeast Pacific and the Philippine Sea sites in Fig. 6.5 are superimposed in Fig. 6.20. These data are characteristic of shipping dominated regions. The levels peak around 50 Hz decreasing 6 to 8 dB/octave with increasing frequency. The Philippine Sea data falls between the lowest Northeast Pacific data from CHURCH OPAL (Site CO) and the data from CHURCH ANCHOR Sites CAC and CAD. In general, the noise level in the Northeast Pacific decreases from north to south, which correlates with the distribution of shipping density.

(U) The nominal shipping density in the Northeast Pacific[28] varies from 10 ships per 5° square at Site CAD to 7 at Site CAC, 4 at Site CAA, and 3 at CHURCH OPAL Site CO. The observed shipping density per 5° square in CHURCH STROKE II at Site B and Site C was on the order of 10 to 15.[10] At Site EN the density was on the order of 13. These density numbers are slightly subjective and variable. In those cases where the sites lay on a 5° boundary an interpolation between 5° squares was made.

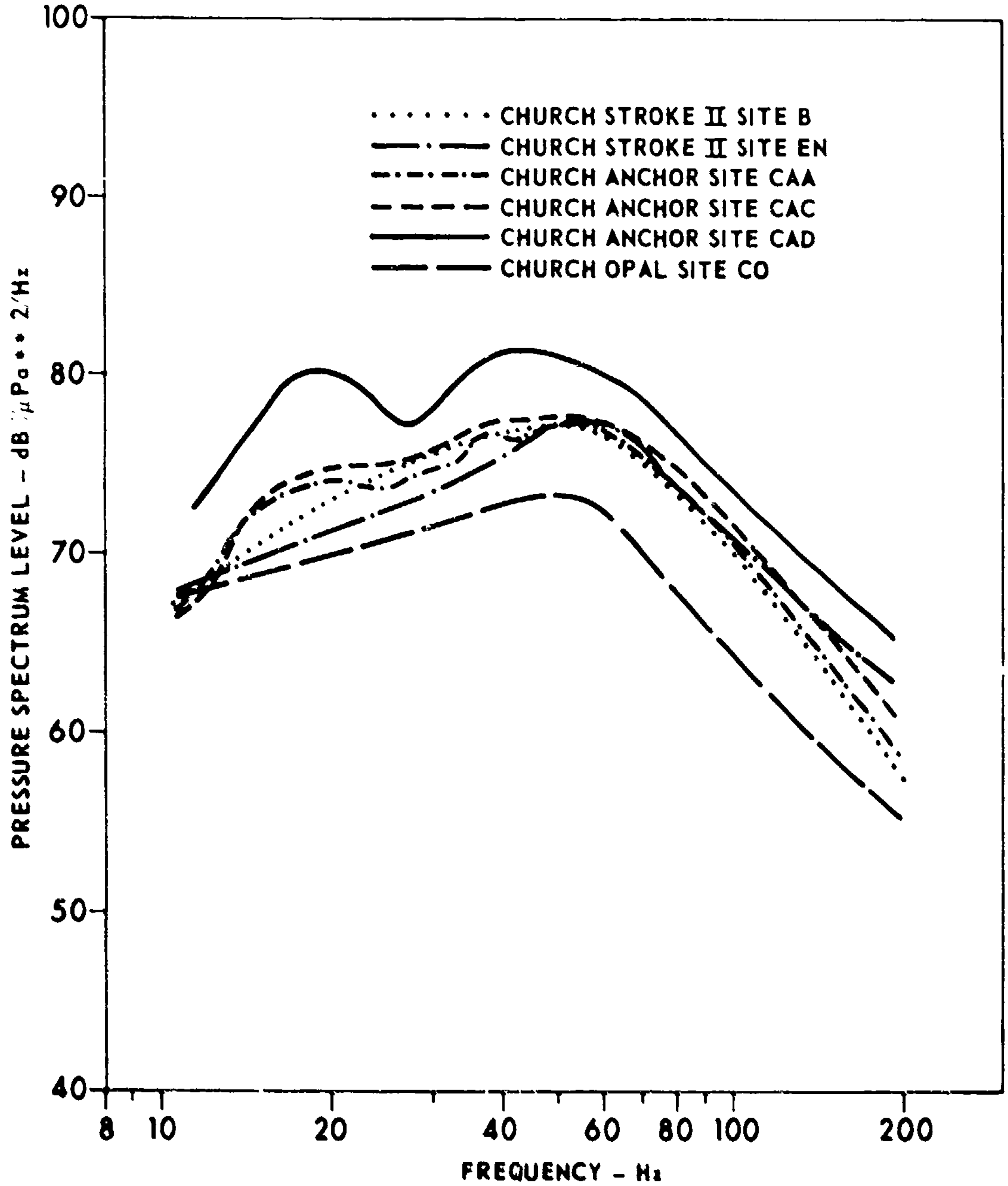

FIGURE 6.20
BACKGROUND NOISE AT CRITICAL DEPTH FOR VARIOUS PACIFIC SITES (U)

ARL UT
AS-79-2130
KCF - GA
10 - 19 - 79

(U) The near-bottom levels are shown in Fig. 6.21 for the three Philippine Sea sites and the CHURCH OPAL site. These levels represent near-minimum conditions during which no single ship appears to dominate the spectrum. The exception is from Site C where only 36 h of data were available and the quietest time found was during a period when a tanker was known to be 50 nmi distant. The CHURCH OPAL data remains as the lowest level data yet recorded on an ACODAC.

(C) One of the more interesting observations in regard to depth dependence is that Sites B and C were bottom limited and Site EN had 1000 m of depth excess. This observation is coupled with the fact that all of the Northeast Pacific data were taken from areas of depth excess and all those data show decreasing noise levels with depth. The significant point is that Site B also showed a decrease in noise level with depth. This is different from the Indian Ocean (BEARING STAKE) data, also bottom limited, which exhibited little or no depth dependence.[18] The difference lies in the shipping densities. The BEARING STAKE 5° shipping densities vary from 149 at Site 1 to 93 at Site 4. In the Indian Ocean, the shipping density is much higher than that of the Philippine Sea, and essentially distant shipping conditions do not exist.

(C) A second factor which may contribute to the depth dependence at Site B is the mechanism of slope coupling of noise from shipping over the sides of the basin which contained Sites B and C (Figs. 2.1 and 4.1). Sources above the slopes of the basin would be expected to contribute relatively little energy to deep near-bottom sensors in the middle of the basin, even though they would be expected to be important at midwater depths.

(C) It should be noted that ambient noise was recorded at Site EN during the passage of Typhoon Lucy. The noise levels increased 25 dB across the spectrum from 7 Hz to 250 Hz during this time. A detailed discussion of the typhoon data was presented in Chapter 3, Section 3.

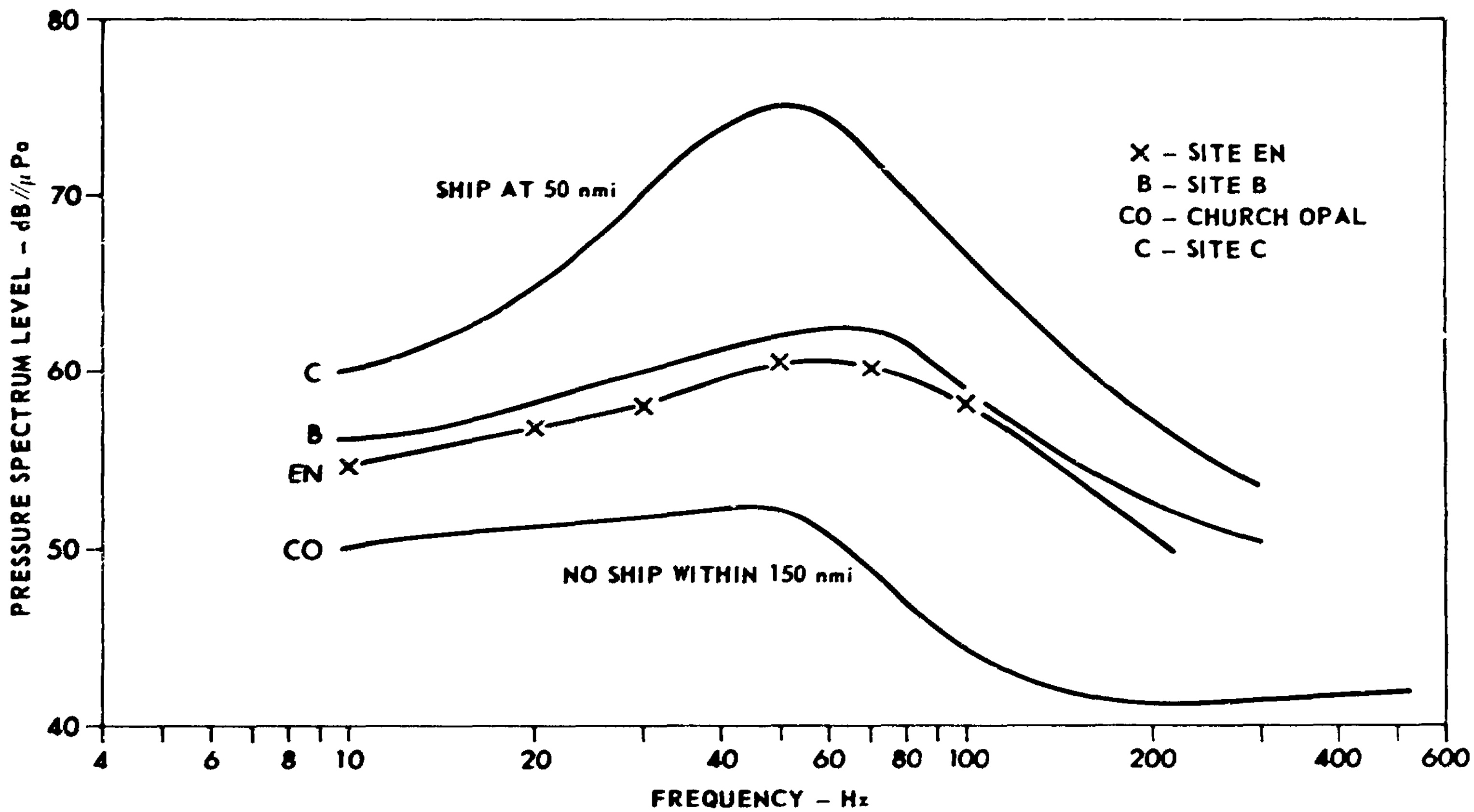

FIGURE 6.21
NEAR-MINIMUM BACKGROUND SPECTRAL LEVELS AT SEVERAL DEEP LOCATIONS (U)

ARL:UT
AS-79-1314
KCF - GA
7 - 11 - 79

APPENDIX A

AMBIENT NOISE/cw PROCESSING

UNCLASSIFIED

(U) The AN/cw processor is a hardware/software configuration designed to perform a narrowband analysis over a variable frequency range handling large volumes of data. The system performs five functions: A/D conversion, spectral estimation, band estimation, editing, and display. Parameters such as bandwidth, frequency range and resolution, and integration or averaging time can readily be adapted to suit different applications. The AN/cw processing flow is shown in Fig. A.1.

(U) The basic signal processing task of the system is to compute and calibrate a narrowband spectrum from contiguous time increments throughout the data period analyzed. Currently, an 8192-point FFT is used to provide a frequency resolution of 0.147 Hz for the frequency range of 10 to 600 Hz.

(U) The ambient noise spectra can be time averaged over a selected period and can be output as narrowband and/or nth octave band time series. Various statistical algorithms are available to furnish the information required to perform an analysis of the acoustical data.

(U) The cw analysis is achieved by using the calibrated narrowband spectra to estimate the signal power in a given frequency band. The spectra are first averaged for a 1 min period; from these averages, two types of band estimates are obtained. For each cw signal, a narrow band (0.5 Hz) centered about the source frequency is searched for its spectral peak, and then the signal power in a narrower band (0.22 Hz) centered about this peak is determined. Peak tracking is used to compensate for any Doppler variation in source frequency that might occur. The second type of band estimate determines the ambient noise power in a wider band (4 Hz) associated with each source frequency. In computing propagation loss, the signal power is corrected for the noise power component.[A.1,A.2] An algorithm is used to minimize the effects of shipping interference and short-term nonstationarities that often contaminate data of this type.

UNCLASSIFIED

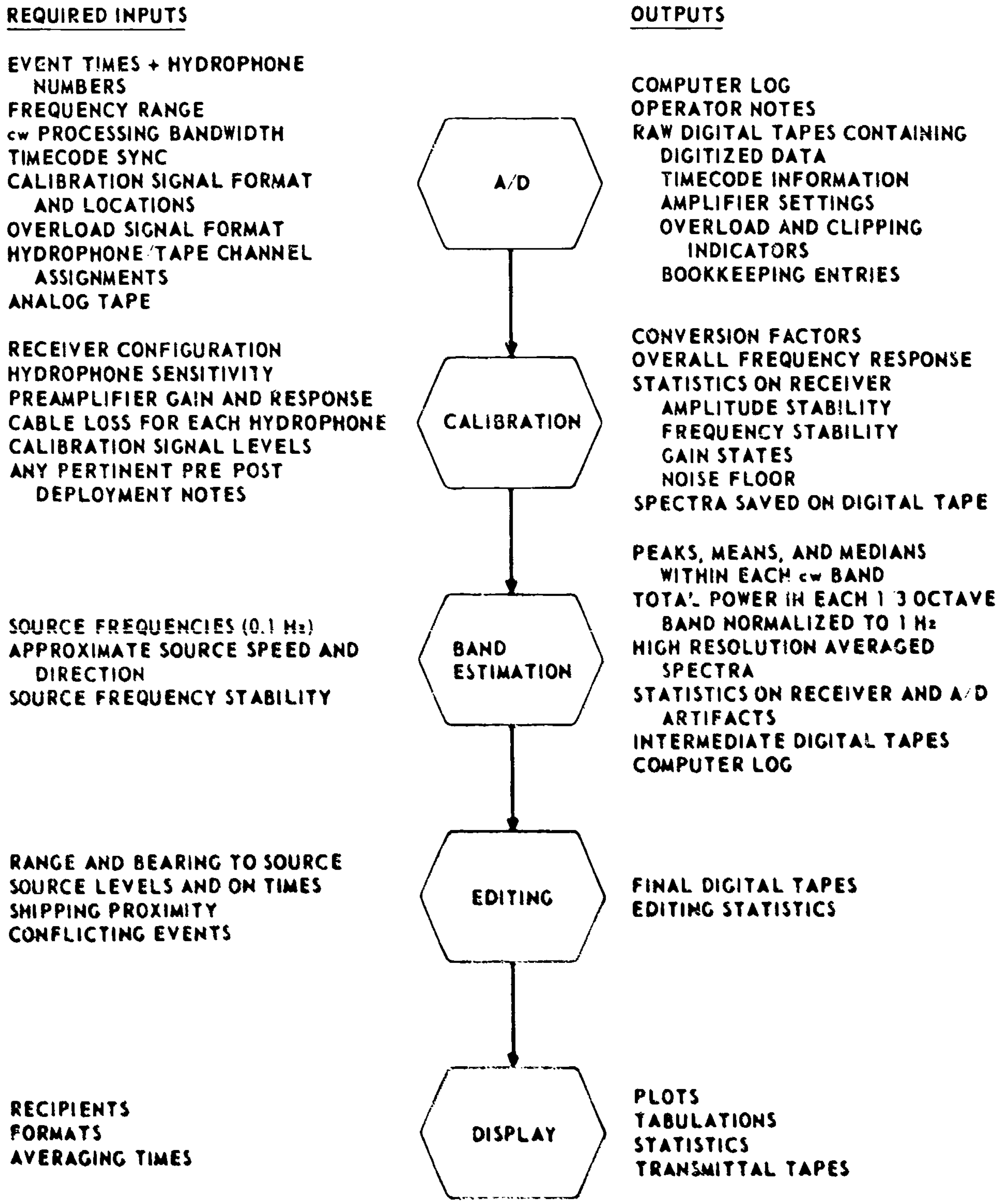

FIGURE A.1
ARL:UT AN/cw PROCESSOR FUNCTIONS

ARL - UT
AS-76-792
CEE - DR
7 - 14 - 76

UNCLASSIFIED

(U) The third task performed by the AN/cw processor is to automatically edit the reduced data for artifacts and contamination from: (1) environmental effects such as biological and seismic noise; (2) exercise effects such as conflicting sources (SUS), source level fluctuations, source timing, and shipping noise; and (3) receiver and recording system effects. The techniques and algorithms used in the editing phase are computerized. These algorithms provide calibrations, data quality indicators, adaptive filters for octave and narrowband noise estimators, peak tracking, and corrrection of artifacts.

Processor Outputs

(U) The following outputs of the AN/cw processor are available for analysis:

1. ambient noise spectra in narrow and/or octave bands,
2. cw signal power, noise power, and S/N estimates in narrow frequency bands, and
3. propagation loss (PL), noise power estimates, and S/N estimates versus range and/or time.

(U) An example of the cw propagation loss display used in this report is shown in Fig. A.2. Each plotted point is derived from an average spectrum over 2 to 4 consecutive minutes. Points are connected when they come from successive averaging intervals. Because of source cycling (10 min on, 5 min off) in this example from BEARING STAKE, there are frequent breaks in the connecting lines. In addition, points are deleted when the signal excess is less than 6 dB.

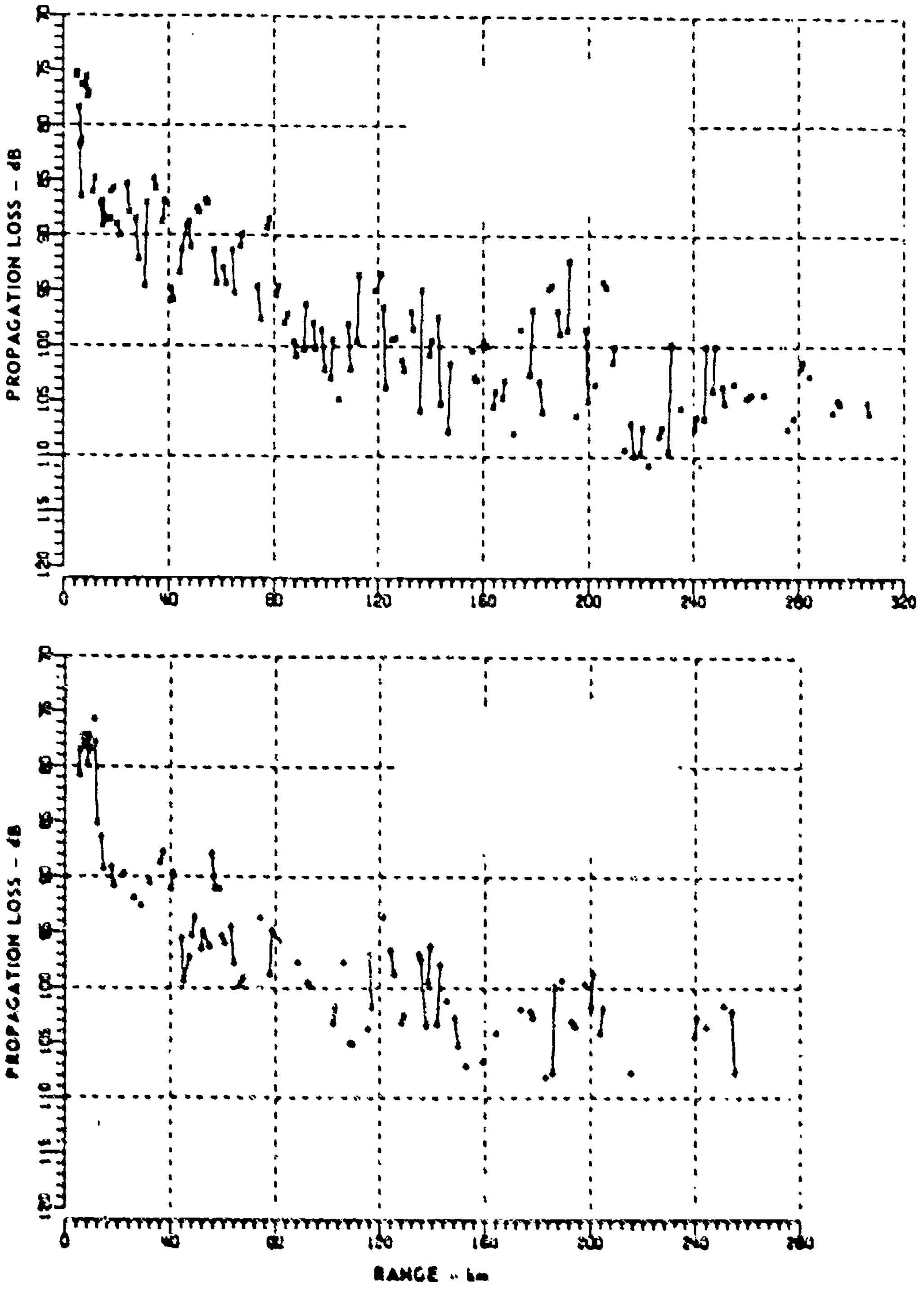

FIGURE A-2
EXAMPLE cw PROPAGATION LOSS DISPLAY

APPENDIX B

SUS PROPAGATION LOSS PROCESSING

(The reverse of this page is blank.)

(U) The general flow of the ARL:UT SUS propagation loss processing is shown in Fig. B.1. The basic inputs are the analog tapes from the ACODAC recordings, SUS detonation times and depths, and navigation information. The primary outputs are propagation loss and S/N in each of the 1/3 octave bands from 12 to 600 Hz and in one octave bands at 12.5, 25, and 50 Hz.

(U) Before digitizing the data, a quality assessment of the ACODAC tapes is performed. At this time decisions are made as to which channels can be processed and potential problems are noted.

(U) As soon as navigation and source information are available, programs are run to calculate the source-to-receiver range and expected arrival time for each shot. These programs provide timing inputs for the analog-to-digital (A/D) conversion program. Typically, a 50 sec time segment starting about 15 sec prior to the expected arrival time for each shot is digitized. An identification record is output along with the time series indicating the source depth, detonation time, and range from source to receiver.

(U) Two channels of SUS data are digitized simultaneously, with 12 bits from each of the two channels packed into one word. At the same time, the predeployment calibration signals are digitized and later processed to provide calibration factors for the digital SUS data. Envelope plots of the type shown in Fig. B.2 indicate that the arrivals are indeed within the window of digitized data, and give an idea as to which shots may be detected.

(U) A computer program is then used to detect the shot, determine its duration, and compute its Fourier spectrum. A noise spectrum is obtained using the first 6.8 sec of the time segment containing the shot, which is then used to correct the shot energy in each frequency band. Calibration factors, ACODAC gain, and ARL:UT gain applied at conversion time are then taken into account in assigning a calibrated propagation loss value for

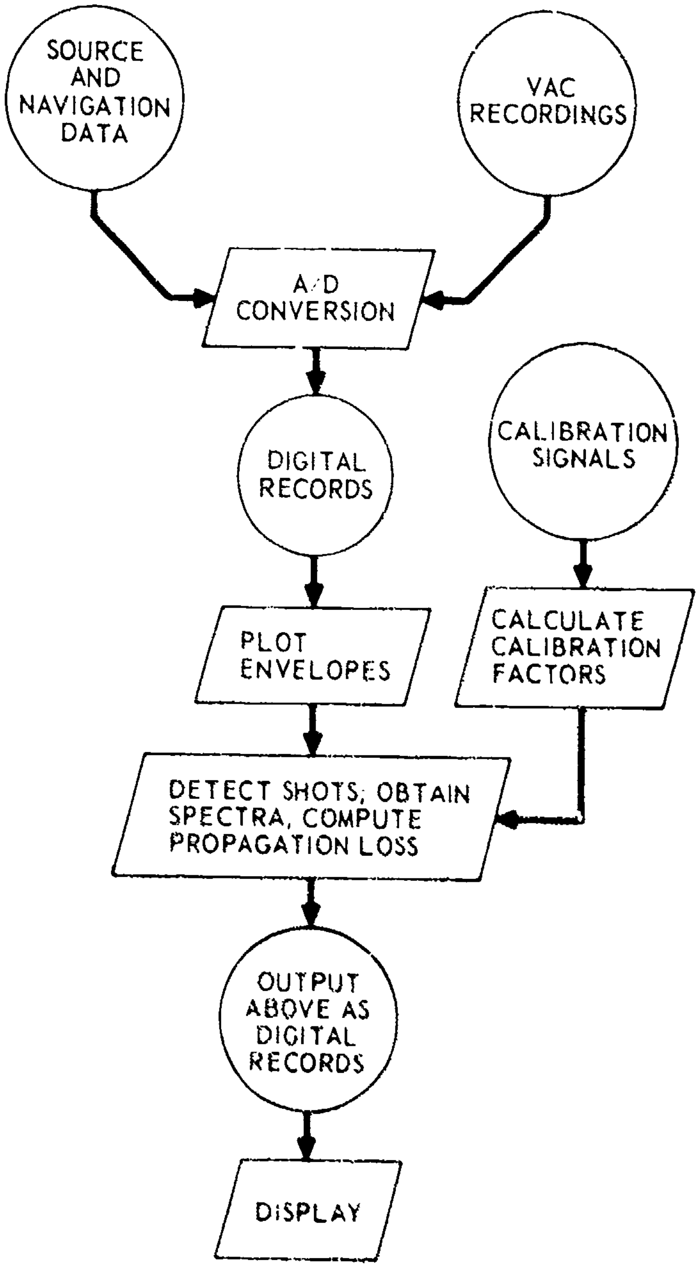

FIGURE B.1
SUS PROPAGATION LOSS PROCESSING FLOWCHART

ARL UT
AS-78-1985
KCF - GA
12-14-78

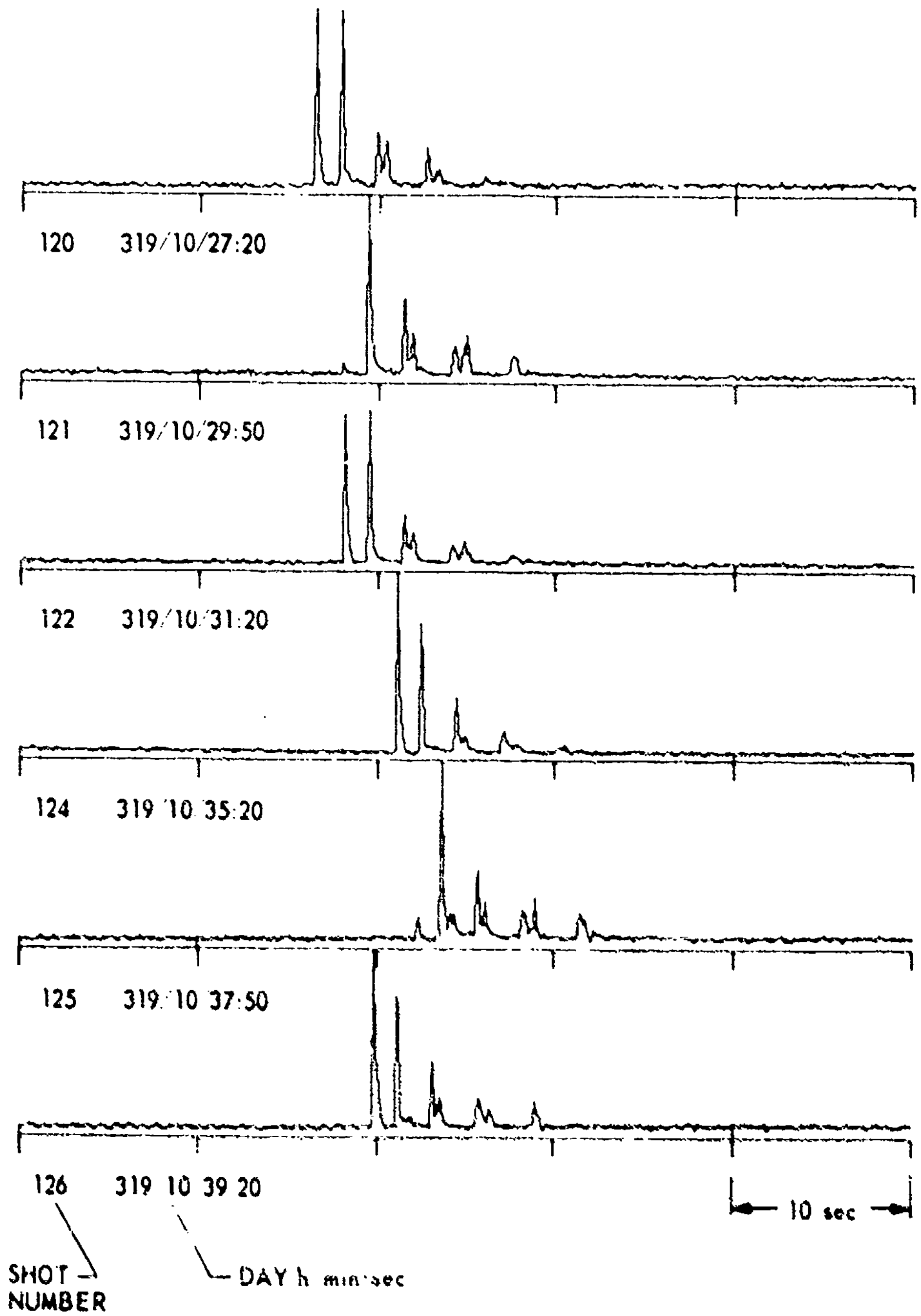

FIGURE B.2
ENVELOPE PLOTS

ARL UT
AS-78-1986
KCF - GA
12-14-78

(U) each frequency band. These values--noise level and S/N in each frequency band, detection time, shot duration, peak level and its time of occurrence, and both the shot and noise transforms--are output on digital tape for each shot.

(U) Additional programs are used to display the data. The primary display is propagation loss versus range for a given source and receiver depth and frequency, as shown in Fig. B.3. Additional displays include travel time from source to receiver, sound speed estimates, shot and noise spectra, noise or S/N versus range, range averaged propagation loss, and differences in propagation loss or S/N as a function of hydrophone depth or frequency.

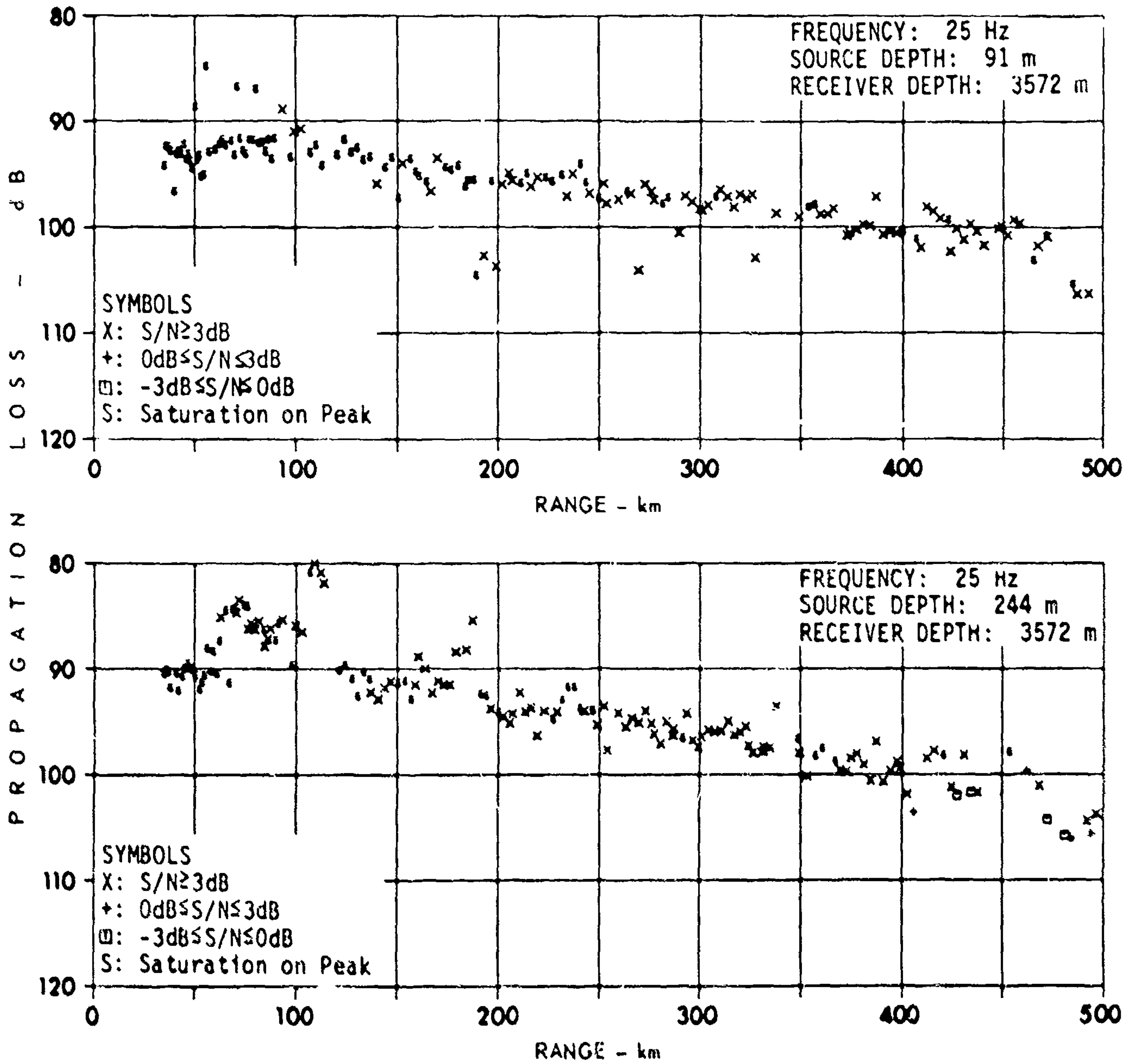

FIGURE B.3
PROPAGATION LOSS versus RANGE PLOTS

ARL UT
AS-78-1987
KCF - GA
12 - 14 - 78

(The reverse of this page is blank.)

APPENDIX C

BOTTOM LOSS PROCESSING

(The reverse of this page is blank.)

(U) The bottom loss processing system is designed to compute bottom loss from recorded multibounce SUS data. There are three elements of the system. First, there is the signal processing element, which is concerned with obtaining calibrated spectral levels for time resolved signal components; this is done using fast Fourier transform analysis of the digitized data. Second, there is a signal modeling element, which is concerned with interpreting and predicting the observable signal components; for the current work, this is done using a ray theory model based on careful calculation of eigenrays. Finally, there is an element of the system which integrates the signal measurements and the model predictions and accomodates small timing discrepancies due to measurement errors or propagation fluctuations; this is achieved by a combination of computer programs and manual intervention.

(U) The general flow of the ARL:UT multipath processing system is shown in Fig. C.1. The basic inputs are the analog tapes from the ACODAC recorders and the associated ancillary data. The ancillary data includes SUS detonation times and depths, navigation inputs, sound velocity profiles, and bathymetry. Bottom losses are computed in all 1/3 octave bands from 21 Hz to 600 Hz and one octave bands at 12, 25, and 50 Hz, and are stored in digital form. Most of the data presented in this report are from the 25, 50, 100, 200, and 400 Hz bands. The source levels used were those reported by Gaspin and Shuler.[C.1]

(U) The initial processing of the ACODAC tapes includes a quality assessment and a data survey. During this time, the ancillary data are used to compute time windows for accepting digital data containing the shot arrivals. Usually, the time window is 50 sec long and begins approximately 15 sec before the expected shot arrival. The data window, together with information such as shot depth and range, are stored on magnetic tape, together with appropriate ancillary information. The predeployment calibration signals (header calibrations) are digitized during the same operation and then processed to provide calibration factors for the digital SUS data.

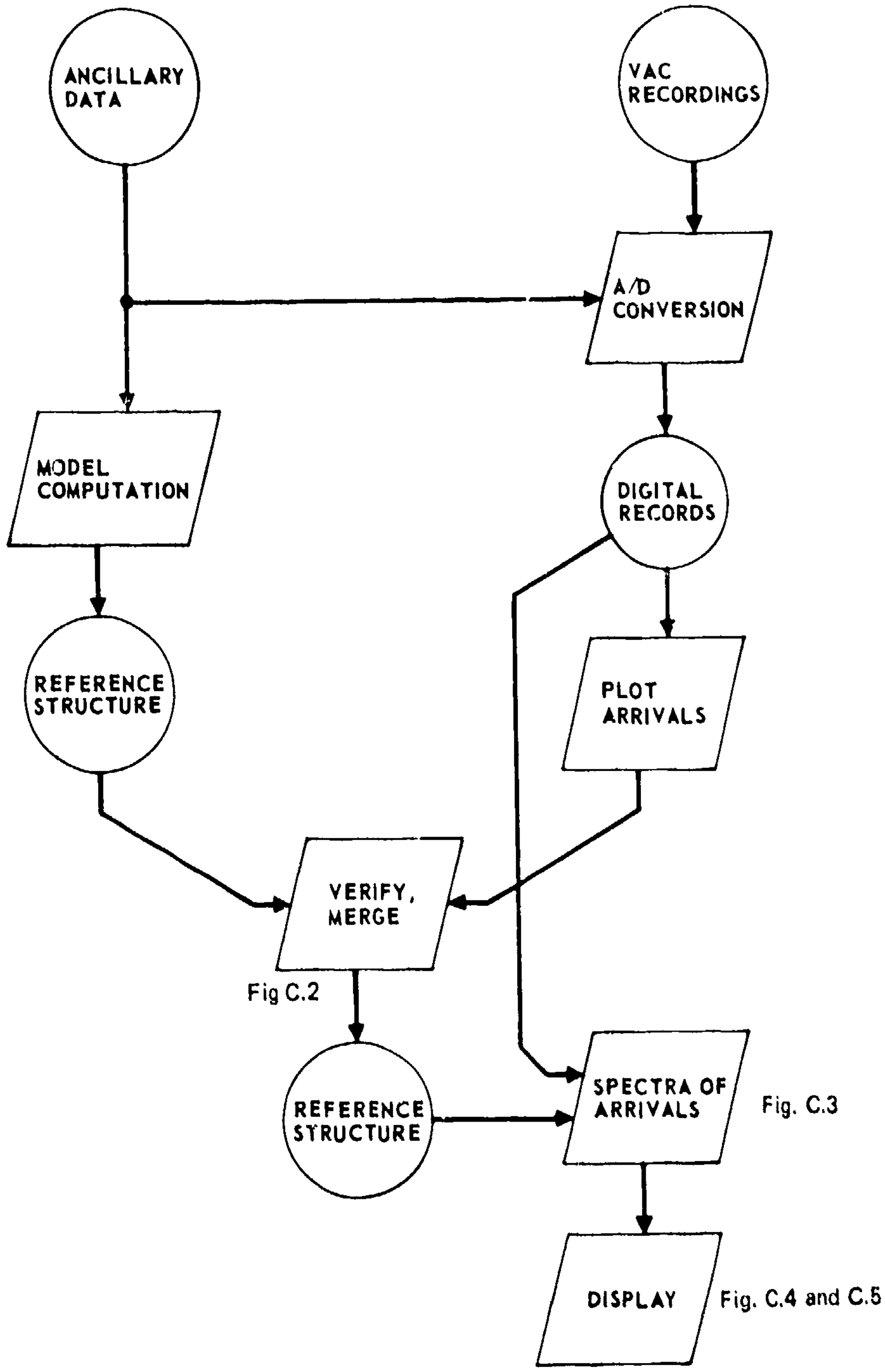

FIGURE C.1
MULTIPATH PROCESSING FLOWCHART

ARL:UT
AS-78-65-P
NRB - GA
2 - 15 - 78
REV 8-15-79

(U) In parallel with the conversion and display of the data, computations are made to determine the ray path arrivals from each shot. These are made using a computer program which determines the eigenrays connecting the source and receiver.[C.2] These computations assume that the bathymetry and sound velocity structure do not vary with range. Within a selected arrival window (usually 10 sec), all of the eigenrays are determined to within 1 m in range. That is, the root-finding iterations to find each ray are terminated when a ray is found which leaves the source and passes through the receiver depth at a range within 1 m of the source range. Thus, the signal travel timing along each ray is determined to better than 1 msec. This information is then stored on a digital magnetic tape.

(U) To reconcile the modeled and the measured arrival structure, the ray arrival structure is plotted to the same scale as the high resolution plots. The one manual step in the multipath processing system uses these two plotted displays in conjunction to verify that the modeled arrival structure is adequate to represent the measurement and to correct for timing errors due to, for example, detonation time uncertainties. Figure C.2 gives an example of agreement typically observed between the ray predictions and the measured signal. In practice, the manual task is to verify such agreement, and then to record the first and last ray indices and the times in the signal at which good agreement has been found. For example, in Fig. C.2 it was noted that there was good agreement from ray 1 at 16.2 sec to ray 22 at 22.8 sec. This information is then input to a subsequent computer operation referred to as "splitup".

(U) The task of splitup is straightforward: to specify the time intervals in the digital data containing groups of multipath arrivals and to associate with these intervals the bottom reflection angle, the number of reflections, and the reference propagation loss. The reflection angle is defined as the average bottom angle of the rays within the time interval. The reference propagation loss is computed by coherently summing the contributions of the rays within the time interval and averaging over the one or 1/3 octave bands used. This computed loss assumes that the ocean

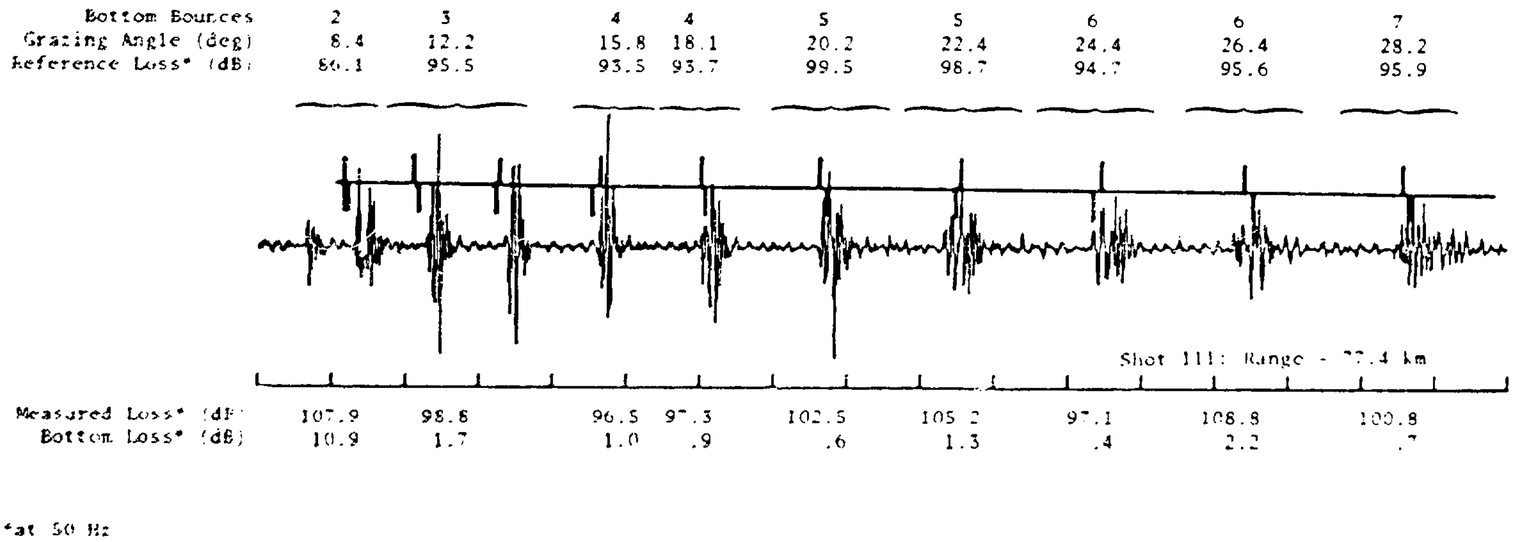

FIGURE C-2
COMPARISON OF MEASURED AND PREDICTED ARRIVAL STRUCTURES

AS-78-70

(U) bottom is perfectly reflecting and that the ocean surface is a pressure release boundary. The difference between the reference and measured propagation losses is then attributed to a bottom loss mechanism. In Fig. C.2, the time intervals computed, together with some of the associated information, are shown.

(U) Finally, the information from the splitup operation is input to the spectral measurement program which computes the Fourier transform and the calibrated propagation loss (and bottom loss) for each of the arrivals. This information is stored on digital tape for subsequent display and analysis. Figure C.3 presents the power spectra for the first nine arrivals in Fig. C.2. Figure C.4 presents the individual bottom loss measurements at 25 Hz and 100 Hz for one SUS run, and Fig. C.5 presents averaged bottom loss at 25, 50, 100, 200, and 400 Hz for the same SUS run.

(U) A more detailed discussion of the bottom loss processing system can be found in Ref. C.3.

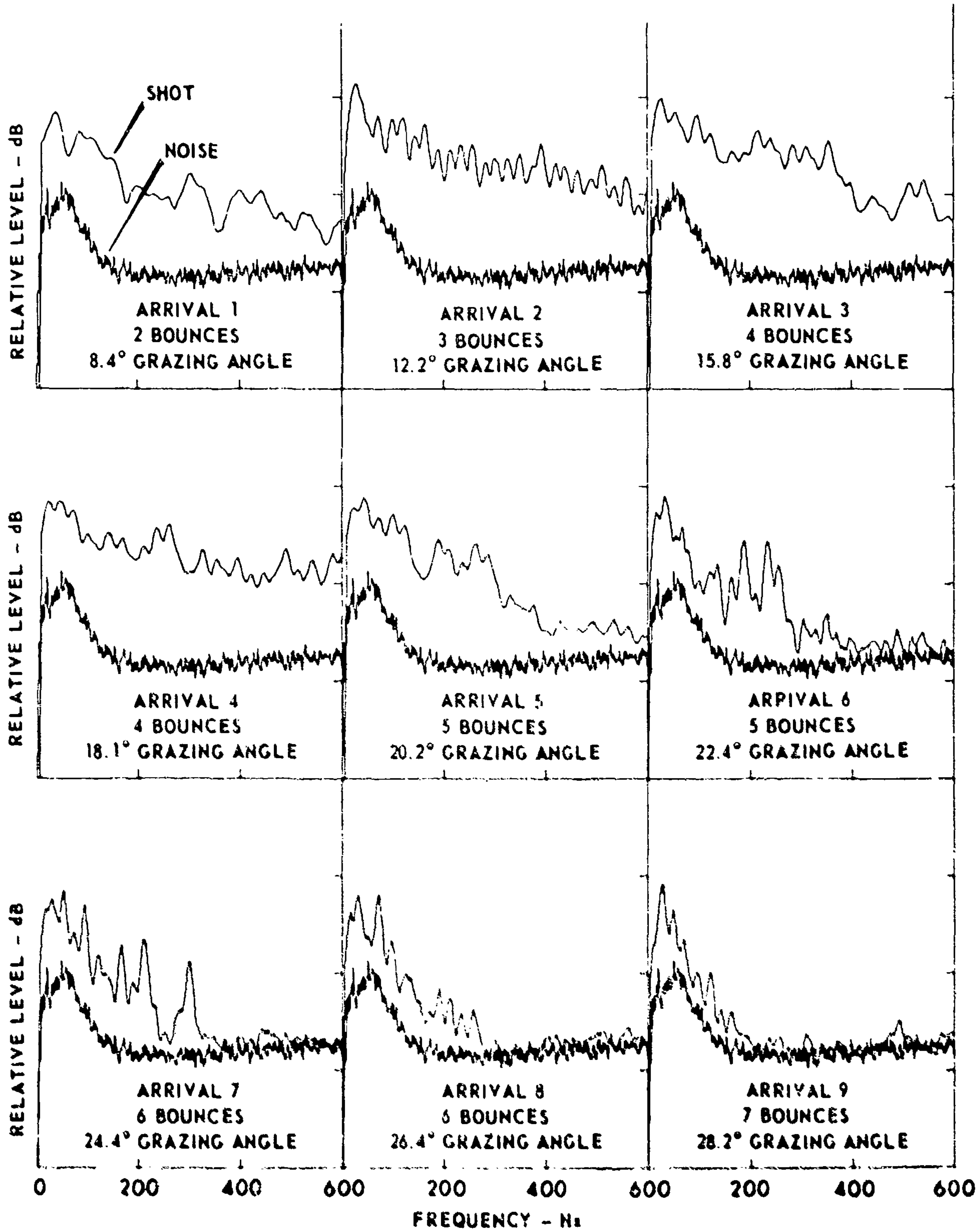

FIGURE C.3
MULTIPATH ARRIVAL AND NOISE POWER SPECTRA
ARRIVALS 1 – 9

ARL UT
AS-78-7.
NRB-GA
3-15-78

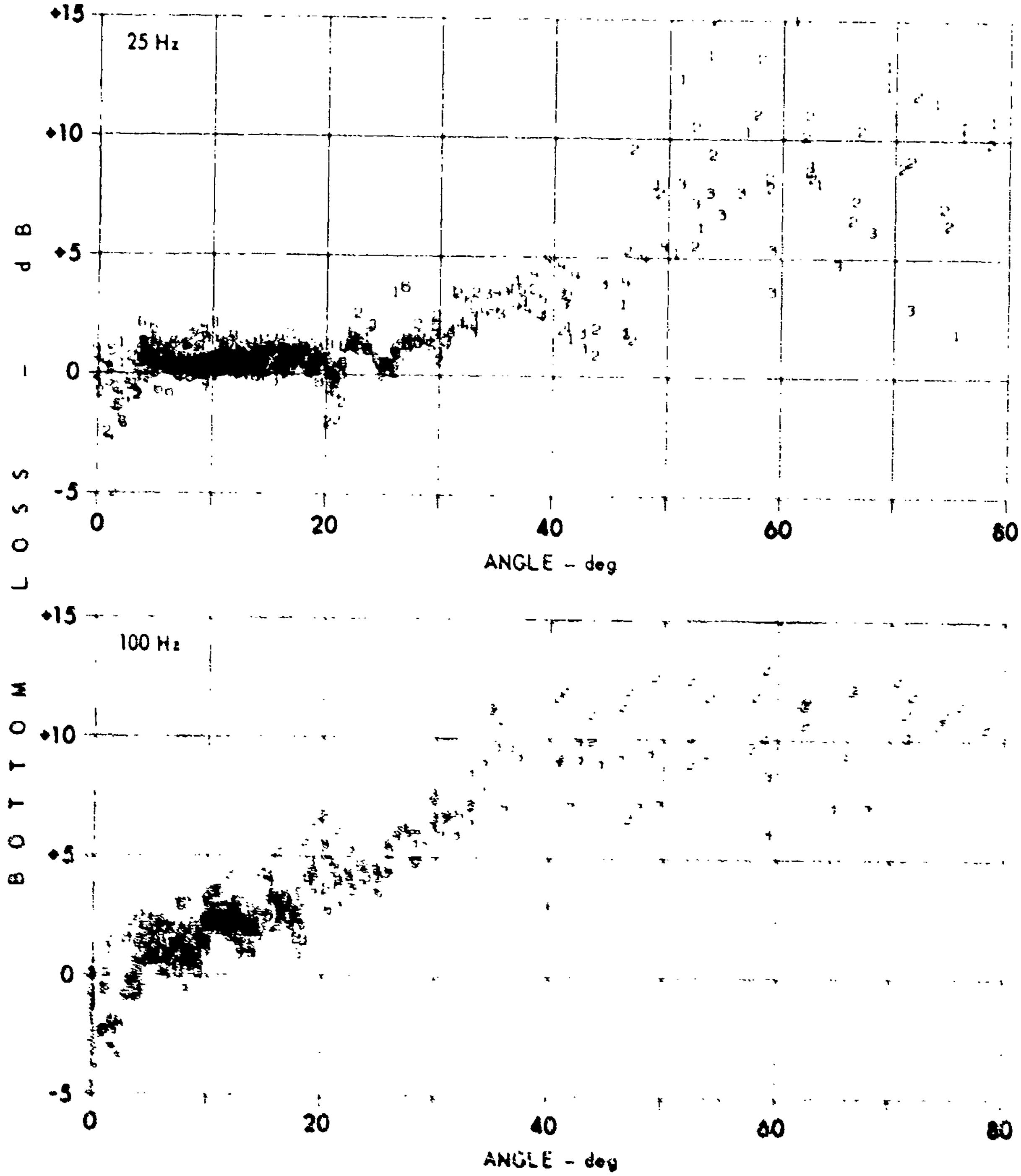

FIGURE C.4
BOTTOM LOSS MEASUREMENTS FOR INDIVIDUAL MULTIPATH ARRIVALS
ENTRIES INDICATE NUMBER OF BOTTOM BOUNCES

ARL UT
AS-78-1988
KCF - GA
12-13-78

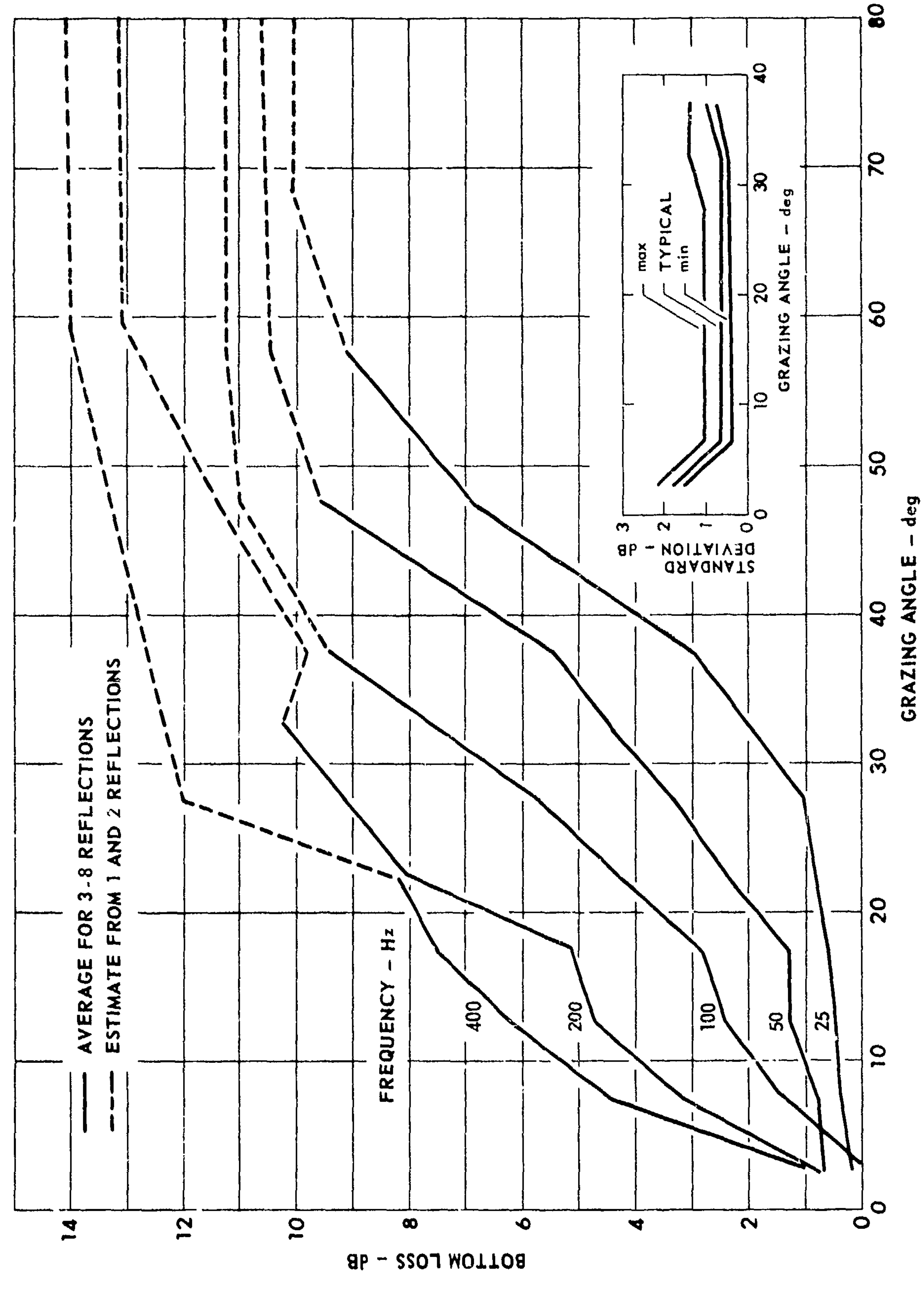

FIGURE C.5
AVERAGED BOTTOM LOSS

ARL:UT
AS-78-58
SKM - GA
5 - 8 - 78

REFERENCES

1. Naval Ocean Research and Development Activity, NSTL Station, MS, "Exercise Plan for CHURCH STROKE II Cruise 5" (U), LRAPP Report No. S77-010, October 1977. (SECRET)

2. D. S. Bitterman, "The ACODAC Ambient Noise System", Proc. IEEE International Conference on Engineering in the Ocean Environment, Vol. 1, 21-23 August 1974, pp. 15-21.

3. Texas Instruments, Inc., Dallas, TX, "Programmable Acoustic Recorder", TI Report No. HB003-EG77, February 1977.

4. J. A. Shooter, "CHURCH STROKE II Cruise 5 Quality Assessment of PAR and ACODAC Tapes", ltr. Ser. F-132 to R. D. Gaul, LRAPP, NORDA, 18 May 1978.

5. J. B. Gaspin and V. K. Shuler, "Source Levels of Shallow Underwater Explosions", NOLTR 71-160, Naval Ordnance Laboratory, White Oak, Silver Spring, MD, 13 October 1971.

6. P. J. Bucca, Bathymetry and Sound Speed Profiles, from ltr. Ser. 341, 340/209-78, Naval Ocean Research and Development Activity, NSTL Station, MS, 22 May 1978.

7. P. J. Bucca, "M/V INDIAN SEAL Projector Logs", Naval Ocean Research and Development Activity, NSTL Station, MS.

8. P. J. Bucca, Source Ship Navigation, from ltr. Ser. 341, 340/142-78, Naval Ocean Research and Development Activity, NSTL Station, MS, 3 April 1978.

9. S. C. Daubin, Jr., SUS Detonation Times, from ltr. Ser. OSD 78-072, Xonics, Inc., Van Nuys, CA, 9 June 1978.

10. C. R. Lunsford, T. Alessi, and L. P. Solomon, "Aircraft Support for the CHURCH STROKE II Cruise 5 Exercises" (U), PSI Report No. TR-091073, Planning Systems, Inc., McLean, VA, 30 March 1978. (CONFIDENTIAL)

11. P. J. Bucca, Site Locations, from ltr. Ser. 341, 340/164-78, Naval Ocean Research and Development Activity, NSTL Station, MS, 19 April 1978.

11a. N. W. Crouch and P. J. Burt, J. Acoust. Soc. Am. 51, 1066-1072 (1962).

12. L. D. Hampton, S. K. Mitchell, and R. Gardner, "Acoustic Bottom Loss Measurement Using Multipath Resolution", Proc. IEEE, EASCON '78, 25-27 September 1978.

13. B. C. Heezen et al., Initial Reports of the Deep Sea Drilling Project, Vol. VI, (U.S. Government Printing Office, Washington, DC, 1971), pp. 293-387.

14. A. F. Whittenborn, private communication, TRACOR, Rockville, MD, April 1978.

15. E. Smith, private communication, Defense Advanced Research Projects Agency, Arlington, VA, April 1978.

16. J. A. Shooter and K. R. Peterman, "Merchant Ship Signatures", Applied Research Laboratories Technical Report No. 77-47 (ARL-TR-77-47), Applied Research Laboratories, The University of Texas at Austin, August 1977. (CONFIDENTIAL)

17. R. D. Gaul, ltr. Ser. 600/110, LRAPP Sea Test Program, Naval Ocean Research and Development Activity, NSTL Station, MS, 23 March 1979.

18. S. K. Mitchell et al., "BEARING STAKE-Vertical ACODAC Acoustic Measurements" (U), Applied Research Laboratories Technical Report No. 78-8 (ARL-TR-78-8), Applied Research Laboratories, The Universtiy of Texas at Austin, February 1978. (CONFIDENTIAL)

19. Maury Center for Ocean Science, Washington, DC, "PARKA II-A Acoustics Measurments" (U), MC Report MC-006, Vol. 1, August 1971.

20. Maury Center for Ocean Science, Washington, DC, "CHURCH ANCHOR Exercise Plan" (U), MC Report MC-011. (CONFIDENTIAL)

21. Xonics, Inc., Van Nuys, CA, "CHURCH OPAL Exercise Plan" (U), Xonics DC No. 1011, August 1975. (SECRET)

22. D. E. Karig, J. C. Ingle, Jr., et al., Initial Reports of the Deep Sea Drilling Project, Vol. 31 (U.S. Government Printing Office, Washington, DC, 1975) pp. 25-47, pp. 169-189.

23. E. L. Hamilton et al., "Sediment Velocities from Sonobuoys: Bay of Bengal, Bering Sea, Japan Sea, and North Pacific", J. Geophys. Res. 2653-2667 (1964).

24. G. Ingram et al., "Analysis of the Acoustic Properties of the Ocean Sediment in the CHURCH STROKE II Area", in preparation.

25. S. K. Mitchell, K. S. Focke, "New Measurement of Compressional Wave Attenuation in Deep Ocean Sediments, submitted to The Journal of The Acoustical Society of America for publication.

26. S. K. Mitchell, K. S. Focke, and M. M. McSwain, "Analysis of Acoustic Bottom Interaction in BEARING STAKE" (U), Applied Research Laboratories Technical Report No. 79-24 (ARL-TR-79-24), Applied Research Laboratories, The University of Texas at Austin, February 1979. (CONFIDENTIAL)

27. J. A. Davis et al., "Acoustic Model Study for Cruise 5 of the CHURCH STROKE II Exercise" (U), NORDA Technical Note 33, Numerical Modeling Division, Naval Oceanographic Laboratory, Washington, DC, November 1977.

28. L. A. Turk, A. E. Barnes, and L. P. Solomon, "CHURCH OPAL: Surveillance of Shipping" (U), PSI Report No. TR-036027, Planning Systems, Inc., January 1976. (SECRET)

REFERENCES

A.1 S. K. Mitchell, "Compensation for Noise in Signal Energy Measurements," J. Acoust. Soc. Am. 60, 967-968 (1976).

A.2 J. A. Shooter and S. L. Watkins, "Estimation of Background Ambient Noise Levels from the Spectral Analysis of Time Series with Application to cw Propagation-Loss Measurements," J. Acoust. Soc. Am. 62, 84-90 (1977).

C.1 J. B. Gaspin and V. K. Shuler, "Source Levels of Shallow Underwater Explosions," NOLTF/FL Technical Report NOLTR-71-160, Naval Ordnance Laboratory, 1971.

C.2 T. L. Foreman, "Acoustic Ray Models Based on Eigenrays," Applied Research Laboratories Technical Report No. 77-1 (ARL-TR-77-1) Applied Research Laboratories, The University of Texas at Austin, 1977.

C.3 L. Hampton, S. Mitchell, and R. Gardner, "Acoustic Bottom Loss Measurement Using Multipath Resolution," Proc. IEEE, EASCON 78, 25-27 September 1978.

(The reverse of this page is blank.)

29 October 1979

DISTRIBTUION LIST FOR
ARL-TR-79-52
UNDER CONTRACT N00014-78-C-0329
CONFIDENTIAL

Copy No.	
	Commanding Officer Naval Ocean Research and Development Activity NSTL Station, MS 39529
1	Attn: Code 110
2	Code 125L
3	Code 115
4	Code 300
5	Code 320
6	Code 340
7	Code 500
8	Code 520 File
	Commanding Officer Naval Research Laboratory Washington, DC 20375
9	Attn: Code 8100
10	Code 8160
11	Code 2627
	Commander Naval Oceanographic Office NSTL Station, MS 39529
12	Attn: Code 7300
13	Code 9210
14	Library
	Commanding Officer Naval Research Laboratory Underwater Sound Reference Division P.O. Box 8337 Orlando, FL 32806
15	Attn: Code 0277
16	Code 8280
17	Code 8289
	Naval Ocean Research and Development Activity Liaison Office Department of the Navy Arlington, VA 22217
18	Attn: Code 130

Distribution List for ARL-TR-79-52 under Contract N00014-78-C-0329 (Cont'd)

Copy No.

Officer in Charge
New London Laboratory
Naval Underwater Systems Center Detachment
New London, CT 06320
19 Attn: Code 31
20 Code 312
21 Code 542

Commander
Naval Ocean Systems Center
San Diego, CA 92152
22 Attn: Code 724
23 Code 7243

Commander
Naval Air Development Center
Warminster, PA 18974
24 Attn: Code 303
25 Code 3032

26 Commanding Officer
Naval Coastal Systems Center
Panama City, FL 32407

27 Officer in Charge
Naval Surface Weapons Center
White Oak Laboratory
Silver Spring, MD 20910

28 Officer in Charge
David W. Taylor Naval Ship Research and Development Center
Carderock Laboratory
Bethesda, MD 20084

29 Director
Naval Ocean Surveillance Information Center
4301 Suitland Road
Washington, DC 20390

30 Commanding Officer
Naval Intelligence Support Center
4301 Suitland Road
Washington, DC 20390

Superintendent
Naval Postgraduate School
Monterey, CA 93940
31 Attn: Library

Distribution List for ARL-TR-79-52 under Contract N00014-78-C-0329 (Cont'd)

Copy No.	
32	Commanding Officer Naval Environmental Prediction Research Facility Monterey, CA 93940
33	Chief Defence Research Establishment, Pacific Fleet Mail Office Canadian Forces Base VICTORIA, BC VOS 1BO
34	Assistant Secretary of the Navy RE&S Department of the Navy Washington, DC 20350 Attn: G. A. Cann
	Chief of Naval Operations Department of the Navy Washington, DC 20350
35	Attn: OP-02
36	OP-03
37	OP-05
38	OP-095
39	OP-096
40	OP-951
41	OP-952
42	OP-951F
43	OP-952D
44 - 45	Headquarters Naval Material Command Washington, DC 20360 Attn: MAT-08T245
46 - 47	Project Manager Antisubmarine Warfare System Project Department of the Navy Washington, DC 20360 Attn: PM-4
48	Director Strategic System Projects Office Department of the Navy Washington, DC 20376 Attn: PM-1

Distribution List for ARL-TR-79-52 under Contract N00014-78-C-0329 (Cont'd)

Copy No.

Chief of Naval Research
Department of the Navy
Arlington, VA 22217
49 Attn: Code 100
50 Code 102B
51 Code 220
52 Code 230
53 Code 460
54 Code 480

Commanding Officer
Office of Naval Research
Branch Office London
FPO New York NY 09510
55 Attn: Code 241

Commander
Naval Electronic Systems Command
Washington, DC 20360
56 Attn: PME-124
57 PME-124TA
58 PME-124/30
59 PME-124/40
60 PME-124/60
61 Code 320

Commander
Naval Sea Systems Command
Washington, DC 20362
62 Attn: Code 06H1

Commander
Naval Air Systems Command
Washington, DC 20361
63 Attn: Code 370
64 PMA-264

65 Deputy Undersecretary of Defense for
Research and Engineering
Department of Defense
Washington, DC 20301

Defense Advanced Research Projects Agency
1400 Wilson Boulevard
Arlington, VA 22209
66 Attn: T. Kooij
67 CDR V. E. Simmons

Distribution List for ARL-TR-79-52 under Contract N00014-78-C-0329 (Cont'd)

Copy No.	
68	Commander Naval Oceanography Command NSTL Station, MS 39529
69	Director of Navy Laboratories Room 1062, Crystal Plaza, Bldg. 5 Department of the Navy Washington, DC 20360
70	Commander in Chief, U.S. Pacific Fleet P.O. Box 3 Pearl Harbor, HI 96860 Attn: Code 3521
71	Commander in Chief U.S. Atlantic Fleet Norfolk, VA 23511 Attn: Code 353
72	Commander Third Fleet Pearl Harbor, HI 96860 Attn: Code N-7
73 - 74	Commander Second Fleet FPO New York, NY 09501
75	Commander Sixth Fleet FPO New York, NY 09501
76	Commander Seventh Fleet FPO San Francisco, CA 96601 Attn: CAPT J. T. Talbert
77	Commander Fleet Air, Mediterranean Commander, Antisubmarine War Force U.S. Sixth Fleet FPO New York, NY 09521
78	Commander Submarine Forces U.S. Pacific Fleet Pearl Harbor, HI 96860

Distribution List for ARL-TR-79-52 under Contract N00014-78-C-0329 (Cont'd)

Copy No.	
79	Commander Submarine Development Group 12 Naval Submarine Base, New London Box 70 Groton, CT 06340
80	Commander Submarine Group Seven Box 50 FPO Seattle, WA 98762 Attn: CAPT J. McNish
81	Commander Operational Test and Evaluation Force Naval Base Norfolk, VA 23511 Attn: Code 42
82	Commander Patrol and Reconnaissance Force Seventh Fleet FPO Seattle, WA 98768 Attn: CDR P. O'Connor
83	Commander U.S. Naval Forces, Marianas FPO San Francisco, CA 96630 Attn: LCDR D. L. Wetherell
84	Commander Patrol Wings U.S. Pacific Fleet Naval Air Station Moffett Field, CA 94035
	Commander Oceanographic System, Atlantic Box 100 Norfolk, VA 23511
85	Attn: LT P. A. Kuhn, N34
86	W. G. Schreiber
	Commander Oceanographic System, Pacific Box 1390 Pearl Harbor, HI 96860
87	Attn: LCDR W. F. Johnson
88	Code N3

Distribution List for ARL-TR-79-52 under Contract N00014-78-C-0329 (Cont'd)

Copy No.	
89	Commander Patrol Wing Two FPO San Francisco, CA 96601
90	Oceanographic Development Squadron 8 Naval Air Station Patuxent River, MD 20670
	Commanding Officer Chesapeake Division Naval Facilities Engineering Command Washington Navy Yard Washington, DC 20374
91	Attn: Code FPO-1E4
	Defense Advanced Research Projects Agency ARPA Research Center Unit 1, Bldg. 301A NAS Moffett Field, CA 94035
92	Attn: E. L. Smith
93 - 94	Commanding Officer and Director Defense Technical Information Center Cameron Station, Building 5 5010 Duke Street Alexandria, VA 22314
95	Chief Defence Research Establishment Atlantic P.O. Box 1012 Dartmouth, NOVA SCOTIA B2Y 327
	Director of Naval Matters Center of Naval Analysis Arlington, VA 22209
96	Attn: C. E. Woods
97	University of California-San Diego P.O. Box 6049 San Diego, CA 92106
	Applied Physics Laboratory The Johns Hopkins University John Hopkins Road Laurel, MD 20810
98	Attn: A. Chwastyk
99	W. L. May
100	G. L. Smith

Distribution List for ARL-TR-79-52 under Contract N00014-78-C-0329 (Cont'd)

Copy No.

101 University of Hawaii
2525 Correa Road
Honolulu, HI 96822

102 Palisades Geophysical Institute, Inc.
131 Erie Street
P.O. Box 396
Blauvelt, NY 10913

103 Applied Physics Laboratory
The University of Washington
1013 Northeast 40th Street
Seattle, WA 98105

Woods Hole Oceanographic Institution
Woods Hole, MA 02543
104 Attn: E. E. Hayes

Analysis & Technology, Inc.
Technology Park
P.O. Box 220, Route 2
North Stonington, CT 06359
105 Attn: S. Elam

Arthur D. Little, Inc.
Acorn Park
Cambridge, MA 02140
106 Attn: G. Raisbeck
107 W. G. Sykes

B-K Dynamics, Incorporated
15825 Shady Grove Road
Rockville, MD 20850
108 Attn: P. G. Bernard

Bell Telephone Laboratories, Inc.
Whippany Road
Whippany, NJ 07961
109 Attn: J. Goldman
110 L. F. Fretwell

111 Bolt, Beranek and Newman, Inc.
1701 North Fort Myer Drive
Arlington, VA 22209

112 Bolt, Beranek, & Newman, Inc.
50 Moulton St.
Cambridge, MA 02138

Distribution List for ARL-TR-79-52 under Contract N00014-78-C-0329 (Cont'd)

Copy No.

113 Claude P. Brancart & Associates, Inc.
17150 Butte Creek, Suite 214
Houston, TX 77090

114 Daniel H. Wagner Associates, Inc.
dba Daniel H. Wagner, Inc.
Station Square One
Paoli, PA 19301

115 Daubin Systems Corporation
104 Crandon Blvd.
Key Biscayne, FL 33149
Attn: S. C. Daubin

116 Envo
800 Follin Lane
Vienna, VA 22130
Attn: C. Matheny

Ocean Data Systems, Inc.
6000 Executive Boulevard
Rockville, MD 20852
117 Attn: [illegible]. V. Jacobs
118 E. Morenoff

119 Ocean Data Systems, Inc.
2400 Garden Road
Monterey, CA 93940

120 Ocean Data Systems, Inc.
3[illegible]75 Wing St.
San Diego, CA 9[illegible]110

ORI, Incorporated
1400 Spring Street
Silver Spring, MD 20910
121 Attn: J. I. Bowen

Planning Systems Incorporated
7900 Westpark Drive
Suite 600
McLean, VA 22101
122 Attn: R. Klinkner
123 R. S. Cavanaugh

Purvis Systems Incorporated
3530 Camino del Rio North
San Diego, CA 92108
124 Attn: T. J. Fitzgerald

Distribution List for ARL-TR-79-52 under Contract N00014-78-C-0329 (Cont'd)

Copy No.	
	Raytheon Company Submarine Signal Division P.O. Box 360 Portsmouth, RI 02871
125	Attn: B. A. Becken
	Sanders Associates, Inc. 95 Canal Street Nashua, NH 03060
126	Attn: L. E. Gagne
127	R. P. White
	Science Applications, Inc. Suite 216 21133 Victory Blvd. Canoga Park, CA 91303
128	Attn: J. H. Wilson
	Science Applications, Inc. P.O. Box 2351 La Jolla, CA 92038
129	Attn: F. J. Ryan
	Science Applications, Inc. P.O. Box 1303 McLean, VA 22101
130	Attn: J. S. Hanna
131	C. W. Spofford
132	Summit Research Corporation 1 West Deer Park Drive Gaithersburg, MD 20760
	SUTRON Corporation Suite 501 1150 Main St. Arlington, VA 22209
133	Attn: C. H. Dabney
	Tracor, Inc. Rockville Laboratory 1601 Research Blvd. Rockville, MD 208[illegible]0
134	Attn: J. T. Gottwald
135	A. F. Wittenborn

Distribution List for ARL-TR-79-52 under Contract N00014-78-C-0329 (Cont'd)

Copy No.	
	TRW Incorporated 7600 Colshire Drive McLean, VA 22101
136	Attn: R. T. Brown
137	I. B. Gereben
	Underwater Systems, Inc. 1776 E. Jefferson St. Silver Spring, MD 20852
138	Attn: M. S. Weinstein
	Western Electric Company, Inc. P.O. Box 20046 Greensboro, NC 27420
139	Attn: R. H. Harris
140	Office of Naval Research Resident Representative Room 582, Federal Building Austin, TX 78712
141	Environmental Sciences Division, ARL:UT
142	Nancy R. Bedford, ARL:UT
143	Karl C. Focke, ARL:UT
144	Kenneth E. Hawker, ARL:UT
145	Stephen K. Mitchell, ARL:UT
146	Jack A. Shooter, ARL:UT
147	Library, ARL:UT

DEPARTMENT OF THE NAVY
OFFICE OF NAVAL RESEARCH
875 NORTH RANDOLPH STREET
SUITE 1425
ARLINGTON VA 22203-1995

IN REPLY REFER TO:

5510/1
Ser 321OA/011/06
31 Jan 06

MEMORANDUM FOR DISTRIBUTION LIST

Subj: DECLASSIFICATION OF LONG RANGE ACOUSTIC PROPAGATION PROJECT (LRAPP) DOCUMENTS

Ref: (a) SECNAVINST 5510.36

Encl: (1) List of DECLASSIFIED LRAPP Documents

1. In accordance with reference (a), a declassification review has been conducted on a number of classified LRAPP documents.

2. The LRAPP documents listed in enclosure (1) have been downgraded to UNCLASSIFIED and have been approved for public release. These documents should be remarked as follows:

   Classification changed to UNCLASSIFIED by authority of the Chief of Naval Operations (N772) letter N772A/6U875630, 20 January 2006.

   DISTRIBUTION STATEMENT A: Approved for Public Release; Distribution is unlimited.

3. Questions may be directed to the undersigned on (703) 696-4619, DSN 426-4619.

BRIAN LINK
By direction

Subj: DECLASSIFICATION OF LONG RANGE ACOUSTIC PROPAGATION PROJECT (LRAPP) DOCUMENTS

DISTRIBUTION LIST:

NAVOCEANO (Code N121LC – Jaime Ratliff)
NRL Washington (Code 5596.3 – Mary Templeman)
PEO LMW Det San Diego (PMS 181)
DTIC-OCQ (Larry Downing)
ARL, U of Texas
Blue Sea Corporation (Dr.Roy Gaul)
ONR 32B (CAPT Paul Stewart)
ONR 321OA (Dr. Ellen Livingston)
APL, U of Washington
APL, Johns Hopkins University
ARL, Penn State University
MPL of Scripps Institution of Oceanography
WHOI
NAVSEA
NAVAIR
NUWC
SAIC

Declassified LRAPP Documents

Report Number	Personal Author	Title	Publication Source (Originator)	Pub. Date	Current Availability	Class.
ARLTR7952	Focke, K. C., et al.	CHURCH STROKE 2 CRUISE 5 PAR/ACODAC ENVIRONMENTAL ACOUSTIC MEASUREMENTS AND ANALYSIS (U)	University of Texas, Applied Research Laboratories	791029	ADC025102; NS; AU; ND	C
Unavailable	Van Wyckhouse, R. J.	SYNBAPS. VOLUME I. DATA BASE SOURCES AND DATA PREPARATION	Naval Ocean R&D Activity	791201	ADC025193	C
NORDATN63	Brunson, B. A., et al.	ENVIRONMENTAL EFFECTS ON LOW FREQUENCY TRANSMISSION LOSS IN THE GULF OF MEXICO (U)	Naval Ocean R&D Activity	800901	ADC029543; ND	C
NORDATN80C	Gereben, I. B.	ACOUSTIC SIGNAL CHARACTERISTICS MEASURED WITH THE LAMBDA III DURING CHURCH STROKE III (U)	Naval Ocean R&D Activity	800915	ADC023527; NS; AU; ND	C
NOSCTR664	Gordon, D. F.	ARRAY SIMULATION AT THE BEARING STAKE SITES	Naval Ocean Systems Center	810401	ADC025992; NS; AU; ND	C
NOSCTR703	Gordon, D. F.	NORMAL MODE ANALYSIS OF PROPAGATION LOSS AT THE BEARING STAKE SITES (U)	Naval Ocean Systems Center	810801	ADC026872; NS; AU; ND	C
NOSCTR680	Neubert, J. A.	COHERENCE VARIABILITY OF ARRAYS DURING BEARING STAKE (U)	Naval Ocean Systems Center	810801	ADC028075; NS; ND	C
HSECO735	Luehrmann, W. H.	SQUARE DEAL R/V SEISMIC EXPLORER FIELD OPERATIONS REPORT (U)	Seismic Engineering Co.	731121	AD0530744; NS; ND	C; U
MPL-C-42/76	Morris, G. B.	CHURCH ANCHOR EXPLOSIVE SOURCE (SUS) PROPAGATION MEASUREMENTS FROM R/P FLIP (U)	Marine Physical Laboratory	760701	ADC010072; AU; ND	C; U
ARLTR7637	Mitchell, S. K., et al.	SQUARE DEAL EXPLOSIVE SOURCE (SUS) PROPAGATION MEASUREMENTS. (U)	University of Texas, Applied Research Laboratories	760719	ADC014196; NS; AU; ND	C; U
NORDAR23	Fenner, D. F.	SOUND SPEED STRUCTURE OF THE NORTHEAST ATLANTIC OCEAN IN SUMMER 1973 DURING THE	Naval Ocean R&D Activity	800301	ADC029546; NS; ND	C; U
NOOTR230	Bucca, P. J.	SOUND VELOCITY CONDITIONS DURING THE CHURCH ANCHOR EXERCISE (U)	Naval Oceanographic Office	751201	NS; AU; ND	C;U
ONR SP 2-69; MC PLAN-01	Unavailable	PARKA II EXPERIMENT UTILIZING SEA SPIDER, ONR SCIENTIFIC PLAN 2-69 (U)	Maury Center for Ocean Science	690626	ADB020846; ND	U
Unavailable	Unavailable	PARKA I EXPERIMENT	Maury Center for Ocean Science	691101	AD0506209	U
USRD CR 3105	Unavailable	SEA SPIDER TRANSPONDER TRANSDUCER	Naval Research Laboratory	700505	ND	U
MC PLAN 05; ONR Scientific Plan 1-71	Unavailable	ATLANTIC TEST BED MEASUREMENT PROGRAM (U)	Maury Center for Ocean Science	701020	ND	U
ACR-170 VOL.1	Hurdle, B. G.	PROJECT NEAT- A COLLABORATIVE LONG RANGE PROPAGATION EXPERIMENT IN THE NORTHEAST ATLANTIC, PART I (U)	Naval Research Laboratory	701118	ND	U
MC-003-VOL-2	Unavailable	THE PARKA I EXPERIMENT. APPENDICES- PACIFIC ACOUSTIC RESEARCH KANEOHE-ALASKA (U)	Maury Center for Ocean Science	710101	ND	U